Cyprus University of Technology

Faculty of Geotechnical Sciences and Environmental Management

Doctoral Dissertation

A novel microbial approach for the valorisation of lupanine containing wastewater emitted from the lupin beans processing industry

Stella Parmaki

Limassol, April 2022

CYPRUS UNIVERSITY OF TECHNOLOGY

FACULTY OF GEOTECHNICAL SCIENCES AND ENVIRONMENTAL MANAGEMENT

DEPARTMENT OF CHEMICAL ENGINEERING

Doctoral Dissertation

A novel microbial approach for the valorisation of lupanine containing wastewater emitted from the lupin beans processing industry

Stella Parmaki

Limassol, April 2022

Approval Form

Doctoral Dissertation

A novel microbial approach for the valorisation of lupanine containing wastewater emitted from the lupin beans processing industry

Presented by

Stella Parmaki

Supervisor: Dr. Michalis Koutinas, Associate Professor

Signature _____

Member of the committee: Dr. Vasileios Fotopoulos, Associate Professor

Signature _____

Member of the committee: Emmanuel M. Papamichael, Prof. Emeritus

Signature _____

Cyprus University of Technology

Limassol, April 2022

Copyrights

Acknowledgements

I would like to express my sincere gratitude to my supervisor Dr. Michalis Koutinas for his patience and continued guidance and support during the time of research and writing of this thesis. I would also like to thank Prof. Carlos Afonso, Prof. Francesca Malpei, Dr. Frederico Ferreira, Dr. Ioannis Vyrides, Dr. Chrysoulla Drouza and Dr. Marlen Vasquez for all the beneficial scientific discussions.

Many thanks to all my colleagues from Environmental Bioprocessing Laboratory and Environmental Engineering Laboratory for all the useful discussions and company during the last six years. Maria P, Maria K, Charis, Panagiota and Antonia thank you for making this long academic journey fun and beautiful.

Also, great thanks to my friends and siblings for their patience and for always being there for me. I owe my deepest gratitude to my life partner, Stelios Mousarris, for his patience and support in my many ups and down and his constant caring. Lastly, my parents deserve endless gratitude: my father for teaching me to stay strong in all the difficult times and my mother for her constant encouragement and unconditional love. To my family, I give everything, including this.

ABSTRACT

Lupin bean processing industries commonly use the debittering process for eliminating the antinutritional and alkaloid content of lupin beans, ensuring a safe product for human consumption. Various debittering processes have been developed for the removal of toxic and bitter alkaloids from lupin beans. However, these methods require the use of large amounts of water, which is eventually disposed as wastewater rich in alkaloids. Lupanine constitutes the major quinolizidine alkaloid present in the specific type of wastewater, which is contained in the effluent as an enantiomeric mixture of D-(+)-lupanine and L-(–)-lupanine. Lupanine is considered a useful molecule exhibiting several applications in pharmaceutical/medical agricultural and chemical industries. Therefore, microbial valorisation of lupanine constitutes a promising approach for the management of wastewater generated from the lupin bean snack industry.

Microorganisms capable of metabolizing racemic lupanine were isolated from different environmental sources, which were identified based on phylogenetic and physiological characteristics. *Rhodococcus rhodochrous* LPK211, *Rhodococcus ruber* LPK111, *Rhodococcus* sp. LPK311 and *Pseudomonas putida* LPK411 were capable of biodegrading racemic lupanine as a single carbon source while generating known and novel lupanine-based alkaloid structures as end products from racemic lupanine bioconversion. Moreover, all strains achieved enantioselective resolutions of lupanine racemate, producing L-(–)-lupanine in high enantiomeric excess. Based on preliminary findings, the most effective isolated strain (*P. putida* LPK411) was further subjected to an extensive study. The aforementioned strain could perform enantioselective resolution of lupanine enantiomeric mixtures existing in both unrefined and pretreated industrial wastewater employing a lab-scale bioreactor while assessing the capacity of LPK411 to perform racemic resolution of lupanine in a repeated fed-batch process exhibited that the microorganism could repetitively perform stable enantioselective resolution. Furthermore, the transcriptional kinetics of key genes for the degradation of lupanine by LPK411 was investigated revealing the transcriptional patterns of the metabolic pathway employed for lupanine metabolism, while an environmental toxicological assessment was performed to evaluate the impact of lupanine and other natural compounds on the ecosystems.

Keywords: lupanine, enantiomers, valorisation, resolution, bioconversion

TABLE OF CONTENTS

LIST OF TABLES

LIST OF FIGURES

LIST OF ABBREVIATIONS

Abbreviations

(–)-DIP-Cl:	(–)-B-chlorodiisopinocampheylborane
ACN:	Accession number
AF-C:	Antifoam controller
ANOVA:	Analysis of variance
APG:	Air pressure generator
APHA:	American Public Health Association
ARB:	Angiotensin II receptor blocker
ASP:	Antifoam syringe pump
AWRP:	effluent generated from anaerobic digestion of wastewater produced from UWRP
AWWA:	American Water Works Association
CI:	Combination index
CM:	CO_2 meter
CCR:	Carbon catabolite repression
cDNA:	Complementary DNA
CI:	Combination index
COD:	Chemical oxygen demand
DH:	Dehumidifier unit
DNA:	Deoxyribonucleic acid
DNS:	Dinitrosalicylic acid
DO:	Dissolved oxygen meter
EC:	European Commission
EC_{50}:	Median effective concentration

ee:	Enantiomeric excesses
EPA:	US Environmental Protection Agency
EPI:	Epichlorohydrin
FDA:	US Food and Drug Administration
FID:	Flame Ionisation Detector
GC:	Gas chromatography
GI:	Germination index
HPLC:	High Performance Liquid Chromatography
IC_{50}:	Half-maximal inhibitory concentration;
ip:	Intraperitoneal administration
ISO:	International Organization for Standardization
ITS:	Internal transcribed spacer sequence
iv:	Intravenous administration
KRED:	KetoREDuctase
LABAs:	Long-acting beta-agonists
LD_{50}:	Lethal dose
LTRA:	Leukotriene receptor antagonist
M9:	Minimal microbial growth medium
mRNA:	Messenger RNA
nAChR:	Nicotinic acetylcholine receptor
NCBI:	National Center for Biotechnology Information
NMR:	Nuclear magnetic resonance spectroscopy
NSAIDs:	Non-steroidal anti-inflammatory drugs
OD:	Optical density
OECD:	Organisation for Economic Co-operation and Development

OFMSW:	Organic fraction of municipal solid waste
PCR:	Polymerase chain reaction
RT-qPCR:	Quantitative reverse transcription PCR
pH-C:	pH controller
PLA:	Poly-L-lactic acid
po:	Oral administration
PP:	Peristaltic pump
REACH:	Registration, Evaluation, Authorisation and Restriction of Chemicals
RNA:	Ribonucleic acid
RWSP:	Retentate water remaining following nanofiltration of wastewater emitted from UWSP
SBLA:	Sewerage Board of Limassol – Amathus
scPTZ:	Subcutaneous pentylenetetrazole
sp.:	species
SP:	Sampling port
spp:	several species
SSRIs:	Selective serotonin-reuptake inhibitors
TC:	Temperature controller
TKN:	Total Kjeldahl nitrogen
UV/VIS:	Ultraviolet-visible
UWRP:	Wastewater generated during the resting phase of the lupin bean snack manufacturing process
UWSP:	Wastewater generated during the sweetening phase of the lupin bean snack manufacturing process
v/v:	Volume/volume

WEF:	Water Environment Federation
w/v:	Weight/volume

Microorganisms and other

A. fischeri	*Aliivibrio fischeri*
A. niger	*Aspergillus niger*
B. coagulans	*Bacillus coagulans*
B. subtilis	*Bacillus subtilis*
C. zeylanoides	*Candida zeylanoides*
C. virginica	*Crassostrea virginica*
D. magna	*Daphnia magna*
E. coli	*Escherichia coli*
G. oxydans	*Gluconobacter oxydans*
G. stearothermophilu	*Geobacillus stearothermophilus*
L. albus	*Lupinus albus*
L. angustifolius	*Lupinus angustifolius*
L. delbrueckii	*Lactobacillus delbrueckii*
L. densiflorus	*Lupinus densiflorus*
L. elegans	*Lupinus elegans*
L. exaltatus	*Lupinus exaltatus*
L. hartwegii	*Lupinus hartwegii*
L. luteus	*Lupinus luteus*
L. macouni	*Lupinus macouni*
L. madrensis	*Lupinus madrensis*
L. mexicanus	*Lupinus mexicanus*

L. montanus	*Lupinus montanus*
L. mutabilis	*Lupinus mutabilis*
L. paracasei	*Lacticaseibacillus paracasei*
L. polyphyllus	*Lupinus polyphyllus*
L. pusillus	*Lupinus pusillus*
L. rotundiflorus	*Lupinus rotundiflorus*
L. sativum	*Lepidium sativum*
L. termis	*Lupinus termis*
L. variusorientalis	*Lupinus variusorientalis*
LPK111	*Rhodococcus ruber* LPK111
LPK211	*Rhodococcus rhodochrous* LPK211
LPK311	*Rhodococcus sp.* LPK311
LPK411	*Pseudomonas putida* LPK411
LPK121	*Pseudomonas citronellolis* LPK121
LPK122	*Rhodobacter sp.* LPK122
LPK221	*Pseudomonas sp.* LPK221
LPK222	*Ochrobactrum tritici* LPK222
O. tritici	*Ochrobactrum tritici*
P. aeruginosa	*Pseudomonas aeruginosa*
P. alcaligenes	*Pseudomonas alcaligenes*
P. citronellolis	*Pseudomonas citronellolis*
P. fluorescens	*Pseudomonas fluorescens*
P. geniculata	*Pseudomonas geniculate*
P. promelas	*Pimephales promelas*
P. putida	*Pseudomonas putida*

P. stutzeri	*Pseudomonas stutzeri*
R. erythropolis	*Rhodococcus erythropolis*
R. opacus	*Rhodococcus opacus*
R. rhodochrous	*Rhodococcus rhodochrous*
R. ruber	*Rhodococcus ruber*
R. subcapitata	*Raphidocelis subcapitata*
S. alba	*Sinapis alba*
S. cerevisiae	*Saccharomyces cerevisiae*
S. costatum	*Skeletonema costatum*
S. saccharatum	*Sorghum saccharatum*

1 INTRODUCTION

1.1 Sustainable technologies for the production of enantiopure added-value molecules

1.1.1 Overview of enantiopure molecules

The capacity to produce pure enantiomers is increasingly important enabling the development of advanced applications for different industries including food, agrochemical, and fine chemicals, but most importantly for the medical and pharmaceutical sectors (Blaser, 2015; Fanali et al., 2019; Leek and Andersson, 2017). The pharmaceutical industry constitutes the major consumer of enantiopure compounds (Sanganyado et al., 2017; Stinson, 2001), exhibiting a continuously growing number of novel drugs manufactured as single-enantiomeric or diastereomeric formulations, given that several currently available racemic drugs are being replaced by their single-enantiomeric counterparts (Abram et al., 2019). Indeed, the number of racemic drugs approved by the US Food and Drug Administration (FDA) has substantially decreased (Agranat et al., 2012; Caner et al., 2004; Sanganyado et al., 2017; Shen et al., 2016) (Fig 1.1), following a regulatory preference towards the production of single enantiomeric molecules to ensure the selective interaction often required between chiral biomolecules and the active pharmaceutical ingredient.

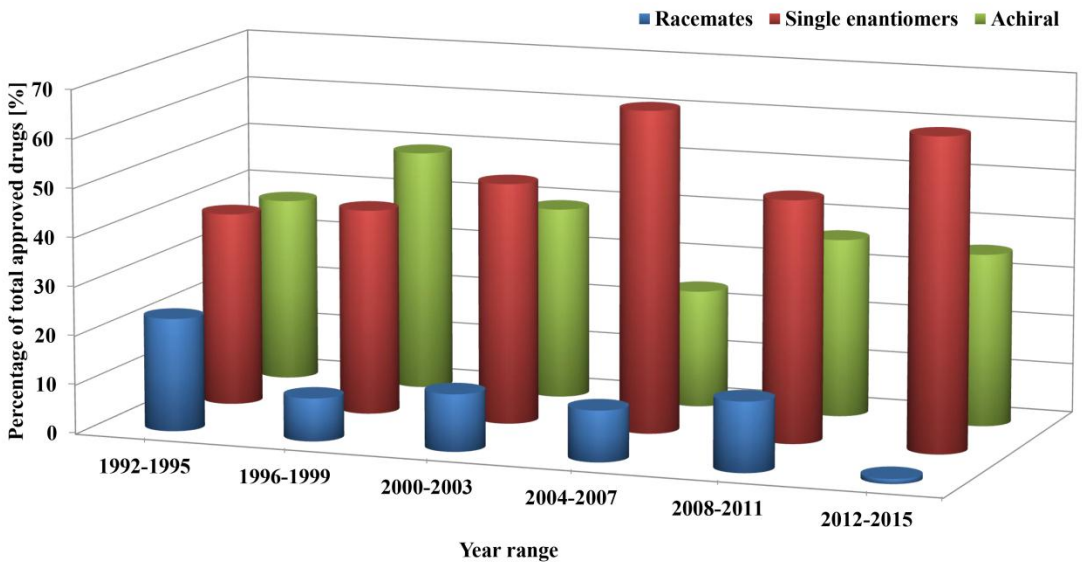

Figure 1.1: Distribution of FDA-approved drugs based on chirality between 1992-2015.

Enantiomerically pure drugs demonstrate significant advantages over racemic options, providing the desired beneficial effect with a reduced total dose of medication and fewer side effects caused by the undesired enantiomer (Alkadi and Jbeily, 2018; Sekhon, 2013). In 1992, FDA established a policy statement to regulate chiral drugs which included guidelines for the development of new stereoisomeric agents, recommending the evaluation of each stereoisomer of the chiral product based on its therapeutic utility and/or toxicological effects (U.S. Food and Drug Administration (FDA), 1992). Ever since several blockbuster drugs have been developed as single isomers, including atorvastatin, simvastatin (HMG-CoA reductase inhibitors), sertraline, paroxetine, duloxetine (selective serotonin-reuptake inhibitors – SSRIs), epoetin alfa (erythropoiesis-stimulating agents – ESAs), montelukast (leukotriene receptor antagonist – LTRA), rituximab (monoclonal antibody), valsartan (angiotensin II receptor blocker – ARB), clopidogrel (antiplatelet agent), oxybutynin (anticholinergic/antimuscarinic), doxazosin (alpha-blocker) and pheniramine (antihistamine) (Ali et al., 2014; Branch and Hutt, 2012; Budau et al., 2017; Gumustas et al., 2018; Sun et al., 2011). Moreover, several successfully commercialized racemic or diastereomeric drugs have been redeveloped as single enantiomeric formulations (Table 1.1).

Table 1.1: Substitution of racemic drugs for single enantiomers through chiral switching.

Generic name of racemic drug	Generic name of enantiopure drug	Class of medication	References
Albuterol	Levalbuterol (*R*-(–)-albuterol)	Bronchodilators	Calcaterra and D'Acquarica, (2018); Caner et al. (2004)
Bupivacaine	Levobupivacaine (*S*-(–)-bupivacaine)	Local anaesthetics	Calcaterra and D'Acquarica, (2018); Caner et al. (2004)
Cetirizine	Levocetirizine (*R*-(–)-cetirizine)	Antihistamines	Calcaterra and D'Acquarica, (2018); Gellad et al. (2014)
Citalopram	Escitalopram (*S*-(+)-citalopram)	SSRIs	Calcaterra and D'Acquarica, (2018); Gellad et al. (2014)
Fenfluramine	Dexfenfluramine (*S*-(+)-fenfluramine)	Antiobesity	Calcaterra and D'Acquarica, (2018); Caner et al. (2004)
Formoterol	Arformoterol (*R,R*-(−)-formoterol)	Long-acting beta agonists (LABAs)	Calcaterra and D'Acquarica, (2018); Gellad et al. (2014)
Ibuprofen	Dexibuprofen (*S*-(+)-Ibuprofen)	Non-steroidal anti-inflammatory drugs (NSAIDs)	Calcaterra and D'Acquarica, (2018)
Ketamine	Esketamine (*S*-(+)-ketamine)	*N*-Methyl-D-aspartate receptor (NMDAR) antagonists	Molero et al. (2018)

Table 1.1: (continued)

Generic name of racemic drug	Generic name of enantiopure drug	Class of medication	References
Ketoprofen	Dexketoprofen (*S*-(+)-ketoprofen)	NSAIDs	Calcaterra and D'Acquarica, (2018)
Lansoprazole	Dexlansoprazole (*R*-(+)-lansoprazole)	Proton pump inhibitors	Calcaterra and D'Acquarica, (2018); Gellad et al. (2014)
Leucovorin	Levoleucovorin (*S*-(−)-leucovorin)	Folic acid analogues	Calcaterra and D'Acquarica, (2018); Gellad et al. (2014)
Methylphenidate	Dexmethylphenidate (*R,R*-(+)-methylphenidate)	Stimulants	Calcaterra and D'Acquarica, (2018); Caner et al. (2004); Gellad et al. (2014)
Modafinil	Armodafinil (*R*-(−)-modanafil)	Wakefulness promoting agents	Calcaterra and D'Acquarica, (2018); Gellad et al. (2014)
Ofloxacin	Levofloxacin (*S*-(–)-ofloxacin)	Quinolone antibiotics	Calcaterra and D'Acquarica, (2018); Caner et al. (2004)
Omeprazole	Esomeprazole (*S*-(–)-omeprazole)	Proton pump inhibitors	Calcaterra and D'Acquarica, (2018); Gellad et al. (2014)
Zopiclone	Eszopiclone (*S*-(+)-zopiclone)	Sedative-hypnotics	Calcaterra and D'Acquarica, (2018); Gellad et al. (2014)

Three main fundamental routes have been proposed to produce enantiomerically pure compounds, categorized as chiral pool, racemic and chiral synthesis approaches (Fig 1.2). The chiral pool approach constitutes the most applicable process producing 55% of the total manufacture of enantiopure drugs, racemic methods are employed for developing 28% of the single enantiomeric drugs available, while chiral synthesis approaches comprise the less desirable route (10%) (Todd, 2014). In the chiral synthesis approach, single enantiomers are formed through the asymmetric synthesis of prochiral substrates following a sequence of reactions (Rouf and Taneja, 2014). Chiral pool methods employ inexpensive naturally occurring chiral molecules (e.g. carbohydrates, amino acids, terpenes, and alkaloids) as feedstocks for the synthesis of optically pure compounds (Lorenz and Seidel-Morgenstern, 2014). Although racemic approach constitutes an easy and simple route where single enantiomers can be obtained through the resolution of racemic mixtures (Schuur et al., 2011).

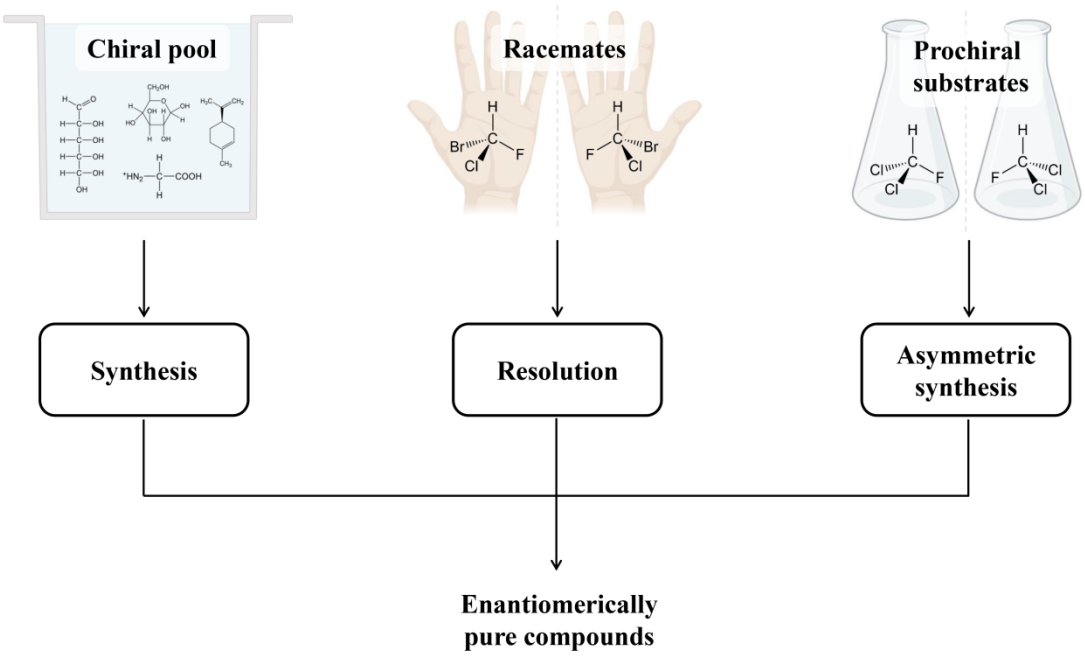

Figure 1.2: Main approaches for the development of enantiomerically pure compounds.

1.1.2 Different routes for the production of enantiopure molecules

1.1.2.1 Chemical production of enantiopure molecules

Over the years, a variety of chemical methods have been developed enabling the manufacture of enantiopure molecules (Fig 1.3). The Chiral pool route is widely applied due to the use of inexpensive and abundant starting materials for the production of enantiomerically pure compounds (Rouf and Taneja, 2014) and the development of products with high chiral purity (Michalska et al., 2017). The chiral pool approaches for the chemical production of enantiomerically pure molecules could be divided into i) the chemical transformation of biomass-derived chiral building blocks involving the amplification of the existing chirality via chiral induction of the existing chiral centre(s) and ii) the removal and/or functional transformation of the existing chiral functional groups of the chiral pool. In the case of natural resources containing a high number of chiral centres, such as carbohydrates, further synthetic transformations are often required to fulfil the removal of certain undesired chiral centres (Ettireddy et al., 2017; Parker et al., 2018).

Racemic resolution constitutes a very powerful approach for the production of enantiomerically pure compounds. The chemical resolution could be usually performed by four major methods including i) crystallization processes, such as direct crystallization of racemates or diastereomeric salts, complexes or compounds (Lorenz and Seidel-Morgenstern, 2014), ii) chiral chromatography (Ward, 2002), iii) kinetic (including dynamic) resolutions conducted via chemical routes (Huerta et al., 2001) and iv) selective liquid-liquid extraction (Pinxterhuis et al., 2018) and v) membrane-based processes (Fernandes et al., 2017).

The asymmetric synthesis of enantiopure molecules using non-chiral building blocks involving the insertion of chirality via non-catalytic (e.g. chiral auxiliaries) or asymmetric catalysis could be also employed. Reusable chiral auxiliaries, including Evans, Corey, Yamada, Enders, Oppolzer and Kunz, have been widely used in the synthesis of enantiomerically pure compounds (Diaz-Munoz et al., 2019), however, this approach exhibits disadvantages such as high cost and low yield. Moreover, asymmetric catalysis constitutes a very appealing approach (Ojima, 2010). Although the production of enantiopure compounds through asymmetric catalysis has been dominated by the use

of metal catalysis, other catalytic routes have also evolved including organocatalysis and Lewis acid catalysis (Pamies and Backvall, 2003).

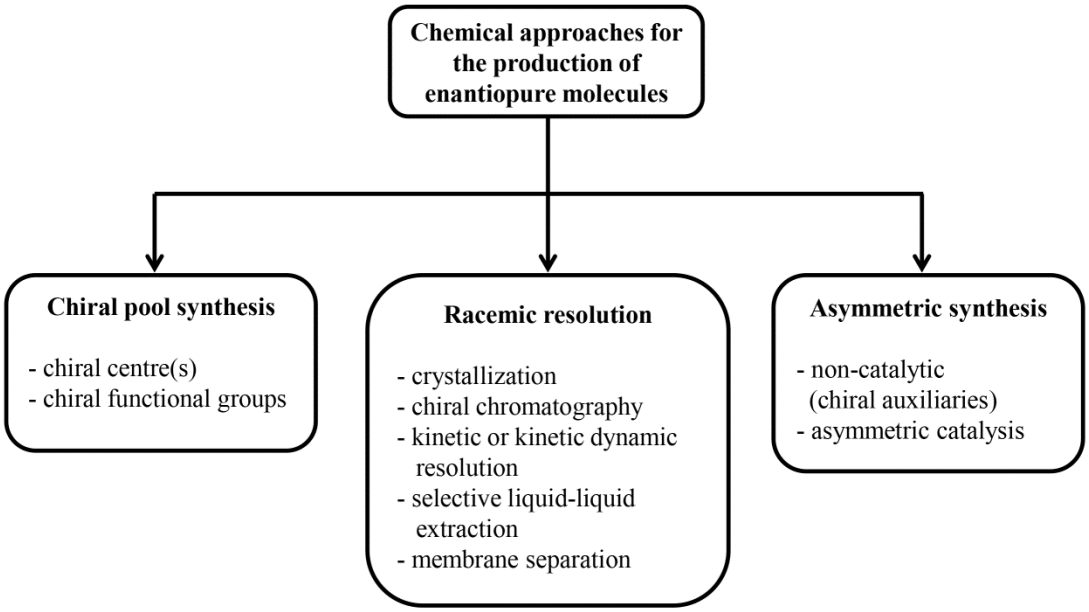

Figure 1.3: Main methods for the chemical production of enantiopure compounds.

1.1.2.2 Biological production of enantiopure molecules

1.1.2.2.1 Microbial production of pure enantiomers via chiral and racemic approaches

The use of whole cells and enzymes for the resolution of racemates and the synthesis of enantiomerically pure compounds from chiral and prochiral substrates has been well documented in the literature. Microbial and enzymatic production of single enantiomers is considered a promising technique based on environmental merits, as well as due to high efficiency, enantioselectivity and yield (Carvalho, 2011; Yuan et al., 2019). Thus, several technologies have been proposed for the manufacture of single enantiomers from a range of starting materials using microbial enzymes and cells. Kinetic resolution and dynamic kinetic resolution constitute methods of high importance for the biological production of enantiopure compounds from stereoisomeric mixtures (enantiomers or diastereomers). The application of kinetic resolution could provide enantiopure compounds at a yield not exceeding 50%, while dynamic kinetic resolution could

convert a racemate into a single stereoisomer completely with 100% theoretical yield (Risi et al., 2019). Moreover, optically pure compounds could be produced from prochiral substrates through desymmetrization and asymmetric synthesis with 100% theoretical yield (Wohlgemuth, 2010), while chiral pool components could be used as raw materials for the synthesis of single enantiomeric agents (Brill et al., 2017).

1.1.2.2.2 Enzymes applied for the production of enantiopure molecules

Biocatalysis allows green production of fine chemicals and pharmaceuticals at a higher yield, mainly due to low energy consumption and environmentally friendly operation (e.g. conducted in water, utilisation of low quantities of organic solvents) (Ahmad et al., 2009). Moreover, enzymes hold the capacity to manufacture enantiomerically pure compounds, often achieving over 99% enantiomeric excesses (ee), based on their high enantioselectivity (Ciriminna and Pagliaro, 2013). The main advantages of the application of enzymes in biocatalysis include specificity for certain reactions, the simple apparatus and procedures employed and in specific cases tolerance to the co-solvents used for dissolving substrates with low water solubility (Carvalho, 2011). Over recent years, a variety of robust and efficient processes have been developed, employing different types of enzymes for the production of compounds in a single enantiomeric form. Moreover, major advances enhancing the functional properties of enzymes have been achieved in the areas of enzymatic immobilization and protein engineering, producing biocatalysts with improved stability, enantioselectivity and activity (Basso and Serban, 2019). The enzymes most commonly explored for the production of enantiomerically enriched molecules include oxidoreductases, lipases and transaminases, while relevant studies also use peptidases, nitrilases, dehalogenases, hydrolases and lyases (Blamey et al., 2017).

Oxidoreductases, including dehydrogenases and oxidases, are widely employed as biocatalysts for the enantioselective production of optically pure chemical compounds (Patil et al., 2018; Y. G. Zheng et al., 2017). Alsafadi et al. (2017) reported that the halophilic alcohol dehydrogenase ADH2 synthesized by *Haloferax volcanii* (*Hv*ADH2) was capable of asymmetric reduction of several prochiral ketones into important enantiopure alcohols with high ee. The specific enzyme achieved >99.9% conversion of 2-fluoro-1-phenylethanol to (*S*)-2-fluoro-1-phenylethanol with excellent ee (>99%) (Fig 1.4 A). Moreover, *Thermoanaerobacter ethanolicus* secondary alcohol dehydrogenase

(TeSADH) mutant W110G demonstrated high resolution of racemic 4-(4′-hydroxyphenyl)-2-butanol, which corresponded to 99% ee of (*S*)-4-(4′-hydroxyphenyl)-2-butanol and >99.5% recovery (Fig 1.4 B) (Karume et al., 2016). Shang et al. (2017) indicated that the recombinant *Escherichia coli* ketoreductase SsCR from *Scheffersomyces stipitis* CBS 604 could asymmetrically reduce 2-chloro-1-(2,4-dichlorophenyl)ethanone into (*R*)-2-chloro-1-(2,4-dichlorophenyl)ethanol with 99% conversion and high ee (>99%) (Fig 1.4 C). Chiral alcohols constitute very important chemicals for synthetic organic and medicinal chemistry, given their wide use as valuable intermediates for the synthesis of several pharmaceutical agents including ezetimibe, fluoxetine and aprepitant. Furthermore, an engineered amine dehydrogenase from *Geobacillus stearothermophilus* (LE-AmDH-v1) was employed to perform the asymmetric reduction of prochiral ketones and kinetic resolution of racemic chiral amines to produce pharmaceutically important enantiopure amines, including sertraline, nor sertraline, rotigotine and rasagiline (Fig 1.4 D, E). The engineered enzyme (LE-AmDH-v1) achieved >98% conversion of aromatic ketones (comprising acetophenone, propiophenone and fluoroacetophenone) into the corresponding *R* enantiomeric amines with >99.7% ee (Tseliou et al., 2019). In addition, the same enzyme was capable of producing (*S*)-amines at high purity (>99% ee) through the kinetic resolution of several racemic amines, such as 1-phenylethylamine, 1-(4-fluorophenyl)ethanamine and 4-chromanamine (Tseliou et al., 2020). Enantiomerically pure 2-hydroxycarboxylic acids constitute multipurpose building blocks for the synthesis of numerous important products, including green solvents, fine and bulk chemicals as well as fuel precursors (Sheng et al., 2016). Thus, the use of D-lactate oxidase (D-LOX) from *Gluconobacter oxydans* 621H, which holds advanced properties (including great solubility, a wide range of substrates and high stereoselectivity), achieved enhanced resolution of racemic 2-hydroxycarboxylic acids into their *S*-enantiomeric form with ee >99% (Fig 1.4 F). Moreover, given that lignocellulose is the most widespread renewable resource worldwide and constitutes a major fraction of municipal, agricultural, forestry and industrial residues, biowaste has been previously applied for the manufacture of enantiopure products (Soccol et al., 2019). Li et al. (2015) demonstrated that (2R,3R)-2,3-butanediol dehydrogenase expressed in *Enterobacter cloacae* SDM achieved the production of (2R,3R)-2,3-butanediol from corn stover hydrolysate with high purity (>96.0%) and yield (95.0%).

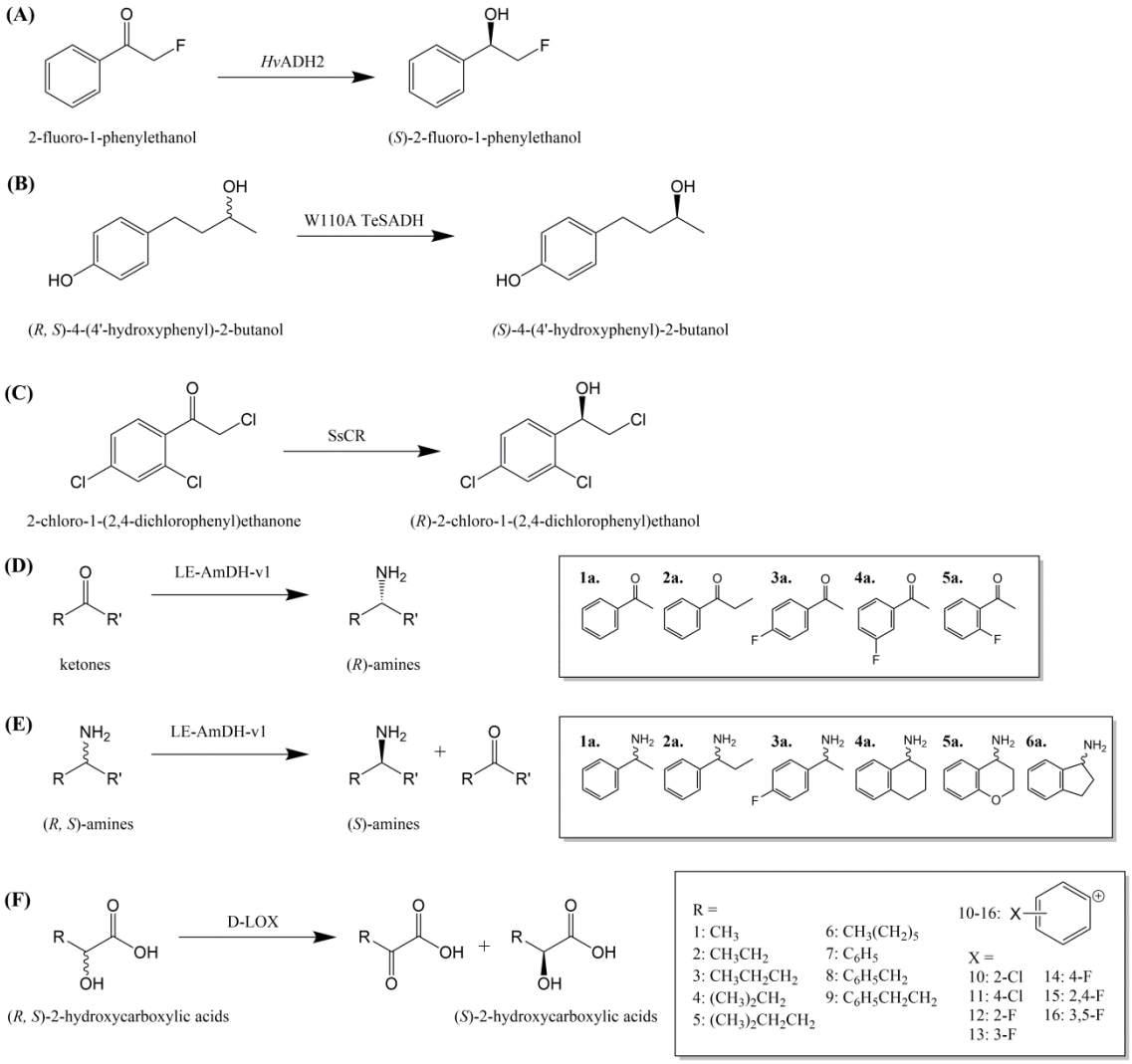

Figure 1.4: Production of enantiomerically pure molecules using oxidoreductases.

Lipases constitute a well-studied group of enzymes for the enantioselective preparation of several substrates including, among others, alcohols and amines (Gotor-Fernandez et al., 2006). Yuan et al. (2019) studied the application of a novel commercial lipase from *Rhizomucor miehei* Novozym 40086 immobilized on acrylic resin beads to perform resolution of (*R,S*)-ibuprofen. Although ibuprofen comprises a well-known anti-inflammatory and analgesic drug, the (*S*)-enantiomer demonstrates higher pharmacological activity as opposed to the corresponding (*R*)-enantiomer. The immobilized enzyme achieved 56% conversion of racemic ibuprofen, while the ee of (*S*)-ibuprofen was 94% (Fig 1.5 A). Moreover, *Burkholderia cepacia* lipase (BCL)

immobilized on phenyl-modified ordered mesoporous silica constitutes a potential biocatalyst for chiral resolution of alcohols (M. Zheng et al., 2017). Thus, immobilized BCL performed resolution of six secondary racemic alcohols (1-phenylethanol, 1-phenyl-1-propanol, 4-phenyl-3-buten-2-ol, 1-(2-naphthyl)ethanol, 1-(4-chlorophenyl)ethanol, 1-(4-bromophenyl)ethanol) achieving 50% conversion of the racemic alcohols tested and >99% ee of the corresponding S-enantiomer (Fig 1.5 B).

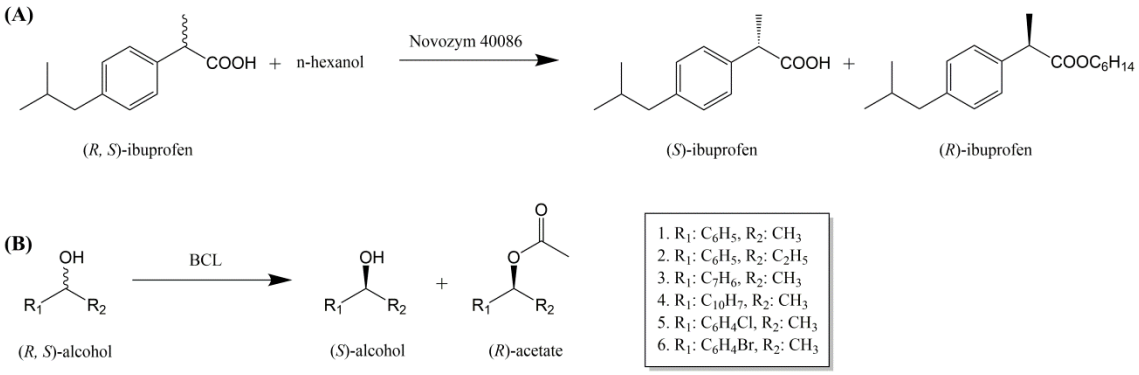

Figure 1.5: Production of enantiomerically pure molecules using lipases.

Transaminases constitute another important group of enzymes for the production of enantiomerically pure compounds exhibiting applications in different industries. Although phosphinothricin (also known as glufosinate) constitutes a commonly used herbicide due to advantages that include high efficiency, a wide range of applications, low toxicity and non-selectivity, only the L-enantiomer performs an herbicidal activity. Therefore, Jin et al. (2019) demonstrated that a new recombinant *E. coli* transaminase from *Pseudomonas fluorescens* ZJB09-108 (*Pf*-TA) could asymmetrically synthesise the active L-enantiomer of phosphinothricin from 4-(hydroxy(methyl)phosphoryl)-2-oxobutanoic acid with 79% yield and 99.9% ee of L-phosphinothricin (Fig 1.6 A). Moreover, the engineered ω-transaminase mutant Trp60Cys from *Chromobacterium violaceum* ($CvTA_{W60C}$) immobilized on bisepoxide-activated polymeric resin performed kinetic resolution of different pharmaceutically relevant racemic amines, such as 4-phenylbutylamine, 1-phenylethylamine, 1,2,3,4-tetrahydronaphthalen-1-amine and 2-heptanamine (Fig 1.6 B). The specific enzyme converted only the *S*-enantiomer of racemic amines, and thus (*R*)-amines remained in high enantiopurity (>96% ee) and significant concentration (Abahazi et al., 2018).

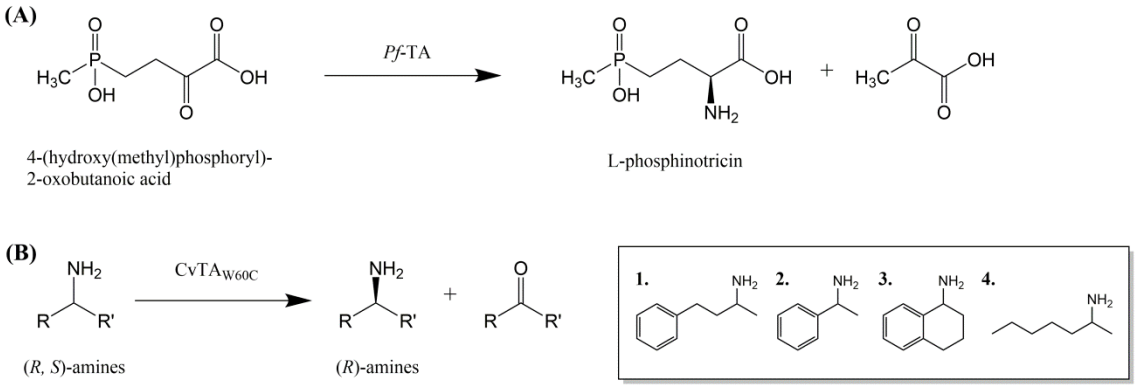

Figure 1.6: Production of enantiomerically pure molecules using transaminases.

Apart from the case studies presented above, several other enzymes hold the capacity to produce important enantiopure compounds. A novel D-aminopeptidase from *Brucella* sp. expressed in *E. coli* demonstrated resolution of racemic 2-aminobutanamide producing (*S*)-2-aminobutanamide, a significant chiral building block for the development of pharmaceutical compounds (Fig 1.7 A). The enantioselective peptidase enzyme achieved 50% conversion of racemic 2-aminobutanamide and high ee (>99%) of the *S*-enantiomer (Tang et al., 2018). Y.C. Zheng et al. (2017) reported that hydroxynitrile lyase isozymes from the sweet almond of *Pyrus communis* (also known as *Prunus dulcis*) expressed in *Pichia pastoris* (*Pc*HNL5) catalysed the asymmetric synthesis of several enantiomerically pure cyanohydrins, which constitute important building blocks for the chemical and pharmaceutical industries. Recombinant *Pc*HNL5 reached >96% conversion of different prochiral aromatic aldehydes to (*R*)-cyanohydrins with elevated optical purity (>99% ee) and excellent yield (>90%) (Fig 1.7 B). Moreover, the new epoxide hydrolase S*l*EH1 from *Solanum lycopersicum* expressed in *E. coli* achieved the production of enantiopure (*R*)-p-chlorostyrene oxide, an important building block for the synthesis of (*R*)-eliprodil, a neuroprotective agent for the treatment of stroke (Fig 1.7 C). The specific enzyme generated (*R*)-p-chlorostyrene oxide from its racemic form, in 98.2% ee and an overall yield of 45.3% (Hu et al., 2020). Xue et al. (2018) indicated that the new halohydrin dehalogenase (HHDH) from *Pseudomonas umsongensis* YCIT1612 expressed in *E. coli* achieved the kinetic resolution of racemic phenyl glycidyl ether to its (*S*) enantiomeric form in high ee (>99%) and 23.5% yield (Fig 1.7 D). Enantiomerically pure epoxides constitute

important building blocks for the manufacture of several medicinal products. (*R*)-(–)-mandelic acid, an important chiral building block used for the synthesis of several pharmaceutical intermediates, could be produced via the enantioselective biotransformation of racemic mandelonitrile in high purity (99% ee) employing nitrilases from different microorganisms, such as *Burkholderia cenocepacia* J2315 (Ni et al., 2013), *Alcaligenes* sp. MTCC 10675 (Bhatia et al., 2014) and *Aspergillus niger* CBS 513.88 (Petrickova et al., 2012; Shen et al., 2021) (Fig 1.7 E).

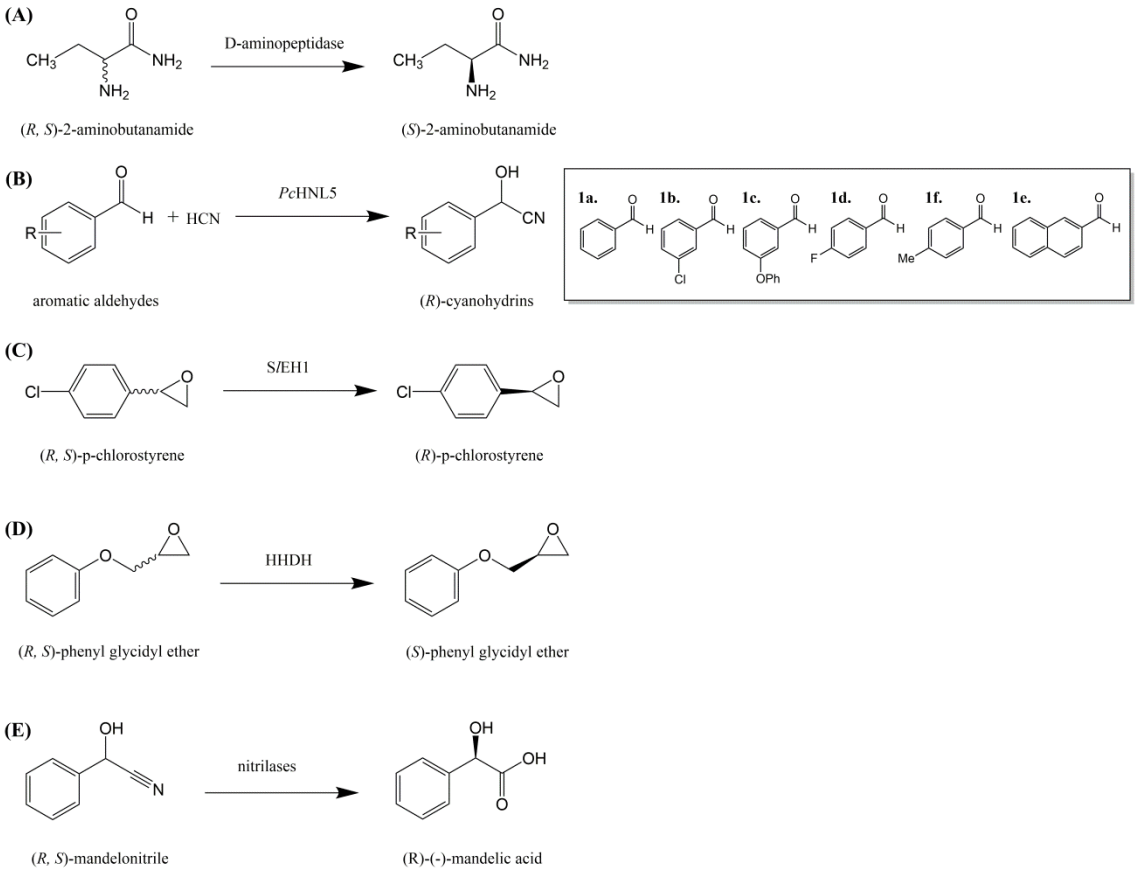

Figure 1.7: Production of enantiomerically pure molecules by different enzymes.

1.1.2.2.3 A selection of microbial methods for the production of pure enantiomers

Apart from employing enzymes for the production of enantiomerically pure compounds, whole cells could be also useful for the resolution of racemic mixtures or the synthesis of optically pure molecules. The use of whole cells entails numerous advantages including the provision of a natural environment that often supports the

required activity and functionality of enzymes preventing potential alterations in protein structure and promoting co-factor regeneration within the cell. Moreover, each microorganism can produce a wide range of enzymes depending on the growth conditions used and cellular development (Carvalho, 2011). Thus, several studies have focused on the production of optically pure compounds employing whole cells under different microbial approaches that include suspended, resting and immobilized cells. Those systems have been explored to produce chiral alcohols, carboxylic acids and sulfoxides among others.

Whole-cell biocatalysis can be employed for microbial production of optically active aromatic alcohols, generated as important chiral building blocks for the manufacture of various natural products and chiral drugs. While the chiral resolution of organic acids and bases could be achieved by chemical/physical methods (e.g. diastereomeric resolution), the separation of neutral racemates is more challenging and therefore whole-cell production of neutral enantiomers is of particular interest. Sahin (2019) demonstrated that *Lacticaseibacillus paracasei* BD87E6 constitutes a potential biocatalyst for asymmetric reduction of 1-(benzofuran-2-yl)-ethanone to (*S*)-1-(benzofuran-2-yl)-ethanol with high stereoselectivity (>99.9% ee) (Fig 1.8 A). Moreover, suspended cultures of *L. paracasei* BD101 performed asymmetric reduction of piperonyl methyl ketone to (*R*)-1-(1,3-benzodioxol-5-yl)-ethanol, which reached 89% yield and >99% ee *Candida zeylanoides* (Fig 1.8 B) (Sahin, 2018). Free cells of the yeast strain *Candida zeylanoides* P1 have been successfully applied in asymmetric reduction of 4-nitroacetophenone producing (*S*)-1-(4-nitrophenyl)ethanol with high yield (89%) and >99% ee (Fig 1.8 C) (Sahin and Dertli, 2017). Interestingly, the industrially important *Saccharomyces cerevisiae* (baker's yeast type 2) could be effectively used for the manufacture of enantiomerically enriched compounds, such as the case of *R*-citronellol production using geraniol, an achiral acyclic monoterpene (Fig 1.8 D) (Valadez-Blanco et al., 2008). Major building blocks, such as D-lactic acid and pyruvic acid holding a range of applications for the production of bioplastics as well as in the chemical, agrochemical and pharmaceutical sectors, could be generated using inexpensive racemic lactic acid as substrate in *Pseudomonas stutzeri* SDM fermentations (Fig 1.8 E). The bioprocess achieved biotransformation of racemic lactate to D-lactic acid with >99.5% ee, producing 25.2 g L^{-1} D-lactic acid and 19.7 g L^{-1}

pyruvic acid from 45 g L^{-1} of racemic lactate (Gao et al., 2009). Moreover, one of the most promising building blocks, L-aspartic acid, could be produced through microbial conversion of fumaric acid by various microorganisms (Choi et al., 2015; Yukawa et al., 2010). A comparative analysis of different strains (*E. coli*, *Klebsiella aerogenes*, *P. fluorescens*, *Pseudomonas aeruginosa*, *Bacillus megatherium* and *Bacillus subtilis*) holding the ability to form L-aspartic acid from fumaric acid demonstrated that *P. fluorescens* 6009-2 could produce pure L-aspartic acid with >85% yield (Fig 1.8 D) (Kisumi et al., 1960). (*R*)-2-hydroxybutyric acid, an important building block for the manufacture of biodegradable materials with medical, pharmaceutical and environmental applications, could be generated from 1,2-butanediol, a by-product formed during the production of 1,4-butanediol from butadiene (Hasegawa and Hayashi, 1986). Gao et al. (2012) reported that suspended cells of *G. oxydans* DSM 2003 achieved elevated conversion of 1,2-butanediol into (*R*)-2-hydroxybutyric acid at high concentration (18.5 g L^{-1}) and ee (99.7%) (Fig 1.8 G).

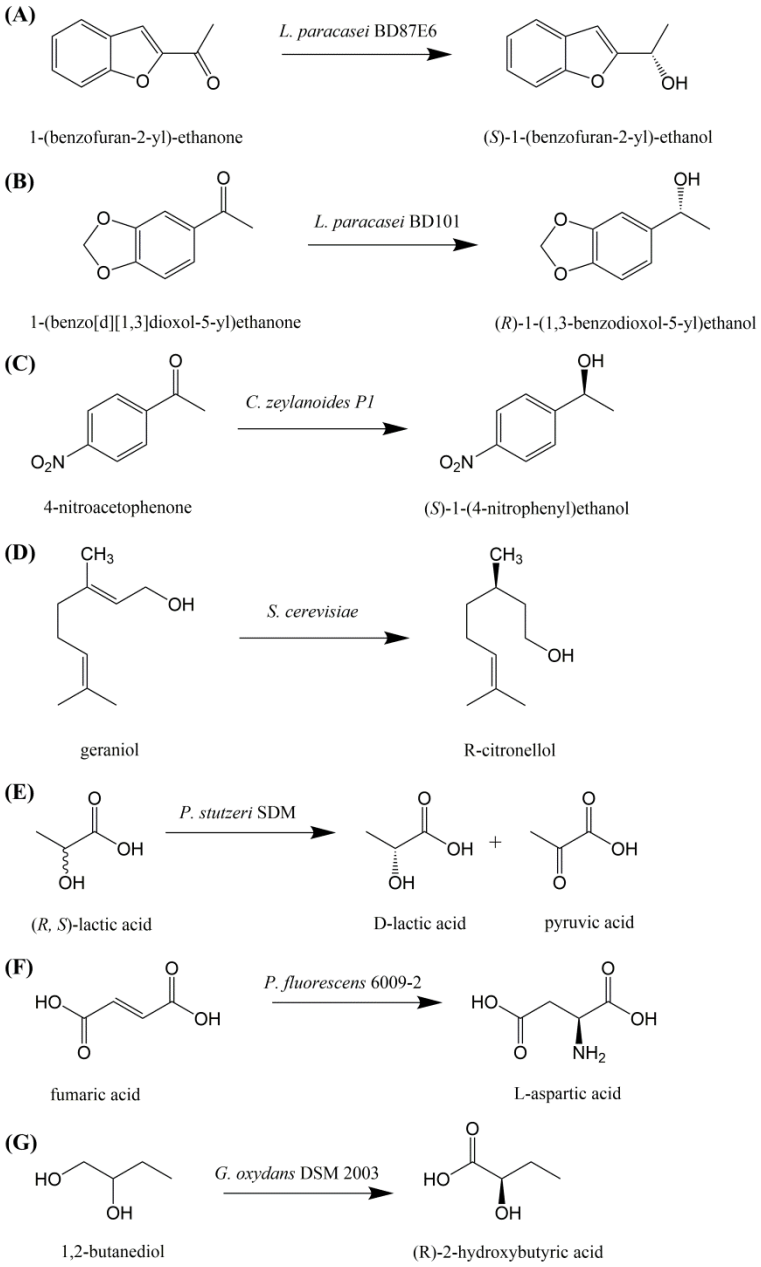

Figure 1.8: Production of enantiomerically pure molecules by free cells.

The use of resting cells constitutes an approach widely applied in biological processes for the manufacture of enantiomerically pure compounds, due to numerous advantages that include stable catalytic activity, simple and flexible operation, as well as ease of product isolation and purification (Sahin, 2019, 2018). Chiral sulfoxides constitute molecules exhibiting extensive applications as intermediates and auxiliaries, ligands and catalysts, as well as drugs. It has been previously reported that resting cells of *Rhodococcus* sp. CCZU10-1 achieved the efficient transformation of phenylmethyl

sulphide into (*S*)-phenylmethyl sulfoxide with ee >99.9% in an *n*-octane–water system under fed-batch conditions (Fig 1.9 A) (He et al., 2013). Moreover, He et al. (2008) demonstrated that (*R*)-(–)-mandelic acid, (*R*)-(–)-*o*-chloromandelic acid, (*S*)-(+)-*m*-chloromandelic acid and (*S*)-(+)-*p*-chloromandelic acid could be produced by their corresponding racemates achieving excellent ee (>99.9%) through use of *Alcaligenes* sp. ECU0401 resting cells (Fig 1.9 B). The aforementioned compounds comprise important chiral synthons applicable to the manufacture of several pharmaceuticals, including semi-synthetic penicillins, cephalosporins, antitumor and antiobesity agents.

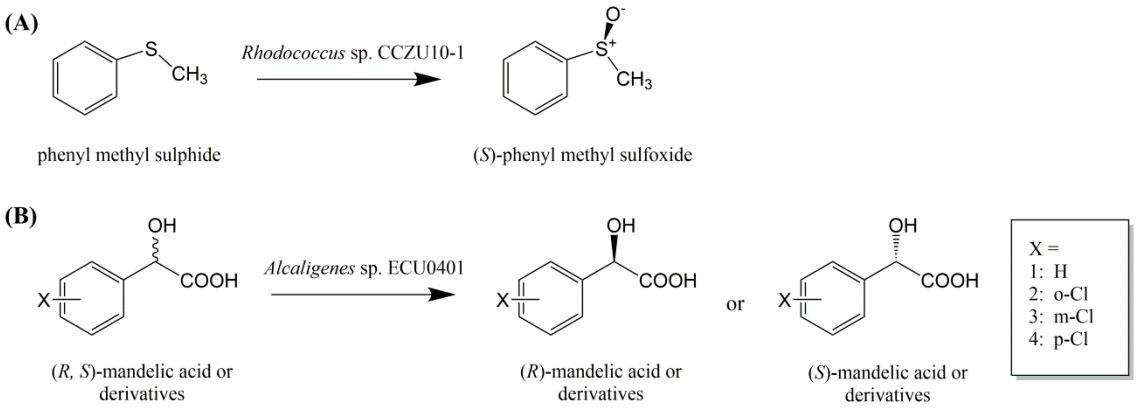

Figure 1.9: Production of enantiomerically pure molecules by resting cells.

Over the last years, immobilized cells have been commonly employed to produce different classes of chemical compounds in a single enantiomeric form. Immobilized cells of *A. niger* (GUFCC5443) and *E. coli* (ATCC9637) have been successfully applied in enantioselective degradation of racemic carvedilol to (*S*)-(–)-carvedilol. Cells entrapped into calcium alginate beads demonstrated 99% and 98% (*S*)-(–)-carvedilol ee respectively, following 10 d of cultivation (Fig 1.10 A) (Ettireddy et al., 2017). Although carvedilol constitutes a cardioprotective drug due to the adrenergic alpha and beta receptors' antagonistic action, the *S*(–) enantiomer exhibits affinity for the cardiac β1ARs, β2ARs and α1ARs, while the *R*(+) enantiomer acts as a pure α1AR-blocker. Thus, separation and use of enantiomerically pure carvedilol could result in administering lower doses for the treatment of high blood pressure and heart failure (Parker et al., 2018). Chaganti et al. (2008) demonstrated the production of lactic acid in its L enantiomeric form from carbohydrates using *Lactobacillus delbrueckii* cells enclosed in functionalized alginate beads, comprising succinylated and palmitoylated

alginate beads (Fig 1.10 B). Cells entrapped in the functionalized alginate beads achieved 99% ee, high product yield (1.44 and 1.74 $mol_{product}$ $mol_{substrate}^{-1}$ respectively) and 14 times lower by-product (e.g. acetic acid, propionic acid, ethanol) formation as compared to free cells.

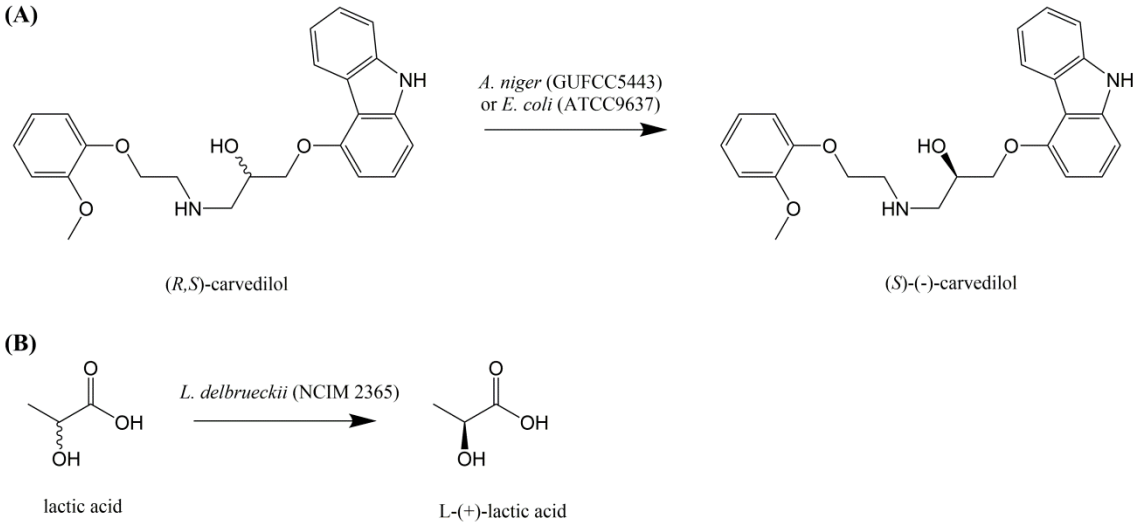

Figure 1.10: Production of pure enantiomers by immobilized cells.

1.1.3 Critical evaluation of biological and chemical approaches for the production of enantiopure molecules

Although various biological and chemical approaches have been used for the development of enantiomerically pure compounds, there is still no commonly applied method recommended to obtain chiral enriched molecules within the biorefinery context. Both biocatalysis and chemical conversion techniques incorporate advantages and disadvantages. Efficiency, applicability, productivity and environmental safety comprise some of the most important factors to determine process feasibility for industrial production of enantiopure molecules. A comparison of the prospects and limitations of the four major approaches (chemical catalysis, biocatalysis, chiral pool and chemical resolution) applied for industrial manufacture of enantiomerically pure or chiral enriched compounds was presented in Blaser et al. (2001), Blaser (2003) and Gumustas et al. (2018) (Table 1.2).

Table 1.2: Prospects and limitations of the main methods applied for the production of enantiopure or enantioenriched compounds.

	Chemical catalysis	**Biocatalysis**	**Chiral pool**	**Chemical resolution**
Enantioselectivity	1-2	1	1	1-2
Activity and productivity	1-2	2-3	-	-
Availability and diversity	1-2	2-3	2	1
Substrate specificity	2	3	1	1-2
Work-up and ecology	1-2	2-3	2	1-2
Development time and effort	2	3	1	1-2
Application in the lab	2	3	1	1-2
Application in development	1-2	2	1	2
Small-scale production	1-2	1-2	1	1-2
Large-scale production	1	2	2-3	1-3

Rating: 1: high prospect, 2: medium prospect, some problems, 3: low prospect, often problematic.

The biological resolution of racemates, as well as the biocatalytic synthesis of enantiopure molecules, often provides numerous advantages as compared to chemical methods comprising relatively green technologies that entail energy and cost savings. In general, biological processes can be conducted in water using mild conditions, such as ambient temperature and neutral pH, without the requirement for large quantities of organic solvents or expensive equipment (Ahmad et al., 2009). Moreover, the enzymatic kinetic resolution has been extensively employed due to various favourable characteristics that include high stereoselectivity and stability, broad substrate specificity, enantioselectivity and reactivity, while the process is usually easy to apply industrially operating in continuous mode (Yuan et al., 2019). Nevertheless, enzymatic resolution incorporates disadvantages that include enzyme activity reduction, narrow application range, low efficiency and decreased number of transfer units per apparatus (Mane, 2016), as well as the prolonged period needed to identify and develop an efficient biocatalyst (Gumustas et al., 2018). Another disadvantage is derived from the need to separate the enzymatic chiral products (e.g. chiral alcohol and chiral ester). Although chromatographic methods can be very efficient to achieve the specific separation, they are rather challenging for large scale applications. To circumvent this limitation, other separation processes have been described such as distillation (Monteiro et al., 2010), polymer-supported substrates (Okudomi et al., 2010), extractions (fluorous medium (Luo et al., 2002), ionic liquids (Gaalova et al., 2020; Ke et al., 2021), eutectic mixtures (Maugeri et al., 2012), supercritical CO_2 (Paiva et al., 2011)) including specific acylating agents such as ionic (Lourenco et al., 2010; Lourenco and Afonso, 2007; Rocha et al., 2017), fatty acid and polyethylene glycol (PEG) (Monteiro et al., 2015) that facilitate the liquid-liquid extraction separation process.

The application of enzymatic dynamic kinetic resolution provides the important benefit to use both enantiomers from the racemate when targeting 100% resolution yield (instead of 50%) of only a single enantiomer. However, besides the high success in this area (Habulin and Knez, 2009; Reetz et al., 2003) the need for simultaneous efficient enzymatic resolution and effectively catalysed racemization (mainly metal-based catalyst) that are compatible with enzymatic reaction conditions, currently limits the large scale and substrate scope applications. In this line, the use of an exclusive

enzymatic dynamic kinetic resolution approach may circumvent some of the limitations derived from the use of non-enzymatic resolution steps (Musa, 2020).

Although the chiral resolution of chiral organic acids or bases is usually possible through the formation of diastereomeric salts and their separation, the chiral resolution of neutral molecules usually includes chemical derivatisation followed by separation and further chemical modification. Therefore, it would be interesting to illustrate the discussion pertinent to the advantages and limitations of biological and chemical routes by employing specific examples where such routes are compared in manufacturing the same product. Herein, the comparison of enzymatic resolutions against either diastereomeric resolution by recrystallization to produce a γ-amino acid or asymmetric synthesis of ketones into chiral alcohol was selected. The example of enantiomerically pure lactic acid production is provided to highlight the superiority of the fermentative route.

A comparative review of the classical and biocatalytic resolution methods available for the development of (*S*)-pregabalin, a medication applied to treat different nervous system disorders (e.g. epilepsy, neuropathic pain and generalized anxiety disorder) has been presented in Dunn et al. (2010). In the classical resolution route, racemic cyanodiester was chemically transformed into (*S*)-pregabalin. The specific route started with hydrolysis and decarboxylation of racemic cyanodiester to β-cyano acid, followed by subsequent reduction of β-cyano acid to racemic pregabalin using Raney nickel. Finally, racemic pregabalin formed a diastereomeric salt with (*S*)-mandelic acid, which was split with wet tetrahydrofuran under neutral conditions to produce (*S*)-pregabalin (Fig 1.11 A). Nevertheless, the enzymatic resolution of racemic cyanodiester to (*S*)-pregabalin was achieved through the action of a lipase synthesised by *Thermomyces lanuginosus*, known as Lipolase (Fig 1.11 B). The study has shown that although the classical route had reduced 12 times the cost of a previously established discovery route that required long synthesis, the enzymatic route employed fewer input materials and energy, which corresponded to a reduction of 80-85% and 82% respectively, as compared to the classical resolution process (Fig 1.11 C, D).

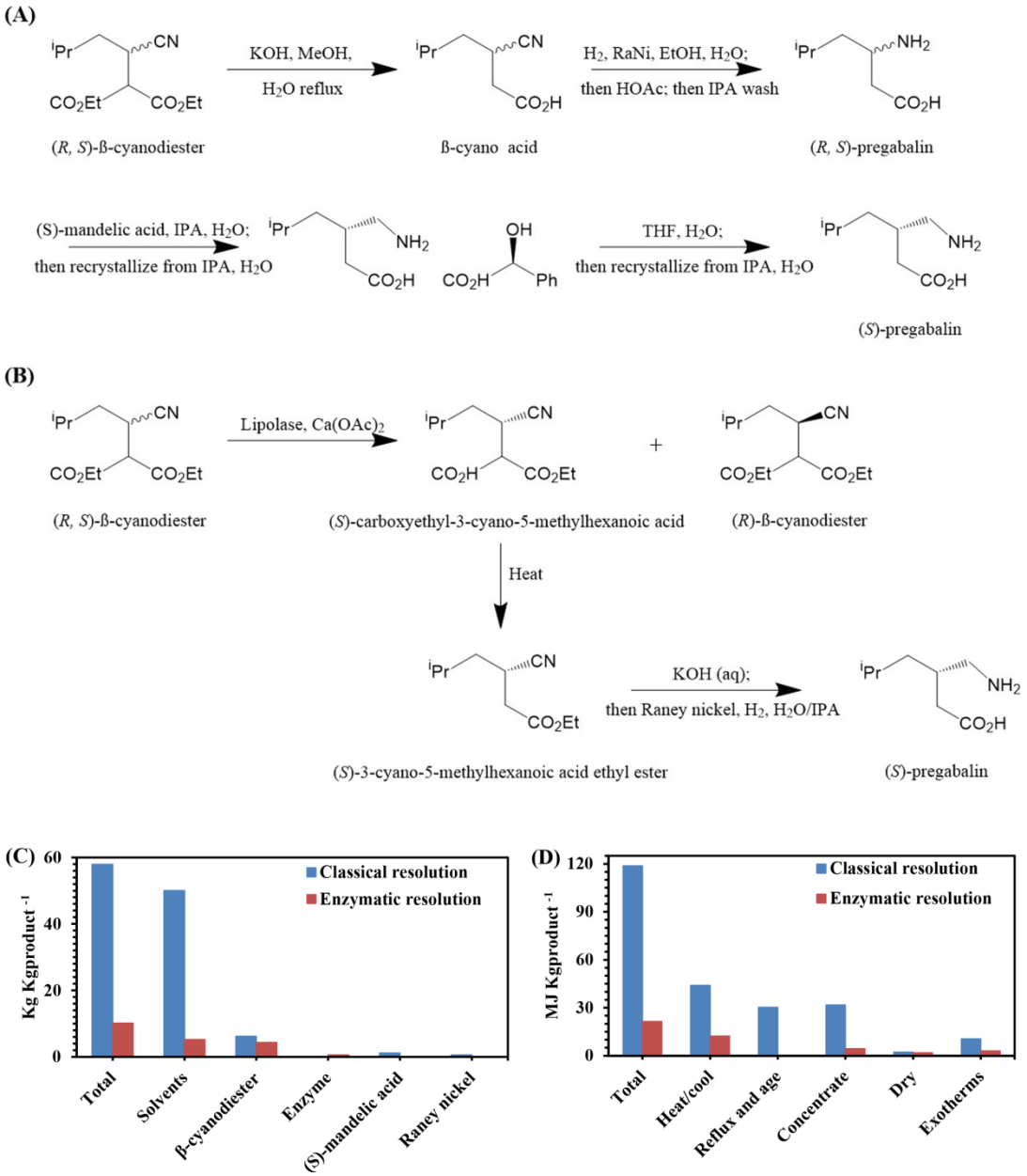

Figure 1.11: Transformation of racemic cyanodiester to (*S*)-pregabalin via (A) classic resolution and (B) enzymatic resolution, and quantity of (C) input materials (expressed as Kg $Kg_{product}^{-1}$) and (D) energy (expressed as MJ $Kg_{product}^{-1}$) used for the production of (*S*)-pregabalin different resolution methods.

The chemical asymmetric ketones reduction by (–)-B-chlorodiisopinocampheylborane ((–)-DIP-Cl) to enantiopure alcohols as opposed to the biocatalytic alternative available by KetoREDuctase (KRED) has been previously explored (Liang et al., 2010). The findings demonstrate that both methods could achieve high optical purity (>99% ee) and yield. However, the (–)-DIP-Cl process required a 25% higher volume of organic solvents, as compared to the KRED bioprocess, and further purification to achieve the desirable enantiopurity. Moreover, Martinkova and Kren (2018) indicated that the dynamic kinetic resolution of mandelonitrile and its analogues to produce (*R*)-mandelic acid or (*R*)-2-chloromandelic acid by nitrilases could serve as a promising alternative to chemical processing. Overall, the benefits identified for the use of biocatalytic reactions include mild process conditions and easy handling, as well as the requirement for small quantities of organic solvents and the production of small volumes of waste. Nevertheless, the chemical catalysis methods developed to demonstrate higher robustness and lower sensitivity to substrate variations as opposed to enzymatic routes.

Enantiomerically pure lactic acids constitute chemical compounds of great importance due to versatile applications, mainly in chemical, pharmaceutical, cosmetic, agriculture and food industries (Ding et al., 2018; Gali et al., 2021), which can be produced through different chemical and biological approaches. D-(–)-lactic acid and L-(+)-lactic acid could be produced via several chemical processes such as chemical synthesis (Sara et al., 2016) or racemic resolution using membrane processes (Boonpan et al., 2013; Hadik et al., 2002), molecular imprinting technology (Huang et al., 2018), chromatography (Henry et al., 2012) and capillary electrophoresis (Saavedra and Barbas, 2002). The chemical production of lactic acid is based on petrochemical resources such as acetaldehyde and hydrocyanic acid, thus 70–90% of the annual worldwide production of lactic acid is achieved by biological processes (Klotz et al., 2016). The biological route for the production of enantiopure lactic acid is enabled through fermentation of low-cost substrates, such as agricultural residues and renewable feedstocks, by *Lactobacillales* and other bacterial strains (Table 1.3). However, the microbial route for fermentative enantiomerically pure lactic acid production also involves challenges, including the production of undesirable by-products (Fan et al.,

2009; Martinkova and Kren, 2018) and the necessity for further precipitation, chromatographic and distillation steps to purify the product.

Table 1.3: Enantiomerically pure lactic acid production on various agricultural residues, wastes and by-products.

Substrate	**Microorganism**	**Purified lactic acid enantiomer**	**Reference**
Sugar cane molasses	*Lactobacillus casei MTCC 1423 immobilized*	L	Thakur et al. (2019)
Soybean vinasse	*Lactobacillus agilis* LPB 56	L	Karp et al. (2011)
Turmeric waste	*L. paracasei*	D	Nguyen et al. (2013)
Brewer's spent grain	*Lactobacillus rhamnosus ATCC 7469*	L	Pejin et al. (2018)
Chicory flour	*Lactobacillus bulgaricus* CGMCC 1.6970	D	Zheng et al. (2018)
Sweet sorghum bagasse	*Bacillus coagulans* LA1507	L	Wang et al. (2016)
Coffee mucilage and pulp	*B. coagulans*	L	Neu et al. (2016); Pleissner et al. (2016)
Cassava starch	*B. coagulans* WCP10-4	L	Ooi and Wu, (2015)
Municipal solid waste	*B. coagulans* A166	L	Lopez-Gomez et al. (2020)
Xylo-oligosaccharides manufacturing waste	*Rhizopus oryzae*	L	Zhang et al. (2015)
Raw potato starch	*G. stearothermophilus* DSM494	L	Smerilli et al. (2015)
Wheat bran	*Sporolactobacillus inulinus* YBS1-5	D	Li et al. (2017)

1.1.4 Perspectives for circular bioeconomy

Sustainability constitutes one of the most urgent challenges of our century. Thus, the development of successful circular bioeconomy concepts could facilitate the development of environmental quality, economic prosperity and social equity for the current and future generations (D'Amato et al., 2017). The circular bioeconomy combines the concept of sustainable consumption of natural resources and their sustainable management. The latter includes the enhancement of resource recovery and recycling, as well as the concept of renewable biological resources' valorisation (non-edible feedstocks and biogenic waste) to produce a range of products, such as biofuels, biochemicals, bioenergy, biomaterials and other high-value bioproducts (Mohan et al., 2016; Santana et al., 2002). Moreover, biorefineries developed using various biomass feedstocks, including lignocellulosic biomass, algae, and numerous waste types could be central for circular bioeconomy advancement (Hopper et al., 1991; Ubando et al., 2020). To illustrate the potential implementation of the above-mentioned concepts when targeting the production of enantiomerically pure or enriched compounds, different examples have been selected in the present study.

Racemic and enantiopure lactic acid constitute major chemical products demonstrating an extensive range of applications in numerous industries. Commercially, lactate can be employed in the food industry as an acidity regulator, flavour enhancer, as well as improving and preserving agent (Ameen and Caruso, 2017). Moreover, lactic acid can be also employed in cosmetic, textile, paper, chemical and pharmaceutical industries (Cubas-Cano et al., 2012). The lactate molecule contains a chiral carbon and it could exist either as a racemate of D-(–)-lactic acid and L-(+)-lactic acid or in the form of single enantiomers. Each enantiomer provides different physical properties to the end product, thus the enantiomeric purity of lactic acid is crucial for the development of specific industrial applications (Oliveira et al., 2018). Over the past decades, L-(+)-lactic acid has stimulated extensive interest as feedstock for the synthesis of poly-L-lactic acid (PLA), a biodegradable and environmental friendly biopolymer, which could be used as an alternative to traditional petrochemical-based plastics (Gawali et al., 2017; Ritter, 2017).

From the circular bioeconomy perspective, various studies have shown that different solid waste and wastewater streams from the industrial and municipal sectors could be employed to produce high-value enantiomerically pure compounds including lactic acid. Lopez-Gomez et al. (2020) reported that the organic fraction of municipal solid waste (OFMSW) could serve as a promising substrate for L-(+)-lactic acid production. The results demonstrated that *B. coagulans* A166 achieved 51.5% racemic lactic acid recovery and 98.7% optical purity of L-(+)-lactic acid following fermentation of pretreated OFMSW. Moreover, *Lactobacillus* species have been extensively applied to produce D-(–)-lactic acid from renewable feedstocks, including pulp mill residue, corn stover, corn cob residue and dairy waste. Therefore, resting cells of *L. delbrueckii* ssp. *delbrueckii* CECT 286 could produce D-(–)-lactic acid with high optical purity (>95%) from an orange peel waste hydrolysate (Torre et al., 2020). Citrus peel waste constitutes an abundant, renewable and inexpensive resource comprising a significant candidate to produce enantiopure lactic acid due to the high sugar content entailed (Torre et al., 2019a). Moreover, citrus peel waste biorefineries could be developed aiming to produce enantiomerically pure lactic acid as well as several other extractable products that include essential oils, pectin (Patsalou et al., 2020), polyphenols (Tsouko et al., 2020) and flavonoids (Torre et al., 2019b), demonstrating a multitude of applications in the food and beverage sector as additives, improving the characteristics and properties of the products manufactured (Neri-Numa et al., 2020; Ozturk et al., 2018; Patsalou et al., 2017). Thus, the development of an integrated biorefinery exploiting citrus peel waste for the production of enantiopure compounds as well as other biomolecules could assist the development of a circular bioeconomy.

Epichlorohydrin is an interesting building block constituting a precursor for the production of epoxy resins and glues, plastics, paints, and biologically active compounds (Jin and OuYang, 2015; Kumar et al., 2016). Thus far, epichlorohydrin was produced in a racemic mixture mainly by chemical synthesis using propene and chlorine (Abraham and Hofer, 2012; Bijsterbosch et al., 1994). However, a novel method of producing racemic epichlorohydrin from glycerol, a renewable feedstock obtained as a biodiesel production by-product, has been developed (Kraff et al., 2017; Pagliaro, 2017; Santacesaria et al., 2010; Simola and Iosco, 2012).

The enantiomeric purity of drugs comprises a very sensitive issue (Kim and Scialli, 2011; Therapontos et al., 2009), thus the production of enantiopure epichlorohydrin is crucial for its application as a building block for the synthesis of active pharmaceutical ingredients (Szekely et al., 2015). The chiral resolution of racemic epichlorohydrin has been mainly achieved by chemical methods, employing hydrolytic kinetic resolution using Co(III)-salen salts as catalysts, which are claimed to be expensive, demonstrating efficient enantioselectivity with >99% ee and >45% yield (Key et al., 2013; Larrow et al., 2003). Although enzymatic based approaches for the preparation of enantiomerically pure epichlorohydrin have been also pursued by kinetic resolution (Jin and OuYang, 2015), Jin et al. (2013) reported that *Agrobacterium radiobacter* epoxide hydrolase (ArEH) expressed in *E. coli* demonstrated resolution of racemic epichlorohydrin producing (*R*)-epichlorohydrin with ≥99% ee and 42.7% yield. Moreover, *Agromyces mediolanus* ZJB120203 epoxide hydrolase (AmEH) mutant W182F/S207V/N240D expressed in *E. coli* achieved high resolution of racemic epichlorohydrin, which corresponded to >99% ee of (*R*)-epichlorohydrin and 45.8% yield (Xue et al., 2015). Thus, the use of a renewable feedstock for the production of enantiopure epichlorohydrin and its wide application in different industrial sectors highlights the potential to develop a sustainable circular bioeconomy concept.

1.2 Production of added-value molecules from lupin beans processing industries wastewater

1.2.1 Properties and processing of lupin beans

The rapidly growing world population has stimulated the need to explore alternative protein sources, including cereals and legumes like soya (*Glycine max*), lupin (*Lupinus albus*), quinoa (*Chenopodium quinoa*) and hemp (*Cannabis sativa*) (Pihlanto et al., 2017). *L. albus* L. is an agronomically and commercially important legume species of the genus *Lupinus* in the family *Leguminosae* (or *Fabaceae*) (Annicchiarico et al., 2014). *L. albus* constitutes an annual plant cultivated in the Mediterranean region as well as in Egypt, Sudan, Ethiopia, Syria, Central and Western Europe, the United States of America and South America, and Tropical and Southern Africa. Also, *L. albus* is widely spread like a wild plant throughout the southern Balkans, the Italian islands of Sicily and Sardinia, the French island of Corsica and the Aegean Sea, as well as in Palestine and western Turkey (Boschin and Resta, 2013). According to FAO, the global lupin production constituted over 1×10^6 t in 2018, while the global production of lupin seeds was over 1.2×10^6 t in 2016 (Schrenk et al., 2019). The lupins and lupin seeds included in the annual compilation of statistics covered comprise *L. albus* (white lupin), *Lupinus angustifolius* (narrow-leafed lupin), *Lupinus luteus* (yellow lupin) and *Lupinus mutabilis* (Andean lupin).

Like other legumes, *L. albus* seeds (lupin beans) are commonly employed as livestock feed (Chiofalo et al., 2012). Studies focused on the application of lupin beans as animal feed show that the use of the specific beans as supplementary in non-ruminants (e.g. poultry and pigs) and ruminants (e.g. sheep) diet cause a positive outcome (Beyene et al., 2014; Prandini et al., 2005; Tadele, 2015). Nevertheless, these beans are important for the human diet, comprising a nutritional product with several applications in the production of existing or novel food products (Jana et al., 2020; Lopez-Cabeza et al., 2017). Lupin beans are commonly consumed as a snack food and they have been gaining increasing interest for application as a protein-rich source and food ingredients for the manufacture of bakery and pastry products, pasta and baked snacks (Magalhaes et al., 2017). Moreover, lupin beans are used as a dairy and meat analogue as well as coffee and egg substitute (Lim, 2012; Yaver and Bilgicli, 2021).

Lupin beans typically consist of 33-47% proteins, 6-13% oils (Kahnt and Hijazi, 1987; Pihlanto et al., 2017), 34-39% dietary fibres (Yorgancilar and Bilgicli, 2012), 0.02-12.73% quinolizidine alkaloids (Kroc et al., 2017) and small amounts of minerals and bioactive compounds. The protein content of *L. albus* seeds comprises 40% of essential amino acids (lysine, methionine, cysteine, threonine, isoleucine, tryptophane, valine, leucine, histidine, phenylalanine, tyrosine) and 60% of non-essential amino acids (arginine, aspartate, serine, glutamate, proline, glycine, alanine) (Sujak et al., 2006). According to Erbas et al. (2005), the oil content of lupin seeds constitutes 13.5% saturated (palmitic acid, stearic acid), 55.4% monounsaturated (oleic acid) and 31.1% polyunsaturated (linoleic acid, linolenic acid) fatty acids, while dietary fibres comprise monosaccharides and Oligosaccharides, including sucrose (70.7%), galactose (8.4%), glucose (6.7%), ribose (5.8%), maltose (5.1%), fructose (2.8%) and xylose (0.6%). Lupin seeds contain also vitamin E (α-, γ- and δ-tocopherols), vitamin B (thiamine, riboflavin and niacin) and vitamin C (Erbas et al., 2005; Frias et al., 2005). The inorganic content of lupin seeds constitutes phosphorus (P), potassium (K), calcium (Ca), magnesium (Mg), iron (Fe), manganese (Mn) and zinc (Zn) (Yorgancilar and Bilgicli, 2012). Moreover, the varieties of *L. albus* with favourable agronomic characteristics contain toxic quinolizidine alkaloids (Carmali et al., 2010). Kroc et al. (2017) documented that the main quinolizidine alkaloids of white lupin comprise lupanine (76.06%), 13-hydroxylupanine (8.23%), multiflorine (5.52%), albine (4.48%), angustifoline (2.07%) and 11,12-seco-12,13-didehydromultiflorine (formerly *N*-methylalbine) (1.74%), as well as low amounts of α-isolupanine, sparteine and different esters of 13α-hydroxylupanine (Annicchiarico et al., 2014; Musco et al., 2017).

Besides the application of lupin beans in the food industry, different compounds derived from lupin beans have stimulated interest for application as ingredients in cosmetic, medical and pharmaceutical products. Amino acid and fatty acid oils derided from lupin beans are used in several cosmetic products, including skin, facial, body and baby care products (Burnett et al., 2014, 2017b, 2017a). Moreover, lupanine, the main quinolizidine alkaloid present in lupin beans, constitutes a valuable molecule exhibiting several applications in pharmaceutical/medical, agricultural and chemical sectors.

1.2.2 Alkaloid compounds as renewable feedstocks for the production of added-value commodities

Alkaloids constitute natural compounds, which incorporate a characteristic ring structure and a nitrogen atom (Mahajan et al., 2010). These molecules occur in certain plant families as well as different bacteria and fungi species. Moreover, alkaloids appear in terrestrial animals, including insects, amphibians, reptiles, birds, mammals and marine animals, such as sponges, asteroids, tunicates, scleractinians and dogfish sharks (Cushnie et al., 2014). Alkaloids are characterized by diverse and complex structures and thus no specific taxonomic principle currently exists for their classification. Nevertheless, the specific natural compounds could be classified based on their biological and ecological activity (bioecological classification), use in chemical and technological innovations (chemotechnological classification), chemical structure (chemo-molecular classification) and biosynthetic pathway (biosynthetic shape-classification) (Table 1.4) (Aniszewski, 2015a).

Table 1.4: Classification of alkaloids.

Bioecological classification
neutral or weakly basic molecules, animal-derived alkaloids, marine alkaloids, moss alkaloids, fungal and bacterial alkaloids, nonnatural alkaloids
Chemotechnological classification
natural alkaloids, biomimetic and bionic alkaloids, synthetic alkaloids
Chemo-molecular classification
acridones, aromatics, bisindoles, carbolines, diterpenes, ergots, ephedras, imidazoles, indoles, indolizidines, manzamines, oxindoles, phenylethylamines, phenylisoquinolines, piperidines, purines, pyrrolidines, pyrrolizidines, pyrrolidones, pyridines, quinolines, quinolizidines, quinazolines, sesquiterpenes, simple tetrahydroisoquinolines, steroids, terpenoids, triterpenes, tropanes.
Biosynthetic shape-classification
true alkaloids, protoalkaloids, pseudoalkaloids

Alkaloids constitute an important group of chemical intermediates and products exhibiting applications in different sectors including chemical, medical, pharmaceutical, food and agricultural industries. In the medical sector, alkaloids include several uses as agents to regulate cell membrane Na^+ ions and channels, as well as regulators of several membrane cell receptors, including muscarinic cholinergic, glycine and opioid receptors. They are used for the regulation of microtubules of the spindle apparatus as well as microbial, schizonticide and antiproliferative activity. Moreover, alkaloids exhibit a range of other medical applications (Aniszewski, 2015b), which has led to the production of important pharmaceutical components (Khalil, 2017). Over the years, several plants and livestock products containing alkaloids have been used for humans as food and beverages. Alkaloids, of different types, are often present in fruits (e.g. blueberries, pineapple and apple), vegetables (e.g. tomatoes, potatoes, aubergines, corn and carrot), nuts (e.g. peanuts, hazelnuts and almonds), legumes (e.g. white lupins) and cereals (e.g. rice, wheat and millet). Besides, animal products such as honey, eggs and milk are known to contain alkaloids, the specific molecules are also contained in several beverages including herbal teas and coffee (Koleva et al., 2012). Furthermore, some alkaloids, including caffeine and quinine, can be used as food additives in soda and energy drinks, as well as other food products (Tan et al., 2018; Y. Wang et al., 2015). Alkaloids usually impart a bitter taste, while they may cause toxic effects on humans and animals when consumed above the daily recommended threshold. In the agricultural industry, alkaloids hold applications as biofertilizers in ecological cultivations of different crops including cereals, legumes, tubers and vegetables (Cushnie et al., 2014; Mahajan et al., 2010), while they could be also used in plant protection as pesticides in organic farming due to their fungicidal, insecticidal and herbicidal activity (Ji et al., 2018; Lopez-Cabeza et al., 2017; Yang et al., 2020). Moreover, based on their distinct chemical structure several alkaloids exhibit different chemical uses including the synthesis of valuable molecules. Recent studies have shown that a high-value molecule that could be synthesised via dearomatization/enantioselective borylation of pyridine alkaloids constitutes the production of paroxetine, a 3,4-disubstituted piperidine compound employed in the pharmaceutical industry as an antidepressant (Koleva et al., 2012; Temple et al., 2017). However, many other opportunities currently exist for the manufacture of building blocks of interest for the pharmaceutical industry from alkaloids.

1.2.2.1 Quinolizidine alkaloids: Lupanine

Quinolizidine alkaloids comprise secondary metabolites that occur mainly within the family *Leguminosae* in the genus *Lupinus*, *Baptisia*, *Thermopsis*, *Genista*, *Cytisus*, *Echinosophora* and *Sophora* (Frick et al., 2017). These lysine-derived alkaloids are biosynthesized in the green tissues of the plant and stored in all plant organs. Quinolizidine alkaloids are important for the survival of plants acting as a defence mechanism against pathogens (fungi, bacteria and viruses) or predators, including insects, slugs, vertebrates and herbivorous animals (Wink, 2019). Moreover, they constitute allelopathic metabolites for competition with other plant species (Bunsupa et al., 2013), while serving as nitrogen reserves in plants (Boschin and Resta, 2013). Quinolizidine alkaloids constitute a type of true alkaloids and involve a chemical structure that is based on the quinolizidine nucleus or pyridone nucleus. Alkaloids with a quinolizidine nucleus can be divided into bicyclic alkaloids (e.g. lupanine, epilupinine and lusitanine), tricyclic alkaloids (e.g. angustifoline and albine) as well as tetracyclic alkaloids (e.g. sparteine and lupanine) (Aniszewski, 2015c).

Tetracyclic lupanine constitutes an important quinolizidine alkaloid formed by two quinolizidine rings and a carbonyl group on the first carbon of the first ring (Boschin and Resta, 2013). In nature, lupanine can occur in two enantiomeric forms, D-(+)-lupanine and L-(–)-lupanine (Fig 1.12). The existence or proportion of each enantiomer is variable in different plant species and even in different cultivars of the same plant, meaning that the ee depends on the genotype and environmental factors of the species origin (Annicchiarico et al., 2014; Boschin et al., 2008; Finefield et al., 2012). Lupanine is one of the most abundant quinolizidine alkaloids in *Lupinus* species (Fig 1.12) (Magalhaes et al., 2017). D-(+)-lupanine occurs in *L. polyphyllus*, *L. angustifolius*, *L. rotundiflorus*, *L. exaltatus*, *L. mexicanus*, *L. montanus*, *L. madrensis* and *L. elegans*, while L-(–)-lupanine occurs only in *L. pusillus* and *L. macouni*. In *L. termis* and *L. albus*, lupanine occurs in an enantiomeric mixture enriched with the D-(+)-lupanine isomer (Carmali et al., 2010; Przybyl and Kubicki, 2011).

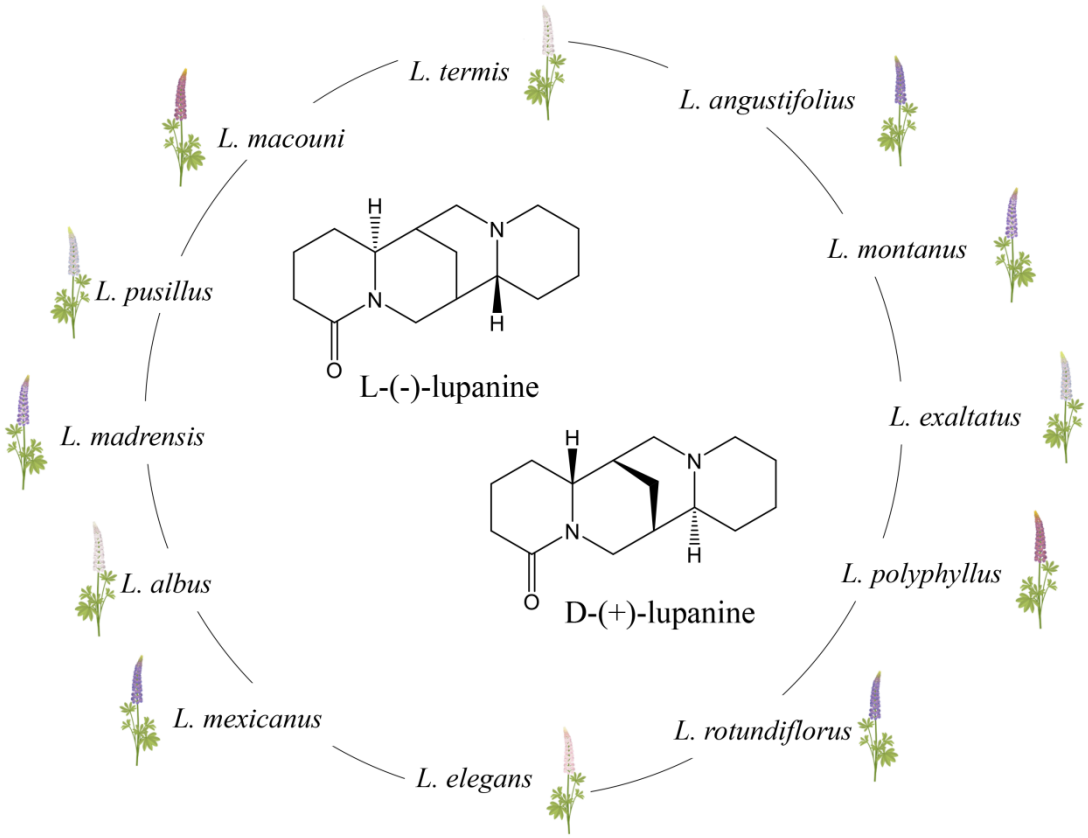

Figure 1.12: Lupanine enantiomers (D-(+)-lupanine and L-(–)-lupanine) and the main *Lupinus* species containing lupanine.

The literature relevant to the intoxication in humans following consumption of lupin beans showed that lupanine can affect the nervous, gastrointestinal and cardiovascular systems. Moderate cases of intoxication demonstrate mydriasis, dizziness, nausea, dryness of the mouth, stomach aches, vomiting, diarrhoea and/or cardiac problems, while in severe cases of intoxication prominent tiredness accompanied by muscular paralysis and convulsions occurs. Death can occur by respiratory paralysis or cardiac arrest as well as choking (Koleva et al., 2012). Thus, Health Authorities of Great Britain, France, Australia and New Zealand have placed a maximum limit of 200 mg kg^{-1} for the content of quinolizidine alkaloids in food products (Resta et al., 2008). Research has focused on the use of lupin beans as feed-in several farm animals, including cattle, swine, poultry and rabbits. These studies have shown that the consumption of lupin beans in higher amounts as compared to that suggested by the European Food Safety Authority could result in a negative impact on animals'

zootechnical performances, including body weight, feed intake, average daily gain and feed conversion ratio (Schrenk et al., 2019). Acute toxicity studies based on the effect of lupanine in experimental animals, including mice, rats and guinea pigs, demonstrated that in the fatal dose animals suffered from tremors, paralysis, convulsions, cyanosis, seizures, trembling, exhaustion, collapse and death caused by asphyxiation, respiratory failure and breathing arrest (Gordon and Henderson, 1951; Petterson et al., 1987; Yovo et al., 1984). Genotoxicity assays performed with lupanine indicated that this alkaloid was unable to bind or intercalate into DNA (Rosenkranz and Wink, 2007; Wink et al., 1998), as well as to induce gene mutations in bacterial and mammalian cells (Quiles et al., 2010). Only a limited number of toxicological assessments have been previously reported and thus the environmental effect of lupanine remains uncertain. Griffiths et al. (2021) demonstrated that EC_{50} values of lupanine using *Daphnia magna* after 48 h and 96 h of exposure were 128 mg L^{-1} and 64 mg L^{-1}, respectively, indicating that lupanine is slightly toxic and practically harmless for the daphnids.

Plants' secondary metabolite, lupanine, is considered a beneficial molecule exhibiting several applications in the pharmaceutical/medical sector (Rasouli et al., 2020). Previous research has documented that lupanine and lupanine derivatives constitute potential compounds for the treatment of type 2 diabetes. Wiedemann et al. (2015) and Lopez et al. (2004) have demonstrated that lupanine, 13-hydroxylupanine and 17-oxolupanine act as modulators of insulin release in rats, by directly affecting K_{ATP} channels and increasing insulin gene expression. Moreover, Garcia-Lopez et al. (2011) reported that lupanine imposes an anticonvulsant effect in rats, acting against the subcutaneous pentylenetetrazole (scPTZ) which causes seizures in humans. A recent study has shown that lupanine is capable of activating the nicotinic acetylcholine receptor (nAChR) inducing neuroprotection in different cellular models. These results suggest that lupanine constitutes a potential molecule for the treatment of the progressive neurological disorder Alzheimer's (Gavilan et al., 2019).

Apart from the benefits of lupanine in human health, this alkaloid could be applicable in the agricultural and chemical industries. Research focusing on the antifungal activity of alkaloids has shown that lupanine inhibits the mycelium growth of *Sclerotium rolfsii*, a fungal pathogen which infects several vegetables, fruits and ornamental plants (Zamora-Natera et al., 2005). Similar antifungal effect of D-(+)-

lupanine was achieved on a pathogenic *Fusarium* strain, which causes disease on economically important food crops (Arias-Garcia et al., 2002). Moreover, lupanine has attracted considerable attention in the chemical industry considering its promising application as feedstock for semi-synthesis of various novel high added-value compounds based on a series of useful functionalities of its asymmetric structure. Racemic and enantiomerically pure lupanine could be chemically transformed into sparteine (Maulide et al., 2016; Przybyl and Kubicki, 2011), an important compound for the pharmaceutical and chemical industries, due to several pharmacological properties and chemical applications as ligand or promoter for various asymmetric reactions. In pharmacology sparteine acts as a cardiovascular agent, exhibiting antiarrhythmic activity, reducing the incidents of ventricular tachycardia and fibrillation which lead to a decrease in heart rate and blood pressure (Boido et al., 2017). Moreover, sparteine demonstrated hypoglycemic properties able to treat type 2 diabetes (Zambrana et al., 2018), diuretic and anti-inflammatory activities, and anticonvulsant effect on seizures (Villalpando-Vargas et al., 2020; Villalpando-Vargas and Medina-Ceja, 2016). Sparteine exhibits also bacteriostatic effects against *Staphylococcus aureus*, *B. subtilis*, *E. coli*, *P. aeruginosa* and *Bacillus thuringiensis* (Boschin and Resta, 2013; Erdemoglu et al., 2007). Besides the various pharmacological properties involved, sparteine includes application in the chemical industry employed as a chiral auxiliary in various asymmetric reactions leading to highly enantioselective transformations (Chuzel and Riant, 2005). The literature shows that sparteine could be used as a chiral ligand for the synthesis of a wide range of compounds including amines (Germain et al., 2011; Stead et al., 2008), aryl alkynes (Priyadarshini et al., 2011), alcohols (Ebner et al., 2008), ferrocenes, esters, phosphines (Metallinos et al., 2003) and piperazines (Andersson et al., 2010).

1.2.3 Lupin beans processing industries' wastewater

The food industry constitutes one of the most important sectors for the expansion of opportunities and economic growth locally and globally (Bigliardi and Galati, 2013). The specific sector comprises different industries including agribusiness, farm production, food processing, food service, retail and wholesale trade, packaging and distribution, marketing and regulations (CED, 2017). Food processing comprises a continuously growing, economically important industrial sector (Lim and Antony, 2019). However, it constitutes one of the largest consumers of energy and freshwater in the manufacturing sector. Freshwater is used throughout the food production chain including process applications as well as non-process applications, such as washing, cooling, heating and cleaning (Bavar et al., 2018). The food processing sector constitutes one of the major water users among manufacturing industries, consuming over 30% of the total utilised freshwater. According to Australian Food Statistics, (2007) regional food processing industries consume approximately 215 million m^3 annually. In Europe, the food manufacturing industry utilises on average 4.9 m^3 of water per inhabitant annually (Forster, 2014). The manufacturing of food products utilized 100 million m^3 of water in the UK in 2010 (Bromley-Challenor et al., 2013) and 34.5 million m^3 in Finland in 2008 (Heponiemi and Lassi, 2012). Due to the exponential growth of the global population, the demand for food is estimated to increase by 60% by 2050. This will cause a direct effect on the food processing industry and the amount of water consumed (Compton et al., 2018). The outcome of the intensive use of freshwater by food processing industries is the generation of high quantities of wastewater. Food factories commonly generate very complex effluents containing pathogen agents and/or chemical contaminants. Moreover, the aforementioned industries generate wastewater in different amounts with varying characteristics depending on the raw material employed (Table 1.5) (Alabaster et al., 2017; Meneses et al., 2017).

Table 1.5: Wastewater produced by different food processing industries

Industry type	**Wastewater production (m^3 $t_{product}^{-1}$)**	**COD (Kg m^{-3})**
Dairy	3-10	1.5-5.2
Fish	8-18	2.5
Meat and poultry	8-18	2-7
Sugar	4-18	1-6
Starch	4-18	1.5-42
Vegetables, fruits and juices	7-35	2-10

Production of the lupin bean snack requires the consumption of high amounts of water to eliminate quinolizidine alkaloids, an antinutritional factor that needs to be removed prior to human or animal consumption. Different processes have been developed for the extraction of undesirable alkaloids from lupin beans. Varieties with low-alkaloid content have been developed and successfully applied in areas where *Lupinus* is not endemic including Australia and Eastern Europe. Sweet lupin varieties were developed in the 1930s and 1940s, indicating that the genetically modified *L. albus* plants produce lupin beans which contain 98-99% fewer alkaloids as compared to wild varieties (Rybinski et al., 2018). Moreover, the capacity of bacterial strains to act as debittering agents has been explored demonstrating low efficiency in quinolizidine alkaloids removal from lupin beans flour (Santana and Empis, 2001). Debittering constitutes the most extensively process used for the elimination of undesirable alkaloids from lupin beans, which typically comprises four steps: i) hydration of dry lupin beans, ii) cooking of water-swollen beans, iii) sweetening of boiled beans (including a debittering stage that achieves significant removal of alkaloids from lupin beans and a washing phase) and iv) a salting final stage required for preservation (Fig 1.13). Different methods have been reported in the literature pertinent to the debittering stage, including normal (freshwater, 25 ^{o}C), alkaline (0.5% $NaHCO_3$, 25 ^{o}C) and thermal (freshwater, 65 ^{o}C) processing. While normal debittering constitutes the most favourable option (Erbas, 2010), it necessitates the consumption of large volumes of freshwater, which result in the generation of significant quantities of effluent (Carmali

et al., 2010) ranging between 10-20 L of wastewater per Kg of dry lupin beans (Esteves et al., 2020). Thus, the wastewater produced from the manufacturing process of the lupin beans snack contains a high amount of quinolizidine alkaloids, which mainly consist of lupanine (Boschin and Resta, 2013; Erbas, 2010).

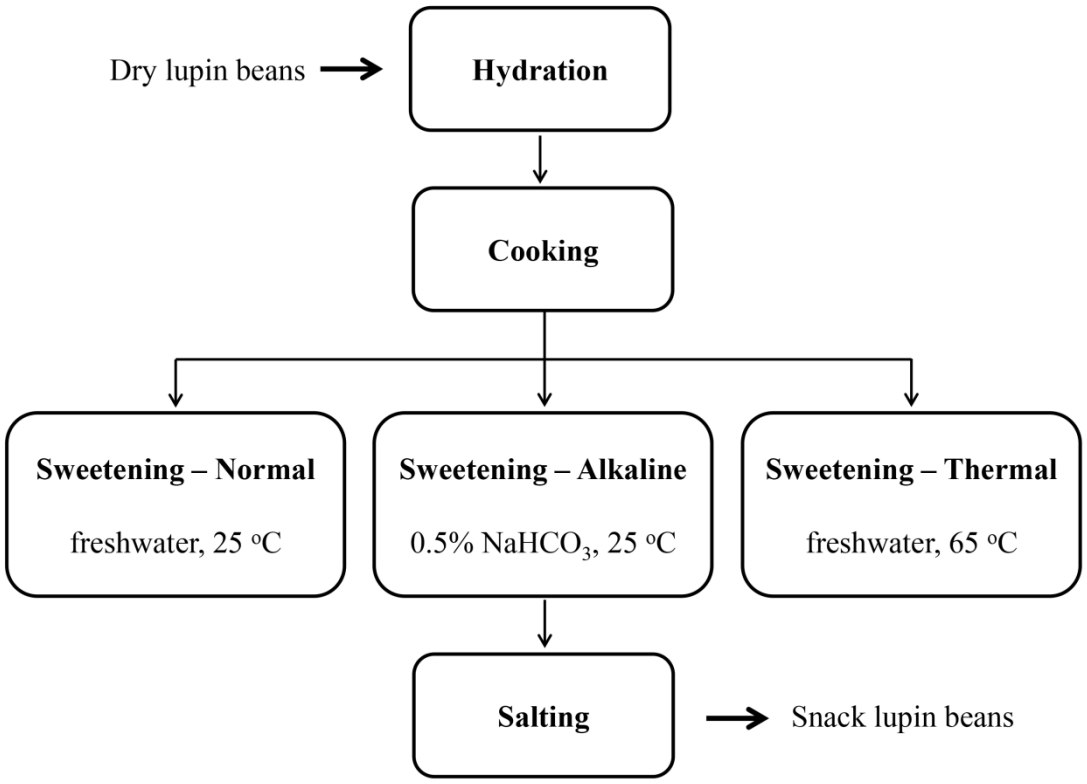

Figure 1.13: Diagram of the lupin beans process with normal, alkaline and thermal debittering stages.

1.2.4 Treatment and valorisation process of lupin beans wastewater

As previously mentioned food processing industries constitute one of the main consumers of available freshwater. However, water scarcity, stricter environmental laws and the increasing cost of wastewater disposal drive food processing industries to develop alternative pathways for the management of the wastewater generated, including water reuse and recycling (Roshan and Kumar, 2020). Throughout the years several physicochemical and biological treatment technologies have been developed for the removal of contaminants from wastewater generated in food industrial units. Among the widely applied physicochemical treatment technologies oxidation, adsorption, ion-

exchange, membrane filtration, solvent extraction and coagulation/flocculation have to be applied, while the biological remediation techniques employed include the use of anaerobic or aerobic microorganisms, enzymes and microbial communities (e.g. activated sludge) for the treatment of industrial wastewater (Barbera and Gurnari, 2018; Crini and Lichtfouse, 2018). A limited number of studies have focused on the treatment of wastewater generated from the lupin bean snack industry. Carmali et al. (2010) constructed a direct method for the recovery of lupanine existing in the industrial lupin bean wastewater using a membrane process as well as osmotic evaporation followed by solvent extraction with ethyl ether. However, the specific approach achieved a significantly low yield (18.5%). Even though the recovery rate of lupanine was low, the process could obtain 0.25 Kg of lupanine with 90% purity per t of dry lupin beans. A recent study shows that nanofiltration could be successfully applied for the treatment of industrial lupin beans wastewater eliminating different organic compounds, including lupanine (Esteves et al., 2020). The use of NF270 membrane achieved 99.5% removal of lupanine that existed in wastewater, while 80% of the treated wastewater could be recycled in the industrial process. Based on this approach 9 Kg of lupanine with 78% purity could be obtained per t of dry lupin beans.

1.3 Aim of current work

The studies presented above indicate that the lupanine enantiomeric mixture existing in the wastewater of lupin bean processing industries constitutes a valuable compound for the pharmaceutical and agricultural sectors, as well as a promising feedstock for semi-synthesis of high added-value compounds in the chemical industry. Thus, a sustainable approach should be followed for the valorisation of the specific waste stream. The current study proposed conducting microbial enantioselective resolution of the lupanine enantiomeric mixture contained in the specific industrial wastewater by employing newly isolated lupanine degrading microorganisms. The study constitutes part of an overall project that aimed to close the loop on the valorisation of the alkaloid rich wastewater generated from the food processing industry, which was performed based on the scheme presented in Fig 1.14.

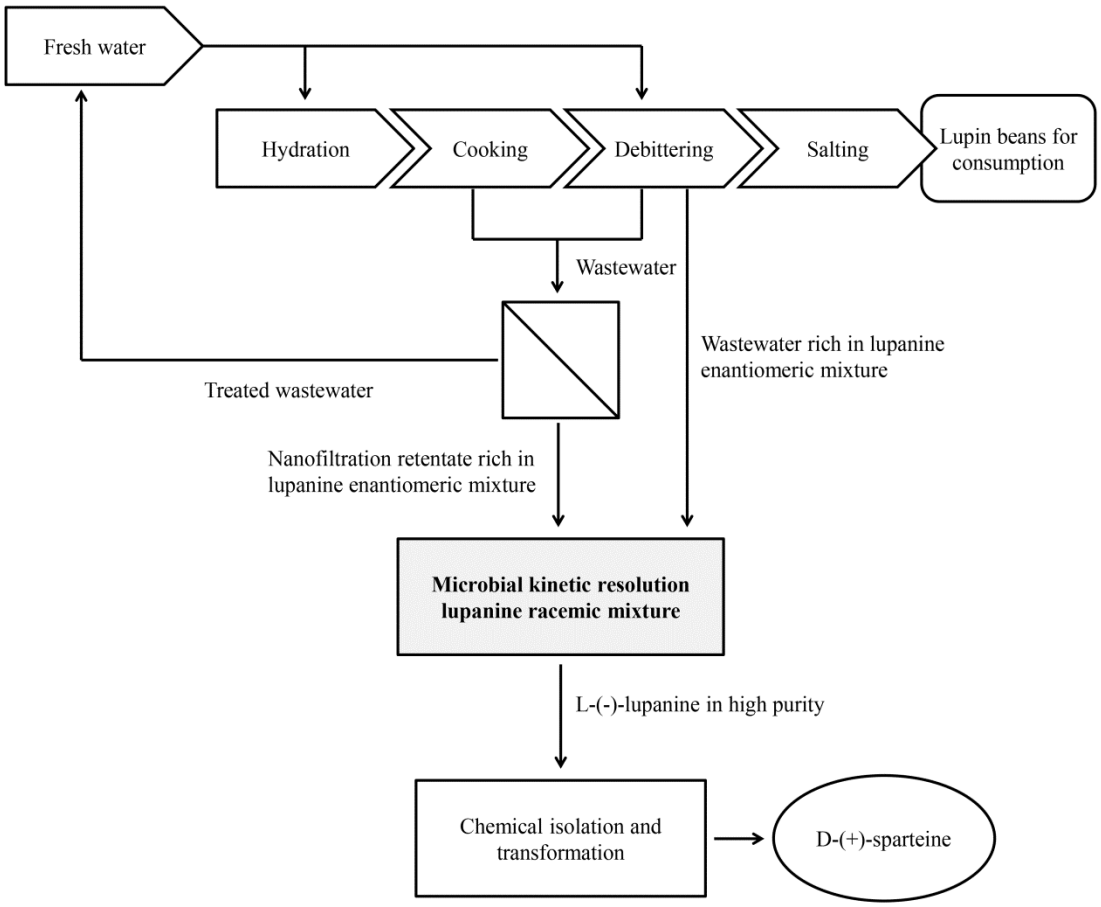

Figure 1.14: Overall scheme for the valorisation of alkaloid rich wastewater generated from the lupin bean processing industry.

1.3.1 Objectives

The development of an efficient technology for bioconversion of the main quinolizidine alkaloid existing in industrial lupine bean processing wastewater required exploring the following specific objectives:

- Bioconversion of racemic lupanine by newly isolated microbial strains for the production of high-value chemicals. To achieve this goal, the isolation of microorganisms from different environmental sources should be conducted based on the ability of each strain to metabolize lupanine. Each microbe should be identified, while their ability to degrade and biotransform lupanine racemate should be evaluated to determine the applicability of each isolate in the process.
- Microbial resolution of racemic lupanine using the isolated strains for the production of enantiomerically pure lupanine. The capacity of each microorganism to degrade enantioselectively racemic lupanine should be assessed for the production of pure lupanine enantiomers in high ee. Moreover, the most promising strains should be studied for their ability to utilize and biotransform each of the lupanine enantiomers as single carbon substrates. The optimal growth conditions of each strain should be evaluated based on different environmental factors.
- The composition of different lupin bean processing wastewater streams in various constituents should be characterized. The capacity of the most promising isolated strain to enantioselectively degrade or biotransform lupanine directly from lupin bean processing wastewater should be evaluated in different bioprocess scales (e.g. shake-flasks, lab-scale bioreactor). Moreover, the microbial valorisation of industrial wastewater should be evaluated under different bioprocess modes (e.g. batch, fed-batch).
- Monitoring of lupanine metabolism by the most promising isolate during biodegradation of pure racemic lupanine and lupanine enantiomers as well as in cultures exposed to the lupanine enantiomeric mixture that exists within the content of organic molecules incorporated in the industrial wastewater. The mRNA expression of key genes during the biodegradation of lupanine should be evaluated

to assess the transcriptional patterns that occur in the metabolic pathway of the alkaloid.

- Environmental toxicological assessment of racemic lupanine, lupanine enantiomers and other natural molecules generated from lignocellulosic biomass should be performed to evaluate if the disposal of these compounds constitutes a safe practice. Different bioindicators, including microbes, animals, planktons and plants, should be employed to determine the impact of the aforementioned components on aquatic and terrestrial ecosystems.

2 RESEARCH METHODOLOGY

2.1 Racemic lupanine, D-(+)-lupanine and L-(–)-lupanine: Purification and storage

The racemic lupanine and lupanine enantiomers (D-(+)-lupanine and L-(–)-lupanine) used in the present work were obtained from the Research Institute for Medicines (iMed ULisboa) of the Faculty of Pharmacy, University of Lisbon and stored at 2-4 ^{o}C until further use.

2.2 Industrial wastewater streams: Origin and storage

The industrial wastewater streams employed constituted the effluents generated during the resting (UWRP) and sweetening phases (UWSP) of the lupin bean snack manufacturing process, which were obtained from a relevant plant (Tremoceira, Charneca da Caparica, Portugal). Moreover, the retentate water remaining following nanofiltration of wastewater emitted from the sweetening processing phase (RWSP) as well as the effluent generated from anaerobic digestion of wastewater produced from the resting phase of the lupin bean snack manufacturing process (AWRP) were obtained from the Institute for Bioengineering and Biosciences (Department of Bioengineering, Instituto Superior Técnico) of the University of Lisbon and the Department of Civil and Environmental Engineering – DICA of the Polytechnic University of Milan respectively. All samples were centrifuged at 5000 rpm for 30 min, filtered through 0.2 mm filters (Whatman, Buckinghamshire, UK) and stored at -20 ^{o}C until further use.

2.3 Microorganisms and culture conditions

2.3.1 Mineral medium

A minimal microbial growth medium (M9) was used for subcultures of microorganisms, which included the following composition (g L^{-1}): $Na_2HPO_4 \cdot 2H_2O$ 8.5, KH_2PO_4 3.0, NaCl 0.5, NH_4Cl 0.5, $MgSO_4 \cdot 7H_2O$ 0.48 and racemic lupanine or pure lupanine enantiomers (D-(+)-lupanine or L-(–)-lupanine) depending on the requirements of each experiment. The medium was sterilized in an autoclave for 15 min at 121 ^oC, while racemic and enantiopure lupanine were added following filter sterilization (Ahlstrom, Bärenstein, Germany, 0.2 μm pore size) when the medium was at room temperature. Solid cultures were performed using M9 medium supplemented with 1.5% (w/v) of agar.

2.3.2 Cultivations for isolation and characterization of newly racemic lupanine metabolizing strains

Microbial strains capable of using racemic lupanine as the sole carbon source have been isolated from four environmental samples that included anaerobic granular sludge obtained from an anaerobic bioreactor treating cheese whey (Charalambides Christis Ltd, Limassol, Cyprus), anaerobically digested sludge and activated sludge derived from a municipal wastewater treatment plant (Sewerage Board of Limassol – Amathus (SBLA), Moni, Cyprus) as well as wastewater from a lupin beans snack manufacturer (Tremoceira, Charneca da Caparica, Portugal). The first three samples were passed through 0.45 μm filters (Whatman, Buckinghamshire, UK) and separated solids were used as 1% (w/v) inoculum for enrichment cultures. Furthermore, wastewater from a lupine beans processing plant was directly used as inoculum (5% v/v) in enrichment cultures. All environmental samples were cultivated under aerobic conditions, while granular and digested sludges were additionally applied under anaerobic conditions.

Aerobic and anaerobic enrichments of microorganisms were carried out using 25 mL working volume in 100 mL and 30 mL flasks respectively. All cultures consisted of M9 medium supplemented with 1.5 g L^{-1} of racemic lupanine and inoculums under sterile conditions as described above, while gas-tight flasks were applied. The flasks were incubated for 7 days and the cultures were maintained at 31 ^oC and 100 rpm.

Following three sequential enrichment cultures, 1 μL of each sample was withdrawn from each flask and plated by the streak method on M9 agar medium aiming to isolate the desired strains. The solid cultures were sealed with parafilm and incubated for 7 days at 31 ^{o}C. Subsequently, single colonies were transferred into a liquid M9 medium and cultivated cells were stored in a medium containing 50% glycerol, at -80 ^{o}C. Isolated strains were also maintained at 4 ^{o}C on M9 agar plates and subcultured onto fresh medium every month.

For characterization of isolated strains, liquid cultures of the pure strains were prepared using M9 medium supplemented with 1.5 g L^{-1} of racemic lupanine and were inoculated by the strains maintained on Petri dishes. The cultures were incubated in a shaking incubator at 100 rpm which was maintained at 31 ^{o}C for 72 h. 0.5 mL of liquid culture samples were transferred into sterile Eppendorf tubes (1.5 mL total volume) that contained 0.5 mL of glycerol.

2.3.3 Inoculum preparation

The inoculum was pregrown overnight at 31 ^{o}C in M9 supplemented with 1.5 g L^{-1} of racemic lupanine. The incubation of the inoculum was performed using flasks of 250 mL (50 mL working volume) for aerobic strains and serum bottles of 35 mL (25 mL working volume) for anaerobic strains in a shaking incubator (Stuart SI600, Staffordshire, UK), which was stirred at 100 rpm.

2.3.4 Cultivations of newly racemic lupanine metabolizing strains

2.3.4.1 Racemic lupanine biodegradation by aerobic and anaerobic cultures

Aerobic cultures were prepared in duplicate inoculating 3 mL of pregrown cells under sterile conditions utilizing flasks of 500 mL (150 mL working volume) and anaerobic cultures were conducted in a similar way using serum bottles of 250 mL (180 mL working volume). Anaerobic conditions were formed through the flashing of serum bottles with CO_2. All experiments were performed using an initial racemic lupanine concentration of 1.5 g L^{-1}, while a control flask, prepared without the additions of cells, was utilized to evaluate that lupanine conversion was due to the microbial action. The cultures were incubated for a period of 36-42 h and they were maintained at 31 ^{o}C, pH 7 and 100 rpm.

2.3.4.2 Microbial resolution of racemic lupanine by aerobic isolated strains

The microbial resolution of racemic lupanine was investigated during the cultures of three microorganisms. Cultures were conducted through the application of 1.5 g L^{-1} racemic lupanine in 500 mL flasks (working volume of 300 mL) and 5% (v/v) of inoculum. All experiments were performed at 31 °C, 100 rpm and pH 7.

2.3.5 Cultivation of *P. putida* LPK411 strain

2.3.5.1 Biodegradation of lupanine enantiomers (D-(+)-lupanine or L-(–)-lupanine)

The biodegradation of each lupanine enantiomer was conducted using 7.5 mL of pregrown LPK411 cells as inoculum in 500 mL flasks (working volume 150 mL) containing M9 medium. The initial D-(+)-lupanine or L-(–)-lupanine concentration used was 0.75 g L^{-1} and the experiments were performed at 31 °C, 100 rpm and pH 7.

2.3.5.2 Biodegradation of racemic lupanine under different culture conditions

Experiments for the determination of optimal conditions for racemic lupanine biodegradation by LPK411 were conducted under different temperatures (25 ^{o}C, 28 ^{o}C, 31 ^{o}C and 34 ^{o}C), pH values (6, 7, 8 and 9) and initial racemic lupanine concentrations (0.3 g L^{-1}, 1.0 g L^{-1}, 1.5 g L^{-1}, 2.5 g L^{-1} and 3.0 g L^{-1}). Cultures were prepared by inoculating 2.5 mL of pregrown cells into 250 mL flasks (working volume of 50 mL) containing M9 medium. Apart from stirring, which was maintained at 100 rpm, culture conditions were varied depending on the requirements of each experiment.

2.3.5.3 Microbial resolution of lupanine enantiomeric mixture in industrial wastewater streams

Cultures aimed at microbial resolution of the lupanine enantiomeric mixture contained in different unrefined and pretreated wastewater streams were conducted using the wastewater stream selected in each case supplemented with M9 salts. Experiments were performed in 1000 mL flasks (200 mL working volume) and 5% (v/v) of inoculum, while the LPK411 cultures were maintained at 31 °C, 100 rpm and pH 7.

2.3.5.4 Microbial resolution of racemic lupanine in repeated fed-batch cultures

Repeated fed-batch cultures were employed to assess the ability of LPK411 to perform enantioselective biodegradation of racemic lupanine in 1000 mL flasks (200 mL working volume). The first feeding was performed using 200 mL of M9 medium supplemented with 1.5 g L^{-1} of racemic lupanine and 5% (v/v) of inoculum. The following three substrate feedings were performed when L-(–)-lupanine ee was <95%, where 60 mL of 2 times concentrated M9 medium containing 3 g L^{-1} of racemic lupanine were added to the existing biomedium. All experiments were performed at 31 °C, 100 rpm and pH 7.

2.3.5.5 Microbial resolution of lupanine enantiomeric mixture in industrial wastewater using a lab-scale bioreactor

Resolution of the lupanine enantiomeric mixture in untreated and pretreated wastewater streams by LPK411 was assessed in a lab-scale bioreactor (Minifor, Lambda, Brno, Czech Republic) in batch mode. A schematic diagram of the bioreactor setup is presented in Fig 2.1. The total volume of the bioreactor was 450 mL, which was operated using 300 mL of working volume completed with wastewater supplemented with M9 salts and 5% (v/v) of inoculum. The pH was controlled at 7 ± 1 by the addition of H_2SO_4 (4 M) or NaOH (4 M) and the temperature was kept constant at 31 ^oC (Inpro 3253/150/Pt100, Mettler-Toledo, Switzerland). Air was supplied continuously to the bioreactor at an inlet flow rate of 1 L min^{-1} by an air compressor (MC 0206 Vakuum Bohemia, Jihlava, Czech Republic). Air was distributed in the biomedium via a sparger. Two fish-tail stirrer discs stirred at 100 rpm provided optimal mixing of the two phases. Dissolved oxygen concentration and carbon dioxide production were monitored during lupanine biodegradation using 800090 DO probe and 8081002 carbometer (Lambda, Brno, Czech Republic). The regulation of foam formation during the experiment was achieved with the use of Antifoam A.

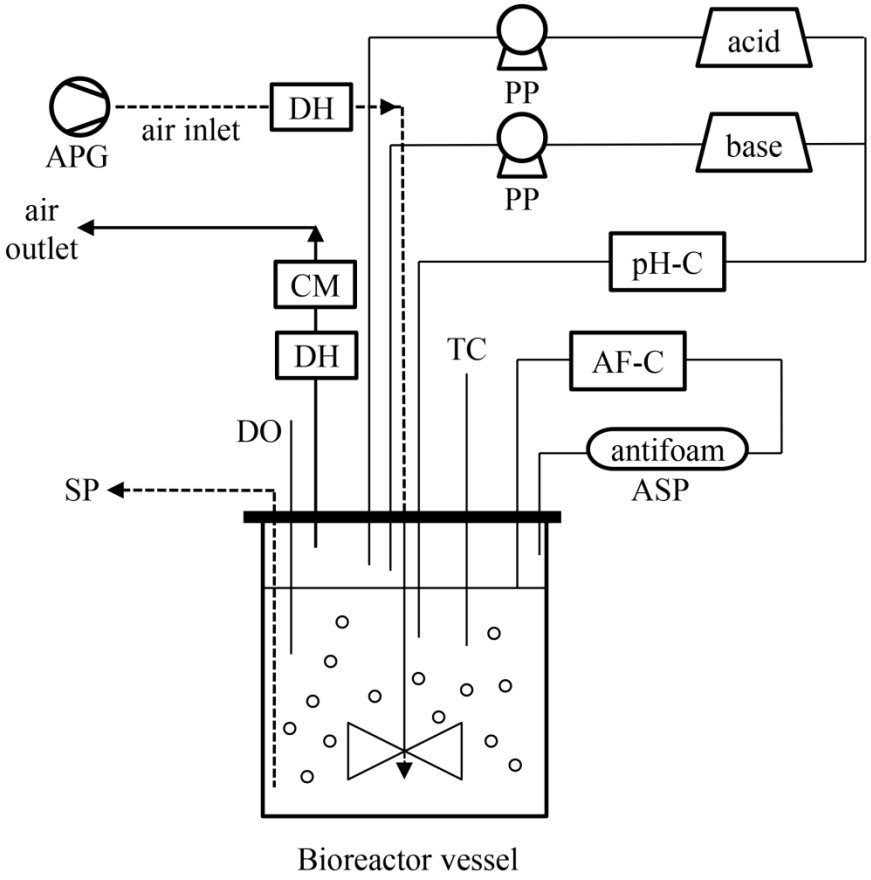

Figure 2.1: Schematic diagram of bioreactor apparatus. AF-C: antifoam controller, APG: air pressure generator, ASP: antifoam syringe pump, CM: CO_2 meter, DH: dehumidifier unit, DO: dissolved oxygen meter, pH-C: pH controller; PP: peristaltic pump, SP: sampling port, TC: temperature controller.

2.3.5.6 Transcriptional kinetics monitoring of luh and crc genes in cultures with lupanine and industrial wastewater

Subcultures of LPK411 conducted for determination of transcriptional kinetics of the *luh* and *crc* genes were pregrown for 18 h at 31 °C in M9 supplemented with 1.5 g L^{-1} of succinic acid. The experiments were prepared by diluting the inoculum in M9 containing either racemic lupanine, lupanine enantiomers (D-(+)-lupanine or L-(–)-lupanine) or UWRP. The optical density (600 nm) at the beginning of the experiment was 0.1 determined using a UV/VIS spectrophotometer (JENWAY 7315, Staffordshire, UK), while cultivation was conducted using 1000 mL flasks (200 mL working volume) at 31 °C, 100 rpm and pH 7.

2.4 Strain identification by 16S rRNA sequence analysis

DNA extraction, PCR (27F/1492R primers), PCR purification (using Montage PCR Clean-up kit) and sequencing alignment were performed by Macrogen (Amsterdam, the Netherlands) using the Big Dye terminator cycle sequencing kit (Applied BioSystems, USA). Sequencing products were resolved on an Applied Biosystems model 3730XL automated DNA sequencing system (Applied BioSystems, USA) and the resulting alignment of the 16S rRNA was compared for homology in the National Center for Biotechnology Information (NCBI) database by BLASTn nucleotide tool analysis. Phylogenetic trees were constructed by the neighbour-joining method using Mega 6.0 software and the most similar sequences according to the NCBI database by BLASTn and boot strapping in 500 replicates.

2.5 Analyses

2.5.1 Dry cell weight

A UV/VIS spectrophotometer (JENWAY 7315, Staffordshire, UK) was used to measure biomass absorbance (600 nm) and dry biomass was determined using a calibration curve of dry cell weight. The calibration was obtained through dilution of a pregrown culture to obtain different OD values. Biomedium samples of 10 mL were dried (105 °C) and placed at 600 °C for 60 min to combust the organic content. The coefficient of variation calculated for 3 samples was 4.5% at a biomass content of 0.1 $g_{biomass}\ L^{-1}$.

2.5.2 Racemic and enantiomeric lupanine concentration

2.5.2.1 Gas chromatography

Gas chromatography (GC) was used to determine the concentration of lupanine in culture samples. The method derived from Santana et al. (1996) was used for the analysis of alkaloids, which was modified as follows: cultures samples were obtained at regular intervals, centrifuged at 4500 rpm for 5 min and filtered with 0.2 μm syringe filters. 0.5 mL of the supernatant was homogenized in 5 mL of 0.5 N HCl and held at room temperature for 30 min. The homogenate was made alkaline (pH 10) with ammonia solution 25% and applied to a standard Extrelut NT 20 column (Merck, Darmstadt, Germany). The alkaloids were eluted with 60 mL of dichloromethane, while the eluates were evaporated to dryness and then taken up in 2 mL of methanol for analysis by GC.

The determination of lupanine was performed using a Shimadzu GC-2014 (Shimadzu, Milton Keynes, UK) equipped with a Flame Ionisation Detector (FID), an AOC-20i auto-injector and a Zebron ZB-5 capillary column (Phenomenex, Macclesfield, UK) with dimensions 30 m × 0.25 mm × 0.25 μm. Nitrogen was used as the mobile phase and the stationary phase of the column consisted of 5% phenyl and 95% dimethylpolysiloxane. 1 μL of alkaloids collected in methanol was injected and the temperature of the column was kept constant at 150 ^{o}C for 2 min followed by an increase of 15 ^{o}C min^{-1} up to 250 ^{o}C. Subsequently, the temperature was further raised to 300 ^{o}C at a rate of 30 ^{o}C min^{-1} and it was maintained at the specific temperature for

an additional 15 min. The samples were analyzed in triplicate and the standard deviation was calculated. All chemicals used were obtained from Sigma-Aldrich Company Ltd (UK) and were of analytical grade.

2.5.2.2 High Performance Liquid Chromatography

The concentration of lupanine existing in unrefined and pretreated wastewater streams was determined through High Performance Liquid Chromatography (HPLC) analysis using a Shimadzu LC-20AD liquid chromatograph (Shimadzu, Milton Keynes, UK) equipped with an SPD-20A UV/VIS detector, a SIL-20A HT autosampler and a CTO-10AS VP column oven. All samples were basified (pH 13) using KOH, centrifuged at 4500 rpm and filtered through 0.2 μm syringe filters. HPLC analysis was performed employing a Kinetex EVO C18 column (Phenomenex, Torrance, CA) with dimensions 4.6 mm × 250 mm × 5 μm and a guard column (3 mm × 4 mm). The mobile phase constituted a mixture of acetonitrile (15%) and Na_2HPO_4 buffer (85%), while the column was eluted isocratically using a flow rate of 1 mL min^{-1} at room temperature. The injection volume was 20 μL and the detection of lupanine was performed at 220 nm. All substances applied were of analytical grade and purchased from Sigma-Aldrich Company Ltd (UK).

2.5.3 Lupanine enantiomeric excess

HPLC was applied to assess the ee of lupanine in cultures. Samples were centrifuged at 4500 rpm and filtered through 0.2 μm syringe filters for biomass removal. 15 mL of the filtrate were basified (pH >11) using 1 M NaOH and the alkaloid content was extracted with the application of 40 mL dichloromethane. Drying of the organic phase was performed employing anhydrous Na_2SO_4 and subsequent concentration was achieved using a Rotavapor R-3 (BUCHI Labortechnik, Switzerland). The concentrated sample was applied to a pipette containing Celite and the alkaloid content was eluted through the application of 4-6 mL dichloromethane. The samples were evaporated until dry and dissolved in 100 μL isopropanol, to which 900 μL of *n*-hexane was added. HPLC analysis was performed using a Lux i-Cellulose-5 column (Phenomenex, Torrance, CA) with dimensions 4.6 mm × 250 mm × 5 μm and a guard column (3 mm × 4 mm). The mobile phase constituted 53% *n*-hexane, 22% isopropanol and 25% *n*-hexane with 0.1% of diethylamine. A flow rate of 1 mL min^{-1} was used, while the

method was conducted at room temperature and UV detection (230 nm). Analytical grade chemicals were used at all times.

2.5.4 Final metabolic products

Nuclear magnetic resonance spectroscopy (NMR) was used to determine the final metabolic products of racemic lupanine and D-(+)-lupanine bioconversion in samples derived from cultures. Liquid samples of 100 mL were first centrifuged for 4 min at 13500 rpm, the supernatant solution was filtered through 0.2 μm syringe filters to remove any remaining solids and it was evaporated to dryness under reduced pressure at 40 ^{o}C in a rotary evaporator (Stuart RE300, Staffordshire, UK).

The samples were dissolved in 600 μL DMSO-d6 (or $CDCl_3$-d) and ^{1}H NMR, ^{13}C NMR, 2D {^{1}H} grCOSY, 2D {^{1}H} TOCSY,2D {^{1}H, ^{13}C} grHSQC and 2D {^{1}H, ^{13}C}HMBC spectra were recorded on a 500 MHz Bruker AvanceII NMR spectrometer. Standard Bruker pulse sequences were used. ^{1}H NMR experiments were performed using 12.00 μs pulse (90°), an acquisition time of 3.17 s, a spectral width of 10330 Hz, 16 scans (+ 4 dummy scans) and delay time 1.00 s. ^{13}C NMR experiments were performed using 9.00 μs pulse (90°), an acquisition time of 1.10 s, a spectral width of 29762 Hz, 4096 scans (+ 4 dummy scans) and delay time 2.00 s. 2D{^{1}H} grCOSY and TOCSY experiments were performed using 12.00 μs pulse (90°), an acquisition time of 0.97 s, a spectral width of 6667 Hz, 64 scans (+ 8 dummy scans) and delay time 2.00 s. 2D {^{1}H, ^{13}C} grHMBC experiments were performed using 12.00 μs pulse (90°), an acquisition time of 0.25 s, a spectral width of 6329 Hz, 80 scans (+ 16 dummy scans) and delay time 1.41 s. 2D {^{1}H, ^{13}C} grHSQC experiments were performed using 12.00 μs pulse (90°), an acquisition time of 0.17 s, a spectral width of 6009 Hz, 32 scans (+ 32 dummy scans) and delay time 2.00 s.

2.5.5 Chemical oxygen demand

Chemical oxygen demand (COD) analysis of the wastewater employed was performed according to the standard COD 5220 D - Closed reflux, colorimetric method (APHA, 2017). Wastewater samples were centrifuged at 4500 rpm for 5 min and filtered through 0.2 μm syringe filters to remove any remaining solids and biomass. 2 mL of sample were digested in a COD-Reactor ET 125 (Lovibond, Dortmund,

Germany) using 1.2 mL of digestion solution ($K_2Cr_2O_7$ 10.216 g L^{-1}, H_2SO_4 167 mL L^{-1} and $HgSO_4$ 33.3 g L^{-1}) and 2.8 mL of sulfuric acid reagent (5.5 g Ag_2SO_4 kg^{-1} H_2SO_4), at 150 ^oC for 2 h. The COD content of wastewater was determined via absorption of dichromate at 600 nm using a UV/VIS spectrophotometer (HACH DR 1900, Colorado, USA).

2.5.6 Total, volatile and fixed solids

Total, fixed and volatile solids of wastewater were determined using standard methods 2540 B and 2540 E SOLIDS (APHA et al., 2017) as well as Method 1684 (U.S. EPA, 2001). 50 g of well-mixed wastewater samples were dried at 105 ^oC for 1 h to determine the total solids content. Volatile and fixed solids were determined by igniting the samples at 550 ^oC for 2 h. According to the weight values obtained total, volatile and fixed solids were calculated using Eq. 1-3, where W_{dish} is the weight of evaporating dish (g), W_{sample} corresponds to the weight of the wet sample and evaporating dish (g), W_{total} is assigned to the weight of dried residue and dish at 105 ^oC (g) and $W_{volatile}$ is the weight of residue and dish after ignition at 550 ^oC (g).

$$\frac{\mathbf{g_{total\ solids}}}{\mathbf{g_{sample}}} = \frac{\mathbf{W_{total} - W_{dish}}}{\mathbf{W_{sample} - W_{dish}}} \quad (1)$$

$$\%\ \text{volatile solids} = \frac{W_{total} - W_{volatile}}{W_{total} - W_{dish}} \times 100 \quad (2)$$

$$\%\ \text{fixed solids} = \frac{W_{volatile} - W_{dish}}{W_{total} - W_{dish}} \times 100 \quad (3)$$

2.5.7 Total protein

The total protein content entailed in the wastewater streams employed here was determined by the Bradford standard assay method as previously described (Kruger, 2009). Wastewater samples were centrifuged at 4500 rpm for 5 min and filtered via 0.2 μm syringe filters to remove any remaining solids and biomass. 5 mL of Bradford reagent (Coomassie® brilliant blue G250 100 mg L^{-1}, ethanol 95% 50 mL L^{-1} and H_3PO_4 85% (w/v) 100 mL L^{-1}) were added in 100 μL of sample. The wastewater protein content was assessed through the absorption of Coomassie® brilliant blue at 595 nm using a UV/VIS spectrophotometer (JENWAY 7315, Staffordshire, UK).

2.5.8 Total lipids

The Bligh and Dyer extraction method was employed for the determination of the lipid content existing in the wastewater samples applied as described in Bligh and Dyer, (1959) and Manirakiza et al. (2001). Wastewater samples were centrifuged at 4 500 rpm for 5 min and filtered via 0.2 μm syringe filters to remove any remaining solids and biomass. Lipids derived from 5 mL of wastewater sample were extracted in organic solvents (methanol and chloroform) through repeated extraction cycles. The eluate was evaporated to dryness using a Rotavapor R-3 (BUCHI Labortechnik, Switzerland) and the residue was further dried at 105 ^{o}C for 1 h. The lipid content of each sample was calculated depending on the sample volume and the weight applied using Eq. 4, where W_{dish} is the weight of flask (g), W_{total} corresponds to the weight of dried residue and flask at 105 ^{o}C (g) and V_{sample} denotes the volume of sample (mL).

$$\text{Total lipids} = \frac{W_{total} - W_{flask}}{V_{sample}} \quad (4)$$

2.5.9 Total and reducing sugars

The phenol-sulfuric acid method was applied to determine the total sugar content of wastewater based on the capacity of the method to detect virtually all classes of carbohydrates, including simple sugars, oligosaccharides, polysaccharides and their derivatives (Dubois et al., 1956; Nielsen, 2010). However, the dinitrosalicylic acid (DNS) method was additionally used to determine the wastewater content in reducing sugars, such as glucose, fructose, glyceraldehydes, lactose, arabinose and maltose (Miller, 1959).

For the determination of total and reducing sugars, wastewater samples were centrifuged at 4500 rpm for 5 min and filtered through 0.2 μm syringe filters. In the phenol-sulfuric acid method, 2 mL of sample were reacted with 0.05 mL of phenol 80% and 5 mL of concentrated H_2SO_4, at 25 ^{o}C for 10 min. Total sugar content in wastewaters was determined via absorption at 490 nm using a UV/VIS spectrophotometer (JENWAY 7315, Staffordshire, UK).

2.5.10 Total Kjeldahl nitrogen

The Total Kjeldahl nitrogen (TKN) content was assessed using the protocols provided by VELP Scientifica (AOAC 973.48-1973, CEN - EN 25663, EPA 351.3, ISO 5663:1984). Wastewater samples were centrifuged at 4500 rpm for 5 min and filtered via 0.2 μm syringe filters. For the determination of TKN 50 mL of homogenised sample was digested using 10 mL of 96-98% H_2SO_4 and 2.5 g of catalyst mixture (K_2SO_4 200 g, $CuSO_4 \cdot 5H_2O$ 20 g and TiO_2 20 g). The mixture was heated at 150 ºC for 30 min, 250 ºC for 30 min and 420 ºC for 1 h using a DK 20 Heating Digester (VELP Scientifica, Monza Brianza, Italy). The tube was then left to cool, and 50 mL of water was added slowly under shaking. Subsequently, TKN was distilled in 30 mL of 0.5 M H_3BO_3 by adding 20 mL of 10 M NaOH and hot steam for 5 min in each digested sample using a UDK 129 Distillation Unit (VELP Scientifica, Monza Brianza, Italy). Finally, distilled samples were titrated using a 0.01 M H_2SO_4 sulfuric acid and bromocresol green-methyl mixed indicator (bromocresol green 1 g L^{-1} and methyl red 0.2 g L^{-1} in ethanol). The content of TKN in g L^{-1} was calculated using Eq. 5, where V_{sample} corresponds to the volume of H_2SO_4 used for the titration of the sample (mL), V_{blank} is the volume of H_2SO_4 used for the titration of the blank (mL) and $V_{digested}$ corresponds to the volume of sample digested (mL).

$$TKN = \frac{V_{sample} - V_{blank}}{V_{digested}} \times 140 \quad (5)$$

2.6 Preparation and isolation of total RNA, cDNA synthesis and quantitative real-time PCR (RT-qPCR)

RT-qPCR analysis was conducted to determine mRNA expression from the *luh* and *crc* genes in LPK411 cultures. Depending on the cell density 3–4.5 mL samples were collected and centrifuged at 9000 rpm for 30 min at 4 °C. The harvested cell pellet was soaked in liquid nitrogen and subsequently stored at − 80 °C. Total RNA isolation and cDNA synthesis were performed as previously described (Koutinas et al., 2010). According to the threshold cycle values obtained relative mRNA expression was estimated using Eqs. 6-8. cDNA synthesis and PCR were performed using a SensoQuest labcycler (SensoQuest GmbH, Göttingen, Germany) and qTower^{3}G real-time PCR (Analytik Jena, Jena, Germany) respectively. The primer pairs of the *luh*, *crc* and *rpoN*, which were used as the reference gene, are displayed in additional data (Table 2.1). Duplicate experiments were conducted and two samples were analysed for each replicate comprising analysis of 4 samples at each time point.

$$\Delta C_{T,luh/crc} = C_{T,luh/crc} - C_{T,rpoN} \tag{6}$$

$$\Delta\Delta C_{T,luh/crc} = \Delta C_{T,luh/crc}(\text{sample}) - \Delta C_{T,\,luh/crc}(\text{calibrator}) \tag{7}$$

$$NE_{luh/crc} = 2^{-\Delta\Delta C_{T,luh/crc}} \tag{8}$$

Table 2.1: Primers used in RT-qPCR

Gene	Pair of primers	Description	Source
luh	Forward	5´- TGCTTGCCACGGTTTCAATG-3´	Current study
	Reverse	3´-TTTCTGATCGCTATGCCCGC-5´	Current study
crc	Forward	5´-AAGTACCTGGACAAGCAGCG-3´	Current study
	Reverse	3′-GACCGCTCTACCCCATACAG-5′	Current study
rpoN	Forward	5′-TAACGAAACCCTGATGAAGG-3′	(Tsipa et al., 2016)
	Reverse	3′-AATGTCATGCAGTACCAACG-5′	(Tsipa et al., 2016)

2.7 Acute toxicity tests

2.7.1 Acute toxicity assessment with a marine bacterium

Bioluminescence inhibition of the marine bacterium *Aliivibrio fischeri* (NRRL B11177, formally known as *Vibrio fischeri*) following exposure to racemic lupanine, lupanine enantiomers and furanic compounds was evaluated by applying a microscale acute toxicity test based on ISO 11348–3:2007 standard. Several dilutions of each studied compound were prepared using stock solutions, while the final salinity was adjusted to 2% NaCl and the pH ranged between 7-7.5. The lyophilized bacterium was rehydrated and kept at 15 ^{o}C throughout the test.

Luminescence of *A. fischeri* was assessed following 0, 5 and 15 min of exposure to tested compounds. Each experimental run was performed in triplicate and the samples collected were analysed in duplicate. Phenol was used as positive control and an EC_{50} ranging between 13-26 mg L^{-1} was considered acceptable. The percentage of bioluminescence inhibition (I) in each sample was determined through a comparison of the bioluminescence value exposed to a control solution (I_c) against that of each tested sample (I_s) using the following formula:

$$I = 100 - (\frac{I_c - I_s}{I_c} \times 100) \quad (9)$$

A linear regression of the inhibition as Γ value (Eq. 10) was logarithmically plotted against the concentration of the compound. The concentration resulting in population bioluminescence inhibition of 50% (EC_{50}) was calculated using linear regression of inhibition.

$$\Gamma = \frac{I}{100 - I} \quad (10)$$

2.7.2 Acute toxicity assessment with crustaceans

D. magna acute immobilisation bioassay was used to determine the toxicity of racemic lupanine to the freshwater organism as described in ISO 6341:2012. Five different concentrations of racemic lupanine were prepared using stock solutions and standard freshwater (67.75 mg L^{-1} NaHCO3, 294 mg L^{-1} $CaCl_2 \cdot 2H_2O$, 123.25 mg L^{-1} $MgSO_4 \cdot 7H_2O$ and 5.75 mg L^{-1} KCl), while the pH value was adjusted to 7-7.5.

Immobilisation of the planktonic microcrustacean was determined following 24 and 48 h of exposure to the tested compounds. Each concentration was tested in triplicate using four internal replicates. Moreover, the number of dead and immobilized daphnids in the control was not significant (<10%), while the EC_{50} value for the quality control test ($K_2Cr_2O_7$) was acceptable (0.8-1.6 mg L^{-1}). The concentration resulting in *D. magna* immobilization of 50% (EC_{50}) was calculated through Probit analysis, which is commonly applied to correlate a dose (concentration of racemic lupanine) with a quantal response (% immobilization) (Bliss, 1934). For this purpose, the immobilization percentage was transformed into Probit values and the concentration of racemic lupanine was log-transformed. A linear regression of the Probit values with the log-transformed concentration was then applied and the EC_{50} values were calculated.

2.7.3 Short-chronic toxicity test with freshwater algae

A microplate short-chronic toxicity bioassay with freshwater green microalgae *Raphidocelis subcapitata* (formerly known as *Selenastrum capricornutum* and *Pseudokirchneriella subcapitata*) was employed to evaluate the toxicity of furanic compounds. The green microalgae strain was purchased from MicroBioTests Inc. (Algaltoxkit F, Gent, Belgium) and maintained at 5 ± 2 ºC. The bioassay for green microalgae was developed based on the standard toxicity procedures OECD 201:2006 and ISO 8692:2012. Subcultures of *R. subcapitata* were pregrown for 4-7 d in 250 mL flasks with a working volume of 100 mL, using Bold's Basal (BB) medium (g L^{-1}: $NaNO_3$ 0.25, $MgSO_4 \cdot 7H_2O$ 0.075, NaCl 0.025, K_2HPO_4 0.075, KH_2PO_4 0.175, $CaCl_2 \cdot 2H_2O$ 0.025, $ZnSO_4 \cdot 7H_2O$ 0.00882, $MnCl_2 \cdot 4H_2O$ 0.00144, MoO_3 0.00071, $CuSO_4 \cdot 5H_2O$ 0.00157, $Co(NO_3)_2 \cdot 6H_2O$ 0.00049, H_3BO_3 0.01142, EDTA 0.05, KOH 0.031, $FeSO_4 \cdot 7H_2O$ 0.00498). Growth inhibition algal toxicity assay was conducted using 96-well clear polystyrene flat-bottom microplates. Several dilutions of each compound studied were prepared using BB medium and the pH range was adjusted between 7-8. The effect of each compound on the freshwater microalgae following 72 h of exposure was determined using 20 μL of inoculum (the initial inoculum cell density was 10^6 mL^{-1}) and 180 μL of the tested compound. Each experimental run was performed in three repetitions and the samples collected were analysed in triplicate. All experiments were performed at 23 ± 2 °C, under continuous illumination (4400–8900

lux) and agitation (70 rpm). The concentration resulting in algae growth inhibition of 50% (EC_{50}) was calculated through the microalgal optical density assessed at 670 nm employing a microplate reader (TECAN, infinite M200PRO, Grodig, Austria). The compound applied as quality control was potassium dichromate ($K_2Cr_2O_7$) (Koutinas et al., 2019; Nagai et al., 2013).

2.7.4 Classification of toxicity for aquatic organisms

Chemical compounds were classified based on the toxicity rating scales for aquatic organisms by the United States Environmental Protection Agency (US EPA). The categories of toxicity for aquatic organisms based on half-maximal effective concentration (EC_{50}) were divided into very highly toxic (<0.1 mg L^{-1}), highly toxic (0.1-1 mg L^{-1}), moderately toxic (1-10 mg L^{-1}), slightly toxic (10-100 mg L^{-1}), practically harmless (100-1000 mg L^{-1}) and nontoxic or harmless (>1000 mg L^{-1}).

2.7.5 Environmental toxicological assessments on terrestrial plants

The direct (intrinsic) effects of tested compounds on the germination and early growth of different terrestrial plants were evaluated through an acute phytotoxicity assay according to a variation of OECD 208:2006 standard as described in Salvatore et al. (2008). The seeds of the dicotyledons *Lepidium sativum* (garden cress) and *Sinapis alba* (white mustard) and monocotyledon *Sorghum saccharatum* (sweet sorghum) were exposed to racemic lupanine and furanic compounds for 72 h. The phytotoxicity test was held in Petri dishes (15 mm × 100 mm) containing a filter paper (Whatman No.1) with 10 seeds and 1 mL of test compounds. Each experiment was repeated at least three times. Petri dishes were maintained at 25 ^{o}C in darkness and the pH ranged between 6.5-7.5. Petri dishes containing only seeds and deionized water were used as the control experiment.

The growth inhibition expressed as the length of roots/shoots, as well as the germination index, given as the number of germinated seeds, were the endpoints evaluated for racemic lupanine experiments. The following equation was applied (A: average number of germinated seeds and average root and shoot length in the control, B: average number of germinated seeds and average root and shoot length in the 5 test concentrations):

$$\% \text{ Inhibition} = \frac{A-B}{A} \times 100 \quad (11)$$

Subsequently, growth inhibition was correlated to racemic lupanine concentration and the corresponding EC_{50} values were calculated.

The germination index (GI) constitutes one of the most complete indicators to represent the effect of chemical compounds on plants combining seed germination and root elongation (Kader, 2005). The specific endpoint was used to determine the toxicity of furanic compounds to dicotyledon plants. The calculation of GI was conducted according to the standard method described in Barrena et al. (2009). The categories of acute toxicity for terrestrial plants based on GI values were classified as inhibitory (<90%), non-effective or nontoxic (90-110%) and stimulant (>110%) (Baran and Tarnawski, 2013).

2.7.6 Growth inhibition toxicity assay with eukaryotic yeast

The toxicity of different furanic compounds to the well-known yeast *S. cerevisiae* was evaluated through a growth inhibition bioassay (Revelles et al., 2005). *S. cerevisiae* was obtained from the Leibniz Institute DSMZ-German Collection of Microorganisms and Cell Cultures (Braunschweig, Germany) and maintained at 4 ^{o}C on YPD agar plates (yeast extract 10 g L^{-1}, peptone 20 g L^{-1}, dextrose 20 g L^{-1}, agar 15 g L^{-1}) and subcultured in fresh medium every month. Subcultures of *S. cerevisiae* were pregrown for 24 h at 30 ^{o}C in 250 mL flasks (working volume of 50 mL) using YPD medium. The effect of each furanic compound on the eukaryotic cells following 6 h, 12 h and 16 h of exposure was determined by diluting the inoculum in YPD medium containing either 100 mg L^{-1} or 500 mg L^{-1} of each furanic compound, while the optical density (600 nm) at the beginning of the experiment was 0.1 corresponding to $3x10^{6}$ cells. All experiments were performed in duplicate using 10 mL test tubes (3 mL working volume) at 30 °C, 100 rpm and pH 7.5-8.5. A UV/VIS spectrophotometer (HACH DR 1900, Colorado, USA) was used to measure biomass absorbance (600 nm). *S. cerevisiae* culture grown in YPD medium was used as the control experiment.

Growth inhibition was expressed as the growth inhibition of test cultures as compared to control cultures following the incubation period. The following equation

was applied (G_c: mean value of OD_{600} of control cultures, G_T: mean value of OD_{600} of test cultures):

$$\% \text{ Inhibition} = \frac{Gc - Gt}{Gc} \times 100 \quad (12)$$

2.8 Statistical analysis

The objective of statistical analysis was to verify the results obtained from analytical methods. Thus, one-way analysis of variance (ANOVA) was conducted and $p<0.05$ was defined as the acceptable level of significance.

3 RESULTS AND DISCUSSION

3.1 Bioconversion of alkaloids to high-value chemicals: Comparative analysis of newly isolated lupanine degrading strains

Bioconversion constitutes a major process for the transformation of organic compounds from one form to another often reducing the persistency and toxicity of environmental pollutants. Moreover, the products of biotransformation maintain the original carbon skeleton, enabling extensive application of bioprocesses for the generation of high added-value metabolites (Bianchini et al., 2015). Thus, bioconversion has been extensively utilized over the past decades both for the bioremediation of toxic organic waste and the production of various organic compounds used in food, pharmaceutical, agrochemical and other industries (Smitha et al., 2017).

Lupanine constitutes a toxic quinolizidine alkaloid existing in the wastewater generated from lupin beans snack manufacture. The specific molecule entails an asymmetric structure that includes useful functionalities for the fine chemicals and pharmaceutical industries and may serve as a starting material for the semisynthesis of a range of new and known alkaloids with high added-value (Villalpando-Vargas and Medina-Ceja, 2016). Nevertheless, lupanine is not considered an easy target for chemical modification due to the presence of stable amide and tertiary amine functionalities (Smith et al., 2002). Thus, apart from the development of biological treatment approaches for detoxification of lupin beans snack industry wastewater, bioconversion could be applied to modify this natural molecule aiming to produce new structures more prone to chemical modification reducing the cost required (Rathbone and Bruce, 2002).

The current chapter provides information about the isolation of microorganisms that hold the capacity to metabolize racemic lupanine under both aerobic and anaerobic conditions, using different environmental samples (Section 3.1.1), the biodegradation of racemic lupanine by aerobic strains (Section 3.1.2) and the identification of the end-products formed via microbial conversion of racemic lupanine (Section 3.1.3). These data have been published in Parmaki et al. (2018).

3.1.1 Isolation and characterization of racemic lupanine metabolizing strains

Samples from four environmental sources were enriched with racemic lupanine as the sole source of carbon under aerobic and anaerobic conditions. Following three sequential enrichment cultivations of the samples in liquid medium significant growth was observed and grown cells were subsequently inoculated into a solid medium. Eight bacterial strains (4 aerobic and 4 anaerobic) were purified holding the capacity to grow on racemic lupanine at a concentration level of 1.5 g L^{-1}. Based on the phylogenetic and physiological characteristics, aerobic strains derived from granular sludge, digested sludge, aerobic sludge and wastewater from the lupin beans snack industry were identified as *Rhodococcus ruber* LPK111 (ACN: MF455224.1), *Rhodococcus rhodochrous* LPK211 (ACN: MF455223.1), *Rhodococcus* sp. LPK311 (ACN: MF455225.1) and *Pseudomonas putida* LPK411 (ACN: MF455219.1) respectively. Moreover, the isolated strains from anaerobic cultures of granular sludge were identified as *Pseudomonas citronellolis* LPK121 (ACN: MF455218.1) and *Rhodobacter* sp. LPK122 (ACN: MF455222.1), while the strains derived from digested sludge were identified as *Pseudomonas* sp. LPK221 (ACN: MF455221.1) and *Ochrobactrum tritici* LPK222 (ACN: MF455217.1) (Table 3.1). All strains demonstrated sequence homology higher than 99% to similar strains and their internal transcribed spacer sequence (ITS) was deposited in GenBank. Thus, the phylogenetic trees (Fig 3.1) based on the ITS were constructed using the neighbour-joining method implemented in the multiple alignment software ClustalW (MEGA 6.0) to correlate the isolated strains with other microorganisms that shared similar ITS gene sequence.

Table 3.1: Newly isolated lupanine metabolizing strains 16S RNA sequence

Microorganism (ACN)	**Nucleotide sequence**
Rhodococcus ruber LPK111 (MF455224.1)	TGAATCATGGCTCAGGACGAACGCTGGCGGCGTGCTTAACACATGCAAGTCGAACGATGAAGCCCAGCTTGCTGGGTGGATTAGTGGCGAACGGGTGAG TAACACGTGGGTGATCTGCCCTGCACTTCGGGATAAGCCTGGGAAACTGGGTCTAATACCGGATAGGACCTCGGGATGCATGTTCCGGGGTGGAAAGGT TTTCCGGTGCAGGATGGGCCCGCGGCCTATCAGCTTGTTGGTGGGGTAACGGCCCACCAAGGCGACGACGGGTAGCCGGCCTGAGAGGGCGACCGGCCA CACTGGGACTGAGACACGGCCCAGACTCCTACGGGAGGCAGCAGTGGGGAATATTGCACAATGGGCGCAAGCCTGATGCAGCGACGCCGCGTGAGGGA TGACGGCCTTCGGGTTGTAAACCTCTTTCAGTACCGACGAAGCGCAAGTGACGGTAGGTACAGAAGAAGCACCGGCCAACTACGTGCCAGCAGCCGCGG TAATACGTAGGGTGCGAGCGTTGTCCGGAATTACTGGGCGTAAAGAGCTCGTAGGCGGTTTGTCGCGTCGTCTGTGAAAACCCGCAGCTCAACTGCGGG CTTGCAGGCGATACGGGCAGACTTGAGTACTGCAGGGGAGACTGGAATTCCTGGTGTAGCGGTGAAATGCGCAGATATCAGGAGGAACACCGGTGGCG AAGGCGGGTCTCTGGGCAGTAACTGACGCTGAGGAGCGAAAGCGTGGGTAGCGAACAGGATTAGATACCCTGGTAGTCCACGCCGTAAACGGTGGGCG CTAGGTGTGGGTTTCCTTCCACGGGATCCGTGCCGTAGCTAACGCATTAAGCGCCCCGCCTGGGGAGTACGGCCGCAAGGCTAAAACTCAAAGGAATTG ACGGGGGCCCGCACAAGCGGCGGAGCATGTGGATTAATTCGATGCAACGCGAAGAACCTTACCTGGGTTTGACATACACCGGACCGCCCCAGAGATGGG GTTTCCCTTGTGGTCGGTGTACAGGTGGTGCATGGCTGTCGTCAGCTCGTGTCGTGAGATGTTGGGTTAAGTCCCGCAACGAGCGCAACCCTTGTCCTGTG TTGCCAGCACGTAATGGTGGGGACTCGCAGGAGACTGCCGGGGTCAACTCGGAGGAAGGTGGGGACGACGTCAAGTCATCATGCCCCTTATGTCCAGGG CTTCACACATGCTACAATGGCCGGTACAGAGGGCTGCGATACCGCGAGGTGGAGCGAATCCCTTAAAGCCGGTCTCAGTTCGGATCGGGGTCTGCAACT CGACCCCGTGAAGTCGGAGTCGCTAGTAATCGCAGATCAGCAACGCTGCGGTGAATACGTTCCCGGGCCTTGTACACACCGCCCGTCACGTCATGAAAG TCGGTAACACCCGAAGCCGGTGGCCTAACCCCTCGTGGGAA

Table 3.1: (continued)

Microorganism (ACN)	Nucleotide sequence
R. rhodochrous LPK211 (MF455223.1)	GAAAGCCTGATGCAGCGACGCCGCGTGAGGGATGACGGCCTTCGGGTTGTAAACCTCTTTCAGCAGGGACGAAGCGAAAGTGACGGTACCTGCAGAAG AAGCACCGGCCAACTACGTGCCAGCAGCCGCGGTAATACGTAGGGTGCGAGCGTTGTCCGGAATTACTGGGCGTAAAGAGCTCGTAGGCGGTTTGTCGC GTCGTCTGTGAAATCCCGCAGCTCAACTGCGGGCTTGCAGGCGATACGGGCAGACTCGAGTACTGCAGGGGAGACTGGAATTCCTGGTGTAGCGGTGAA ATGCGCAGATATCAGGAGGAACACCGGTGGCGAAGGCGGGTCTCTGGGCAGTAACTGACGCTGAGGAGCGAAAGCGTGGGTAGCGAACAGGATTAGAT ACCCTGGTAGTCCACGCCGTAAACGGTGGGCGCTAGGTGTGGGTTTCCTTCCACGGGATCCGTGCCGTAGCCAACGCATTAAGCGCCCCGCCTGGGGAGT ACGGCCGCAAGGCTAAAACTCAAAGGAATTGACGGGGGCCCGCACAAGCGGCGGAGCATGTGGATTAATTCGATGCAACGCGAAGAACCTTACCTGGG TTTGACATGTACCGGACGACTGCAGAGATGTGGTTTCCCTTGTGGCCGGTAGACAGGTGGTGCATGGCTGTCGTCAGCTCGTGTCGTGAGATGTTGGGTT AAGTCCCGCAACGAGCGCAACC
Rhodococcus sp. LPK311 (MF455225.1)	CTCAGGACGAACGCTGGCGGCGTGCTTAACACATGCAAGTCGAACGATGAAGCCCAGCTTGCTGGGTGGATTAGTGGCGAACGGGTGAGTAACACGTGG GTGATCTGCCCTGCACTTCGGGATAAGCCTGGGAAACTGGGTCTAATACCGGATAGGACCTCGGGATGCATGTTCCGGGGTGGAAAGGTTTTCCGGTGCA GGATGGGCCCGCGGCCTATCAGCTTGTTGGTGGGGTAACGGCCCACCAAGGCGACGACGGGTAGCCGGCCTGAGAGGGCGACCGGCCACACTGGGACT GAGACACGGCCCAGACTCCTACGGGAGGCAGCAGTGGGGAATATTGCACAATGGGCGCAAGCCTGATGCAGCGACGCCGCGTGAGGGATGACGGCCTT CGGGTTGTAAACCTCTTTCAGTACCGACGAAGCGCAAGTGACGGTAGGTACAGAAGAAGCACCGGCCAACTACGTGCCAGCAGCCGCGGTAATACGTAG GGTGCGAGCGTTGTCCGGAATTACTGGGCGTAAAGAGCTCGTAGGCGGTTTGTCGCGTCGTCTGTGAAAACCCGCAGCTCAACTGCGGGCTTGCAGGCG ATACGGGCAGACTTGAGTACTGCAGGGGAGACTGGAATTCCTGGTGTAGCGGTGAAATGCGCAGATATCAGGAGGAACACCGGTGGCGAAGGCGGGTC TCTGGGCAGTAACTGACGCTGAGGAGCGAAAGCGTGGGTAGCGAACAGGATTAGATACCCTGGTAGTCCACGCCGTAAACGGTGGGCGCTAGGTGTGG GTTTCCTTCCACGGGATCCGTGCCGTAGCTAACGCATTAAGCGCCCCGCCTGGGGAGTACGGCCGCAAGGCTAAAACTCAAAGGAATTGACGGGGGCCC GCACAAGCGGCGGAGCATGTGGATTAATTCGATGCAACGCGAAGAACCTTACCTGGGTTTGACATACACCGGACCGCCCCAGAGATGGGGTTTCCCTTG TGGTCGGTGTACAGGTGGTGCATGGCTGTCGTCAGCTCGTGTCGTGAGATGTTGGGTTAAGTCCCGCAACGAGCGCAACCCTTGTCCTGTGTTGCCAGCA CGTAATGGTGGGGACTCGCAGGAGACTGCCGGGGTCAACTCGGAGGAAGGTGGGGACGACGTCAAGTCATCATGCCCCTTATGTCCAGGGCTTCACACA TGCTACAATGGCCGGTACAGAGGGCTGCGATACCGCGAGGTGGAGCGAATCCCTTAAAGCCGGTCTCAGTTCGGATCGGGGTCTGCAACT

Table 3.1: (continued)

Microorganism (ACN)	Nucleotide sequence
P. putida LPK411 (MF455219.1)	AGAGTTTGAATCATGGCTCAGATTGAACGCTGGCGGCAGGCCTAACACATGCAAGTCGAGCGGATGACGGGAGCTTGCTCCTTGATTCAGCGGCGGACG GGTGAGTAATGCCTAGGAATCTGCCTGGTAGTGGGGGACAACGTTTCGAAAGGAACGCTAATACCGCATACGTCCTACGGGAGAAAGCAGGGGACCTTC GGGCCTTGCGCTATCAGATGAGCCTAGGTCGGATTAGCTAGTTGGTGGGGTAATGGCTCACCAAGGCGACGATCCGTAACTGGTCTGAGAGGATGATCA GTCACACTGGAACTGAGACACGGTCCAGACTCCTACGGGAGGCAGCAGTGGGGAATATTGGACAATGGGCGAAAGCCTGATCCAGCCATGCCGCGTGTG TGAAGAAGGTCTTCGGATTGTAAAGCACTTTAAGTTGGGAGGAAGGGCAGTAAGTTAATACCTTGCTGTTTTGACGTTACCGACAGAATAAGCACCGGCT AACTCTGTGCCAGCAGCCGCGGTAATACAGAGGGTGCAAGCGTTAATCGGAATTACTGGGCGTAAAGCGCGCGTAGGTGGTTTGTTAAGTTGGATGTGA AAGCCCCGGGCTCAACCTGGGAACTGCATCCAAAACTGGCAAGCTAGAGTACGGTAGAGGGTGGTGGAATTTCCTGTGTAGCGGTGAAATGCGTAGATA TAGGAAGGAACACCAGTGGCGAAGGCGACCACCTGGACTGATACTGACACTGAGGTGCGAAAGCGTGGGGAGCAAACAGGATTAGATACCCTGGTAGT CCACGCCGTAAACGATGTCAACTAGCCGTTGGAATCCTTGAGATTTTAGTGGCGCAGCTAACGCATTAAGTTGACCGCCTGGGGAGTACGGCCGCAAGG TTAAAACTCAAATGAATTGACGGGGGCCCGCACAAGCGGTGGAGCATGTGGTTTAATTCGAAGCAACGCGAAGAACCTTACCAGGCCTTGACATGCAGA GAACTTTCCAGAGATGGATTGGTGCCTTCGGGAACTCTGACACAGGTGCTGCATGGCTGTCGTCAGCTCGTGTCGTGAGATGTTGGGTTAAGTCCCGTAA CGAGCGCAACCCTTGTCCTTAGTTACCAGCACGTTATGGTGGGCACTCTAAGGAGACTGCCGGTGACAAACCGGAGGAAGGTGGGGATGACGTCAAGTC ATCATGGCCCTTACGGCCTGGGCTACACACGTGCTACAATGGTCGGTACAGAGGGTTGCCAAGCCGCGAGGTGGAGCTAATCTCACAAAACCGATCGTA GTCCGGATCGCAGTCTGCAACTCGACTGCGTGAAGTCGGAATCGCTAGTAATCGCGAATCAGAATGTCGCGGTGAATACGTTCCCGGGCCTTGTACACAC CGCCCGTCACACCATGGGAGTGGGTTGCACCAGAAATAGCTAGTCTAACCTTCAGGGGGACGGTTACCACGGTGTGATTCACGACTGGGGTGAA

Table 3.1: (continued)

Microorganism (ACN)	Nucleotide sequence
P. citronellolis LPK121 (MF455218.1)	CTTCCGGATTCAGCGGCGGACGGGTGAGTAATGCCTAGGAATCTGCCTGGTAGTGGGGGACAACGTTCCGAAAGGAGCGCTAATACCGCATACGTCCTA CGGGAGAAAGTGGGGGATCTTCGGACCTCACGCTATCAGATGAGCCTAGGTCGGATTAGCTAGTAGGTGGGGTAATGGCTCACCTAGGCGACGATCCGT AACTGGTCTGAGAGGATGATCAGTCACACTGGAACTGAGACACGGTCCAGACTCCTACGGGAGGCAGCAGTGGGGAATATTGGACAATGGGCGAAAGC CTGATCCAGCCATGCCGCGTGTGTGAAGAAGGTCTTCGGATTGTAAAGCACTTTAAGTTGGGAGGAAGGGCAGTAAGTTAATACCTTGCTGTTTTGACGT TACCAACAGAATAAGCACCGGCTAACTTCGTGCCAGCAGCCGCGGTAATACGAAGGGTGCAAGCGTTAATCGGAATTACTGGGCGTAAAGCGCGCGTAG GTGGTTTGGTAAGATGGATGTGAAATCCCCGGGCTCAACCTGGGAACTGCATCCATAACTGCCTGACTAGAGTACGGTAGAGGGTGGTGGAATTTCCTGT GTAGCGGTGAAATGCGTAGATATAGGAAGGAACACCAGTGGCGAAGGCGACCACCTGGACTGATACTGACACTGAGGTGCGAAAGCGTGGGGAGCAAA CAGGATTAGATACCCTGGTAGTCCACGCCGTAAACGATGTCGACTAGCCGTTGGGATCCTTGAGATCTTAGTGGCGCAGCTAACGCGATAAGTCGACCGC CTGGGGAGTACGGCCGCAAGGTTAAAACTCAAATGAATTGACGGGGGCCCGCACAAGCGGTGGAGCATGTGGTTTAATTCGAAGCAACGCGAAGAACC TTACCTGGCCTTGACATGTCCGGAATCCTGCAGAGATGCGGGAGTGCCTTCGGGAATCGGAACACAGGTGCTGCATGGCTGTCGTCAGCTCGTGTCGTGA GATGTTGGGTTAAGTCCCGTAACGAGCGCAACCCTTGTCCTTAGTTACCAGCACGTTATGGTGGGCACTCTAAGGAGACTGCCGGTGACAAACCGGAGG AAGGTGGGGATGACGTCAAGTCATCATGGCCCTTACGGCCAGGGCTACACACGTGCTACAATGGTCGGTACAGAGGGTTGCCAAGCCGCGAGGTGGAGC TAATCCCAGAAAACCGATCGTAGTCCGGATCGCAGTCTGCAACTCGACTGCGTGAAGTCGGAATCGCTAGTAATCGTGAATCAGAATGTCACGGTGAAT ACGTTCCCGGGCCTTGTACACACCGCCCGTCACACCATGGGAGTGGGTTGCTCCAGAAGTAGCTAGTCTAACCGCAAGGGGGACGGTTACCACGGAGTG ATTCATGACTGGGGTGAAGTCGTA

Table 3.1: (continued)

Microorganism (ACN)	Nucleotide sequence
Rhodobacter sp. LPK122 (MF455222.1)	CCCTTTGCTTCGGAATAGCCTCGGGAAACTGGGAGTAATACCGAATGTGCCCTACGGGGGAAAGATTTATCGGCAAAGGATCGGCCCGCGTTGGATTAG GTAGTTGGTGAGGTAATGGCTCACCAAGCCGACGATCCATAGCTGGTTTGAGAGGATGATCAGCCACACTGGGACTGAGACACGGCCCAGACTCCTACG GGAGGCAGCAGTGGGGAATCTTAGACAATGGGGGAAACCCTGATCTAGCCATGCCGCGTGAGCGATGAAGGCCTTAGGGTTGTAAAGCTCTTTCAGCTG GGAAGATAATGACGGTACCAGCAGAAGAAGCCCCGGCTAACTCCGTGCCAGCAGCCGCGGTAATACGGAGGGGGCTAGCGTTGTTCGGAATTACTGGG CGTAAAGCGCACGTAGGCGGATTATTAAGTCGGGGGTGAAATCCCGGGGCTCAACCCCGGAACTGCCTTCGATACTGGTAGTCTTGAGGTCGAGAGAGG TGAGTGGAATTCCGAGTGTAGAGGTGAAATTCGTAGATATTCGGAGGAACACCAGTGGCGAAGGCGGCTCACTGGCTCGATACTGACGCTGAGGTGCGA AAGCGTGGGGAGCAAACAGGATTAGATACCCTGGTAGTCCACGCCGTAAACGATGAATGCCAGTCGTCGGGCAGCATGCTGTTCGGTGACACACCTAAC GGATTAAGCATTCCGCCTGGGGAGTACGGTCGCAAGATTAAAACTCAAAGGAATTGACGGGGGCCCGCACAAGCGGTGGAGCATGTGGTTTAATTCGAA GCAACGCGCAGAACCTTACCAACCCTTGACATCGAGATCGCGGTTACCAGAGATGGTTTCCTTCAGTTCGGCTGGATCTTAGACAGGTGCTGCATGGCTG TCGTCAGCTCGTGTCGTGAGATGTTCGGTTAAGTCCGGCAACGAGCGCAACCCACGTCTTCAGTTGCCAGCATTCAGTTGGGCACTCTGAAGAAACTGCC GATGATAAGTCGGAGGAAGGTGTGGATGACGTCAAGTCCTCATGGCCCTTACGGGTTGGGCTACACACGTGCTACAATGGCGATGACAATGGGCCAATC CCAAAAAGTCGTCTCAGTTCGGATTGGGGTCTGCAACTCGACCCCATGAAGTCGGAATCGCTAGTAATCGCGTAACAGCATGACGCGGTGAATACGTTCC CGGGCCTTGTACACACCGCCCGTCACACCATGGGAATTGGGTCTACCCTAAGATGGTGCGCCAACCTGTAAAGGAGGCAGCCAGCCACGGTAGGCTCAG TGACTGGGGTGAAGTCGTAACAA

Table 3.1: (continued)

Microorganism (ACN)	Nucleotide sequence
Pseudomonas sp. LPK221 (MF455221.1)	GAAAGGGACGCTAATACCGCATACGTCCTACGGGAGAAAGTGGGGGATCTTCGGACCTCACGCTATCAGATGAGCCTAGGTCGGATTAGCTAGTAGGTG GGGTAATGGCTCACCTAGGCGACGATCCGTAACTGGTCTGAGAGGATGATCAGTCACACTGGAACTGAGACACGGTCCAGACTCCTACGGGAGGCAGCA GTGGGGAATATTGGACAATGGGCGAAAGCCTGATCCAGCCATGCCGCGTGTGTGAAGAAGGTCTTCGGATTGTAAAGCACTTTAAGTTGGGAGGAAGGG CTGCAAGTTAATACCTTGTAGTTTTGACGTTACCAACAGAATAAGCACCGGCTAACTTCGTGCCAGCAGCCGCGGTAATACGAAGGGTGCAAGCGTTAAT CGGAATTACTGGGCGTAAAGCGCGCGTAGGTGGTTTGGTAAGATGGATGTGAAATCCCCGGGCTCAACCTGGGAACTGCATCCATAACTGCCTGACTAG AGTACGGTAGAGGGTGGTGGAATTTCCTGTGTAGCGGTGAAATGCGTAGATATAGGAAGGAACACCAGTGGCGAAGGCGACCACCTGGACTGATACTG ACACTGAGGTGCGAAAGCGTGGGGAGCAAACAGGATTAGATACCCTGGTAGTCCACGCCGTAAACGATGTCGACTAGCCGTTGGGATCCTTGAGATCTT AGTGGCGCAGCTAACGCGATAAGTCGACCGCCTGGGGAGTACGGCCGCAAGGTTAAAACTCAAATGAATTGACGGGGGCCCGCACAAGCGGTGGAGCA TGTGGTTTAATTCGAAGCAACGCGAAGAACCTTACCTGGCCTTGACATGTCCGGAATCCTGCAGAGATGCGGGAGTGCCTTCGGGAATCGGAACACAGG TGCTGCATGGCTGTCGTCAGCTCGTGTCGTGAGATGTTGGGTTAAGTCCCGTAACGAGCGCAACCCTTGTCCTTAGTTACCAGCGC
O. tritici LPK222 (MF455217.1)	GGGGAGCGGCAGACGGGTGAGTAACGCGTGGGAACGTACCTTTTGCTACGGAATAACTCAGGGAAACTTGTGCTAATACCGTATGTGCCCGAAAGGGGA AAGATTTATCGGCAAAGGATCGGCCCGCGTTGGATTAGCTAGTTGGTGAGGTAAAGGCTCACCAAGGCGACGATCCATAGCTGGTCTGAGAGGATGATC AGCCACACTGGGACTGAGACACGGCCCAGACTCCTACGGGAGGCAGCAGTGGGGAATATTGGACAATGGGCGCAAGCCTGATCCAGCCATGCCGCGTG AGTGATGAAGGCCCTAGGGTTGTAAAGCTCTTTCACCGGTGAAGATAATGACGGTAACCGGAGAAGAAGCCCCGGCTAACTTCGTGCCAGCAGCCGCGG TAATACGAAGGGGGCTAGCGTTGTTCGGATTTACTGGGCGTAAAGCGCACGTAGGCGGACTTTTAAGTCAGGGGTGAAATCCCGGGGCTCAACCCCGGA ACTGCCTTTGATACTGGAAGTCTTGAGTATGGTAGAGGTGAGTGGAATTCCGAGTGTAGAGGTGAAATTCGTAGATATTCGGAGGAACACCAGTGGCGA AGGCGGCTCACTGGACCATTACTGACGCTGAGGTGCGAAAGCGTGGGGAGCAAACAGGATTAGATACCCTGGTAGTCCACGCCGTAAACGATGAATGTT AGCCGTTGGGGAGTTTACTCTTCGGTGGCGCAGCTAACGCATTAAACATTCCGCCTGGGGAGTACGGTCGCAAGATTAAAACTCAAAGGAATTGACGGG GGCCCGCACAAGCGGTGGAGCATGTGGTTTAATTCGAAGCAACGCGCAGAACCTTACCAGCCCTTGACATACCGGTCGCGGACACAGAGATGTGTCTTT CAGTTCGGCTGGACCGGATACAGGTGCTGCATGGCTGTCGTCAGCTCGTGTCGTGAGATGTTGGGTTAAGTCCCGCAACGAGCGCAACCCTCGCCCTTAG TTGCCAGCATTTAGTTGGGCACTCTAAGGGGACTGCCGGTGATAAGCCGAGAGGAAGGTGGGGATGACGTCAAGTCCTCATGGCCCTTACGGGCTGGGC TACACACGTGCTACAATGGTGGTGACAGTGGGCAGCGAGCACGCGAGTGTGAGCTAATCTCCAAAAGCCATCTCAGTTCGGATTGCACTCTGCAACTCG AGTGCATGAAGTTGGAATCGCTAGTAATCGCGGATCAGCATGCCGCGGTGAATACGTTCCCGGGCCTTGTACACACCGCCCGTCACACCATGGGAGTTG GTTTTACCCGAAGGCGCTGTGCTAACCGCAAGGAGGCAGGCGACCACGGTAGGGTCAGCGACTGGGGTGAAGTCGTAACAAGGTAACCAG

Pseudomonas sp. LPK221 exhibited close similarity to *Pseudomonas* sp. IBP-A36, which holds the capacity to produce polyhydroxyalkanoates (Galia et al., 2014), while *P. citronellolis* LPK121 and *P. putida* LPK411 were similar to *P. citronellolis* P3B5 and *P. putida* OBS-2 isolated from the medicinal plants *Ocimum basilicum* and *Morinda citrifolia* respectively (Remus-Emsermann et al., 2016; unpublished results, NCBI). *O. tritici* LPK222 showed close similarity to *O. tritici* TJ3, a phenol-degrading and nitrate-reducing bacterial strain (Baek et al., 2003), and *Rhodobacter* sp. LPK122 was related to *Rhodobacter* sp. R076N. Furthermore, Fig 3.1 D demonstrates that *R. rhodochrous* LPK211 was alike *R. rhodochrous* LAZC-8, an actinomycete isolated from a clinical environment in Mexico, *Rhodococcus* sp. LPK311 was similar to *Rhodococcus* sp. K-39 (a hydrocarbon-degrading bacterial strain) and *R. ruber* LPK111 showed close similarity to *R. ruber* 2S12 (unpublished results, NCBI). Thus, the lupanine metabolizing strains isolated belong to genera strongly associated with the biodegradation of recalcitrant and toxic pollutants.

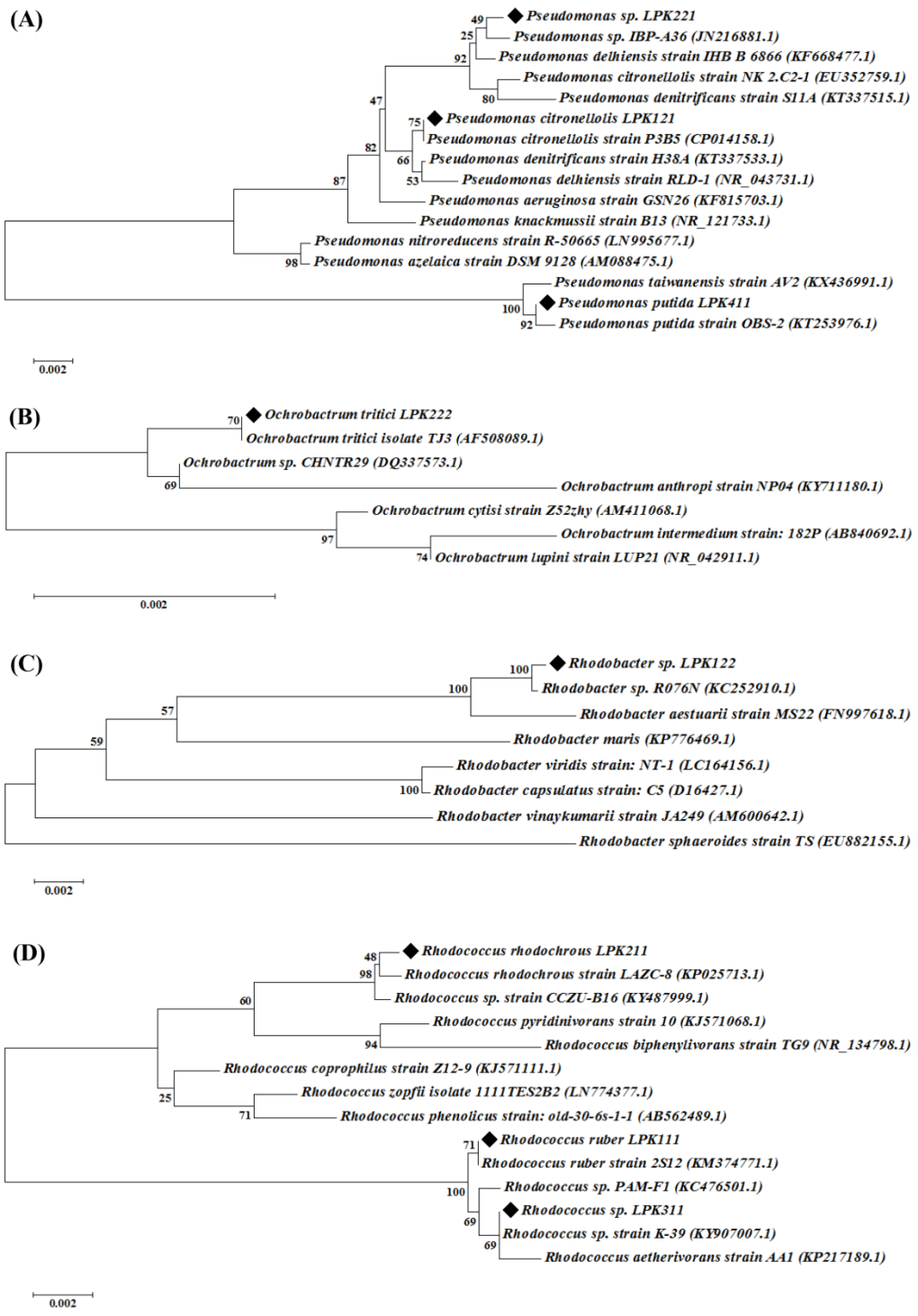

Figure 3.1: Phylogenetic trees of microbial isolates obtained through neighbour-joining analysis exhibiting the position of purified microorganisms among similar strains. Bootstrap values (expressed as percentages of 500 replications) are shown at the branch points and the scale bar represents a distance of 0.002. (A) *P. putida* LPK411, *P. citronellolis* LPK121 and *Pseudomonas* sp. LPK221, (B) *O. tritici* LPK222, (C) *Rhodobacter* sp. LPK122 and (D) *R. ruber* LPK111, *R. rhodochrous* LPK211 and *Rhodococcus* sp. LPK311.

3.1.2 Biodegradation of racemic lupanine by aerobic isolates

The microorganisms isolated under aerobic conditions (*R. rhodochrous* LPK211, *R. ruber* LPK111, *Rhodococcus* sp. LPK311 and *P. putida* LPK411), holding the capacity to utilize racemic lupanine as the sole carbon source, were grown in M9 medium containing 1.5 g L^{-1} of the alkaloid. The cultures were maintained at 31 ^{o}C, pH 7 and 100 rpm for 36-42 h, while the results demonstrate that lupanine was substantially biodegraded by all isolated strains (Fig 3.2). *R. rhodochrous* LPK211 achieved high removal of lupanine at 36 h, which corresponded to 81%, while under the same conditions *R. ruber* LPK111 and *Rhodococcus* sp. LPK311 demonstrated 66% and 71% removal of lupanine within 42 h and 36 h respectively. However, although *P. putida* LPK411 produced the lowest biomass content as compared to the three *Rhodococcus* strains, it demonstrated the shortest lag phase and significant removal of lupanine which reached 80% following 36 h of cultivation. The four anaerobic strains isolated, demonstrated very slow growth on lupanine under tested conditions and therefore these strains were not studied any further.

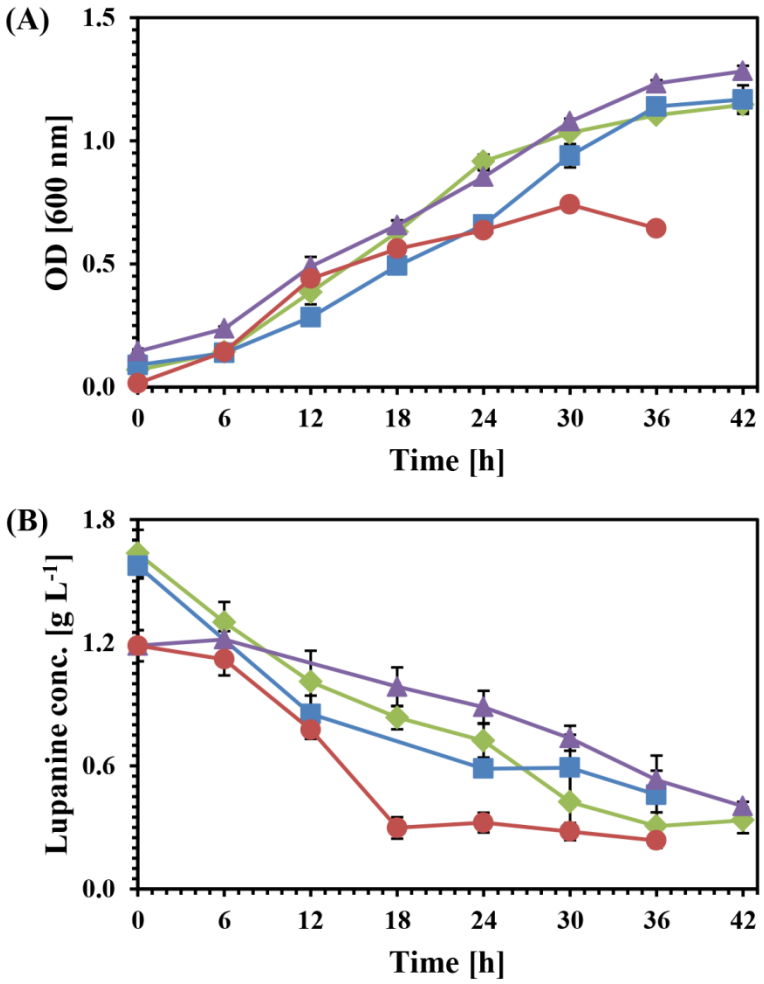

Figure 3.2: Biodegradation of racemic lupanine from aerobic microorganisms. (A) Microbial growth (expressed as OD) and (B) concentration of lupanine in cultures were performed. ■ : *Rhodococcus* sp. LPK311, ● : *P. putida* LPK411, ◆ : *R. rhodochrous* LPK211, ▲ : LPK111.

Previous studies have confirmed that *Pseudomonas* and *Rhodococcus* species hold the capacity to biodegrade a wide range of alkaloids, including among others nicotine, caffeine, codeinone and ergot alkaloids (Table 3.2). Wang et al. (2012) reported that *Pseudomonas* sp. S16 was capable of complete biodegradation of 3 g L^{-1} of nicotine within 10 h at 30 ^{o}C. Furthermore, *Pseudomonas* sp. GSC 1182 removed 80% of caffeine (1.2 g L^{-1}) within 48 h (Gokulakrishnan et al., 2007), while *Rhodococcus* sp. Y22 demonstrated 100% degradation of nicotine following 8 h of cultivation (Gong et al., 2009). *Rhodococcus erythropolis* MTHt3 could remove 5 mg L^{-1} of ergotamine and ergine within 24 h, which were converted to lysergic acid accumulating as the final metabolic product in the medium. Only a limited number of studies have led to the isolation of microorganisms capable of biodegrading lupanine. A bacterial strain isolated from soil, *Pseudomona lupanini* (recently renamed as *P. putida* Psp-LUP (Detheridge et al., 2018), achieved 88% removal of 0.7 g L^{-1} of lupanine at 27 ^{o}C within 96 h of cultivation (Mozejko-Toczko, 1960). Similar performance was achieved by bacterial strains IST20B and IST40D demonstrating 99% removal for 1 and 2 g L^{-1} of lupanine at 27 ^{o}C respectively (Santana et al., 2002). However, the specific isolated strains could not be identified.

Table 3.2: Microbial bioconversion of different alkaloids

Microorganism	Alkaloid	Removal (%)	Time (h)	Metabolites	Conc. (g L^{-1})	Reference
R. rhodochrous LPK211	Lupanine	81	36	–	1.5	Current study
R. ruber LPK111	Lupanine	66	42	lupanine *N*-oxide	1.5	Current study
R. sp. LPK311	Lupanine	71	36	lupanine *N*-oxide	1.5	Current study
P. putida LPK411	Lupanine	80	36	17-oxolupanine, molecules D-E (Fig 3.3)	1.5	Current study
P. putida Psp-LUP	Lupanine	85	96	17-hydroxylupanine	0.7	Mozejko-Toczko, (1960); Toczko, (1966)
IST20B	Lupanine	99	24	3-hydroxylupanine, 13-hydroxylupanine, 17-oxosparteine	3.0	Santana et al. (2002)
IST40D	Lupanine	99	24	3,4- dehydrolupanine, α-isolupanine	3.0	Santana et al. (2002)
Pseudomonas alcaligenes CFR 1708	Caffeine	100	30	–	1.0	Babu et al. (2005)
Pseudomonas **sp.** HF−1	Nicotine	99.6	25	–	1.3	Ruan et al. (2005)

Table 3.2: (continued)

Microorganism	Alkaloid	Removal (%)	Time (h)	Metabolites	Conc. (g L^{-1})	Reference
Pseudomonas sp. ZUTSKD	Nicotine	97	12	–	1.6	Zhong et al. (2010)
Pseudomonas sp. S16	Nicotine	100	10	–	3.0	Wang et al. (2012)
P. putida M10	Codeinone	100	72	14β-hydroxycodeine, 14β-hydroxycodeinone	3.0	Lister et al. (1999)
Rhodococcus sp. Y22	Nicotine	100	8	–	1.0	Gong et al. (2009)
R. erythropolis MTHt3	Ergotamine, ergine	100	24	Lysergic acid	0.005	Thamhesl et al. (2015)
Ochrobactrum intermedium DN2	Nicotine	97.7	36	–	0.5	Yuan et al. (2005)

3.1.3 Bioconversion of racemic lupanine for the production of high-value products

Lupanine comprises an asymmetric structure and may serve as a starting material for the semisynthesis of a range of other alkaloids (Carmali et al., 2010). Thus, apart from current efforts focusing on the use of microorganisms for debittering of lupin bean flours as well as detoxification of lupin beans industrial wastewater, the bioconversion of lupanine into modified structures could substantially enhance the effectiveness of lupanine-based chemical conversion technologies for the production of biopharmaceuticals. In line with the above, we have performed a preliminary assessment of the final metabolic products generated during bioconversion of racemic lupanine by the four aerobic strains isolated by applying NMR analysis in samples obtained at the end of the experiments presented in the previous section (Fig 3.3). There were no end-products detected for *R. rhodochrous* LPK211 indicating that racemic lupanine could be mineralized to a large extent. LPK111 and *Rhodococcus* sp. LPK311 produced the same molecule (B, Fig 3.3), the most possible structure of which constitutes 12-(l1-oxidanyl)tetradecahydro-4H-12l4-7,14-methanodipyrido[1,2-a:1',2'-e][1,5]diazocin-4-one (lupanine *N*-oxide). Three compounds (molecules C, D and E in Fig 3.3) have been observed as end-products of racemic lupanine bioconversion using *P. putida* LPK411. A ketone group at C-17 was formed at molecules C and D, while a C-N (2-1) bond was cleaved and a hydroxyl group was added to C-2 in products D and E. The potential structures of these products could be 4-(6-oxodecahydro-2H-1,5-methanopyrido[1,2-a][1,5]diazocin-4-yl)butanoic acid, 4-(decahydro-2H-1,5-methanopyrido[1,2-a][1,5]diazocin-4-yl)butanoic acid and decahydro-2H,6H-7,14-methanodipyrido[1,2-a:1',2'-e][1,5]diazocine-6,11(7H)-dione (17-oxolupanine).

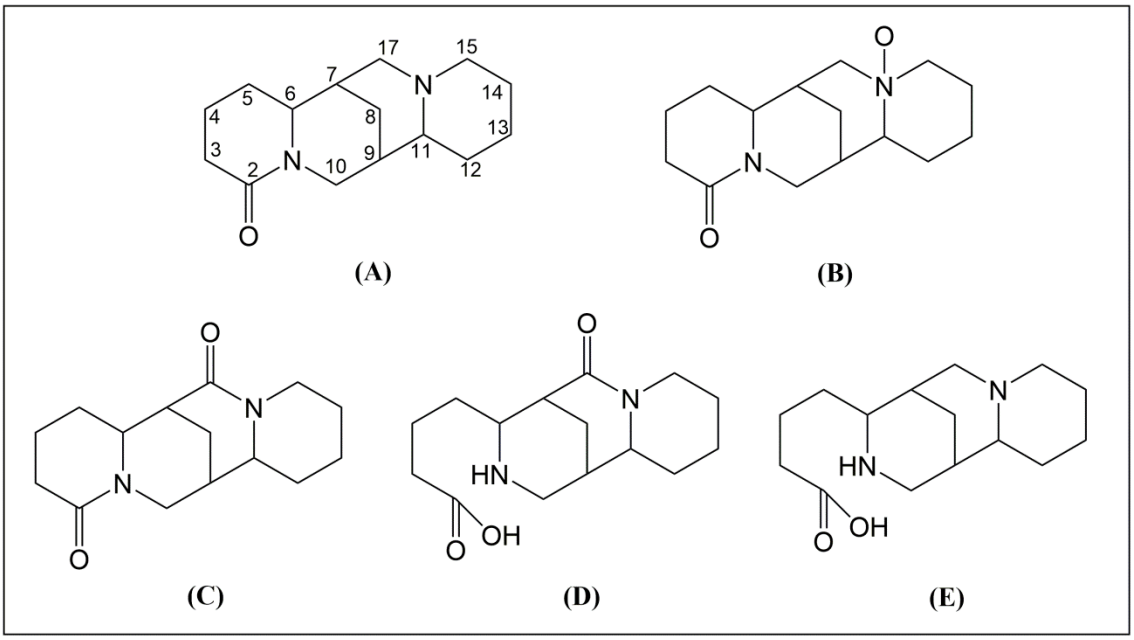

Figure 3.3: Chemical structure of lupanine and final metabolic products from racemic lupanine bioconversion identified through NMR analysis. (A): lupanine; (B): lupanine-*N*-oxide; (C): 17-oxolupanine; (D) and (E): novel structures.

Although the metabolites presented above have not been previously identified as products formed in similar biocatalytic processes, lupanine *N*-oxide (molecule B, Fig 3.3), as well as other epi-*N*-oxides, have been synthetically prepared from sparteine in a laboratory scale (Brukwicki and Wysocka, 2003). Moreover, 17-oxolupanine (molecule C, Fig 3.3) as well as lupanine, sparteine, albine, angustifoline, multiflorine and some of their derivatives have been isolated from *Lupinus* species of *L. albus*, *L. variusorientalis*, *L. hartwegii*, and *L. densiflorus* (El-Shazly et al., 2001). However, the non-rigid lupanine derivatives produced in *P. putida* LPK411 cultures (molecules D and E, Fig 3.3) constitute novel structures reported here for the first time. A few studies have been conducted to date concerning the chemical and biological conversion of lupanine. Hopper et al. (1991) reported that lupanine can be metabolized by *P. putida* Psp-LUP, where the first reaction included hydroxylation of lupanine into 17-hydroxylupanine, through the action of lupanine 17-hydroxylase. The production of 3-hydroxylupanine, 13-hydroxylupanine, 17-oxosparteine, 3,4-dehydrolupanine and α-isolupanine has been confirmed employing the two bacterial strains IST40D and IST20B (Santana et al., 2002). Moreover, Maulide et al. (2014) achieved the chemical conversion of lupanine into sparteine using $NaBH_4$ and I_2 in an organic solvent. Pertinent to the molecular structures of the final metabolic products depicted in Fig 3.3, molecules C and D derived from site-specific oxidation at carbon C-17 to the corresponding amide constitute the most promising compounds for generating useful products. The formed amide bond allows the creation of new generation sparteine analogues via alkylation on the amide bond. Thus, the present study demonstrates that both known and novel lupanine-based alkaloid structures can be produced with the use of the isolated strains.

3.2 Resolution of alkaloid racemate: A novel microbial approach for the production of enantiopure lupanine via industrial wastewater valorisation

Over the past few years, there is a growing interest in producing enantiomerically pure compounds for the food, fine chemicals, agrochemical and pharmaceutical sectors (Blaser, 2015; Fanali et al., 2019; Leek and Andersson, 2017). There is clear evidence of the advantage offered by the preparation of enantiomerically pure drugs, providing the required physiological effect, while reducing the total dose and side effects caused by the undesired enantiomer (Calcaterra and D'Acquarica, 2018). Moreover, enantiopure compounds are important for chemical industries, employing these molecules as build blocks for the production of other enantiomerically pure compounds (Maier et al., 2001).

Lupanine exists in nature as an enantiomeric mixture of D-(+)-lupanine and L-(–)-lupanine. Enantiomerically pure lupanine has attracted considerable attention in the biotechnological sector and it could be employed as feedstock for the synthesis of other enantiopure compounds with high added value (Villalpando-Vargas and Medina-Ceja, 2016). Only a few studies have currently achieved chemical resolution of racemic lupanine producing D-(+)-lupanine and L-(–)-lupanine in high purity employing chiral acids and organic solvents (Maulide et al., 2016; Przybyl and Kubicki, 2011). Thus, the development of a microbial process for the resolution of lupanine enantiomeric mixture constitutes a promising approach for the valorisation of the alkaloid existing in industrial wastewater.

This chapter provides information about the resolution of racemic lupanine by the newly isolated *P. putida* LPK411, *R. rhodochrous* LPK211 and *Rhodococcus* sp. LPK311 (Section 3.2.1), the capacity of LPK411 to utilize each of the enantiomers as single carbon substrates and the structure of the end-products formed from D-(+)-lupanine bioconversion (Section 3.2.2). Moreover, the optimal conditions of racemic lupanine biodegradation by *P. putida* LPK411 have been additionally assessed (Section 3.2.3). Data from Section 3.2.1 and Section 3.2.2 have been published in Parmaki et al. (2020).

3.2.1 Microbial resolution of racemic lupanine by aerobic isolated strains

Enantiomers comprise molecules that include the same chemical formula, as well as physical and chemical properties in a chiral environment (Fanali et al., 2019). However, the biological activity of two enantiomers could be significantly different constituting the cost-effective enantioselective synthesis an important industrial topic (Casado et al., 2019). Several processes have been employed for the manufacture of enantiopure compounds. The racemic approach includes processes of extensive industrial use, such as enantioselective liquid-liquid extraction, membrane applications and chromatography. However, employing these methods often requires the use of expensive equipment and significant amounts of organic solvents (Yuan et al., 2019). Thus, microbial resolution of racemic mixtures could be an environmentally friendly and low-cost alternative for chiral separation. In this study, the enantioselective degradation of racemic lupanine was investigated during the cultivation of three microorganisms (*P. putida* LPK411, *R. rhodochrous* LPK211, *Rhodococcus* sp. LPK311), which are capable of utilizing racemic lupanine as single carbon substrate. The results demonstrate that all microorganisms could perform resolution degrading faster D-(+)-lupanine (Fig 3.4). LPK211 and LPK311 exhibited high resolution of racemic lupanine at 42 h, which corresponded to 100% and 98% of L-(–)-lupanine ee respectively. Moreover, approximately 60% of the initial lupanine content remained in the biomedium following 42 h at both cultures demonstrating that a substantial part of L-(–)-lupanine could still be potentially present. However, *P. putida* LPK411 reached L-(–)-lupanine ee of 95% more rapidly (36 h) as compared to *Rhodococcus* strains, which was further increased to 99% at 42 h. The remaining lupanine from LPK411 cultivation at 36 h was 53% highlighting the great potential of the strain for microbial L-(–)-lupanine purification.

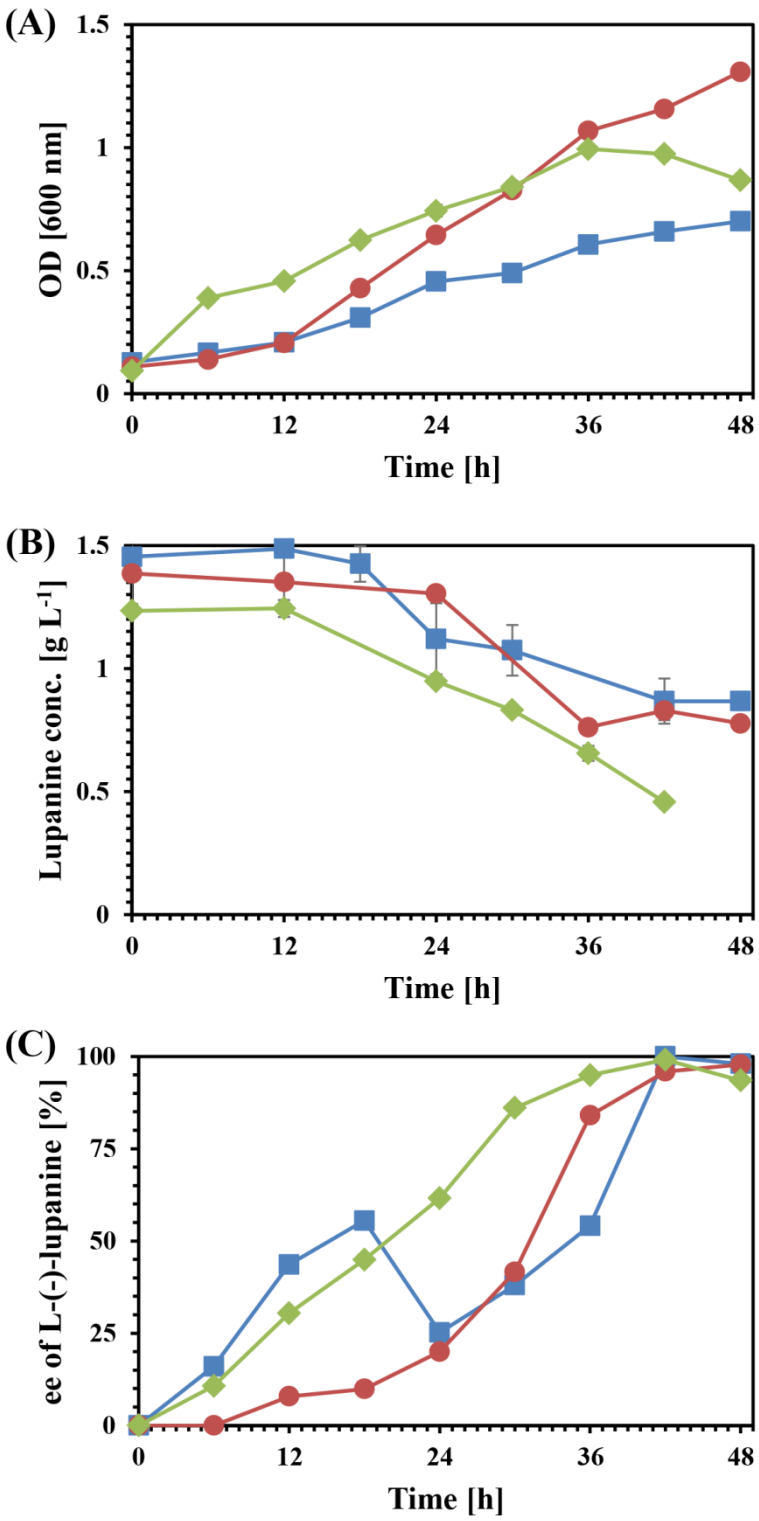

Figure 3.4: Microbial resolution of racemic lupanine. (A) Biomass growth (OD), (B) lupanine concentration and (C) ee of L-(–)-lupanine (expressed as %). ■ : *R. rhodochrous* LPK211, ● : *Rhodococcus* sp. LPK311, ◆ : *P. putida* LPK411.

The literature has shown that *Pseudomonas* and *Rhodococcus* species are capable of biodegrading enantioselectively various compounds, including aromatic and other organic molecules (Table 3.3). Ettireddy et al. (2017) reported that immobilized cells of *P. putida* (NCIB9494) were capable of resolution racemic carvedilol within 10 h, accumulating (*S*)-(–)-carvedilol at a concentration of 34.92% and purity that included 94.67% ee. Furthermore, resting cells of *Rhodococcus* sp. CCZU10-1 could remove 44.7% of racemic phenyl methyl sulfoxide, achieving enantioselectivity of (*S*)-phenyl methyl sulfoxide that reached ee >99.9% (He et al., 2013). Resolution of racemic mixtures has been also achieved through the use of purified enzymes. Wu et al. (2017) demonstrated that ω-transaminase from *P. putida* NBRC 14164 entailed high enantioselectivity to different racemic amines and amino alcohols, including α-methylbenzylamine and 2-amino-2-phenylethanol. The enzyme PpspuC achieved ee >99.0% of (*R*)-α-methylbenzylamine and (*S*)-2-amino-2-phenylethanol within 4 h and 24 h respectively, while the removal of racemic α-methylbenzylamine was 50.2% and that of racemic 2-amino-2-phenylethanol reached 50.7%. Moreover, the oxidase *Rhodococcus opacus* L-AAO incorporated wide substrate specificity and it was capable of performing resolution of racemic amino acid mixtures, including leucine and phenylalanine (Geueke and Hummel, 2002). The results show that the purified enzyme achieved ee >99.5% for D-phenylalanine and ee >99.2% for D-leucine within 24 h, demonstrating that D-leucine and D-phenylalanine concentrations were constant during the process. However, Mesnard et al. (2001) reported that in the presence of racemic nicotine, *Nicotiana plumbaginifolia* could degrade more rapidly (*R*)-nicotine as compared to the natural isomer (*S*)-nicotine. Thus far, studies have mainly focused on the application of chemical methods for the purification of lupanine enantiomers from the racemic mixture. Specifically, separation of the enantiomers could be achieved using solvents such as (+)-dibenzoyltartaric acid and ethanol in several steps (Maulide et al., 2016; Przybyl and Kubicki, 2011). The findings of the present study suggest that a two-stage process could be developed, including microbial resolution of racemic lupanine to produce enantiopure L-(–)-lupanine followed by chemical transformation of the latter into high added-value D-(+)-sparteine. Thus, the application of biocatalysts for lupanine racemate resolution could substantially reduce the experimentation required for the achievement of a cost-effective process.

Table 3.3: Biocatalytic resolution of racemic mixtures

Biocatalyst	Racemic compound	Purified enantiomer	Initial racemate conc. (g L^{-1})	Remaining racemate conc. (%)	ee (%)	Reference
P. putida LPK411	Lupanine	L-(–)-lupanine	1.23	39	99	Current study
R. rhodochrous LPK211	Lupanine	L-(–)-lupanine	1.45	60	100	Current study
Rhodococcus sp. LPK311	Lupanine	L-(–)-lupanine	1.39	60	96	Current study
P. putida (NCIB9494)	Carvedilol	*(S)*-(–)-carvedilol	0.25	34.92	95	Ettireddy et al. (2017)
Rhodococcus sp. CCZU10-1	Phenyl methyl sulfoxide	*(S)*-phenyl methyl sulfoxide	14.02	55.3	>99.9	He et al. (2013)
P. putida NBRC 14164 ω-transaminase	α-methylbenzylamine	*(R)*-α-methylbenzylamine	6.06	49.8	>99.0	Wu et al. (2017)
	2-amino-2-phenylethanol	*(S)*-2-amino-2-phenylethanol	5.49	49.3	>99.0	Wu et al. (2017)
R. opacus L-AAO oxidase	Leucine	D-leucine	0.91	50	>99.2	Geueke and Hummel, (2002)
	Phenylalanine	D-phenylalanine	1.16	50	>99.5	Geueke and Hummel, (2002)

3.2.2 Biodegradation of lupanine enantiomers by *P. putida* LPK411

The most effective microorganism in performing racemic lupanine resolution was *P. putida* LPK411. Thus, the specific strain was grown in M9 medium containing D-(+)-lupanine and L-(–)-lupanine, which were fed in separate cultures as single substrates (Fig 3.5). The results demonstrate that only D-(+)-lupanine could be metabolized substantially by the microorganism. *P. putida* LPK411 achieved D-(+)-lupanine removal of 92% following 30 h of incubation, which resulted in net biomass production of 0.21 g L^{-1}. Nevertheless, under the same conditions L-(–)-lupanine biodegradation was insignificant as confirmed by statistical analysis. Moreover, NMR was applied to identify the metabolites generated from D-(+)-lupanine biodegradation by *P. putida* LPK411 following 30 h of incubation. A single compound (molecule C3 in Fig 3.5 C) was formed as an end-product of D-(+)-lupanine biodegradation, which was identified as (trans)-6-oxooctahydro-1H-quinolizine-3-carboxylic acid.

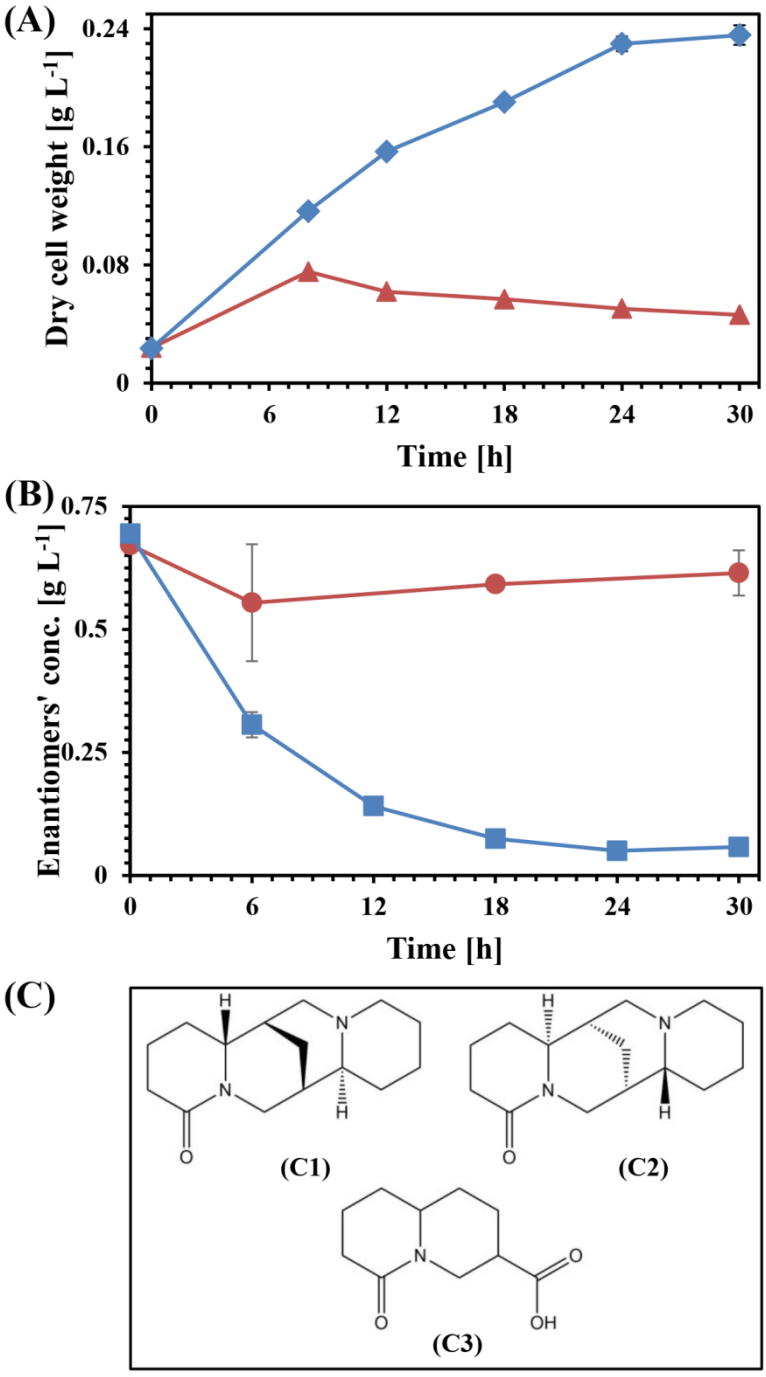

Figure 3.5: Biodegradation of D-(+)-lupanine and L-(–)-lupanine by *P. putida* LPK411. (A) Biomass growth (dry cell weight concentration), (B) concentration of D-(+)-lupanine and L-(–)-lupanine in cultures, (C) chemical structure of lupanine enantiomers and end-product formed from D-(+)-lupanine biodegradation. (C1) : D-(+)-lupanine; (C2) : L-(–)-lupanine; (C3) : (trans)-6-oxooctahydro-1H-quinolizine-3-carboxylic acid; ◆ : biomass growth on D-(+)-lupanine; ▲ : biomass growth on L-(–)-lupanine; ■ : D-(+)-lupanine concentration, ● : L-(–)-lupanine concentration.

A few studies have focused on the biodegradation of racemic quinolizidine alkaloid mixtures, while significantly less attention has been placed on the biodegradation of other racemic alkaloids. Hopper and Kaderbhai, (2003) suggested that the first step of lupanine biodegradation by *Pseudomonas* sp. occurred through the action of lupanine hydroxylase, an inducible enzyme which was active only when the microorganism was grown on D-(+)-lupanine. The enzyme remained inactive in the presence of L-(–)-lupanine indicating that it could be induced only by the growth of the strain on D-(+)-lupanine. Santana et al. (2002) demonstrated that the molecules 3-hydroxylupanine, 13-hydroxylupanine, 17-oxosparteine, 3,4-dehydrolupanine and α-isolupanine can be produced during lupanine bioconversion by unidentified microorganisms. Moreover, bioconversion experiments of racemic lupanine using *R. ruber* LPK111 and *Rhodococcus* sp. LPK311 generated the same compound (lupanine *N*-oxide) as the final metabolic product (Section 3.1.3). However, the use of *P. putida* LPK411 resulted in accumulation of three metabolic products from racemic lupanine biodegradation (17-oxolupanine and two derivatives incorporating open ring structures). The final metabolic product of D-(+)-lupanine biodegradation by *P. putida* LPK411 identified in the current study has not been previously reported as a metabolite from microbial cultivation on lupanine. However, the presence of the amide and carboxyl functionalities opens the possibility for further chemoselective functional group modifications.

3.2.3 Biodegradation of racemic lupanine by *P. putida* LPK411 under different culture conditions

The effect of different culture conditions (temperatures, pH values and initial racemic lupanine concentrations) was investigated during cultures of *P. putida* LPK411 (Fig 3.6), which is capable of utilizing racemic lupanine as a single carbon substrate. The biodegradation of racemic lupanine by *P. putida* LPK411 was initially studied under various temperatures. LPK411 achieved the highest removal of lupanine at 31 ^{o}C, which corresponded to 76%, following 12 h of cultivation. At the specific time point, the microorganism was grown at 28 ^{o}C and 34 ^{o}C demonstrating significantly lower removal of lupanine that reached 60% and 61% respectively. At the lowest temperature tested (25 ^{o}C) the removal of lupanine was further reduced to 55% following 12 h of LPK411 cultivation demonstrating that 31 ^{o}C was the temperature level enhancing both the biodegradation of the alkaloid as well as biomass production. An additional factor varied to assess its impact on the biodegradation of racemic lupanine by *P. putida* LPK411 was the pH value applied. The microorganism achieved higher lupanine removal within 12 h of cultivation using pH values between 6-7, which reached 81% (pH 7) and 79% (pH 6). Moreover, the biomass growth rate was maximised at neutral pH, while the use of an alkaline environment substantially reduced both the growth rate and the removal of lupanine, which was calculated at 69% and 49% for pH values of 8 and 9 respectively. Moreover, the biodegradation of the alkaloid by *P. putida* LPK411 was evaluated in different initial racemic lupanine concentrations. The highest lupanine removal achieved by the specific strain within 12 h was 81%, which was performed at the initial racemic lupanine concentration of 1.5 g L^{-1}. LPK411 grown at 1.0 g L^{-1} and 2.5 g L^{-1} initial racemic lupanine concentration exhibited reduced lupanine removal efficiencies, which reached 62% and 72% within 12 h and 18 h respectively. Although the use of 0.3 g L^{-1} and 3.0 g L^{-1} of initial racemic lupanine concentration further reduced the removal to 53% and 47% respectively, smaller variations were observed in the growth rate that occurred in different initial substrate contents. Based on the results obtained, the optimal culture conditions for racemic lupanine biodegradation by *P. putida* LPK411 comprise 31 ^{o}C, pH 6-7 and 1.5 g L^{-1} of initial lupanine concentration.

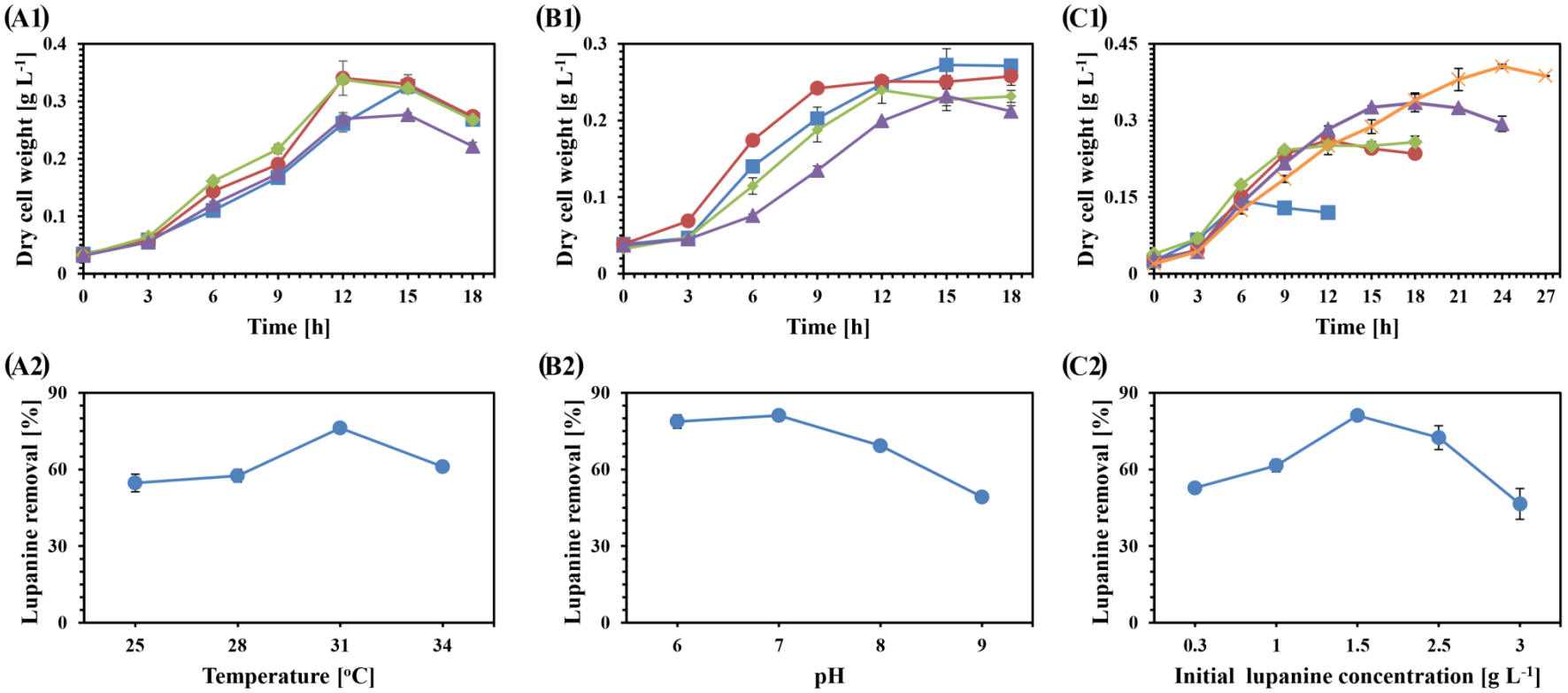

Figure 3.6: Biodegradation of racemic lupanine in different culture conditions. Subfigures show the effect of (A) temperature (: 25 °C, : 28 °C, : 31 °C, : 34 °C), (B) pH value (: 6, : 7, : 8, : 9), and (C) initial racemic lupanine concentration (: 0.3 g L^{-1}, : 1.0 g L^{-1}, : 1.5 g L^{-1}, : 2.5 g L^{-1}, : 3.0 g L^{-1}). (A1), (B1), (C1): Microbial growth (expressed as dry cell weight); (A2), (B2), (C2): Lupanine removal (expressed as percentage).

Several publications have previously indicated that *Pseudomonas* species are capable of biodegrading a wide range of organic compounds, including alkaloid and aromatic molecules, in moderate temperatures and neutral pH values (Table 3.4). Similarly to the present work, a different study focusing on lupanine biodegradation isolated *P. putida* Psp-LUP, which was capable of metabolising lupanine at an optimal temperature of 27 ^{o}C and pH value that ranged between 6-7 (Mozejko-Toczko, 1960). The unidentified bacterial strains IST20B and IST40D grown in a liquid medium simulating lupin bean processing wastewater demonstrated that the highest lupanine removal was performed at 27 ^{o}C and a pH value of 7 (Santana et al., 2002). Moreover, various studies have assessed the culture conditions required for biodegradation of well-known alkaloids, including nicotine and caffeine, by *Pseudomonas* spp. Liu et al. (2014) reported that the conditions maximising the removal of nicotine by *Pseudomonas geniculata* N1 included 30 ^{o}C and pH 6.5, while *P. alcaligenes* CFR 1708 was capable of biodegrading caffeine at an optimal temperature of 37 ^{o}C and pH value that ranged between 7-8. Furthermore, Eltoukhy et al. (2020) and Wang et al. (2015) demonstrated that *P. putida* strains LY1 and YC-AE1 could biodegrade phenol and/or phenol-based compounds exhibiting the highest substrate removal at 25-30 ^{o}C and pH values ranging between 7-8. *Pseudomonas* sp. BTEX-30 was capable of metabolising a mixture of aromatic compounds (BTEX) with optimal culture conditions of 28.9 ^{o}C and pH 7.6 (Khodaei et al., 2017), while *P. aeruginosa* LVD-10 treated toluene with the highest efficiency at 30 ^{o}C and pH 7 (Drakou et al., 2015).

Table 3.4: Culture conditions maximising the biodegradation of different substrates by *Pseudomonas* spp.

Microorganism	Temperature (ºC)	pH	Substrate	Reference
P. putida LPK411	31	6-7	Lupanine	Current study
P. putida Psp-LUP	27	6-7	Lupanine	Mozejko-Toczko, (1960)
IST20B	27	6	Lupanine	Santana et al. (2002)
IST40D	27	6	Lupanine	Santana et al. (2002)
P. geniculata N1	30	6.5	Nicotine	Liu et al. (2014)
*P. **alcaligenes*** CFR 1708	37	7-8	Caffeine	Babu et al. (2005)
P. putida LY1	25	7-8	Phenol and 4-chlorophenol	Wang et al. (2015)
P. putida YC-AE1	25-30	7.2	Bisphenol A	Eltoukhy et al. (2020)
Pseudomonas sp. BTEX-30	28.9	7.6	BTEX (benzene, toluene, ethylbenzene and xylenes)	Khodaei et al. (2017)
P. aeruginosa LVD-10	30	7	Toluene	Drakou et al. (2015)

3.3 Valorisation of alkaloid rich industrial wastewater: A novel approach for the production of enantiopure lupanine via enantioselective microbial resolution

The food processing industry requires the use of large amounts of water for the production of high quality and safe products for human consumption while generating significant quantities of wastewater (Valta et al., 2015). Lupin bean processing industries mainly employ the debittering process to eliminate the antinutritional and alkaloid contents of lupin beans, ensuring a safe snack for human consumption (Curti et al., 2018). However, the debittering process utilizes significant volumes of freshwater, which is inevitably disposed as wastewater rich in alkaloids (Carmali et al., 2010). Lupanine comprises the major quinolizidine alkaloid present in the specific wastewater (Kroc et al., 2017) constituting a neurotoxin (Wink, 2019), which in nature exists as an enantiomeric mixture (D-(+)-lupanine and L-(–)-lupanine).

Several treatment methods have been used for the remediation of wastewater emitted from the food industry, including physical, chemical, thermal and biological processes (Barbera and Gurnari, 2018). Thus far, Carmali et al. (2010) and Esteves et al. (2020) indicated that membrane processes were capable of removing lupanine from lupin bean industrial leaching waters. However, biological remediation could be an environmentally friendly, inexpensive and efficient alternative for the treatment of wastewater generated in the specific industrial sector (Azubuike et al., 2020).

The present chapter provides information about the characterization of unrefined and pretreated wastewaters generated from the lupin bean processing industry (Section 3.3.1), the microbial resolution of lupanine enantiomeric mixture achieved directly in industrial wastewater by LPK411 grown in shake-flasks (Section 3.3.2) and a lab-scale bioreactor in batch operation mode (Section 3.3.4). Moreover, the enantioselective biodegradation of racemic lupanine in repeated fed-batch cultures by LPK411 has been additionally explored (Section 3.3.3).

3.3.1 Characterization of different wastewater streams

Wastewater emitted from agricultural products processing industries could comprise inexpensive raw materials for the manufacture of high-value products due to their high nutrient content (Chen et al., 2020). Thus, characterization of the wastewater emitted from lupin beans processing could lead to the development of an integrated treatment plan enhancing the potential for the valorisation of the specific waste stream. In this study, unrefined and pretreated wastewaters of the lupin beans processing industry (UWRP, UWSP, RWSP and AWRP) were characterized for their content on different constituents (Table 3.5). UWRP contained 5-fold and 5.7-fold higher amounts of COD and lupanine as compared to UWSP respectively. RWSP constitutes a stream which was obtained via concentration of UWSP via membrane filtration, thus it contained substantially higher contents of COD and lupanine. AWRP included the lowest amounts of COD and lupanine due to pretreatment with anaerobic digestion.

Table 3.5: Characterization of different lupin bean processing wastewater streams.

Parameters	**UWSP**	**UWRP**	**RWSP**	**AWRP**
COD (g L^{-1})	9.65	48.08	52.60	1.32
Lupanine concentration (g L^{-1})	0.56	3.21	4.13	0.16
D-(+)-lupanine (%)	55	64	75	41
L-(–)-lupanine (%)	45	36	25	59
Total sugars (g L^{-1})	0.09	3.16	2.28	0.02
Reducing sugars (g L^{-1})	*	0.18	0.18	*
Total proteins (g L^{-1})	*	0.08	0.07	*
Total lipids (g L^{-1})	1.50	3.11	5.44	1.44
Total Kjeldahl nitrogen (g L^{-1})	*	0.38	0.42	0.25
Total solids ($g_{total\ solids}$ g_{sample} $^{-1}$)	0.01	0.03	0.03	-
Volatile solids (%)	81	71	88	-
Fixed solids (%)	19	29	12	-
pH value	4.16	4.09	4.07	8.35

* Bellow detection limit

To the best of our knowledge, this is the first study reporting the composition of wastewater generated from the lupin bean snack industry. However, industrial effluent has been previously applied for the production of added value commodities. Specifically, Kahnt and Hijazi, (1991) presented Lupinex, a product formed using wastewater from the lupin beans debittering process, which was developed by Mittex AG (Germany). Lupinex was used as a growth regulator and fertilizer in different crops and its composition consisted of 9.4% N, 1.26% P, 2.01% K, 0.32%, Ca, 0.52% Mg, 0.03% Na (in dry matter), 23 mg Kg^{-1} Cu, 209 mg Kg^{-1} Fe, 149 mg Kg^{-1} Mn, 226 mg Kg^{-1} Zn, 10% water, 9% residual sugars, 6% disaccharides and 5% alkaloids. However, the industrial wastewater generated from different lupin beans snack manufacturers or different batches of the same manufacturer could differ greatly in composition, due to variations in processing and raw material composition.

3.3.2 Microbial resolution of lupanine enantiomeric mixture from industrial wastewater in batch mode

Microbial resolution of the lupanine enantiomeric mixture existing in the alkaloid rich industrial wastewater exploited in the current study could provide an eco-friendly and low-cost approach for the production of useful enantiomerically pure molecules. Thus, the enantioselective biodegradation of the lupanine enantiomeric mixture contained in industrial wastewater was investigated in cultures of *P. putida* LPK411, which is capable of performing racemic lupanine resolution. The specific strain was grown in the two industrial wastewater streams (UWRP and UWSP), while although the aforementioned samples were employed without any prior treatment, the use of LPK411 in lupanine enantiomeric mixture resolution was also tested with the application of pretreated wastewaters, RWSP and AWRP. The results demonstrate that LPK411 was capable of performing enantioselective biodegradation of lupanine in different types of wastewater emitted from the lupin beans processing industry as well as pre-processed effluents (Fig 3.7). *P. putida* LPK411 grown in UWRP and UWSP wastewaters exhibited 47% and 94% of L-(–)-lupanine ee, while the removal of lupanine that existed in unrefined wastewater streams was 32% and 57% following 48 h of cultivation respectively. Moreover, LPK411 exhibited high resolution of lupanine (100% of L-(–)-lupanine ee) and 52% removal of the initial lupanine content following 6 h of cultivation in AWRP wastewater. However, the specific stain could not perform the resolution of the lupanine enantiomeric mixture existing in RWSP.

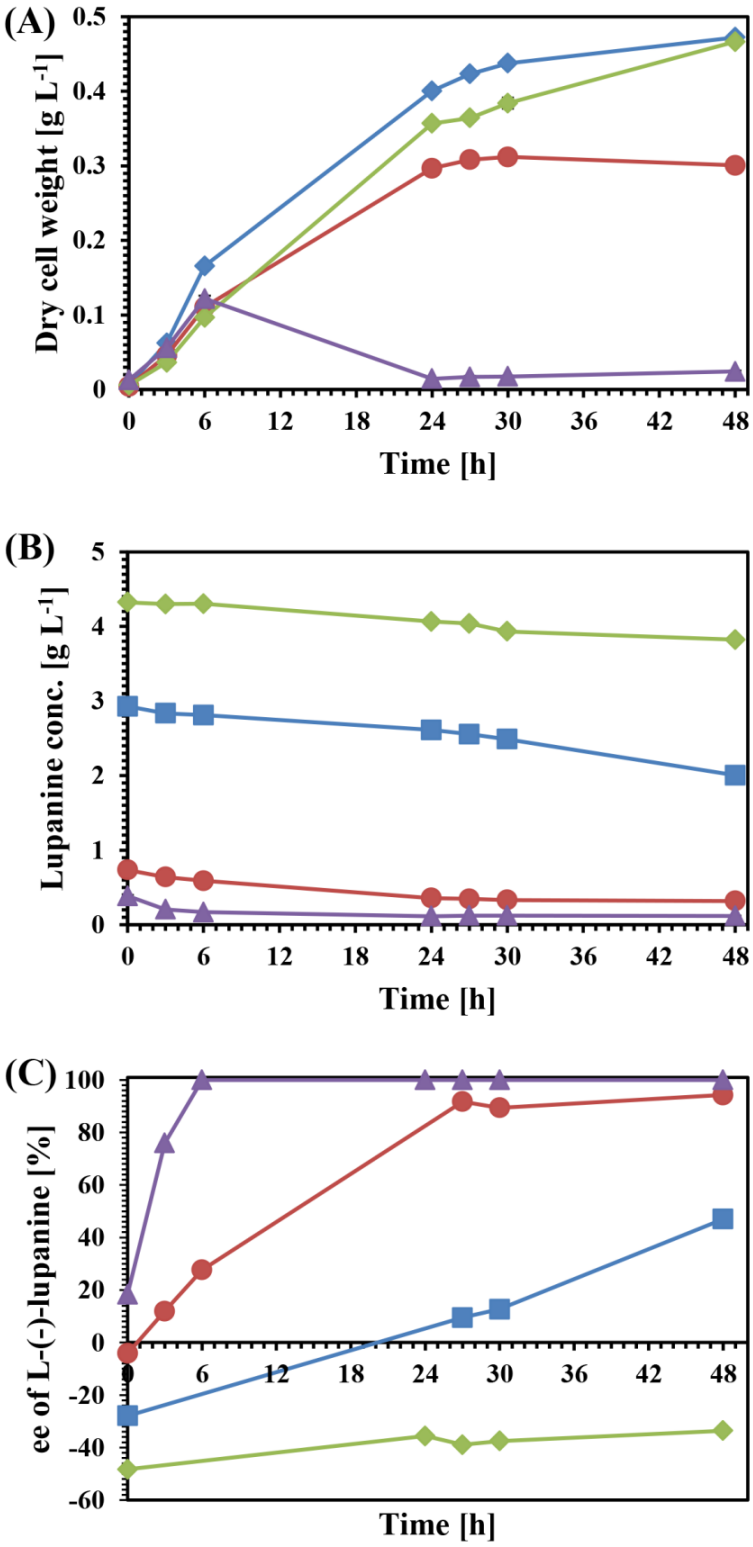

Figure 3.7: Microbial resolution of lupanine enantiomeric mixture in unrefined and pretreated industrial wastewater streams by *P. putida* LPK411. (A) Microbial growth (expressed as dry cell weight), (B) concentration of lupanine in cultures and (C) L-(–)-lupanine ee. ■ : UWRP; ● : UWSP; ◆ : RWSP; ▲ : AWRP.

A number of studies have documented that different strains are capable of biodegrading lupanine (Mozejko-Toczko, 1960; Santana et al., 1996), while significantly less attention has been placed on the valorisation of the lupanine existing in the specific wastewater streams. The current study reported that strain LPK411 exhibited high resolution and significant biodegradation of racemic lupanine at 36 h (Section 3.2.1), which corresponded to 95% of L-(–)-lupanine ee and 47% of lupanine removal. Thus, the results of Fig 3.7 indicate that the resolution of the lupanine enantiomeric mixture by LPK411 was negatively affected by the use of unrefined and pretreated wastewater streams as an alkaloid rich source. Similar performance was achieved by the Gram-negative bacterial strains IST20B and IST40D. Although the aforementioned microorganisms demonstrated 99% removal for 1 g L^{-1} and 2 g L^{-1} of lupanine respectively, IST20B performed 85% removal of alkaloids (including lupanine) from an aqueous extract of lupin beans (Santana et al., 1996), while both strains could biodegrade 77% of lupanine from an aqueous extract simulating the lupin beans industrial wastewater, Lupinex (Santana et al., 2002). Moreover, a previous study targeting lupanine valorisation has indicated that the alkaloid could be recovered by industrial wastewater via a physicochemical process, which included concentration of the alkaloid content through osmotic evaporation and lupanine isolation using organic solvents (Carmali et al., 2010). Moreover, nanofiltration could be successfully applied for the treatment of industrial lupin bean wastewater eliminating different organic compounds contained in the effluent including lupanine (Esteves et al., 2020).

3.3.3 Microbial resolution of racemic lupanine in repeated fed-batch cultures

Fed-batch bioreactor operation constitutes a widely used process in industrial applications due to the high yield and productivity that often occurs as a result of controlled substrate addition (Shimizu, 2011). Thus, the resolution of lupanine enantiomeric mixtures under fed-batch mode could serve as a promising approach for the valorisation of the wastewater generated by the lupin beans snack industry. A repeated fed-batch process for the resolution of racemic lupanine by *P. putida* LPK411 was performed (Fig 3.8). The first feeding was conducted using 200 mL of M9 medium supplemented with 1.5 g L^{-1} of racemic lupanine, while the following three substrate feedings were applied when L-(–)-lupanine ee reached higher content than 95%. Each feeding added to the existing biomedium comprised 60 mL of twice concentrated M9 medium containing 3 g L^{-1} of racemic lupanine. The results demonstrated that LPK411 achieved high resolution of lupanine racemate, which corresponded to 96% of L-(–)-lupanine ee, while 0.88 g L^{-1} of lupanine concentration remained following 9 h of cultivation. The process was significantly improved in the fourth subsequent batches performed exhibiting ee of L-(–)-lupanine, following 3 h from the beginning of the intermediate feeding, which remained higher than 92%. Moreover, biomass productivity was 0.19 $g_{biomass}$ L^{-1} h^{-1} at the first batch, which continuously decreased following subsequent feedings, reaching 0.06 $g_{biomass}$ L^{-1} h^{-1} at the final feeding. However, the lupanine utilization rate increased from 0.56 $g_{lupanine}$ L^{-1} h^{-1} to 0.70 $g_{lupanine}$ L^{-1} h^{-1} following the first repeated feeding, while at the second and third repeated feedings reached 0.82 $g_{lupanine}$ L^{-1} h^{-1} and 0.69 $g_{lupanine}$ L^{-1} h^{-1}, respectively. The results obtained from the fed-batch process indicated that LPK411 achieved a significant increase in D-(+)-lupanine biodegradation, as well as L-(–)-lupanine and biomass production, as compared to the batch cultures. Under fed-batch conditions, LPK411 additionally degraded 53% of D-(+)-lupanine and produced 49% more biomass as opposed to the corresponding batch cultures, while L-(–)-lupanine concentration increased by 49%. These findings exhibit that a repeated fed-batch process for the resolution of the lupanine enantiomeric mixture could be effective for the valorisation of lupanine existing in industrial wastewater streams.

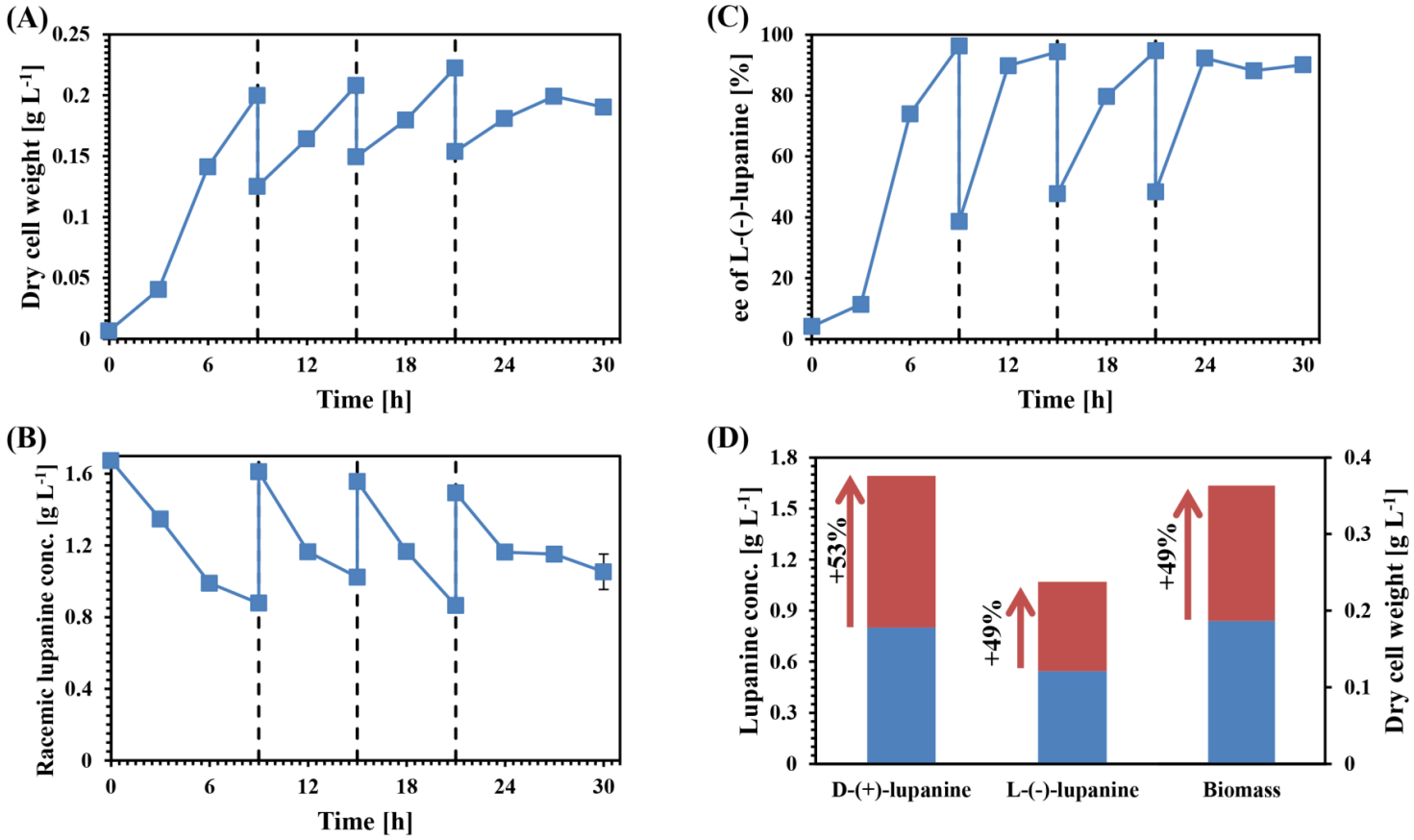

Figure 3.8: Microbial resolution of racemic lupanine in a repeated fed-batch process. (A) Microbial growth (expressed as dry cell weight), (B) concentration of lupanine in cultures, (C) L-(–)-lupanine ee and (D) D-(+)-lupanine biodegradation, as well as L-(–)-lupanine and biomass production in batch (■), and fed-batch (■) conditions.

3.3.4 Microbial resolution of lupanine enantiomeric mixture in industrial wastewater using a lab-scale bioreactor

Biotechnological processes, based on different economic advantages, have been utilized in a multitude of industrial applications, such as pharmaceutical, agrochemical and food/beverage production, as well as wastewater and biowaste treatment (Rischer et al., 2020; Roy and Bharadvaja, 2018; Vasquez et al., 2019). Thus, there is a growing interest in developing industrial batch processes for the production of speciality high added-value biomolecules (Basso and Serban, 2019). Herein, the enantioselective biodegradation of lupanine enantiomeric mixture in different unrefined wastewater streams (UWRP and UWSP) and pre-processed wastewaters (RWSP and AWRP) by *P. putida* LPK411 was assessed in a lab-scale bioreactor under batch operation to evaluate the effectiveness of the bioprocess at higher scale employing controlled conditions. The strain achieved high L-(–)-lupanine ee in unrefined and pretreated wastewaters emitted from lupin beans processing using the batch bioreactor (Fig 3.9). LPK411 grown in UWRP and UWSP wastewaters exhibited 93% and 95% of L-(–)-lupanine ee, while the removal of lupanine from both wastewater streams was 69% following 56 h and 24 h of cultivation respectively. Moreover, LPK411 performed 94% of L-(–)-lupanine ee and 83% of lupanine removal from RWSP at 48 h of cultivation, while exhibiting high-resolution capacity (100% of L-(–)-lupanine ee) and 74% removal of the initial lupanine content following 16 h of cultivation in AWRP.

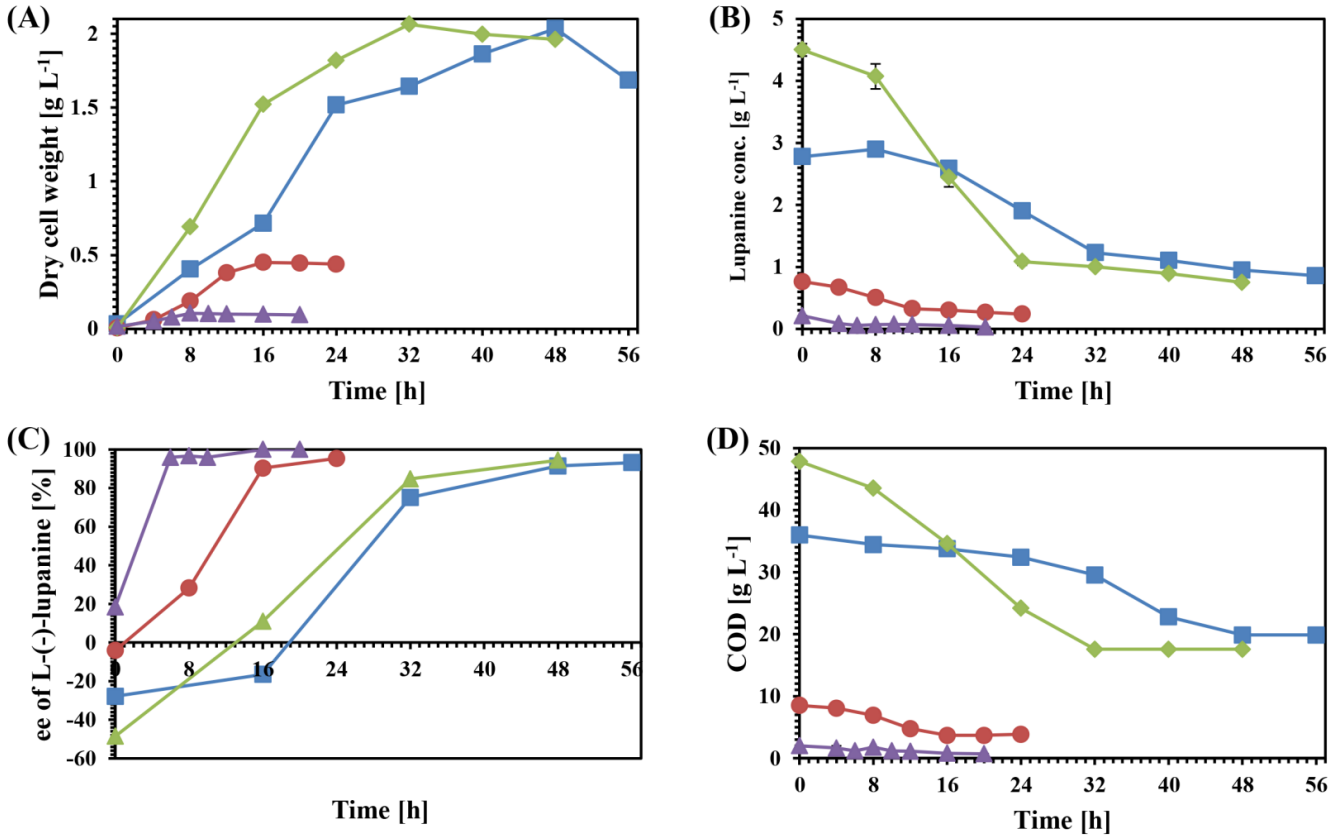

Figure 3.9: Microbial resolution of lupanine enantiomeric mixture in unrefined and pretreated industrial wastewater streams by *P. putida* LPK411 using a lab-scale bioreactor. (A) Microbial growth (expressed as dry cell weight), (B) concentration of lupanine in cultures, (C) L-(–)-lupanine ee and (D) COD concentration. ■ : UWRP; ● : UWSP; ◆ : RWSP; ▲ : AWRP.

In aerobic bioprocesses, oxygen constitutes a key substrate for microbial growth and metabolic activity. However, oxygen exhibits low solubility in water and aqueous-based culture media (Garcia-Ochoa et al., 2010). Bioreactor systems provide controlled conditions, including temperature, pH value and agitation, while continuously supplying air to ensure that oxygen limitation does not occur. A comparison of the results obtained at the bioreactor scale as compared to the use of shake flasks exhibited that the cultivation of LPK411 in the bioreactor significantly improved the resolution of the lupanine demonstrating >93% of L-(–)-lupanine ee in all wastewater streams applied. Moreover, the biomass yield was substantially enhanced in the bioreactor using the unrefined effluent UWRP and pretreated RWSP achieving 0.25 $g_{biomass}\ g_{COD}^{-1}$ and 0.06 $g_{biomass}\ g_{COD}^{-1}$ as opposed to shake flask cultures that reached 0.05 $g_{biomass}\ g_{COD}^{-1}$ and 0.03 $g_{biomass}\ g_{COD}^{-1}$, respectively. The use of UWSP achieved a similar biomass yield of LPK411 as compared to that obtained in cells grown in shake flasks and the bioreactor, corresponding to 0.10 $g_{biomass}\ g_{COD}^{-1}$. In the aforementioned wastewater streams (UWRP, UWSP, RWSP) lupanine removal rates were higher in the bioreactor achieving 0.32 $g_{lupanine}\ L^{-1}\ h^{-1}$, 0.18 $g_{lupanine}\ L^{-1}\ h^{-1}$ and 0.78 $g_{lupanine}\ L^{-1}\ h^{-1}$, while in shake-flask cultures lupanine removal rate was 0.09 $g_{lupanine}\ L^{-1}\ h^{-1}$, 0.07 $g_{lupanine}\ L^{-1}\ h^{-1}$ and 0.06 $g_{lupanine}\ L^{-1}\ h^{-1}$, respectively. Experiments performed using AWRP at bioreactor scale and shake-flasks exhibited that the biomass yield was similar at both systems reaching 0.08 $g_{biomass}\ g_{COD}^{-1}$ and 0.13 $g_{biomass}\ g_{lupanine}^{-1}$, respectively. However, the lupanine removal rate was significantly lower in the bioreactor achieving 0.10 $g_{lupanine}\ L^{-1}\ h^{-1}$, as opposed to shake-flask cultures that reached 0.14 $g_{lupanine}\ L^{-1}\ h^{-1}$.

Table 3.6: Biomass yield and lupanine removal rate for each experiment.

Wastewater	Biomass yield ($g_{biomass}\ g_{COD}^{-1}$)		Lupanine removal rate ($g_{lupanine}\ L^{-1}\ h^{-1}$)	
	shake flask	lab-scale bioreactor	shake flask	lab-scale bioreactor
UWRP	0.05	0.25	0.09	0.32
UWSP	0.10	0.10	0.07	0.18
RWSP	0.13	0.06	0.06	0.78
AWRP	0.03	0.08	0.17	0.10

3.4 Metabolism of quinolizidine alkaloids: A preliminary study of lupanine metabolism by *P. putida* LPK411

An increased research interest over the past few years in understanding and optimizing the production of added-value commodities by microbial producers has stimulated various studies pertinent to the metabolism of quinolizidine alkaloids, including lupanine and sparteine (Detheridge et al., 2018; Santana et al., 2002). Determination of transcriptional kinetics in microorganisms enables obtaining important information relevant to the expression of CCR mechanism's genes improving the knowledge about waste streams' bioconversion to high added-value chemicals and the biodegradation process triggered (Tsipa et al., 2016). Thus, future optimization of the bioprocess could be enabled through the use of important transcriptional information for the development of coupled gene expression-growth kinetic models (Koutinas et al., 2011; Tsipa et al., 2018).

The first step in lupanine biodegradation by *Pseudomonas* sp. was performed via the action of the *luh* gene, which encodes for the lupanine hydroxylase enzyme responsible for the conversion of lupanine to 17-hydroxylupanine (Hopper et al., 2002; Hopper and Kaderbhai, 2003). Moreover, carbon catabolite repression (CCR) constitutes an important mechanism in *Pseudomonas* sp. controlling the selective utilization of a preferred compound among a mixture of different carbon sources. Thus, monitoring the metabolic route responsible for metabolizing the alkaloid as well as the potential activation of the CCR mechanism in racemic lupanine biodegradation cultures of LPK411 could provide important insight into the function of the bioprocess.

This chapter provides information relevant to the expression from the gene encoding for the first enzyme of the lupanine metabolic pathway during biodegradation of racemic lupanine and lupanine enantiomers by LPK411 (Section 3.4.1) as well as the activation of the CCR mechanism in racemic lupanine and lupanine rich wastewater during biodegradation by LPK41 (Section 3.4.2). Data from Section 3.4.1 have been published in Parmaki et al. (2020).

3.4.1 Transcriptional kinetics of *luh* gene in *P. putida* LPK411 during racemic lupanine and lupanine enantiomers degradation

Gene *luh* could be the first gene expressed in the catabolic pathway of lupanine used by LPK411. Herein, systematic monitoring of transcription from the *luh* gene was performed during *P. putida* LPK411 growth in M9 medium containing the racemic alkaloid mixture or lupanine enantiomers (D-(+)-lupanine, L-(–)-lupanine) until biomass reached the stationary phase (Fig 3.10). mRNA expression of *luh* was at basal level upon racemic lupanine entry, while at the first stages of the cultures, *luh* transcription continuously increased ($p < 0.05$) reaching a peak of expression at 6 h. The direct decrease of lupanine concentration observed since the beginning of the cultures supported this claim. Thus, the maximal expression of *luh* occurred at the onset of exponential growth, where racemic lupanine biodegradation had already started, suggesting complete activation of the lupanine biodegradation pathway. Subsequently, *luh* mRNA expression was reduced to basal levels between 12 and 15 h ($p < 0.05$), where lupanine removal reached 57%. Similarly to racemic lupanine biodegradation, the addition of D-(+)-lupanine triggered the same response of *luh* transcription demonstrating a similar mRNA expression pattern ($p < 0.05$). The only difference was identified at 15 h of microbial cultivation where *luh* expression due to D-(+)-lupanine catabolism was significantly higher as compared to expression triggered by racemic lupanine. Interestingly, *luh* was not expressed immediately following L-(–)-lupanine addition remaining at a basal level for the first h of substrate induction. However, expression of *luh* sharply increased following 6 h of enantiomer addition exhibiting similar mRNA levels as compared to the use of racemic and D-(+)-lupanine ($p < 0.05$). Although expression from the catabolic gene was activated with the use of L-(–)-lupanine, which was not biodegraded in the experiment, *luh* mRNA was decreased to basal level for the rest of the cultures.

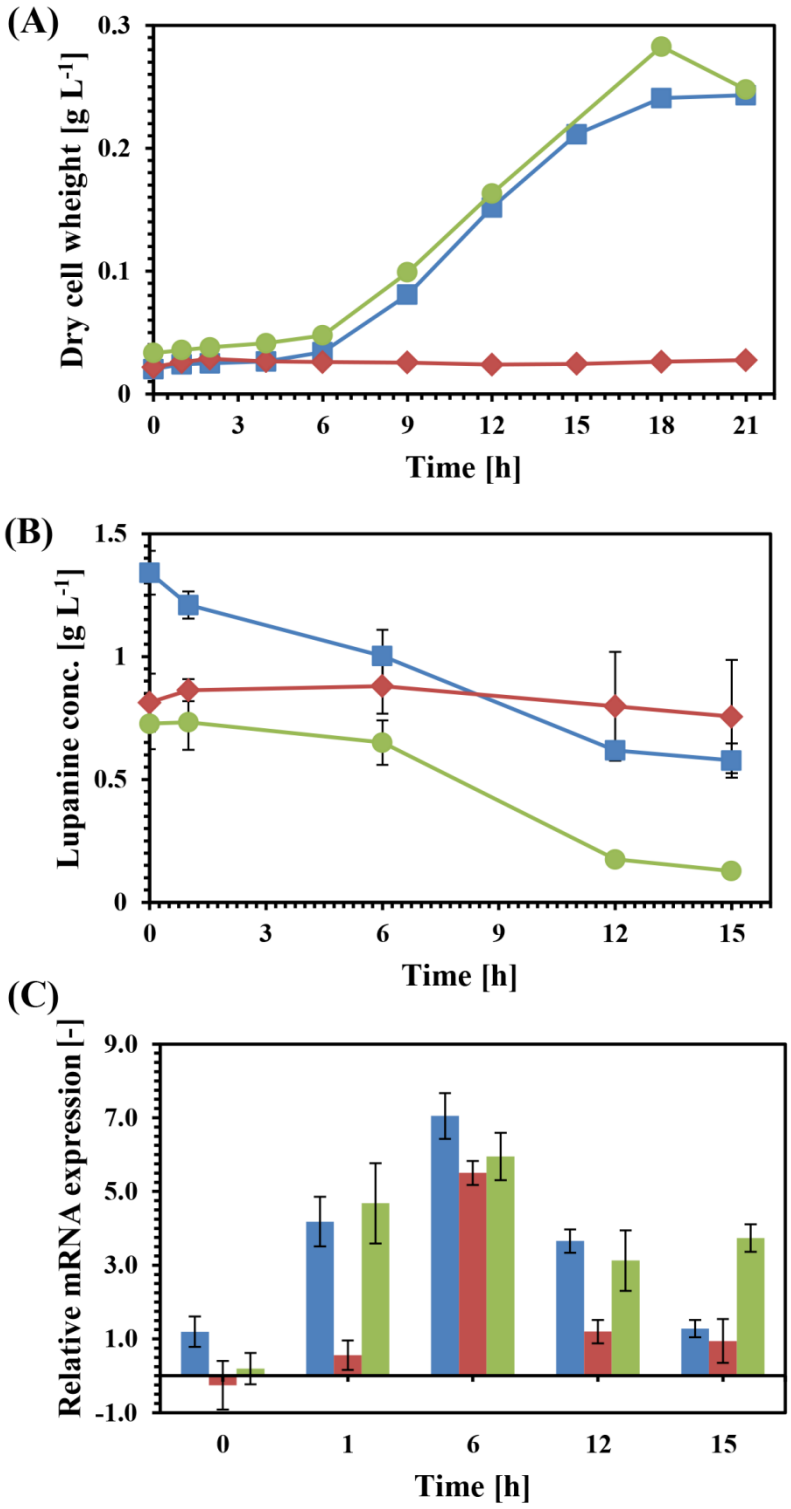

Figure 3.10: Expression from the *luh* gene of *P. putida* LPK411 during biodegradation of racemic lupanine and lupanine enantiomers. (A) Biomass growth (dry cell weight), (B) concentration of racemic lupanine and lupanine enantiomers and (C) *luh* gene relative mRNA expression. ■ : racemic lupanine, ◆ : L-(–)-lupanine, ● : D-(+)-lupanine.

The response of *luh* upon exposure to lupanine enantiomers and the racemic mixture indicates stimulation of the gene by all the molecules used. However, although these results confirm the production of the precursor mRNA molecules required for lupanine hydroxylase formation, which catalyses lupanine bioconversion to the first intermediate of the metabolic pathway, L-(–)-lupanine was not biodegraded. Thus, given that the gene is transcribed in the presence of L-(–)-lupanine either the translation process or the activation of lupanine hydroxylase cannot proceed due to the environmental signal preventing its biodegradation. Moreover, the delay of *luh* activation in the cultures conducted using L-(–)-lupanine as compared to the cultures supplemented with D-(+)-lupanine and the racemate indicate that an alternative gene activation mechanism could be potentially followed in the presence of L-(–)-lupanine.

A limited number of publications have focused on the microbial metabolism of quinolizidine alkaloids. Detheridge et al. (2018) demonstrated that the initial step in lupanine and sparteine degradation was performed through hydroxylation on carbon C-17 by hydroxylase and dehydrogenase enzymes respectively. Moreover, lupanine hydroxylase was active in *P. putida* only when D-(+)-lupanine was supplemented (Hopper and Kaderbhai, 2003). Previous studies exhibited that lupanine dehydrogenase from *P. putida* Psp-LUP is a stereospecific enzyme which catalyses only D-(+)-lupanine (Niedzielska and Rogozinski, 1973; Toczko, 1966). According to Adamu et al. (2018), stereospecific/stereoselective enzymes recognize and bind to a specific enantiomeric substrate. The present study further supports this claim through monitoring of *luh* transcriptional kinetics, confirming for the first time that *luh* mRNA gene expression is triggered by the racemate and both lupanine enantiomers, which supports the potential stereospecificity of lupanine catabolic enzymes.

3.4.2 Transcriptional kinetics of *luh* and *crc* genes in *P. putida* LPK411 during racemic lupanine and wastewater biodegradation

Herein, systematic monitoring of transcription from the *luh* and *crc* genes was performed during LPK411 growth in M9 medium supplemented with the racemic alkaloid as well as the industrial wastewater stream UWRP containing an enantiomeric mixture of lupanine (Fig 3.11). As previously described in Section 3.4.1, mRNA expression of *luh* during racemic lupanine biodegradation in the synthetic medium was continuously increased ($p < 0.05$) reaching a peak of expression at the beginning of exponential growth following 6 h of cultivation. Subsequently, *luh* mRNA expression was reduced at 12 h ($p < 0.05$), where lupanine removal reached 48%. During biodegradation of the lupanine enantiomeric mixture existing in industrial wastewater, expression from *luh* was low and remained at a constant level between 0-12 h. However, expression from *luh* sharply increased following 24 h of cultivation ($p < 0.05$), while the relative mRNA content of the gene at 36 h was reduced at the basal level. mRNA expression from the *crc* gene, which encodes for the CCR control protein, remained at a basal level between 0-12 h during racemic lupanine biodegradation, indicating that the CCR mechanism was inactive during the cultivation of the strain using racemic lupanine as the sole carbon source. Thus, although LPK411 cannot metabolize L-(–)-lupanine, the presence of the specific enantiomer during D-(+)-lupanine biodegradation does not trigger the CCR metabolic effect. However, *crc* mRNA expression during LPK411 cultivation in industrial wastewater remained at high levels between 0-12 h, while the relative activity of the gene decreased following 24 and 36 h of the process ($p < 0.05$). These results suggest that due to the presence of multiple carbon sources in the wastewater stream, *P. putida* LPK411 could potentially prefer to utilise other carbon sources existing in the effluent over lupanine. The specific effect is exhibited both by the suppression of the lupanine catabolic pathway via induction of the CCR mechanism monitored as well as the substantially low lupanine consumption rate that occurred using the industrial wastewater as compared to the application of lupanine racemate in synthetic medium.

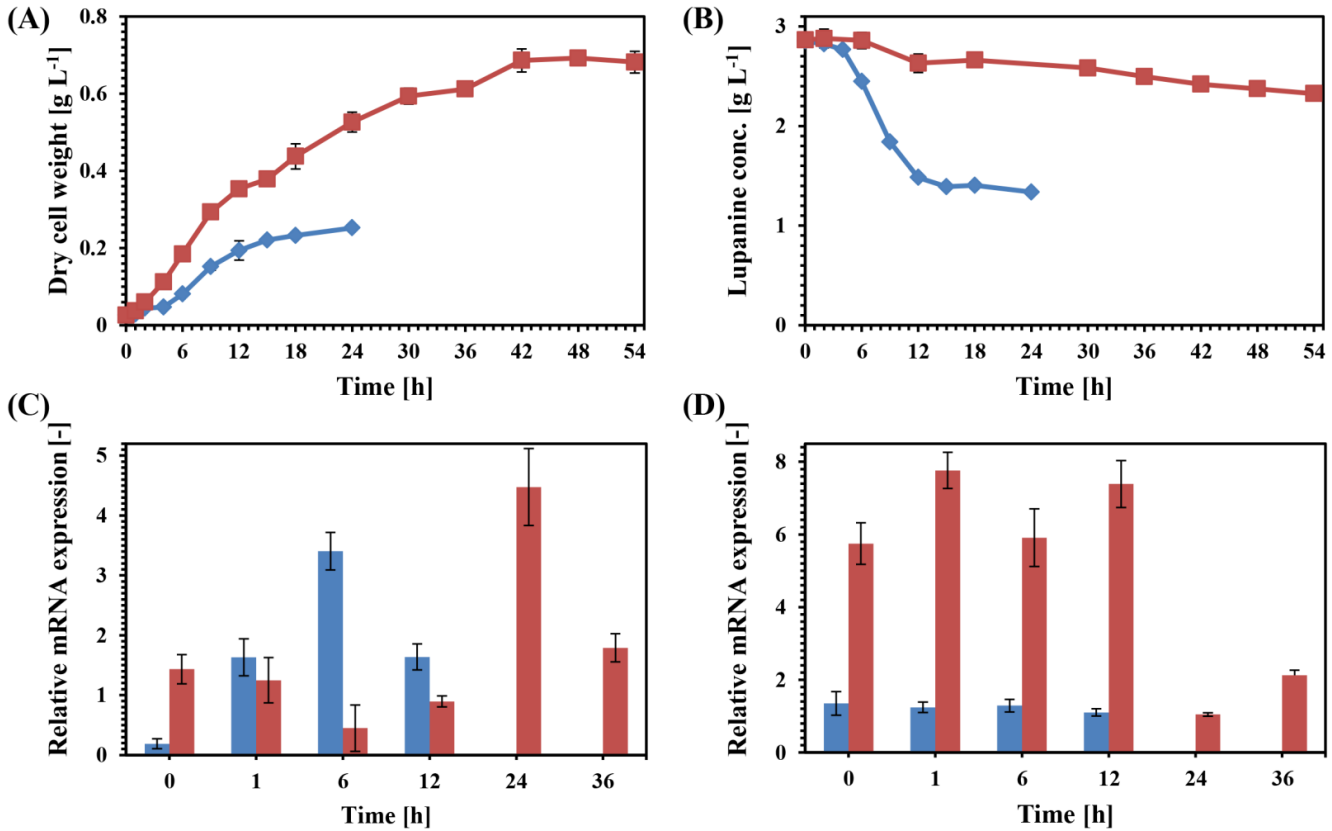

Figure 3.11: Expression from the *luh* and *crc* genes of *P. putida* LPK411 during biodegradation of racemic lupanine as the sole carbon source and the lupanine enantiomeric mixture content of industrial wastewater. (A) Biomass concentration (dry cell weight), (B) concentration of lupanine, (C) *luh* gene relative mRNA expression and (D) *crc* gene relative mRNA expression. Blue colour: racemic lupanine in M9 medium, red colour: lupanine enantiomeric mixture in UWRP wastewater.

To the best of our knowledge, this is the first work studying the simultaneous biodegradation of alkaloids and other carbon sources. Previous research has shown that in contrast to other bacteria including *E. coli* and *Bacillus* species, *Pseudomonas* prefer to biodegrade organic acids, amino acids and aromatic compounds over carbohydrates (Bharwad and Rajkumar, 2019; Rojo, 2010). The industrial wastewater (UWRP) used in the current study, apart from the lupanine enantiomeric mixture also contained lipids and sugars. Based on the mRNA expression of *crc* and *luh* genes, as well as the growth and lupanine biodegradation monitored during LPK411 cultivation in industrial wastewater, the strain could be preferentially consuming other carbon substrates available as opposed to lupanine. Thus, although the consumption of 1.52 g L^{-1} racemic lupanine as the sole substrate resulted in the production of 0.23 g L^{-1} dry cell weight, the use of 0.54 g L^{-1} of the alkaloid content of the industrial wastewater generated 0.66 g L^{-1} dry cell weight, demonstrating that the mixture of organic compounds contained in the effluent significantly affected the preference of the strain in consuming other available substrates. Moreover, expression from the *luh* gene exhibited that the catabolic pathway of lupanine was not activated since the beginning of the cultures, confirming the inhibitory effect of the presence of alternative substrates on the metabolism of the alkaloid.

3.5 Environmental toxicological assessment of natural compounds

Over the past decades, increasing concerns about human health and the environment began to arise, stimulating the development of legislative frameworks to control chemicals. Regulation (EC) No. 1907/2006 of the European Parliament and the Council of December 18, 2006, concerning the Registration, Evaluation, Authorisation and Restriction of Chemicals (REACH) was established for the protection of both human health and the environment from the potential impacts that can be caused by a chemical substance (REACH, 2006). Moreover, REACH legislation in ecotoxicology aims at evaluating and managing the toxic effects of chemical substances on ecosystems (Perazzolo and Saouter, 2013).

Different standardization organizations, including European Committee for Standardization (CEN), International Organization for Standardization (ISO), Organization for Economic Co-operation and Development (OECD) and the United States Environmental Protection Agency (US EPA), have established standardized procedures in toxicological testing. The standardization of toxicological methods has several advantages, such as facilitated comparison of data and results, increased accuracy of the data, as well as reliable replication and conduction of the test (Taylor and Scroggins, 2013).

Different bioindicators, including marine bioluminescent bacteria, freshwater crustaceans, green algae and terrestrial plants, are employed in toxicological bioassays to determine the impact of chemical compounds in aquatic and terrestrial ecosystems. *A. fischeri* is a Gram-negative, rod-shaped bacterium inhabiting marine ecosystems globally constituting a widely employed organism in ecotoxicology due to its luminescence ability. The specific marine bacterium produces light proportionally to the metabolic activity of the bacterial population, while any inhibition of enzymatic activity caused by toxicity or cell death results in a decrease in the bioluminescence produced (Parvez et al., 2006). Thus, *A. fischeri* bioluminescence inhibition bioassay is a widely used, easy, sensitive and cost-effective microscale biomonitoring tool employed to assess the acute toxicity of different compounds in the marine environment (Abbas et al., 2018). *Daphnia* species constitute common planktonic invertebrate microcrustaceans inhabiting various freshwater ecosystems, while considered very

useful model organisms in ecotoxicology. Moreover, daphnids play a significant role in the food chain, bridging the gap between primary producers and secondary consumers, while exhibiting high sensitivity to a range of substances and easy acclimation to laboratory conditions. Therefore, the acute toxicity bioassay of *D. magna* is a well-developed standard toxicity test, suitable to assess the toxicity of chemical compounds in the freshwater environment (Bownik, 2017; Wieczerzak et al., 2016). Another group of freshwater organisms used in ecotoxicological assays comprise green algae. Green algae are very important for the aquatic ecosystems, providing food to other organisms as primary producers in aquatic food webs and maintaining the ecological balance of these ecosystems (Alho et al., 2019). The specific photosynthetic cells occur in several freshwater bodies, including river streams, lakes, ponds, puddles and ditches, and they are widely used as model organisms in toxicity testing (Mani and Dinabandhu, 2015). Thus, the growth inhibition toxicity bioassay employing the green algae *R. subcapitata* is considered an appropriate test to determine the toxicity effect of chemical compounds on freshwater algae. Besides aquatic organisms, plants constitute important members of terrestrial ecosystems considering that primary producers provide food and habitat to higher trophic levels (Vonk and Kraak, 2020). Thus, damage at the first trophic level could damage the ecosystem (Rosenbaum et al., 2018). Therefore, determining the toxicity effect of chemical compounds on plants is significantly important for terrestrial ecosystems. Phytotoxicity assays using the dicotyledonous plants *L. sativum* and *S. alba* as well as the monocotyledonous plant *S. saccharatum* are frequently employed to evaluate the toxicity of different chemical compounds and effluents. The acute phytotoxicity assay constitutes an easy and quick toxicity test, while the plants selected display rapid germination and growth of roots (Antonkiewicz et al., 2019; Lago-Vila et al., 2019). Monocotyledonous and dicotyledonous plant species most obviously differ in the number of embryonic leaves (or cotyledons) within their seeds. The presence of one or two cotyledons in the embryo is associated with different morphological, physiological and biochemical features that characterize developing seeds (Sabelli, 2012). Therefore, the differences between monocotyledonous and dicotyledonous plants could lead to different sensitivities (toxicities) when exposed to chemicals (Matzke et al., 2008). *S. cerevisiae* constitutes one of the most extensively studied monocellular eukaryotic microorganisms in molecular and cell biology. Moreover, its cellular structure and functional organization has holds great similarities to cells of higher-level

organisms. Thus, the effect of different chemical compounds on *S. cerevisiae* could provide important information about the impact on higher-level organisms. The growth inhibition bioassay using *S. cerevisiae* constitutes a simple and inexpensive method to determine the effect of different compounds on eukaryotic organisms (Hung et al., 2018).

This chapter provides information about the environmental toxicity of racemic lupanine and lupanine enantiomers, L-(–)-lupanine and D-(+)-lupanine (Section 3.5.1), as well as furanic compounds (Section 3.5.2) on marine bacteria, freshwater crustaceans, green algae, monocotyledonous and dicotyledonous plants and unicellular eukaryotic organisms.

3.5.1 Environmental toxicological assessment of racemic lupanine and lupanine enantiomers

Lupanine constitutes the major alkaloid existing in the wastewater of the lupin beans snack industry. Thus far, the specific wastewater is mainly collected and treated in municipal wastewater treatment plants. However, the environmental effect of lupanine remains uncertain and a toxicological assessment should be performed to assess the environmental impact of lupin beans processing wastewater release. Herein, different toxicological tests were employed to evaluate the environmental effect of racemic lupanine (Section 3.4.1.1) and lupanine enantiomers (Section 3.4.1.2) in aquatic organisms and plants. These data have been published in Parmaki et al. (2018) and Parmaki et al. (2020).

3.5.1.1 Toxicological assessment of racemic lupanine

The toxicity of racemic lupanine was evaluated through the calculation of the half-maximal effective concentration (EC_{50}) of the two aquatic organisms, the fluorescent marine bacterium *A. fischeri* and the planktonic crustacean *D. magna*, while root growth inhibition of the plants *S. alba* and *S. saccharatum* was also determined (Fig 3.12). To evaluate the EC_{50} of *A. fischeri* nine different concentrations of racemic lupanine that varied between 8 and 2000 mg L^{-1} were tested, while to determine the EC_{50} value of *D. magna* five different concentrations of racemic lupanine that ranged between 3.125 and 100 mg L^{-1} were used. The toxicity of racemic lupanine on aquatic organisms was tested in two different durations of exposure to the alkaloid. Thus, the EC_{50} values calculated for *A. fischeri* were 89 mg L^{-1} and 47 mg L^{-1} for 5 min and 15 min of exposure, while the corresponding values for *D. magna* reached 60 mg L^{-1} and 12 mg L^{-1} following 24 h and 48 h of exposure, respectively. Moreover, the phytotoxicity imposed on dicotyledonous *S. alba* and monocotyledonous *S. saccharatum* was assessed during exposure to different racemic lupanine concentrations for 96 h. Racemic lupanine severely impacted the root growth of *S. saccharatum* demonstrating inhibition that ranged between 97-99.7% for the four highest alkaloid concentrations employed (100, 50, 25 and 12.5 mg L^{-1}). The alkaloid also inhibited the germination of *S. saccharatum* (40-80%) in the four highest concentrations tested. However, exposure to

racemic lupanine exhibited a positive effect on the root growth and it did not affect the germination of *S. alba*, which constitutes a dicotyledonous plant similarly to *L. albus*.

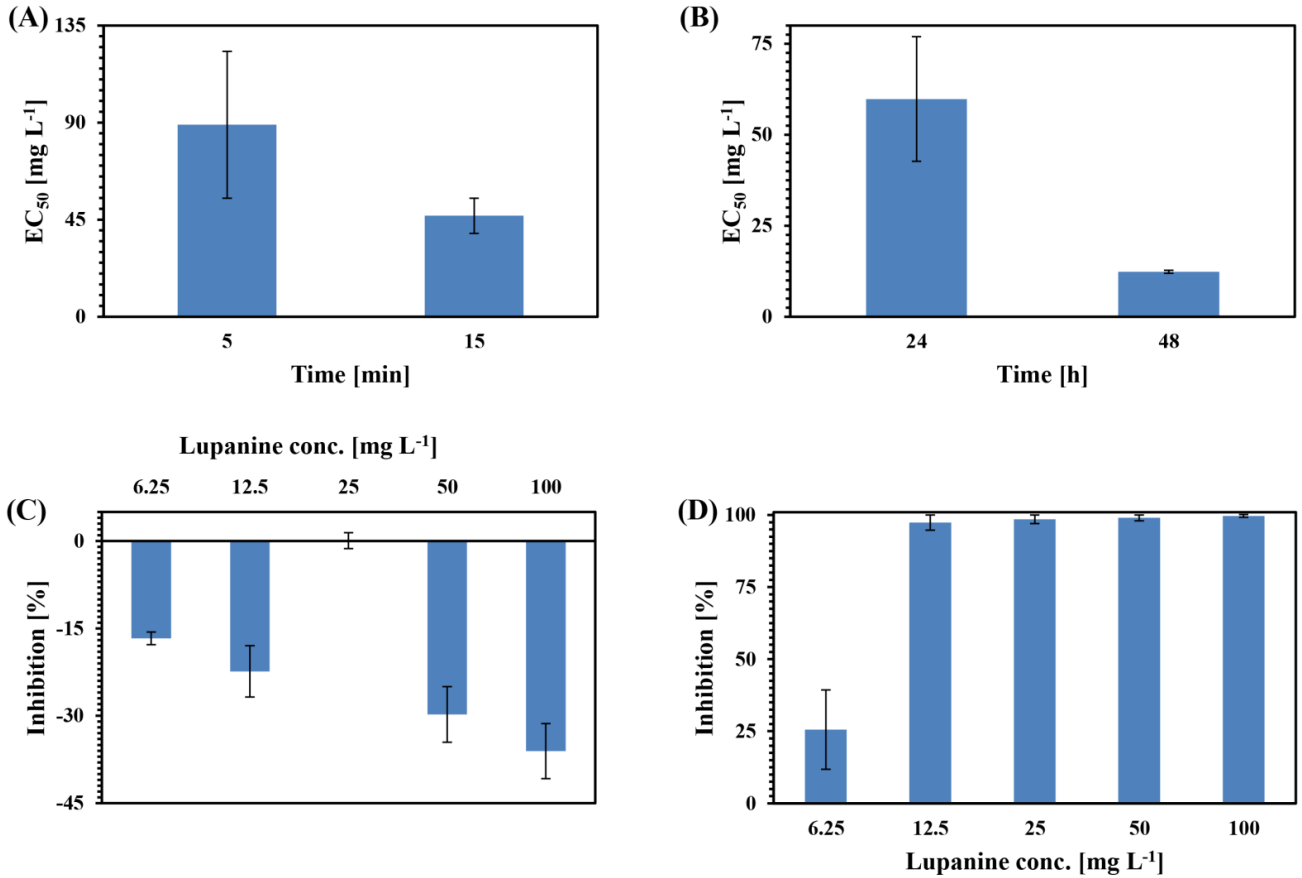

Figure 3.12: Environmental toxicological assessment of racemic lupanine on aquatic organisms and plants. EC_{50} (mg L^{-1}) values were calculated for (A) *A. fischeri* (5 min and 15 min of exposure to racemic lupanine) and (B) *D. magna* (24 h and 48 h of exposure to racemic lupanine). Inhibition of root growth was determined for (C) *S. alba* and (D) *S. saccharatum* (expressed as % root growth inhibition).

Toxicological studies have been previously conducted to assess the effect of various quinolizidine alkaloids in rodents, including mice and rats, as well as guinea pigs (Table 3.7). Thus, the corresponding LD_{50} values for intra peritoneal administration of lupanine, sparteine, 13-hydroxylupanine and 17-oxolupanine in mice were 175, 36, 172 and 690 mg kg^{-1} respectively. These results demonstrate that lupanine and 13-hydroxylupanine express equal toxicity in mice, while lupanine is more toxic as compared to 17-oxolupanine and less toxic than sparteine. Well-known alkaloids, such as caffeine and nicotine, have gained substantial interest relevant to their toxicological effect on the environment. The EC_{50} values calculated for caffeine using the *D. magna* assay were 161-684 mg L^{-1} and 182 mg L^{-1} for 24 h and 48 h of exposure respectively (Camacho-Muñoz et al., 2010) exhibiting lower toxicity as compared to lupanine. However, although Jiménez et al. (2017) reported that nicotine is non-toxic for *V. ficsheri*, the effect of lupanine on *D. magna* was less toxic than that of nicotine, which comprised EC_{50} values that reached 4-6 mg L^{-1} and 0.79 mg L^{-1} for 24 h and 48 h of exposure respectively (Jiménez et al., 2017; Martins et al., 2007). A similar toxicological study demonstrated the toxicity of lupanine to *D. magna* after 48 h and 96 h of exposure, where the EC_{50} values obtained comprised 128 mg L^{-1} and 64 mg L^{-1}, respectively (Griffiths et al., 2021). The specific study shows that the EC_{50} for *D. magna* after 48 h of exposure was approximately 10-fold higher as compared to the results obtained here while demonstrating that sparteine exhibited higher toxicity than lupanine on *D. magna*. Only a few studies have been conducted for evaluating the toxicity of alkaloids to plants. The toxic alkaloid cylindrospermopsin has been reported to inhibit the growth of *S. alba* demonstrating an IC_{50} value of 18.2 μg mL^{-1} (Vasas et al., 2002). However, quinolizidine alkaloids, such as lupanine, are important for the survival of plants acting as a defence mechanism against pathogens or predators and constitute allelopathic metabolites for competition with other plant species (Bunsupa et al., 2013). Previous studies (Cahill and Lamb, 2007) exhibit that dicotyledonous plants (e.g. *L. albus* and *S. alba*) constitute stronger competitors compared to monocotyledonous (e.g. *S. saccharatum*) suggesting that dicotyledonous develop mechanisms enabling a significant competitive advantage over other plants.

Table 3.7: Toxicological effects of alkaloids in different organisms (intraperitoneal administration (ip); intravenous administration (iv); oral administration (po)).

Alkaloid	Species	Test	Value	Reference
Lupanine	*A. fischeri*	EC_{50} (5 min)	89 mg L^{-1}	Current study
	A. fischeri	EC_{50} (15 min)	47 mg L^{-1}	Current study
	D. magna	EC_{50} (24 h)	60 mg L^{-1}	Current study
	D. magna	EC_{50} (48 h)	12 mg L^{-1}	Current study
	D. magna	EC_{50} (48 h)	128 mg L^{-1}	Griffiths et al. (2021)
	D. magna	EC_{50} (96 h)	64 mg L^{-1}	Griffiths et al. (2021)
	Mouse	LD_{50} (ip)	175 mg Kg^{-1}	Yovo et al. (1984)
	Mouse	LD_{50} (po)	410 mg Kg^{-1}	Yovo et al. (1984)
	Mouse	LD50 (ip)	80 mg Kg^{-1}	Gordon and Henderson, (1951)
	Rat	LD_{50} (ip)	177 mg Kg^{-1}	Pothier et al. (1998)
	Rat	LD_{50} (po)	1440-1664 mg Kg^{-1}	Pothier et al. (1998)
	Guinea pig	LD_{50} (ip)	210 mg Kg^{-1}	Ohmiya et al. (1995)
Sparteine	*D. magna*	EC_{50} (48 h)	28.6 mg L^{-1}	Griffiths et al. (2021)
	D. magna	EC_{50} (96 h)	14.3 mg L^{-1}	Griffiths et al. (2021)
	Mouse	LD_{50} (ip)	36 mg Kg^{-1}	Yovo et al. (1984)
	Mouse	LD_{50} (po)	220 mg Kg^{-1}	Yovo et al. (1984)
	Rat	LD_{50} (ip)	42-44 mg Kg^{-1}	Ohmiya et al. (1995)
	Rat	LD_{50} (iv)	68-75 mg Kg^{-1}	Ohmiya et al. (1995)
13-hydroxylupanine	Mouse	LD_{50} (ip)	172 mg Kg^{-1}	Ohmiya et al. (1995)
	Rat	LD_{50} (ip)	199 mg Kg^{-1}	Ohmiya et al. (1995)
17-oxolupanine	Mouse	LD_{50} (ip)	690 mg Kg^{-1}	Ohmiya et al. (1995)

Table 3.7: (continued)

Alkaloid	Species	Test	Value	Reference
Caffeine	Mouse	LD_{50} (ip)	369 mg Kg^{-1}	Mitkov et al. (2007)
	Mouse	LD_{50} (po)	527 mg Kg^{-1}	Mitkov et al. (2007)
	D. magna	EC_{50} (24 h)	161-684 mg L^{-1}	Martins et al. (2007)
	D. magna	EC_{50} (48 h)	182 mg L^{-1}	Camacho-Muñoz et al. (2010)
	D. magna	LC_{50} (24 h)	684 mg L^{-1}	Martins et al. (2007)
Nicotine	D. magna	EC_{50} (24 h)	4-6 mg L^{-1}	Martins et al. (2007)
	D. magna	EC_{50} (48 h)	0.79 mg L^{-1}	Jiménez et al. (2017)

3.5.1.2 Toxicological assessment of lupanine enantiomers on a marine bacterium

The toxicity imposed on the aquatic bacterium *A. fischeri* was calculated as the EC_{50} value corresponding to two distinct durations of exposure to each enantiomer (D-(+)-lupanine and L-(–)-lupanine). Several dilutions that varied between 75 and 1000 mg L^{-1} were prepared for each lupanine enantiomer to evaluate the toxic effect of both enantiomers on the marine bacterium. The toxicological assessment demonstrates that both D-(+)-lupanine and L-(–)-lupanine induced similar levels of toxicity for *A. fischeri*, based on EC_{50} values obtained for 5 min and 15 min of exposure that ranged between 317-320 mg L^{-1} and 372-457 mg L^{-1} respectively. Moreover, the enantiomers interaction assessment (Fig 3.13) demonstrates a very strong synergistic effect of D-(+)-lupanine and L-(–)-lupanine mixture toxicity for *A. fischeri* (CI <1).

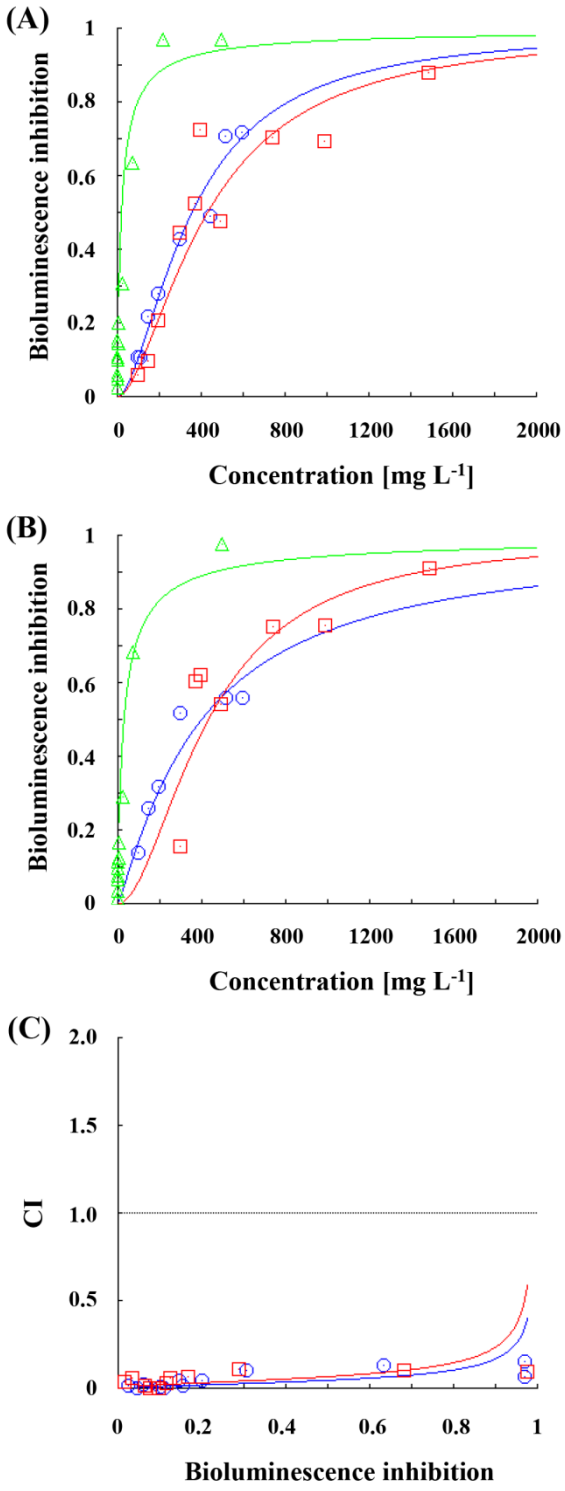

Figure 3.13: Toxicological assessment of racemate and lupanine enantiomers on *A. fischeri*. (A) Bioluminescence inhibition for 5 min of exposure, (B) bioluminescence inhibition for 15 min of exposure (△ : racemic lupanine, □ : L-(–)-lupanine, ○ : D-(+)-lupanine) and (C) toxicity interaction (expressed as CI) values calculated for different durations of exposure (○ : 5 min, □ : 15 min) to the alkaloid.

Previous studies on intravenous administration of coniine, ammodendrine and *N*-methylammodendrine enantiomers in mice demonstrated that the two molecules can incorporate similar LD_{50} values, which could be similar to that of the racemic mixture (Table 3.8). Moreover, the toxicity of the racemate often constitutes the additive result of both enantiomers, demonstrating an effect that ranges between the toxicity values of the respective enantiomers (Zhou et al., 2009). However, toxicological studies in mice report that racemic anabasine expressed higher toxicity as compared to the enantiomers (Green et al., 2012). The EC_{50} values calculated for racemic lupanine on *A. fischeri* have been determined for 5 min and 15 min of exposure as 89 mg L^{-1} and 47 mg L^{-1} respectively (Section 3.5.1.1). Thus, the results presented here indicate that lupanine enantiomers are less toxic as compared to racemic lupanine, confirming the presence of a strong synergistic effect in the toxicity action of these molecules when they exist in the form of a racemic mixture. This response is aligned with a potential absence of a specific mechanism for detoxification/transformation of these compounds in the metabolism of *A. fischeri* that could result in at least an additive effect on bioluminescence inhibition following exposure to the racemic mixture. Lin et al. (2008) reported that enantioselective biological reactions, such as in vivo chiral inversion or enantiomerization, could cause antagonistic or synergistic interactions. Nevertheless, only a few studies have yet attempted to understand the interactions between the enantiomers of chiral molecules.

Table 3.8: Toxicological effects of racemic mixtures and the respective enantiomers in different organisms (intravenous administration (iv)).

Compound	**Species**	**Test**	**Concentration**			**Reference**
			Racemate	**(+), (*R*), D**	**(–), (*S*), L**	
Lupanine	*A. fischeri*	EC_{50} (5 min)	89 mg L^{-1}	320 mg L^{-1}	317 mg L^{-1}	Current study
	A. fischeri	EC_{50} (15 min)	47 mg L^{-1}	457 mg L^{-1}	372 mg L^{-1}	Current study
Coniine	Mouse	LD_{50} (iv)	7.7 mg kg^{-1}	12.1 mg kg^{-1}	7.0 mg kg^{-1}	Lee et al. (2013)
Ammodendrine	Mouse	LD_{50} (iv)	134 mg kg^{-1}	94.1 mg kg^{-1}	115 mg kg^{-1}	Green et al. (2012)
Anabasine	Mouse	LD_{50} (iv)	1.6 mg kg^{-1}	11 mg kg^{-1}	16 mg kg^{-1}	Green et al. (2012)
N-methylammodendrine	Mouse	LD_{50} (iv)	-	56.3 mg kg^{-1}	63.4 mg kg^{-1}	Lee et al. (2005)

3.5.2 Furanic compounds: Environmental toxicological assessment of biomass-derived platform chemicals

Over the past few decades, economical and political concerns, as well as environmental issues, such as global warming, overpopulation and natural resource depletion, have increased the interest in renewable raw materials which could replace fossil fuels (Mariscal et al., 2018; Wu et al., 2016). Lignocellulosic biomass constitutes a widely available, inexpensive and abundant feedstock, which represents a promising alternative for the production of biofuels, biomaterials and biomolecules (Kabir and Hameed, 2017; Luo et al., 2019). Furanic compounds have gained high importance as value-added chemicals derived from biomass, while exhibiting various applications in different industries, including chemical, pharmaceutical, energy and food sectors (Dalvand et al., 2018; Mariscal et al., 2018). Nowadays, several furanic compounds are mainly used as green solvents, biofuels and fuel additives, lubricants, resins and plasticizers, while they can be also added to food and drinks as flavour enhancers or as intermediate in the synthesis of pharmaceuticals, chemicals and biopolymers/biomonomers (Chatterjee et al., 2014; Guigo et al., 2019; Li et al., 2016; Peleteiro et al., 2016; Qian et al., 2015). Among these molecules, furfural, 5-hydroxymethylfurfural (HMF) and furan-2,5-dicarboxylic acid (FDCA) comprise some of the most important building blocks holding the capacity to produce a wide range of valuable chemicals as determined by the U.S. Department of Energy (Choi et al., 2015). However, furanic compounds could be only commercialized if they satisfy the requirements of the REACH legislation. The specific legislation requires the protection of both human health and the environment from the potential impacts that could be caused by a chemical substance (REACH, 2006). Therefore, ecotoxicity testing is necessary to determine the toxicity imposed by furanic compounds on the environment, as well as to validate their “green” character.

Previous toxicological studies have mainly focused on furans’ effect in rodents, including mice and rats (Arts et al., 2004; Bauer-Marinovic et al., 2012; Hall et al., 1993; Høie et al., 2016; Sujatha, 2008). Furan, the parent compound for the synthesis of other furans, has been classified as carcinogenic in rodents, even at relatively low doses. Furan and its derivatives' negative impact on human health remain unclear (Batool et

al., 2020). Recent toxicological assessments of furans on aquatic organisms, including the marine bacterium *A. fischeri* and the planktonic freshwater crustacean *D. magna*, reported that furan derivatives exhibit different levels of toxicity (Ventura et al., 2016; Zuriaga et al., 2018). Given that the aforementioned studies indicated that furans were more toxic as compared to conventional solvents, their "greenness" is questionable. Nevertheless, further research is still required to confirm the environmental effects of furans.

The current section represents a comprehensive environmental toxicological assessment of fourteen furanic compounds that serve as valuable building blocks for the chemical industry, on aquatic organisms and plants. The furanic compounds used in the current study were furan-2-yl-methanol (furfuryl alcohol), furan-2-carbaldehyde (furfural), furan-2-carboxylic acid or 2-furoic acid (FA), ethyl 2-furoate or ethyl furan-2-carboxylate (EFA), 2,5-dimethylfuran (DMF), furan-2,5-diyldimethanol or 2,5-bis(hydroxymethyl)furan (DHMF), 5-hydroxymethyl furfural or 5-(hydroxymethyl)furan-2-carbaldehyde (HMF), 5-(hydroxymethyl)furan-2-carboxylic acid (HMFA), 2,5-furandicarboxaldehyde or furan-2,5-dicarbaldehyde (DFA), 2,5-furandicarboxylic acid or furan-2,5-dicarboxylic acid (FDCA), dimethyl furan-2,5-dicarboxylate (DFDC), (5,5'-(oxybis(methylene))bis(furan-5,2-diyl))dimethanol (OBMFA), 5,5'-(oxybis(methylene))bis(furan-2-carbaldehyde) (OBMF) and 5,5'-(oxybis(methylene))bis(furan-2-carboxylic acid) (OBCA) (Table AP 1). The impact of furanic compounds on the environment was investigated employing two aquatic organisms, consisting of the marine bioluminescent bacterium *A. fischeri* and the freshwater green microalgae *R. subcapitata*. The phytotoxicity of furanic compounds was investigated employing two dicotyledonous plants, *S. alba* and *L. sativum*. Moreover, the growth inhibition effect of the furanic molecules was studied on the unicellular eukaryotic yeast *S. cerevisiae*.

3.5.2.1 Toxicological assessment of furan compounds for marine bacterium and green algae

The toxicity of the furanic compounds selected on the marine bacterium *A. fischeri* was calculated as the half-maximal effective concentration (EC_{50}) value for 5 min and 15 min of exposure to each tested compound (Table 3.9). The toxicological assessment demonstrated that the majority of furanic compounds, including furfuryl alcohol, FA, EFA, DMF, DHMF, HMF, DFA, FDCA and OBMFA, exhibited similar levels of toxicity for *A. fischeri* in the different durations of exposure. However, HMFA, DFDC, OBMF and OBCA exhibited lower levels of toxicity on the marine bacterium, while the toxicity of furfural increased between 5 min and 15 min of exposure. The toxicity of furanic compounds on *A. fischeri* determined upon 5 min of exposure exhibited the following descending order: (toxic) DMF > OBMF > FA > OBMFA > DFA > FDCA > OBCA > DHMF > furfuryl alcohol > DFDC > EFA > HMF > furfural > HMFA (nontoxic). However, following 15 min of exposure the decreasing order of toxicity was configured as: (toxic) DMF > FA > OBMFA > FDCA > DFA > OBMF > furfuryl alcohol > DHMF > OBCA > EFA > HMF > DFDC > furfural > HMFA (nontoxic).

The toxicity of furanic compounds on the freshwater algae was expressed as an EC_{50} value for 72 h of exposure to the selected molecule (Table 3.9). The specific assessment demonstrates that several furanic compounds, including furfuryl alcohol, furfural, FA, DHMF, HMF, HMFA and OBCA were practically harmless for green algae, while EFA, DMF, DFA, DFDC, OBMFA and OBMF exhibited slight toxicity for the green algae. The toxicity of furanic compounds on *R. subcapitata* upon 72 h of exposure exhibited the following descending order: (toxic) DFA > DFDC > OBMF > OBMFA > DMF > EFA > DHMF > furfural > furfuryl alcohol > FDCA > OBCA > FA > HMF > HMFA (nontoxic).

Table 3.9: Toxicity classification of furan compounds in different aquatic organisms based on EC_{50}.

Compound	*A. fischeri* (mg L^{-1})		*R. subcapitata* (mg L^{-1})
	5 min	**15 min**	**72 h**
Furfuryl alcohol	127.35 ± 2.28	99.63 ± 19.11	143.79 ± 14.37
Furfural	369.36 ± 4.34	295.47 ± 5.12	133.72 ± 10.34
FA	41.41 ± 5.58	41.19 ± 9.04	163.33 ± 26.78
EFA	142.41 ± 13.17	161.54 ± 24.22	82.25 ± 9.25
DMF	20.22 ± 2.07	15.87 ± 1.13	64.24 ± 6.68
DHMF	126.77 ± 12.76	122.18 ± 10.21	103.39 ± 16.29
HMF	183.57 ± 19.37	188.55 ± 11.52	273.63 ± 33.89
HMFA	1128.53 ± 90.95	1521.77 ± 2.22	529.77 ± 11.87
DFA	50.55 ± 11.30	65.78 ± 8.59	10.16 ± 0.43
FDCA	55.05 ± 10.29	56.46 ± 5.96	145.48 ± 6. 47
DFDC	131.74 ± 6.86	263.75 ± 3.01	11.56 ± 1.94
OBMFA	48.91 ± 6.06	47.71 ± 5.97	55.19 ± 8.57
OBMF	37.24 ± 2.61	73.30 ± 8.64	37.49 ± 1.83
OBCA	90.59 ± 4.66	142.65 ± 14.04	162.21 ± 17.31

■ : very highly toxic, ■ : highly toxic, ■ : moderately toxic,

■ : slightly toxic, ■ : practically harmless, ☐ : nontoxic or harmless

3.5.2.2 Comparative analysis of the toxicological effects monitored for furan compounds

A comprehensive literature review on the toxicological effect of furan compounds on aquatic organisms based on the EC_{50} values demonstrated for different molecules is shown in Table 3.10. The data demonstrated that the furan compounds assessed were mainly slightly toxic, practically harmless or nontoxic for the marine and freshwater organisms tested. The comparative analysis showed that furfural could exhibit higher toxicity than furfuryl alcohol and HMF for different freshwater organisms, including green algae, crustacean *D. magna* and fish fathead minnow. Moreover, Zuriaga et al. (2018) reported that furfural was moderately toxic for the freshwater fish bluegill and rainbow trout. The marine bacterial strain *A. fischeri* constitutes a widely employed microorganism for the determination of furan compounds toxicity. Thus, furfuryl alcohol, furfural, DHMF and HMF were practically harmless for the marine bacterium, while FA, DMF and DFA were slightly toxic for all exposure times assessed (5 min, 15 min and 30 min). Ventura et al. (2016) reported that FDCA exhibited slight toxicity on *A. fischeri* at 5 min, while in longer exposures (15 min and 30 min) FDCA was moderately toxic for the marine bacterium. The toxicity of furfural to other marine organisms, including marine algae *Skeletonema costatum* and marine mollusc *Crassostrea virginica*, demonstrated that the specific furan compound was slightly toxic for both organisms.

Table 3.10: Median effective concentration (EC_{50}) values of furan compounds for different aquatic organisms.

Chemical name	Organism scientific name	Organism common name	Concentration (mg L^{-1})	Exposure time	Toxicity classification	Reference
Freshwater algae						
Furfuryl alcohol	*Chlorococcales*	Green algae	>1000	1 d	nontoxic	ECOTOX (EPA)
Furfural	*Anabaena flosaquae*	Blue-green algae	61 (39-93)	4 d	slightly toxic	ECOTOX (EPA)
	Chlorococcales	Green algae	570	1 d	practically harmless	ECOTOX (EPA)
	Navicula pelliculosa	Diatom	32 (23-45)	4 d	slightly toxic	ECOTOX (EPA)
	R. subcapitata	Green algae	19.9	3 d	slightly toxic	Zuriaga et al. (2018)
			43 (39-48)	4 d	slightly toxic	ECOTOX (EPA)
HMF	*R. subcapitata*	Green algae	110.2 (106.8-115.5)	3 d	practically harmless	Muralidhara et al. (2019)
Freshwater crustaceans						
Furfuryl alcohol	*D. magna*	Water flea	110 ± 2	1 d	practically harmless	Zuriaga et al. (2018)
			328	1 d	practically harmless	ECOTOX (EPA)
Furfural	*D. magna*	Water flea	29	1 d	slightly toxic	ECOTOX (EPA)
			20.4 (16.4-25.2)	2 d	slightly toxic	ECOTOX (EPA)

Table 3.10: (continued)

Chemical name	Organism scientific name	Organism common name	Concentration (mg L^{-1})	Exposure time	Toxicity classification	Reference
HMF	*D. magna*	Water flea	>500	1 d	practically harmless	Muralidhara et al. (2019)
			36.5 (30.0-45.1)	2 d	slightly toxic	Muralidhara et al. (2019)
			55.3 (50.3-60.9)	2 d	slightly toxic	Swart et al. (2019)
Freshwater fish						
Furfuryl alcohol	*Pimephales promelas*	Fathead minnow	7240	0.0833 d	nontoxic	ECOTOX (EPA)
Furfural	*Lepomis macrochirus*	Bluegill	5.8	4 d	moderately toxic	Zuriaga et al. (2018)
	Oncorhynchus mykiss	Rainbow trout	3.62	4 d	moderately toxic	Zuriaga et al. (2018)
	P. promelas	Fathead minnow	726	0.0833 d	practically harmless	ECOTOX (EPA)
			20.6	4 d	slightly toxic	Zuriaga et al. (2018)
	Poecilia reticulata	Guppy	10.6	14d	slightly toxic	Zuriaga et al. (2018)
Marine algae						
Furfural	*S. costatum*	Diatom	24 (17-33)	4 d	slightly toxic	ECOTOX (EPA)

Table 3.10: (continued)

Chemical name	Organism scientific name	Organism common name	Concentration (mg L^{-1})	Exposure time	Toxicity classification	Reference
Marine molluscs						
Furfural	C. virginica	American/virginia oyster	18 (14-22)	4 d	slightly toxic	ECOTOX (EPA)
Marine bacteria						
Furfuryl alcohol	*A. fischeri*		167.00 ± 57.50	5 min	practically harmless	Ventura et al. (2016)
			131.00 ± 38.40	15 min	practically harmless	Ventura et al. (2016)
			101.00 ± 25.65	30 min	practically harmless	Ventura et al. (2016)
			116.00 ± 9.00	30 min	practically harmless	Ventura et al. (2016)
Furfural	*A. fischeri*		339.00 ± 84.50	5 min	practically harmless	Ventura et al. (2016)
			255.00 ± 66.50	15 min	practically harmless	Ventura et al. (2016)
			188.00 ± 46.50	30 min	practically harmless	Ventura et al. (2016)
			454.00 ± 50	30 min	practically harmless	Ventura et al. (2016)
FA	*A. fischeri*		15.60 ± 0.85	5 min	slightly toxic	Ventura et al. (2016)
			15.40 ± 1.05	15 min	slightly toxic	Ventura et al. (2016)
			14.90 ± 0.70	30min	slightly toxic	Ventura et al. (2016)

Table 3.10: (continued)

Chemical name	Organism scientific name	Organism common name	Concentration (mg L^{-1})	Exposure time	Toxicity classification	Reference
DMF	*A. fischeri*		33.50 ± 14.65	5 min	slightly toxic	Ventura et al. (2016)
			24.30 ± 9.50	15 min	slightly toxic	Ventura et al. (2016)
			23.40 ± 6.80	30 min	slightly toxic	Ventura et al. (2016)
DHMF	*A. fischeri*		314.00 ± 53.50	5 min	practically harmless	Ventura et al. (2016)
			306.00 ± 39.50	15 min	practically harmless	Ventura et al. (2016)
			290.00 ± 43.00	30 min	practically harmless	Ventura et al. (2016)
HMF	*A. fischeri*		407.00 ± 73.00	5 min	practically harmless	Ventura et al. (2016)
			385.00 ± 63.50	15 min	practically harmless	Ventura et al. (2016)
			389.00 ± 103.50	30 min	practically harmless	Ventura et al. (2016)
DFA	*A. fischeri*		39.20 ± 12.50	5 min	slightly toxic	Ventura et al. (2016)
			21.30 ± 6.25	15 min	slightly toxic	Ventura et al. (2016)
			22.80 ± 10.30	30 min	slightly toxic	Ventura et al. (2016)
FDCA	*A. fischeri*		10.40 ± 1.10	5 min	slightly toxic	Ventura et al. (2016)
			9.66 ± 1.14	15 min	moderately toxic	Ventura et al. (2016)
			9.57 ± 1.25	30 min	moderately toxic	Ventura et al. (2016)

3.5.2.3 Toxicological assessment of furan compounds for terrestrial plants

The effects of furan compounds on the germination and early growth of two dicotyledonous plants were studied for 72 h of exposure to each tested compound, at a concentration of 150 mg L^{-1}. The results demonstrate that furanic compounds display different sensitivity levels in plants (Fig 3.14). The toxicological assessment exhibited that the majority of the furanic compounds studied do not affect the growth of *L. sativum* and *S. alba* at the concentration tested. Furans including FA, DHMF, HMF, HMFA, DFA, FDCA, OBMF and OBMCA were nontoxic for *L. sativum*, while furfuryl alcohol, FA, DMF, DHMF, DFA, DFDC and OBMFA did not impose toxicity on *S. alba*. A number of furanic molecules stimulated the growth of *S. alba* (HMF, HMFA, FDCA and OBMF), though only OBMF acted positively on *L. sativum* growth. Moreover, only a few furanic compounds were inhibitory on *L. sativum* (furfuryl alcohol, furfural, EFA, DMF and DFDC) and *S. alba* (furfural, EFA and OBCA).

Previous studies dealing with the impact of furan compounds on dicotyledonous and monocotyledonous plants demonstrated that the furan nucleus could impose a significant effect on the growth of plants (Matusiak et al., 2013; Zou et al., 2010). Thus, furfural holds applications in agriculture and horticulture sectors as fungicide and nematocide (Zeitsch, 2000), while furfural residues can be used to improve the quality of the soil, enhancing its chemical and physical properties. Moreover, furfural could be employed as organic fertilizer increasing the yield of several crops (Anthonia and Steele, 2015; Sun et al., 2019).

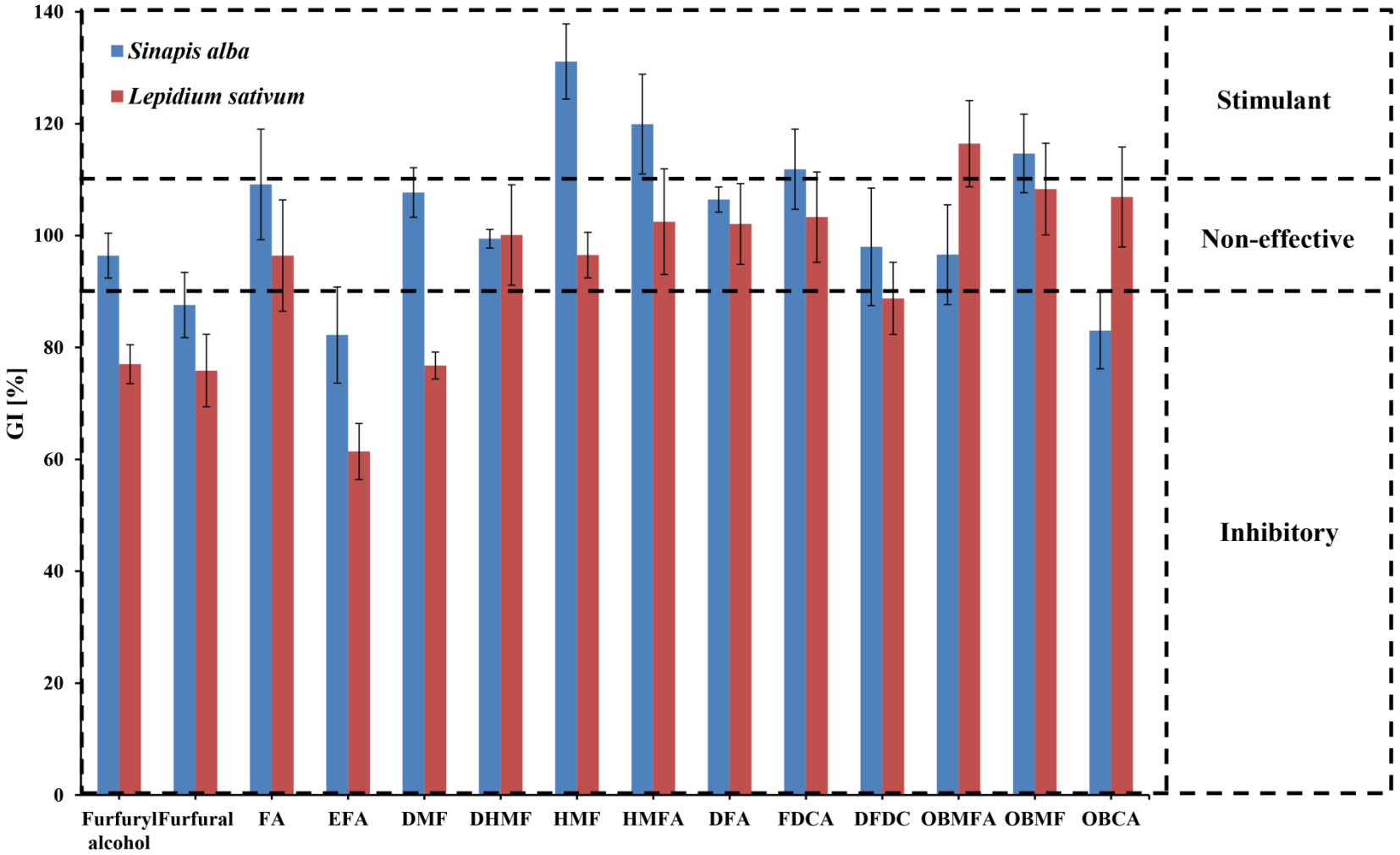

Figure 3.14: Toxicity classification of furanic compounds on dicotyledonous plants. ■ : *S. alba* and ■ : *L. sativum*.

3.5.2.4 Toxicological assessment of furan compounds for unicellular eukaryotic yeast

Furan derivatives produced from the partial degradation of cellulose, hemicellulose and lignin present in lignocellulosic material, constitute some of the most common fermentation inhibitors (Lopez et al., 2021). Herein, the toxic effect of fourteen furanic compounds on the unicellular eukaryotic yeast *S. cerevisiae* was studied as the growth inhibition following 6 h, 12 h and 16 h of exposure to each tested compound, at a concentration of 500 mg L^{-1}. The toxicological assessment demonstrated that all furanic compounds exhibited low levels of toxicity to *S. cerevisiae* at the tested concentration in the different durations of exposure. The results showed that growth inhibition remained below 10% following 6 h, 12 h and 16 h of exposure to all molecules, indicating that the specific compounds cause insignificant inhibition on eukaryotic cell growth for the concentration applied.

Several publications have reported that furanic compounds occur in different fermentation processes employing lignocellulosic material. Furfuryl alcohol constitutes an upgraded product of furfural bioconversion, holding wide application in fine chemical and polymer industries. However, furfural is a well-known inhibitor of numerous microorganisms, including *S. cerevisiae*. Yan et al. (2019) reported that *S. cerevisiae* NL22 exhibited a reduction in productivity and selectivity for the production of furfuryl alcohol upon exposure to furfural concentrations higher than 6 g L^{-1}. Moreover, Erkan et al. (2021) have recently shown that the production of bioethanol using immobilized cells of *S. cerevisiae* was increased at furfural concentrations higher than 6 g L^{-1}. Considering that insignificant inhibition was reported here for the application of furfural, future research should focus on determining the concentration level required to stimulate significant levels of inhibition to the growth of the eukaryotic yeast.

4 PROJECT REVIEW

The valorisation of wastewater generated from food processing industries constitutes an advanced solution as compared to waste management approaches since it combines wastewater treatment and the production of added-value compounds alleviating a range of environmental concerns while contributing toward the shift to a circular economy. Lupin bean processing manufacturers commonly use the debittering process to eliminate the antinutritional and alkaloid content of lupin beans, ensuring a safe for human consumption product. However, the specific production process generates large amounts of wastewater rich in alkaloids, mainly lupanine. This alkaloid is considered an important molecule exhibiting several applications in pharmaceutical/medical, agricultural and chemical industries. Therefore, this thesis focused on the development of a promising microbial process for the valorisation of lupanine existing in the wastewater generated from the lupin beans snack industry.

Microorganisms capable of metabolizing racemic lupanine were isolated using four different environmental samples that included anaerobic granular sludge obtained from an anaerobic bioreactor treating cheese whey, anaerobic digested sludge and activated sludge derived from a municipal wastewater treatment plant as well as wastewater obtained from a lupin bean snack manufacturer. Strains isolated under aerobic conditions were studied further to assess their ability to biodegrade racemic lupanine as a single carbon source, while the potential end-products formed via the microbial conversion of racemic lupanine were identified for each isolated strain (Chapter 3.1).

Apart from the bioconversion of racemic lupanine, the microbial resolution of the lupanine enantiomeric mixture existing in the industrial effluent in high ee constituted a promising route for the production of enantiopure lupanine. The ability of the aerobic strains to produce enantiomerically pure lupanine was investigated using racemic lupanine. Based on the findings obtained, the most effective isolated strain, *P. putida* LPK411, was extensively studied. The capacity of LPK411 to utilize each of the lupanine enantiomers and the end-products formed from D-(+)-lupanine bioconversion was investigated using D-(+)-lupanine and L-(–)-lupanine as single carbon substrates. Moreover, the optimal culture conditions of LPK411 were determined during racemic lupanine degradation (Chapter 3.2).

The work performed relevant to the resolution of racemic lupanine led towards a novel research direction enabling the valorisation of the lupanine enantiomeric mixture existing in industrial wastewater. Four different unrefined and pretreated wastewater streams of the lupin bean processing industry were characterized and used as feedstocks of the alkaloid racemate. The ability of LPK411 to enantioselective biodegrade the lupanine enantiomeric mixture in industrial wastewater was studied using shake flasks and a lab-scale bioreactor in batch mode. Subsequently, a fed-batch process was employed to improve the resolution of racemic lupanine by LPK411 (Chapter 3.3).

The transcriptional kinetics of *luh* and *crc* genes of *P. putida* LPK411 during racemic lupanine and lupanine enantiomers biodegradation was determined. The specific task aimed to provide information relevant to the metabolic pathway of lupanine biodegradation by *Pseudomonas* sp. during the supply of the alkaloid as a single carbon source. Moreover, the *crc* gene was additionally monitored to identify any potential inhibitory response due to activation of the CCR mechanism during simultaneous biodegradation of lupanine and other substrates available in the industrial effluent (Chapter 3.4).

An environmental toxicological assessment was performed to determine the effect of racemic lupanine, lupanine enantiomers as well as a wide range of furan compounds in the environment. The safety of these compounds was evaluated via a range of standard toxicological bioassays (Chapter 3.5).

The concluding remarks of the current Thesis are presented in the following Section, while based on these remarks, future directions are additionally suggested.

4.1 Conclusions

4.1.1 Bioconversion of racemic lupanine by newly isolated microbial strains for the production of high-value chemicals

The first objective of the current thesis required the isolation of new microbial strains from different environmental sources based on their ability to metabolize lupanine. Moreover, the isolates were identified along with their capacity to biodegrade and biotransform lupanine racemate to determine their applicability in the process.

4.1.1.1 Isolation and characterization of racemic lupanine metabolizing strains

Eight bacterial strains (4 aerobic and 4 anaerobic) capable of using racemic lupanine as the sole carbon source, at a concentration level of 1.5 g L^{-1}, have been isolated from four environmental samples that included anaerobic granular sludge obtained from an anaerobic bioreactor treating cheese whey, anaerobic digested sludge and activated sludge derived from a municipal wastewater treatment plant, as well as wastewater from a lupin bean snack manufacturer. The aerobic strains derived from granular sludge, digested sludge, aerobic sludge and wastewater from the lupin bean processing industry wastewater were identified as *R. ruber* LPK111, *R. rhodochrous* LPK211, *Rhodococcus* sp. LPK311 and *P. putida* LPK411, respectively. The strains isolated from the anaerobic cultures of granular sludge were identified as *P. citronellolis* LPK121 and *Rhodobacter* sp. LPK122, while the microorganisms derived from digested sludge were identified as *Pseudomonas* sp. LPK221 and *O. tritici* LPK222.

4.1.1.2 Biodegradation of racemic lupanine by aerobic isolates

The new microbial strains isolated under aerobic conditions (*R. rhodochrous* LPK211, *R. ruber* LPK111, *Rhodococcus* sp. LPK311 and *P. putida* LPK411) were further studied for their capacity to biodegrade racemic lupanine as the sole carbon source, at a concentration level of 1.5 g L^{-1}. All isolated strains achieved significant removal of racemic lupanine under the same culture conditions (M9 medium, 31 ºC, pH 7 and 100 rpm). *R. rhodochrous* LPK211 and *P. putida* LPK411 achieved the highest removal of racemic lupanine at 36 h of cultivation, corresponding to 81% and 80%

respectively. *R. ruber* LPK111 and *Rhodococcus* sp. LPK311 demonstrated 66% and 71% removal of lupanine within 42 h and 36 h respectively.

4.1.1.3 Final metabolic products from racemic lupanine bioconversion by aerobic isolates

The final metabolic products generated during the bioconversion of racemic lupanine were identified in cultures of the isolated aerobic strains. There were no end-products detected for *R. rhodochrous* LPK211 indicating that racemic lupanine could be mineralized to a large extent. *R. ruber* LPK111 and *Rhodococcus* sp. LPK311 produced the same molecule, the most possible structure of which constitutes lupanine *N*-oxide. Three molecules have been observed as end-products of racemic lupanine bioconversion by *P. putida* LPK411 including 17-oxolupanine and two non-rigid lupanine derivatives, while the potential structures of these products could be 4-(6-oxodecahydro-2H-1,5-methanopyrido[1,2-a][1,5]diazocin-4-yl)butanoic acid and 4-(decahydro-2H-1,5-methanopyrido[1,2-a][1,5]diazocin-4-yl)butanoic acid. The aforementioned molecules constitute novel structures reported for the first time and constitute promising molecules for the production of other high-value alkaloids. Thus, these results could lead to the development of a lupanine bioconversion process based on the newly isolated P. putida LPK411 for the valorization of industrial wastewater.

4.1.2 Microbial resolution of racemic lupanine by newly isolated microbial strains for the production of enantiomerically pure lupanine

This objective required assessing the ability of the isolated strains to enantioselectivity biodegrade racemic lupanine for the production of pure lupanine enantiomers at high ee. Moreover, the evaluation of the capacity of the most promising microorganisms to utilize and biotransform each enantiomer as a single carbon substrate as well as identifying the optimal growth conditions of the strain was required.

4.1.2.1 Microbial resolution of racemic lupanine enantiomeric by aerobic isolates

The enantioselective biodegradation of racemic lupanine was tested during cultures of *P. putida* LPK411, *R. rhodochrous* LPK211, and *Rhodococcus* sp. LPK311. All microorganisms were able to perform resolution degrading faster D-(+)-lupanine. *Rhodococcus* strains LPK211 and LPK311 produced 100% and 98% of L-(–)-lupanine

ee respectively, while approximately 60% of the initial racemic lupanine content remained in the biomedium following 42 h at both cultures. *P. putida* LPK411 reached L-(–)-lupanine ee of 95% more rapidly (36 h) as compared to *Rhodococcus* strains, which was further increased to 99% at 42 h. The remaining racemic lupanine from LPK411 cultivation at 36 h was 53%. These results demonstrated that LPK411 constitutes a promising microorganism for the enantioselective resolution of lupanine enantiomeric mixture existing in industrial wastewater.

4.1.2.2 Biodegradation of lupanine enantiomers by P. putida LPK411

The most effective microorganism in performing bioconversion and resolution of racemic lupanine was *P. putida* LPK411, thus the biodegradation and bioconversion of lupanine enantiomers (D-(+)-lupanine and L-(–)-lupanine) by the specific strain were studied. Results demonstrated that only D-(+)-lupanine could be metabolized substantially by LPK411. *P. putida* LPK411 achieved D-(+)-lupanine removal of 92% following 30 h of incubation, while under the same conditions L-(–)-lupanine biodegradation was insignificant as confirmed by statistical analysis. The end-product formed via D-(+)-lupanine biodegradation by LPK411 was identified as (trans)-6-oxooctahydro-1H-quinolizine-3-carboxylic acid. The final metabolic product of D-(+)-lupanine biodegradation by *P. putida* LPK411 identified in the current study has not been previously reported as a metabolite generated from microbial cultivation on lupanine. However, the presence of the amide and carboxyl functionalities opens the possibility for further chemoselective functional group modifications.

4.1.2.3 Biodegradation of racemic lupanine by P. putida LPK411 under different culture conditions

The effect of different culture conditions, including temperature, pH value and initial racemic lupanine concentration, were assessed during lupanine degradation by *P. putida* LPK411. The results demonstrate that the specific strain could adapt to a range of cultural conditions. LPK411 achieved the highest removal of lupanine at 31 ^{o}C, which corresponded to 76%, following 12 h of cultivation. At the same time point, the growth of the microorganism at 28 ^{o}C and 34 ^{o}C demonstrated 60% and 61% removal of lupanine respectively. However, at the lowest temperature tested (25 ^{o}C) the removal of lupanine reached 55% following 12 h of cultivation. Moreover, LPK411 achieved

higher lupanine removal within 12 h of cultures at neutral to slightly acidic pH values, which corresponded to 81% and 79% respectively. The use of an alkaline environment for the growth of *P. putida* LPK411 demonstrated 69% and 49% removal of lupanine within 12 h of cultivation respectively. The highest lupanine removal exhibited by LPK411 was achieved using 1.5 g L^{-1} of initial racemic lupanine concentration, which corresponded to 81%. The specific strain was grown at 1.0 g L^{-1} and 2.5 g L^{-1} initial racemic lupanine concentration demonstrated 62% and 72% removal of lupanine within 12 h and 18 h respectively, while at the use of 0.3 g L^{-1} and 3.0 g L^{-1} of initial racemic lupanine concentration substantially reduced the effectiveness of the process. These findings demonstrate that the optimal culture conditions for racemic lupanine biodegradation by *P. putida* LPK411 comprise 31 ^{o}C, pH 6-7 and 1.5 g L^{-1} of initial racemic lupanine concentration.

4.1.3 Valorisation of the lupanine enantiomeric mixture in industrial wastewater by microbial resolution

Lupin bean processing industrial wastewater streams should be characterized based on their content in lupanine, COD, sugars, proteins, lipids, nitrogen and solids. The ability of the most promising isolated strain to enantioselective biodegrade lupanine directly from lupin bean processing industrial wastewater streams was evaluated using shake flasks and a lab-scale bioreactor. Moreover, the valorisation of industrial wastewater employing the newly isolated strain was evaluated under different bioprocess scenarios.

4.1.3.1 Characterization of different wastewater streams

Four unrefined and treated wastewaters of the lupin beans processing industry (UWRP, UWSP, RWSP, and AWRP) were characterized based on different parameters. UWRP constituted the retentate of unrefined wastewater, containing significantly higher COD (500%) and lupanine (600%) contents as compared to UWSP. RWSP stream constitutes the retentate of a membrane filtration process employed for UWSP pretreatment, which resulted in substantially higher concentrations of COD and lupanine. AWRP wastewater contained lower quantities of COD and lupanine due to the anaerobic digestion process employed as pretreatment.

4.1.3.2 Microbial resolution of the lupanine enantiomeric mixture in industrial wastewater in batch mode

The ability of *P. putida* LPK411 to enantioselectively biodegrade the lupanine enantiomeric mixture existing in the food process effluents was investigated using two unrefined industrial wastewater streams (UWSP, UWRP) and two pre-processed wastewater streams (RWSP, AWRP). The results demonstrate that LPK411 was capable of performing selective biodegradation of lupanine directly in the different types of wastewater emitted from the lupine bean processing industry as well as pre-processed effluents. *P. putida* LPK411 grown in UWRP and UWSP exhibited 47% and 94% of L-(–)-lupanine ee, while the removal of lupanine from unrefined wastewater streams comprised 32% and 57% respectively. Moreover, LPK411 exhibited high resolution of lupanine (100% of L-(–)-lupanine ee) and 52% removal of the initial lupanine content following 6 h of cultivation in AWRP. However, the specific stain grown was not able to perform resolution of the lupanine enantiomeric mixture content of RWSP.

4.1.3.3 Microbial resolution of racemic lupanine in a fed-batch process

A fed-batch process was additionally applied to enhance the resolution of racemic lupanine by *P. putida* LPK411. The results demonstrated that LPK411 achieved high resolution of lupanine racemate exhibiting 96% of L-(–)-lupanine ee, while 0.95 g L^{-1} of racemic lupanine concentration remained following 9 h of cultivation. The specific strain continued to perform enantioselective resolution of racemic lupanine in the subsequent three feedings applied, reaching L-(–)-lupanine ee > 92% following 6 h from each feeding conducted. Moreover, the biomass growth rate at the first batch was 0.19 $g_{biomass}$ L^{-1} h^{-1}, while the rate continuously decreased following subsequent feedings, reaching 0.06 $g_{biomass}$ L^{-1} h^{-1} at the final feeding. However, the utilization rate of the alkaloid increased from 0.47 $g_{lupanine}$ L^{-1} h^{-1} to 0.70 $g_{lupanine}$ L^{-1} h^{-1} as a result of the first refeed, while at the second and third refeeds it reached 0.82 $g_{lupanine}$ L^{-1} h^{-1} and 0.69 $g_{lupanine}$ L^{-1} h^{-1} respectively. The results obtained from the fed-batch process indicated that LPK411 achieved a significant increase in D-(+)-lupanine biodegradation, as well as L-(–)-lupanine and biomass production, as compared to the batch cultures. Under fed-batch conditions, LPK411 biodegraded an additional quantity of 53% D-(+)-lupanine and produced 49% more biomass as compared to the corresponding batch cultures, while L-(–)-lupanine concentration increased by 49%. These findings exhibit

that a fed-batch process could be effectively employed to enhance the resolution of the lupanine enantiomeric mixture using the specific microorganism for the valorisation of lupanine directly from industrial wastewater streams.

4.1.3.4 Microbial resolution of lupanine enantiomeric mixture in industrial wastewater using a lab-scale bioreactor

The enantioselective biodegradation of different wastewater streams (UWSP, UWRP) and pre-processed wastewaters (RWSP, AWRP) was studied during the growth of *P. putida* LPK411 in a batch mode lab-scale bioreactor. The results demonstrated that the specific strain achieved high L-(–)-lupanine ee in unrefined and pretreated wastewaters emitted from lupine bean processing in a batch bioreactor. LPK411 grown in UWRP and UWSP exhibited 93% and 95% of L-(–)-lupanine ee, while the removal of lupanine in both wastewater streams comprised 69%. Moreover, LPK411 reached 94% of L-(–)-lupanine ee and 83% removal of the initial lupanine concentration existing in RWSP, while exhibiting high resolution of lupanine (100% of L-(–)-lupanine ee) and 74% of lupanine removal from the AWRP stream. A comparison of the results obtained at the bioreactor scale as opposed to the use of shake flasks exhibited that employing the bioreactor for LPK411 growth enabled substantially improved resolution of the lupanine enantiomeric mixture from all the wastewater streams applied, which corresponded to L-(–)-lupanine ee values >93%.

4.1.4 Metabolic pathway for the degradation of lupanine by *Pseudomonas* spp.

The mRNA expression of key genes involved in the catabolic route of the alkaloid as well as the CCR mechanisms activation of LPK411 during lupanine biodegradation was evaluated. Thus, transcription from the *luh* and *crc* genes were monitored over time during the biodegradation of racemic lupanine and each lupanine enantiomer in M9 medium, as well as in LPK411 cultures using industrial wastewater.

4.1.4.1 Transcriptional kinetics of luh gene in P. putida LPK411 during racemic lupanine and lupanine enantiomers biodegradation

Monitoring the transcription from the first gene expressed in the catabolic pathway of lupanine (*luh*) during *P. putida* LPK411 growth in M9 medium containing the racemic lupanine or lupanine enantiomers (D-(+)-lupanine, L-(–)-lupanine)

demonstrated that *luh* was expressed in the presence of both lupanine enantiomers as single carbon sources as well as the racemic mixture. However, although these results confirm the production of the precursor mRNA molecules required for lupanine hydroxylase formation, which catalyses lupanine bioconversion into the first intermediate of the metabolic pathway, L-(–)-lupanine was not biodegraded. Thus, given that the gene is transcribed in the presence of L-(–)-lupanine either the translation process or the activation of lupanine hydroxylase cannot proceed. Moreover, the delay of *luh* activation in the cultures conducted using L-(–)-lupanine as compared to the experiments supplemented with D-(+)-lupanine and the racemate indicate that an alternative gene activation mechanism could be potentially followed in the presence of L-(–)-lupanine.

4.1.4.2 Transcriptional kinetics of luh and crc genes in P. putida LPK411 during racemic lupanine and wastewater biodegradation

Transcription from the *luh* and *crc* genes performed during LPK411 growth in M9 medium containing the racemic alkaloid as well as employing an industrial wastewater stream containing the enantiomeric mixture of lupanine and other organic substrates demonstrated that *P. putida* LPK411 preferably utilised other carbon molecules in the wastewater over lupanine, suppressing the catabolic pathway of the alkaloid via the CCR mechanism.

4.1.5 Environmental toxicological assessment of natural compounds

Toxicological assessment of racemic lupanine, lupanine enantiomers and furan molecules employed as valuable building blocks in the chemical industry was performed to evaluate the safety of these compounds. Different bioindicators, including microbes, animals, planktons and plants were employed to determine the impact of these substances in aquatic and terrestrial ecosystems.

4.1.5.1 Environmental toxicological assessment of lupanine and lupanine enantiomers

The toxicity of racemic lupanine was evaluated for the aquatic organisms *A. fischeri* and *D. magna*, as well as for the terrestrial plants *S. alba* and *S. saccharatum*. The EC_{50} values calculated for *A. fischeri* were 89 mg L^{-1} and 47 mg L^{-1} for 5 min and 15 min of

exposure, while the corresponding values for *D. magna* reached 60 mg L^{-1} and 12 mg L^{-1} following 24 h and 48 h of exposure respectively. These results demonstrated that racemic lupanine exhibited slight toxicity to the marine bacterium and the freshwater crustaceans. Moreover, the phytotoxicity assays exhibited that racemic lupanine inhibited the root growth and seed germination of *S. saccharatum* at a concentration level higher than 12.5 mg L^{-1} for 96 h of exposure. However, exposure to racemic lupanine imposed a positive effect on the root growth and it did not affect the germination of *S. alba*. These findings show that racemic lupanine demonstrates a negative impact on the germination and growth of monocotyledon plants while improving the growth and germination of dicotyledon plants.

Toxicological tests of D-(+)-lupanine and L-(–)-lupanine show that both enantiomers induced similar levels of toxicity on *A. fischeri* for 5 min and 15 min of exposure, corresponding to EC_{50} levels that ranged between 317-320 mg L^{-1} and 372-457 mg L^{-1} respectively. The enantiomers' interaction assessment demonstrated a very strong synergistic effect for the mixture of D-(+)-lupanine and L-(–)-lupanine on the toxicity imposed to *A. fischeri* (CI <1).

4.1.5.2 Environmental toxicological assessment of furanic compounds

The toxicological assessment demonstrated that the majority of the furanic compounds tested, including furfuryl alcohol, FA, EFA, DMF, DHMF, HMF, DFA, FDCA and OBMFA, exhibited similar levels of toxicity for *A. fischeri* following 5 and 15 min of exposure. However, HMFA, DFDC, OBMF and OBCA were less toxic for marine bacterium, while the toxicity of furfural increased between 5 and 15 min of exposure. The toxicity imposed by furanic compounds to *A. fischeri* following 5 min of exposure exhibited the following descending order: (toxic) DMF > OBMF > FA > OBMFA > DFA > FDCA > OBCA > DHMF > furfuryl alcohol > DFDC > EFA > HMF > furfural > HMFA (nontoxic). However, upon 15 min of exposure the decreasing order of toxicity was configured as: (toxic) DMF > FA > OBMFA > FDCA > DFA > OBMF > furfuryl alcohol > DHMF > OBCA > EFA > HMF > DFDC > furfural > HMFA (nontoxic).

The use of freshwater algae demonstrated that several furanic compounds, including furfuryl alcohol, furfural, FA, DHMF, HMF, HMFA and OBCA were practically

harmless for the specific organisms, while EFA, DMF, DFA, DFDC, OBMFA and OBMF demonstrated slight toxicity on green algae. The toxicity of furanic compounds to *R. subcapitata* after 72 h of exposure presented the following descending order: (toxic) DFA > DFDC > OBMF > OBMFA > DMF > EFA > DHMF > furfural > furfuryl alcohol > FDCA > OBCA > FA > HMF > HMFA (nontoxic).

The phytotoxicity assessment demonstrated that the majority of furanic compounds do not affect the growth of *L. sativum* and *S. alba* at the concentration tested. Furanic compounds including FA, DHMF, HMF, HMFA, DFA, FDCA, OBMF and OBMCA were nontoxic for *L. sativum*, while furfuryl alcohol, FA, DMF, DHMF, DFA, DFDC and OBMFA displayed no toxicity for *S. alba*. A number of furanic molecules stimulated the growth of *S. alba* (HMF, HMFA, FDCA and OBMF), while only OBMF acted positively on *L. sativum* growth. However, only a few furans were inhibitory for *L. sativum* (furfuryl alcohol, furfural, EFA, DMF and DFDC) and *S. alba* (furfural, EFA and OBCA).

The growth inhibition toxicity assay of *S. cerevisiae* showed that furanic compounds exhibited insignificant inhibition on eukaryotic cell growth following 6 h, 12 h and 16 h of exposure to each furanic compound at a concentration level of 500 mg L^{-1}.

4.2 Future directions

4.2.1 Bioconversion of lupanine for the production of high-value products

Lupanine comprises an asymmetric structure and may serve as a starting material for the semisynthesis of a range of other alkaloids (Carmali et al., 2010). The present thesis demonstrates that both known and novel lupanine-based alkaloid structures can be produced by the newly isolated strains *R. ruber* LPK111, *Rhodococcus* sp. LPK311 and *P. putida* LPK411 during the degradation of racemic lupanine. Moreover, a new lupanine-based alkaloid structure was formed during D-(+)-lupanine biodegradation by *P. putida*. Further research is needed to assess the potential use of the specific molecules as starting materials for the chemical synthesis of other valuable products. Thus, the isolation of the specific compounds via novel and existing processes, such as the liquid-liquid extraction methods proposed by Maulide et al. (2014) and Przybyl and Kubicki, (2011), and their separation through different chromatographic techniques, including Thin-layer Chromatography (TLC) and Gas Chromatography Mass Spectrometry (GC-MS) will enable a more specific and detailed study of the structures produced during the bioconversion of racemic and enantiopure lupanine.

4.2.2 Resolution of the lupanine enantiomeric mixture content from industrial wastewater

The current Thesis demonstrated that it is possible to enantioselectively biodegradation the lupanine enantiomeric mixture directly from the wastewater derived from the lupin bean processing industry. The results have shown that the newly isolated *P. putida* LPK411 was capable of performing enantioselective resolution of lupanine, while the experiments conducted using a lab-scale bioreactor exhibited that controlled cultivation conditions could improve the production of pure L-(–)-lupanine. Thus, studying the enantioselective biodegradation of lupanine employing a lab-scale bioreactor under different bioprocess operating conditions (fed-batch, continuous) could potentially further improve the production of enantiomerically pure lupanine. Moreover, in case the data obtained from the aforementioned task are promising a pilot bioreactor could be applied to assess the effectiveness of the developed process.

4.2.3 Deciphering lupanine metabolism in *Pseudomonas* sp.

The first step in racemic lupanine biodegradation by *P. putida* Psp-LUP was performed via the action of the *luh* gene, which encodes for the lupanine hydroxylase enzyme responsible for the conversion of lupanine to 17-hydroxylupanine (Hopper et al., 2002; Hopper and Kaderbhai, 2003). As mentioned in Section 3.4.1 *luh* mRNA gene expression is triggered by the racemate and both lupanine enantiomers, which supports the potential stereospecificity of lupanine catabolic enzymes. Further research is needed to assess the complete metabolic pathway followed by *Pseudomonas* sp. for racemic lupanine and lupanine enantiomers biodegradation. Lupanine constitutes a lysine-derived quinolizidine alkaloid, according to Revelles et al. (2005), while lysine racemate catabolism in *P. putida* KT2440 occurs via the aminovalerate pathway for L-lysine and the aminoadipate route for D-lysine. Thus, the specific pathways could be potentially employed during the catabolism of lupanine enantiomers by *P. putida* LPK411. Systematic monitoring of transcription from specific genes expressed in aminovalerate (e.g. *dav*A, *dav*B) and aminoadipate (e.g. *dpk*A, *ama*A) pathways will provide more information pertinent to the catabolic mechanism of lupanine by *Pseudomonads*. Moreover, deciphering of the molecular events that control the lupanine metabolic pathway in *P. putida* LPK411 could lead to future optimization of the bioprocess through the use of important transcriptional information for the development of coupled gene expression-growth kinetic models.

4.2.4 Recovery and valorisation of enantiopure lupanine

Recovery of high-value products generated during the microbial treatment of the wastewater from the lupin beans snack industry constitutes an important factor to evaluate the efficiency and applicability of this process. Previous studies have shown that osmotic evaporation and nanofiltration comprise potential solutions for the removal of lupanine from industrial wastewater (Carmali et al., 2010; Esteves et al., 2020). Consequently, the development of a physicochemical process for the recovery of enantiomerically pure lupanine generated from microbial metabolism could be promising for the valorisation of lupin bean wastewater. The application of an existing or newly developed physicochemical process for the recovery of enantiomerically pure lupanine generated from microbial metabolism could lead to the further valorisation of

the alkaloid. Enantiopure lupanine produced from the microbial metabolism of industrial wastewater could be chemically transformed into the enantiomerically pure sparteine, an alkaloid with several chemical and pharmaceutical applications.

REFERENCES

Abahazi, E., Satorhelyi, P., Erdelyi, B., Vertessy, B.G., Land, H., Paizs, C., Berglund, P., Poppe, L., 2018. Covalently immobilized Trp60Cys mutant of ω-transaminase from *Chromobacterium violaceum* for kinetic resolution of racemic amines in batch and continuous-flow modes. Biochem. Eng. J. 132, 270–278.

Abbas, M., Adil, M., Ehtisham-ul-Haque, S., Munir, B., Yameen, M., Ghaffar, A., Shar, G.A., Tahir, M.A., Iqbal, M., 2018. *Vibrio fischeri* bioluminescence inhibition assay for ecotoxicity assessment: A review. Sci. Total Environ. 626, 1295–1309.

Abraham, T.W., Hofer, R., 2012. Lipid-based polymer building blocks and polymers, in : Moeller, M., Matyjaszewski, K. (Eds.), Polymer science: A comprehensive reference 15–58.

Abram, M., Jakubiec, M., Kamiński, K., 2019. Chirality as an important factor for the development of new antiepileptic drugs. ChemMedChem 14, 1744–1761.

Adamu, A., Firdausi, A., Huyop, F., Wahab, R.A., 2018. Molecular basis and engineering of enzymes stereospecificity. J. Mol. Biol. Methods 1, e1.

Agranat, I., Wainschtein, S.R., Zusman, E.Z., 2012. The predicated demise of racemic new molecular entities is an exaggeration. Nat. Rev. Drug Discov. 11, 972–973.

Ahmad, A.L., Oh, P.C., Abd Shukor, S.R., 2009. Sustainable biocatalytic synthesis of L-homophenylalanine as pharmaceutical drug precursor. Biotechnol. Adv. 27, 286–296.

Alabaster, G., Dzikus, A., Otieno, P., 2017. Municipal and urban wastewater, in : The united nations world water development Report 2017. Wastewater: The untapped resource 48–57.

Alho, L.O.G., Gebara, R.C., Paina, K.A., Sarmento, H., Melão, M.G.G., 2019. Responses of *Raphidocelis subcapitata* exposed to Cd and Pb: Mechanisms of toxicity assessed by multiple endpoints. Ecotoxicol. Environ. Saf. 169, 950–959.

Ali, I., Al-Othman, Z.A., Al-Warthan, A., Alam, S.D., Farooqi, J.A., 2014. Enantiomeric separation and simulation studies of pheniramine, oxybutynin, cetirizine, and brinzolamide chiral drugs on amylose- based columns. Chirality 26,

136–143.

Alkadi, H., Jbeily, R., 2018. Role of chirality in drugs: An overview. Infect. Disord. - Drug Targets 18, 88–95.

Alsafadi, D., Alsalman, S., Paradisi, F., 2017. Extreme halophilic alcohol dehydrogenase mediated highly efficient syntheses of enantiopure aromatic alcohols. Org. Biomol. Chem. 15, 9169–9175.

Ameen, S.M., Caruso, G., 2017. The importance of lactic acid in the current food industry: An introduction, in : Lactic acid in the food industry. Springer briefs Mol. Sci. Chem. foods 1–5.

Andersson, H., Banchelin, T.S.L., Das, S., Gustafsson, M., Olsson, R., Almqvist, F., 2010. Complete regioselective addition of grignard reagents to pyrazine *N*-oxides, toward an efficient enantioselective synthesis of substituted piperazines. Org. Lett. 12, 284–286.

Aniszewski, T., 2015a. Definition, typology, and occurrence of alkaloids, in : Alkaloids: Chemistry, biology, ecology and applications 1–97.

Aniszewski, T., 2015b. Applied potential and current applications of alkaloids, in : Alkaloids: Chemistry, biology, ecology and applications 345–420.

Aniszewski, T., 2015c. Alkaloid chemistry, in: Alkaloids: Chemistry, Biology, Ecology and Applications 99–193.

Annicchiarico, P., Manunza, P., Arnoldi, A., Boschin, G., 2014. Quality of *Lupinus albus* L.(white lupin) seed: extent of genotypic and environmental effects. J. Agric. Food Chem. 62, 6539–6545.

Anthonia, E.E., Steele, P.H., 2015. An overview of the applications of furfural and its derivatives. Int. J. Adv. Chem. 3, 42–47.

Antonkiewicz, J., Baran, A., Pełka, R., Wisła-Świder, A., Nowak, E., Konieczka, P., 2019. A mixture of cellulose production waste with municipal sewage as new material for an ecological management of wastes. Ecotoxicol. Environ. Saf. 169, 607–614.

AOAC 973.48-1973 - Association of Official Agricultural Chemists. Nitrogen(Total) in Water - Kjeldahl Method, n.d.

APHA, AWWA, WEF, 2017. Standard methods for the examination of water and wastewater, 23rd edition.

Arias-Garcia, A., Garcia-Lopez, P.M., Ruiz-Lopez, M.A., Wysocka, W., 2002. Growth inhibition of *Fusarium* by a new lupanine thioanalogue, (+)-2-thionosparteine, and (+) lupanine, in : Santen, E., Hill, G.D. (Eds.), Wild and cultivated lupins from the tropics to the poles 256–257.

Arts, J.H.E., Muijser, H., Appel, M.J., Kuper, C.F., Bessems, J.G.M., Woutersen, R.A., 2004. Subacute (28-day) toxicity of furfural in Fischer 344 rats: A comparison of the oral and inhalation route. Food Chem. Toxicol. 42, 1389–1399.

Australian Food Statistics, 2007. Water sustainability in the Australian food processing industry 27–34.

Azubuike, C.C., Chikere, C.B., Okpokwasili, G.C., 2020. Bioremediation: An eco-friendly sustainable technology for environmental management, in : Saxena, G., Bharagava, R. (Eds.) Bioremediation of industrial waste for environmental safety 19–39.

Babu, V.S., Patra, S., Thakur, M.S., Karanth, N.G., Varadaraj, M.C., 2005. Degradation of caffeine by *Pseudomonas alcaligenes* CFR 1708. Enzyme Microb. Technol. 37, 617–624.

Baek, S.H., Kim, K.H., Yin, C.R., Jeon, C.O., Im, W.T., Kim, K.K., Lee, S.T., 2003. Isolation and characterization of bacteria capable of degrading phenol and reducing nitrate under low-oxygen conditions. Curr. Microbiol. 47, 462–466.

Baran, A., Tarnawski, M., 2013. Phytotoxkit/Phytotestkit and Microtox® as tools for toxicity assessment of sediments. Ecotoxicol. Environ. Saf. 98, 19–27.

Barbera, M., Gurnari, G., 2018. Wastewater treatment and reuse in the food industry 1–47.

Barrena, R., Casals, E., Colón, J., Font, X., Sánchez, A., Puntes, V., 2009. Evaluation of the ecotoxicity of model nanoparticles. Chemosphere 75, 850–857.

Basso, A., Serban, S., 2019. Industrial applications of immobilized enzymes - A review. Mol. Catal. 479, e110607.

Batool, Z., Xu, D., Zhang, X., Li, X., Li, Y., Chen, Z., Li, B., Li, L., 2020. A review on

furan: Formation, analysis, occurrence, carcinogenicity, genotoxicity and reduction methods. Crit. Rev. Food Sci. Nutr. 61, 395–406.

Bauer-Marinovic, M., Taugner, F., Florian, S., Glatt, H., 2012. Toxicity studies with 5-hydroxymethylfurfural and its metabolite 5-sulphooxymethylfurfural in wild-type mice and transgenic mice expressing human sulphotransferases 1A1 and 1A2. Arch. Toxicol. 86, 701–711.

Bavar, M., Sarrafzadeh, M.H., Asgharnejad, H., Norouzi-Firouz, H., 2018. Water management methods in food industry: Corn refinery as a case study. J. Food Eng. 238, 78–84.

Beyene, G., Ameha, N., Urge, M., Estifanos, A., 2014. Replacing soybean meal with processed Lupin (*Lupinus albus*) meal as poultry layers feed. Livest. Res. Rural Dev. 26, e208.

Bharwad, K., Rajkumar, S., 2019. Rewiring the functional complexity between Crc, Hfq and sRNAs to regulate carbon catabolite repression in *Pseudomonas*. World J. Microbiol. Biotechnol. 35, e140.

Bhatia, S.K., Mehta, P.K., Bhatia, R.K., Bhalla, T.C., 2014. Optimization of arylacetonitrilase production from *Alcaligenes* sp. MTCC 10675 and its application in mandelic acid synthesis. Appl. Microbiol. Biotechnol. 98, 83–94.

Bianchini, L.F., Arruda, M.F.C., Vieira, S.R., Campelo, P.M.S., Gregio, A.M.T., Rosa, E.A.R., 2015. Microbial biotransformation to obtain new antifungals. Front. Microbiol. 6, e1433.

Bigliardi, B., Galati, F., 2013. Innovation trends in the food industry: the case of functional foods. Trends Food Sci. Technol. 31, 118–129.

Bijsterbosch, J.W., Das, A., Kerkhof, F.P.J.M., 1994. Clean technology in the production of epichlorohydrin. J. Clean. Prod. 2, 181–184.

Blamey, J.M., Fischer, F., Meyer, H.P., Sarmiento, F., Zinn, M., 2017. Enzymatic biocatalysis in chemical transformations: A promising and emerging field in green chemistry practice, in : Brahmachari, G. (Eds.), Biotechnology of microbial enzymes production, biocatalysis and industrial applications 347–403.

Blaser, H.U., 2015. Looking back on 35 years of industrial catalysis. Chimia (Aarau).

69, 393–406.

Blaser, H.U., 2003. Enantioselective catalysis in fine chemicals production. Chem. Commun. 293–296.

Blaser, H.U., Spindler, F., Struder, M., 2001. Enantioselective catalysis in fine chemicals production. Appl. Catal. A Gen. 221, 119–143.

Bligh, E.G., Dyer, W.J., 1959. A rapid method of total lipid extraction and purification. Can. J. Biochem. Physiol. 37, 911–917.

Bliss, C.I., 1934. The method of probits. Science. 79, 38–39.

Boido, V., Ercoli, M., Tonelli, M., Novelli, F., Tasso, B., Sparatore, F., Cichero, E., Fossa, P., Dorigo, P., Froldi, G., 2017. New arylsparteine derivatives as positive inotropic drugs. J. Enzyme Inhib. Med. Chem. 32, 588–599.

Boonpan, A., Pivsa-Art, S., Pongswat, S., Areesirisuk, A., Sirisangsawang, P., 2013. Separation of D, L-lactic acid by filtration process. Energy Procedia 34, 898–904.

Boschin, G., Annicchiarico, P., Resta, D., D'Agostina, A., Arnoldi, A., 2008. Quinolizidine alkaloids in seeds of lupin genotypes of different origins. J. Agric. Food Chem. 56, 3657–3663.

Boschin, G., Resta, D., 2013. Alkaloids derived from lysine: quinolizidine (a focus on lupin alkaloids), in : Ramawat, K.G., Mérillon, J.M. (Eds.), Natural Products 381–403.

Bownik, A., 2017. Daphnia swimming behaviour as a biomarker in toxicity assessment: A review. Sci. Total Environ. 601–602, 194–205.

Branch, S.K., Hutt, A.J., 2012. Regulatory perspective on the development of new stereoisomeric drugs, in : Jozwiak, K., Lough, W.J., Wainer, I.W. (Eds.), Drug stereochemistry: Analytical methods and pharmacology 240–273.

Brill, Z.G., Condakes, M.L., Ting, C.P., Maimone, T.J., 2017. Navigating the chiral pool in the total synthesis of complex terpene natural products. Chem. Rev. 117, 11753–11795.

Bromley-Challenor, K., Kowalski, M., Barnard, R., Lynn, S., 2013. Water use in the UK food and drink industry. Technical report. Project code: PAD 101 202.

Brukwicki, T., Wysocka, W., 2003. NMR spectra and geometry of epi *N*-oxides of sparteine and some of its derivatives in solution. J. Mol. Struct. 647, 275–286.

Budau, M., Hancu, G., Rusu, A., Carcu-Dobrin, M., Muntean, D.L., 2017. Chirality of modern antidepressants: An overview. Adv. Pharm. Bull. 7, 495–500.

Bunsupa, S., Saito, K., Yamazaki, M., 2013. Molecular biology and biotechnology of quinolizidine alkaloid biosynthesis in *Leguminosae* plants, in : Chandra, S., Lata, H., Varma, A. (Eds.), Biotechnology for medicinal plants: Micropropagation and Improvement 263–273.

Burnett, C., Heldreth, B., Bergfeld, W.F., Belsito, D.V., Hill, R.A., Klaassen, C.D., Liebler, D.C., Marks, J.G., Shank, R.C., Slaga, T.J., Snyder, P.W., Andersen, F.A., 2014. Safety assessment of animal- and plant- derived amino acids as used in cosmetics. Int. J. Toxicol. 33, 5S-12S.

Burnett, C.L., Boyer, I., Heldreth, B., Bergfeld, W.F., Belsito, D.V., Hill, R.A., Klaassen, C.D., Liebler, D.C., Marks, J.G., Shank, R.C., Slaga, T.J., Snyder, P.W., 2017a. Safety assessment of plant-derived proteins and peptides as used in cosmetics. Cosmet. Ingred. Rev. 1–25.

Burnett, C.L., Fiume, M.M., Bergfeld, W.F., Belsito, D.V., Hill, R.A., Klaassen, C.D., Liebler, D., Marks, J.G., Shank, R.C., Slaga, T.J., Snyder, P.W., Andersen, F.A., 2017b. Safety assessment of plant-derived fatty acid oils. Int. J. Toxicol. 36, 51S-129S.

Cahill, J.F., Lamb, E.G., 2007. Interactions between root and shoot competition and plant traits. HortScience 42, 1110–1112.

Calcaterra, A., D'Acquarica, I., 2018. The market of chiral drugs: Chiral switches versus *de novo* enantiomerically pure compounds. J. Pharm. Biomed. Anal. 147, 323–340.

Camacho-Muñoz, D., Martín, J., Santos, J.L., Aparicio, I., Alonso, E., 2010. Occurrence, temporal evolution and risk assessment of pharmaceutically active compounds in Doñana Park (Spain). J. Hazard. Mater. 183, 602–608.

Caner, H., Groner, E., Levy, L., Agranat, I., 2004. Trends in the development of chiral drugs. Drug Discov. Today 9, 105–110.

Carmali, S., Alves, V.D., Coelhoso, I.M., Ferreira, L.M., Lourenço, A.M., 2010. Recovery of lupanine from *Lupinus albus* L. leaching waters. Sep. Purif. Technol. 74, 38–43.

Carvalho, C.C.C.R., 2011. Enzymatic and whole cell catalysis: Finding new strategies for old processes. Biotechnol. Adv. 29, 75–83.

Casado, N., Valimaña-Traverso, J., García, M.Á., Marina, M.L., 2019. Enantiomeric determination of drugs in pharmaceutical formulations and biological samples by electrokinetic chromatography. Crit. Rev. Anal. Chem. 50, 554–584.

CED, 2017. Economic contribution of the food and beverage industry. A report by the Committe for Economic Development of The Conderence Board 1–48.

CEN - EN 25663 - European Committee for Standardization. Water Quality - Determination of Kjeldahl Nitrogen – Method After Mineralization with Selenium, n.d.

Chaganti, S.R., Prakasham, R.S., Rao, B.A., Yadav, J.S., 2008. Production of L (+) lactic acid by *Lactobacillus delbrueckii* immobilized in functionalized alginate matrices. World J. Microbiol. Biotechnol. 24, 1411–1415.

Chatterjee, M., Ishizaka, T., Kawanami, H., 2014. Selective hydrogenation of 5-hydroxymethylfurfural to 2,5-bis-(hydroxymethyl)furan using Pt/MCM-41 in an aqueous medium: A simple approach. Green Chem. 16, 4734–4739.

Chen, W., Oldfield, T.L., Patsios, S.I., Holden, N.M., 2020. Hybrid life cycle assessment of agro-industrial wastewater valorisation. Water Res. 170, e115275.

Chiofalo, B., Presti, V.L., Chiofalo, V., Gresta, F., 2012. The productive traits, fatty acid profile and nutritional indices of three lupin (*Lupinus* spp.) species cultivated in a Mediterranean environment for the livestock. Anim. Feed Sci. Technol. 171, 230–239.

Choi, S., Song, C.W., Shin, J.H., Lee, S.Y., 2015. Biorefineries for the production of top building block chemicals and their derivatives. Metab. Eng. 28, 223–239.

Chuzel, O., Riant, O., 2005. Sparteine as a chiral ligand for asymmetric catalysis, in: Lemaire, M., Mangeney, P. (Eds.), Chiral diazaligands for asymmetric synthesis 59–92.

Ciriminna, R., Pagliaro, M., 2013. Green chemistry in the fine chemicals and pharmaceutical industries. Org. Process Res. Dev. 17, 1479–1484.

Compton, M., Willis, S., Rezaie, B., Humes, K., 2018. Food processing industry energy and water consumption in the Pacific northwest. Innov. Food Sci. Emerg. Technol. 47, 371–383.

Crini, G., Lichtfouse, E., 2018. Wastewater treatment: An overview, in : Green adsorbents for pollutant removal : Fundamentals and design 1–22.

Cubas-Cano, E., Gonzalez-Fernandez, C., Ballesteros, M., Tomas-Pejo, E., 2012. Biotechnological advances in lactic acid production by lactic acid bacteria: Lignocellulose as novel substrate. Biofuels, Bioprod. Biorefining 12, 290–303.

Curti, C.A., Curti, R.N., Bonini, N., Ramón, A.N., 2018. Changes in the fatty acid composition in bitter *Lupinus* species depend on the debittering process. Food Chem. 263, 151–154.

Cushnie, T.P.T., Cushnie, B., Lamb, A.J., 2014. Alkaloids: An overview of their antibacterial, antibiotic-enhancing and antivirulence activities. Int. J. Antimicrob. Agents 44, 377–386.

D'Amato, D., Droste, N., Allen, B., Kettunen, M., Lahtinen, K., Korhonen, J., Leskinen, P., Matthies, B.D., Toppinen, A., 2017. Green, circular, bio economy: A comparative analysis of sustainability avenues. J. Clean. Prod. 168, 716–734.

Dalvand, K., Rubin, J., Gunukula, S., Wheeler, M.C., Hunt, G., 2018. Economics of biofuels: Market potential of furfural and its derivatives. Biomass and Bioenergy 115, 56–63.

Detheridge, A.P., Griffith, G.W., Hopper, D.J., 2018. Genome sequence analysis of two *Pseudomonas putida* strains to identify a 17-hydroxylase putatively involved in sparteine degradation. Curr. Microbiol. 75, 1649–1654.

Diaz-Munoz, G., Miranda, I.L., Sartori, S.K., Rezende, D.C., Diaz, M.A.N., 2019. Use of chiral auxiliaries in the asymmetric synthesis of biologically active compounds: A review. Chirality 31, 776–812.

Ding, X., Lin, S., Weng, H., Liang, J., 2018. Separation and determination of the enantiomers of lactic acid and 2-hydroxyglutaric acid by chiral derivatization

combined with gas chromatography and mass spectrometry. J. Sep. Sci. 41, 2576–2584.

Drakou, E.M., Koutinas, M., Pantelides, I., Tsolakidou, M., Vyrides, I., 2015. Insights into the metabolic basis of the halotolerant *Pseudomonas aeruginosa* strain LVD-10 during toluene biodegradation. Int. Biodeterior. Biodegrad. 99, 85–94.

Dubois, M., Gilles, K.A., Hamilton, J.K., Rebers, P.A., Smith, F., 1956. Colorimetric method for determination of sugars and related substances. Anal. Chem. 28, 350–356.

Dunn, P.J., Hettenbach, K., Kelleher, P., Martinez, C.A., 2010. The development of a green, energy efficient, chemoenzymatic manufacturing process for pregabalin, in : Dunn, P.J., Wells, A.S., Williams, M.T. (Eds.), Green chemistry in the pharmaceutical industry 171–177.

Ebner, D.C., Trend, R.M., Genet, C., McGrath, M.J., O'Brien, P., Stoltz, B.M., 2008. Palladium-catalyzed enantioselective oxidation of chiral secondary alcohols: Access to both enantiomeric series. Angew. Chemie - Int. Ed. 47, 6367–6370.

El-Shazly, A., Ateya, A.M.M., Wink, M., 2001. Quinolizidine alkaloid profiles of *Lupinus* varius orientalis, *L. albus albus*, *L. hartwegii*, and *L. densiflorus*. Zeitschrift für Naturforsch. C 56, 21–30.

Eltoukhy, A., Jia, Y., Nahurira, R., Abo-Kadoum, M.A., Khokhar, I., Wang, J., Yan, Y., 2020. Biodegradation of endocrine disruptor Bisphenol A by *Pseudomonas putida* strain YC-AE1 isolated from polluted soil, Guangdong, China. BMC Microbiol. 20, e11.

EPA, n.d. United States Environmental Protection Agency (US EPA). ECOTOX Knowledgebase http://www.epa.gov/ecotox/.

EPA 351.3 - U.S. Environmental Protection Agency. Nitrogen, Kjeldahl, Total (Colorimetric; Titrimetric; Potentiometric), n.d.

Erbas, M., 2010. The effects of different debittering methods on the production of lupin bean snack from bitter *Lupinus albus* L. seeds. J. Food Qual. 33, 742–757.

Erbas, M., Certel, M., Uslu, M.K., 2005. Some chemical properties of white lupin seeds (*Lupinus albus* L.). Food Chem. 89, 341–345.

Erdemoglu, N., Ozkan, S., Tosun, F., 2007. Alkaloid profile and antimicrobial activity of *Lupinus angustifolius* L. alkaloid extract. Phytochem. Rev. 6, 197–201.

Erkan, S.B., Yatmaz, E., Germec, M., Turhan, I., 2021. Effect of furfural concentration on ethanol production using Saccharomyces cerevisiae in an immobilized cells stirred-tank bioreactor with glucose-based medium and mathematical modeling. J. Food Process. Preserv. 45, e14635.

Esteves, T., Mota, A.T., Barbeitos, C., Andrade, K., Afonso, C.A.M., Ferreira, F.C., 2020. A study on lupin beans process wastewater nanofiltration treatment and lupanine recovery. J. Clean. Prod. 277, e123349.

Ettireddy, S., Chandupatla, V., Veeresham, C., 2017. Enantioselective resolution of (*R,S*)-carvedilol to (*S*)-(−)-carvedilol by biocatalysts. Nat. Products Bioprospect. 7, 171–179.

Fan, Y., Zhou, C., Zhu, X., 2009. Selective catalysis of lactic acid to produce commodity chemicals. Catal. Rev. - Sci. Eng. 51, 293–324.

Fanali, C., D'Orazio, G., Gentili, A., Fanali, S., 2019. Analysis of enantiomers in products of food interest. Molecules 24, e1119.

Fernandes, C., Tiritan, M.E., Pinto, M.M.M., 2017. Chiral separation in preparative scale: A brief overview of membranes as tools for enantiomeric separation. Symmetry (Basel). 9, e206.

Finefield, J.M., Sherman, D.H., Kreitman, M., Williams, R.M., 2012. Enantiomeric natural products: Occurrence and biogenesis. Angew. Chemie - Int. Ed. 51, 4802–4836.

Forster, J., 2014. Archive: Water use in industry. Eurostat https://ec.europa.eu/eurostat/statistics-explained.

Frias, J., Miranda, M.L., Doblado, R., Vidal-Valverde, C., 2005. Effect of germination and fermentation on the antioxidant vitamin content and antioxidant capacity of *Lupinus albus* L. var. Multolupa. Food Chem. 92, 211–220.

Frick, K.M., Kamphuis, L.G., Siddique, K.H.M., Singh, K.B., Foley, R.C., 2017. Quinolizidine alkaloid biosynthesis in lupins and prospects for grain quality improvement. Front. Plant Sci. 8, e87.

Gaalova, J., Yalcinkaya, F., Curinova, P., Kohout, M., Yalcinkaya, B., Kostejn, M., Jirsak, J., Stibor, I., Bara, J.E., Van der Bruggen, B., Izak, P., 2020. Separation of racemic compound by nanofibrous composite membranes with chiral selector. J. Memb. Sci. 596, e117728.

Gali, K.K., Tadi, S.R.R., E.V.R., A., Mohan, N., Swaminathan, N., Katiyar, V., Sivaprakasam, S., 2021. Cost-effective valorization of cassava fibrous waste into enantiomerically pure D-lactic acid: Process engineering and kinetic modelling approach. Environ. Technol. Innov. 22, e101519.

Galia, M.B., Rivas, S.A., Molinari, G., Timmis, K.N., 2014. Utilization of the novel, environmental isolate *Pseudomonas* sp. IPB-A36 for the efficient production of mcl/lcl-PHAs and specialty-PHAs. U.S. Patent No.: US 2014/0378647A1.

Gao, C., Qiu, J., Li, J., Ma, C., Tang, H., Xu, P., 2009. Enantioselective oxidation of racemic lactic acid to D-lactic acid and pyruvic acid by *Pseudomonas stutzeri* SDM. Bioresour. Technol. 100, 1878–1880.

Gao, C., Zhang, W., Huang, Y., Ma, C., Xu, P., 2012. Efficient conversion of 1,2-butanediol to (R)-2-hydroxybutyric acid using whole cells of *Gluconobacter oxydans*. Bioresour. Technol. 115, 75–78.

Garcia-Lopez, P.M., Mora, P.G., Meneses-Medina, M.I., Zermeno, A.E.R., Moreno-Sandoval, V., Toro-Urena, I.D., Garcia-Preciado, L.E., Gurrola-Diaz, C., Ramos-Zuniga, R., Wysocka, W., 2011. *Lupinus exaltatus* obtained lupanine and its measured anticonvulsive activity, in : Naganowska, B., Kachlicki, P., Wolko, B. (Eds.), Lupin crops: An opportunity for today, a promise for the future 195–200.

Garcia-Ochoa, F., Gomez, E., Santos, V.E., Merchuk, J.C., 2010. Oxygen uptake rate in microbial processes: An overview. Biochem. Eng. J. 49, 289–307.

Gavilan, J., Mennickent, D., Ramirez-Molina, O., Trivino, S., Perez, C., Silva-Grecchi, T., Godoy, P.A., Becerra, J., Aguayo, L.G., Moraga-Cid, G., Martin, V.S., Yevenes, G.E., Castro, P.A., Guzman, L., Fuentealba, J., 2019. 17 oxo sparteine and lupanine, obtained from *Cytisus scoparius*, exert a neuroprotection against soluble oligomers of amyloid-β toxicity by nicotinic acetylcholine receptors. J. Alzheimer's Dis. 67, 343–356.

Gawali, V.S., Simeonov, S., Drescher, M., Knott, T., Scheel, O., Kudolo, J., Kahlig, H., Hochenegg, U., Roller, A., Todt, H., Maulide, N., 2017. C2-modified sparteine derivatives are a new class of potentially long-acting sodium channel blockers. ChemMedChem 12, 1819–1822.

Gellad, W.F., Choi, P., Mizah, M., Good, C.B., Kesselheim, A.S., 2014. Assessing the chiral switch: Approval and use of single-enantiomer drugs, 2001 to 2011. Am. J. Manag. Care 20, 90–97.

Germain, A.R., Bruggemeyer, D.M., Zhu, J., Genet, C., O'Brien, P., Porco, J.A., 2011. Synthesis of the azaphilones (+)-sclerotiorin and (+)-8- O -methylsclerotiorinamine utilizing (+)-sparteine surrogates in copper-mediated oxidative dearomatization. J. Org. Chem. 76, 2577–2584.

Geueke, B., Hummel, W., 2002. A new bacterial L-amino acid oxidase with a broad substrate specificity: Purification and characterization. Enzyme Microb. Technol. 31, 77–87.

Gokulakrishnan, S., Chandraraj, K., Gummadi, S.N., 2007. A preliminary study of caffeine degradation by *Pseudomonas* sp. GSC 1182. Int. J. Food Microbiol. 113, 346–350.

Gong, X.W., Yang, J.K., Duan, Y.Q., Dong, J.Y., Zhe, W., Wang, L., Li, Q.H., Zhang, K.Q., 2009. Isolation and characterization of *Rhodococcus* sp. Y22 and its potential application to tobacco processing. Res. Microbiol. 160, 200–204.

Gordon, W.C., Henderson, J.H.M., 1951. The alkaloidal content of blue lupine (*Lupinus angustifolius*) and its toxicity on small laboratory animals. J. Agric. Sci. 41, 141–145.

Gotor-Fernandez, V., Brieva, R., Gotor, V., 2006. Lipases: Useful biocatalysts for the preparation of pharmaceuticals. J. Mol. Catal. B Enzym. 40, 111–120.

Green, B.T., Lee, S.T., Panter, K.E., Brown, D.R., 2012. Piperidine alkaloids: Human and food animal teratogens. Food Chem. Toxicol. 50, 2049–2055.

Griffiths, M.R., Strobel, B.W., Hama, J.R., Cedergreen, N., 2021. Toxicity and risk of plant-produced alkaloids to *Daphnia magna*. Environ. Sci. Eur. 33, e10.

Guigo, N., Forestier, E., Sbirrazzuoli, N., 2019. Thermal properties of biobased

polymers: Furandicarboxylic acid (FDCA)-based polyesters. Adv. Polym. Sci. 283, 189–218.

Gumustas, M., Ozkan, S.A., Chankvetadze, B., 2018. Analytical and preparative scale separation of enantiomers of chiral drugs by chromatography and related methods. Curr. Med. Chem. 25, 4152–4188.

Habulin, M., Knez, Z., 2009. Optimization of (*R*,*S*)-1-phenylethanol kinetic resolution over *Candida antarctica* lipase B in ionic liquids. J. Mol. Catal. B Enzym. 58, 24–28.

Hadik, P., Szabo, L.P., Nagy, E., 2002. D,L-lactic acid and D,L-alanine enantioseparation by membrane process. Desalination 148, 193–198.

Hall, I.H., Wong, O.T., Reynolds, D.J., Chang, J.J., 1993. The hypolipidemic effects of 2- furoic acid in Sprague- Dawley rats. Arch. Pharm. (Weinheim). 326, 15–23.

Hasegawa, R., Hayashi, K., 1986. Polyester containing impure 1,2-butanediol. U.S. Patent No. 4596886.

He, Y.C., Ma, C.L., Yang, Z.X., Zhou, M., Xing, Z., Ma, J.T., Yu, H.L., 2013. Highly enantioselective oxidation of phenyl methyl sulfide and its derivatives into optically pure (*S*)-sulfoxides with *Rhodococcus* sp . CCZU10-1 in an *n*-octane–water biphasic system. Appl. Microbiol. Biotechnol. 97, 10329–10337.

He, Y.C., Xu, J.H., Pan, J., Ouyang, L.M., Xu, Y., 2008. Preparation of (*R*)-(-)-mandelic acid and its derivatives from racemates by enantioselective degradation with a newly isolated bacterial strain *Alcaligenes* sp. ECU0401. Bioprocess Biosyst. Eng. 31, 445–451.

Henry, H., Conus, N.M., Steenhout, P., Beguin, A., Boulat, O., 2012. Sensitive determination of D-lactic acid and L-lactic acid in urine by high-performance liquid chromatography-tandem mass spectrometry. Biomed. Chromatogr. 26, 425–428.

Heponiemi, A., Lassi, U., 2012. Advanced oxidation processes in food industry wastewater treatment – A review, in : Valdez, B., (Eds.), Food Industrial Processes: Methods and Equipment 313–338.

Høie, A.H., Svendsen, C., Rasmussen, T., Alexander, J., Husøy, T., 2016. Intestinal

tumor development in C57BL/6J-ApcMin/+ mice expressing human sulphotransferases 1A1 and 1A2 after oral exposure to 2,5-dimethylfuran. Anticancer Res. 36, 545–554.

Hopper, D.J., Kaderbhai, M.A., 2003. The quinohaemoprotein lupanine hydroxylase from *Pseudomonas putida*. Biochim. Biophys. Acta (BBA)-Proteins Proteomics 1647, 110–115.

Hopper, D.J., Kaderbhai, M.A., Marriott, S.A., Young, M., Rogozinski, J., 2002. Cloning, sequencing and heterologous expression of the gene for lupanine hydroxylase, a quinocytochrome c from a *Pseudomonas* sp. Biochem. J. 367, 483–489.

Hopper, D.J., Rogozinski, J., Toczko, M., 1991. Lupanine hydroxylase, a quinocytochrome *c* from an alkaloid-degrading *Pseudomonas* sp. Biochem. J. 279, 105–109.

Hu, B.C., Hu, D., Li, C., Xu, X.F., Wen, Z., Wu, M.C., 2020. Near-perfect kinetic resolution of racemic p-chlorostyrene oxide by SlEH1, a novel epoxide hydrolase from *Solanum lycopersicum* with extremely high enantioselectivity. Int. J. Biol. Macromol. 147, 1213–1220.

Huang, Q., Li, H., Guo, T., Li, S., Shen, G., Ban, C., Liu, J., 2018. Chiral separation of (D,L)-lactic acid through molecularly imprinted cellulose acetate composite membrane. Cellulose 25, 3435–3448.

Huerta, F.F., Minidis, A.B.E., Backvall, J.E., 2001. Racemisation in asymmetric synthesis. Dynamic kinetic resolution and related processes in enzyme and metal catalysis. Chem. Soc. Rev. 30, 321–331.

Hung, C.W., Martinez-Marquez, J.Y., Javed, F.T., Duncan, M.C., 2018. A simple and inexpensive quantitative technique for determining chemical sensitivity in *Saccharomyces cerevisiae*. Sci. Rep. 8, e11919.

ISO 11348–3:2007 - International Organization for Standardization. Water quality– Determination of the inhibitory effect of water samples on the light emission of *Vibrio fischeri*.

ISO 5663:1984 - International Organization for Standardization. Water quality —

Determination of Kjeldahl nitrogen — Method after mineralization with selenium.

ISO 6341:2012 - International Organization for Standardization. Water quality — Determination of the inhibition of the mobility of *Daphnia magna* Straus (Cladocera, Crustacea) — Acute toxicity test.

ISO 8692:2012 - International Organization for Standardization. Water quality–Fresh water algal growth inhibition test with unicellular green algae.

Jana, S., Sarkar, S., Morris, S.A., 2020. Recent developments towards the synthesis of paroxetine: A 3,4-disubstituted piperidine. Tetrahedron 76, e131215.

Ji, X., Guo, J., Liu, Y., Lu, A., Wang, Z., Li, Y., Yang, S., Wang, Q., 2018. Marine-Natural-Product development: First discovery of nortopsentin alkaloids as novel antiviral, anti-phytopathogenic-fungus, and insecticidal agents. J. Agric. Food Chem. 66, 4062–4072.

Jiménez, A.L.O., Floro, A.M., Palma, P., 2017. Toxic potential of the emerging contaminant nicotine to the aquatic ecosystem. Environ. Sci. Pollut. Res. 24, 16605–16616.

Jin, H.X., Liu, Z.Q., Hu, Z.C., Zheng, Y.G., 2013. Biosynthesis of (*R*)-epichlorohydrin at high substrate concentration by kinetic resolution of racemic epichlorohydrin with a recombinant epoxide hydrolase. Eng. Life Sci. 13, 385–392.

Jin, H.X., OuYang, X.K., 2015. Enzymatic approaches to the preparation of chiral epichlorohydrin. RSC Adv. 5, 92988–92994.

Jin, L.Q., Peng, F., Liu, H.L., Cheng, F., Jia, D.X., Xu, J.M., Liu, Z.Q., Xue, Y.P., Zheng, Y.G., 2019. Asymmetric biosynthesis of L-phosphinothricin by a novel transaminase from *Pseudomonas fluorescens* ZJB09-108. Process Biochem. 85, 60–67.

Kabir, G., Hameed, B.H., 2017. Recent progress on catalytic pyrolysis of lignocellulosic biomass to high-grade bio-oil and bio-chemicals. Renew. Sustain. Energy Rev. 70, 945–967.

Kader, M.A., 2005. A comparison of seed germination calculation formulae and the associated interpretation of resulting data. J. Proceeding R. Soc. New South Wales 138, 65–75.

Kahnt, G., Hijazi, L.A., 1991. Use of lupinex to increase crop yield and improve harvest quality with lesser nitrogen fertilization. J. Agron. Crop Sci. 166, 228–237.

Kahnt, G., Hijazi, L.A., 1987. Effect of bitter lupin extract on growth and yield of different crops. J. Agron. Crop Sci. 159, 320–328.

Karp, S.G., Igashiyama, A.H., Siqueira, P.F., Carvalho, J.C., Vandenberghe, L.P.S., Thomaz-Soccol, V., Coral, J., Tholozan, J.L., Pandey, A., Soccol, C.R., 2011. Application of the biorefinery concept to produce l-lactic acid from the soybean vinasse at laboratory and pilot scale. Bioresour. Technol. 102, 1765–1772.

Karume, I., Takahashi, M., Hamdan, S.M., Musa, M.M., 2016. Deracemization of secondary alcohols by using a single alcohol dehydrogenase. ChemCatChem 8, 1459–1463.

Ke, J., Yang, K., Bai, X., Luo, H., Ji, Y., Chen, J., 2021. A novel chiral polyester composite membrane: Preparation, enantioseparation of chiral drugs and molecular modeling evaluation. Sep. Purif. Technol. 255, e117717.

Key, R.E., Venkatasubbaiah, K., Jones, C.W., 2013. Evaluation of enantiopure and non-enantiopure Co(III)-salen catalysts and their counter-ion effects in the hydrolytic kinetic resolution (HKR) of racemic epichlorohydrin. J. Mol. Catal. A Chem. 366, 1–7.

Khalil, A., 2017. Role of biotechnology in alkaloids production, in : Naeem, M., Aftab, T., Khan, M.M.A. (Eds.), Catharanthus roseus: Current research and future prospects 59–70.

Khodaei, K., Nassery, H.R., Asadi, M.M., Mohammadzadeh, H., Mahmoodlu, M.G., 2017. BTEX biodegradation in contaminated groundwater using a novel strain (*Pseudomonas* sp. BTEX-30). Int. Biodeterior. Biodegrad. 116, 234–242.

Kim, J.H., Scialli, A.R., 2011. Thalidomide: The tragedy of birth defects and the effective treatment of disease. Toxicol. Sci. 122, 1–6.

Kisumi, M., Ashikaga, Y., Chibata, I., 1960. Studies on the fermentative preparation of L-aspartic acid from fumaric acid. J. Agric. Chem. Soc. Japan 24, 296–305.

Klotz, S., Kaufmann, N., Kuenz, A., Prüße, U., 2016. Biotechnological production of enantiomerically pure D-lactic acid. Appl. Microbiol. Biotechnol. 100, 9423–9437.

Koleva, I.I., van Beek, T.A., Soffers, A.E., Dusemund, B., Rietjens, I.M., 2012. Alkaloids in the human food chain–natural occurrence and possible adverse effects. Mol. Nutr. Food Res. 56, 30–52.

Koutinas, M., Kiparissides, A., Lam, M.C., Silva-Rocha, R., Godinho, M., Lorenzo, V., Santos, V.A.P.M., Pistikopoulos, E.N., Mantalaris, A., 2011. Improving the prediction of *Pseudomonas putida* mt-2 growth kinetics with the use of a gene expression regulation model of the TOL plasmid. Biochem. Eng. J. 55, 108–118.

Koutinas, M., Lam, M.C., Kiparissides, A., Silva-Rocha, R., Godinho, M., Livingston, A.G., Pistikopoulos, E.N., de Lorenzo, V., dos Santos, V.A.P.M., Mantalaris, A., 2010. The regulatory logic of m-xylene biodegradation by *Pseudomonas putida* mt-2 exposed by dynamic modelling of the principal node Ps/Pr of the TOL plasmid. Environ. Microbiol. 12, 1705–1718.

Koutinas, M., Vasquez, M.I., Nicolaou, E., Pashali, P., Kyriakou, E., Loizou, E., Papadaki, A., Koutinas, A.A., Vyrides, I., 2019. Biodegradation and toxicity of emerging contaminants: Isolation of an exopolysaccharide-producing *Sphingomonas* sp. for ionic liquids bioremediation. J. Hazard. Mater. 365, 88–96.

Kraff, P., Gilbeau, P., Gosselin, B., 2017. Process for produce epichlorohydrin. U.S. Patent No.: US9633427B2.

Kroc, M., Rybinski, W., Wilczura, P., Kamel, K., Kaczmarek, Z., Barzyk, P., Swiecicki, W., 2017. Quantitative and qualitative analysis of alkaloids composition in the seeds of a white lupin (*Lupinus albus* L .) collection. Genet. Resour. Crop Evol. 64, 1853–1860.

Kruger, N.J., 2009. The Bradford method for protein quantitation, in: Walker, J.M. (Eds.), The protein protocols handbook, 3rd edition 15–21.

Kumar, C.V., Vasa, P.K., Kumar, Y.R., Aparna, P., Pratyusha, P., 2016. Enantiomeric separation of *S*-epichlorohydrin and *R*-epichlorohydrin by capillary gas chromatography with FID detector. Am. J. Anal. Chem. 7, 772–784.

Lago-Vila, M., Rodríguez-Seijo, A., Vega, F.A., Arenas-Lago, D., 2019. Phytotoxicity assays with hydroxyapatite nanoparticles lead the way to recover firing range soils. Sci. Total Environ. 690, 1151–1161.

Larrow, J.F., Hemberger, K.E., Jasmin, S., Kabir, H., Morel, P., 2003. Commercialization of the hydrolytic kinetic resolution of racemic epoxides: Toward the economical large-scale production of enantiopure epichlorohydrin. Tetrahedron Asymmetry 14, 3589–3592.

Lee, S.T., Green, B.T., Welch, K.D., Jordan, G.T., Zhang, Q., Panter, K.E., Hughes, D., Chang, C.W.T., Pfister, J.A., Gardner, D.R., 2013. Stereoselective potencies and relative toxicities of γ-coniceine and *N*-methylconiine enantiomers. Chem. Res. Toxicol. 26, 616–621.

Lee, S.T., Molyneux, R.J., Panter, K.E., Chang, C.W.T., Gardner, D.R., Pfister, J.A., Garrossian, M., 2005. Ammodendrine and *N*-methylammodendrine enantiomers: Isolation, optical rotation, and toxicity. J. Nat. Prod. 68, 681–685.

Leek, H., Andersson, S., 2017. Preparative scale resolution of enantiomers enables accelerated drug discovery and development. Molecules 22, e158.

Li, J., Sun, J., Wu, B., He, B., 2017. Combined utilization of nutrients and sugar derived from wheat bran for D-Lactate fermentation by *Sporolactobacillus inulinus* YBS1-5. Bioresour. Technol. 229, 33–38.

Li, L., Li, K., Wang, Y., Chen, C., Xu, Y., Zhang, L., Han, B., Gao, C., Tao, F., Ma, C., Xu, P., 2015. Metabolic engineering of *Enterobacter cloacae* for high-yield production of enantiopure (2*R*,3*R*)-2,3-butanediol from lignocellulose-derived sugars. Metab. Eng. 28, 19–27.

Li, X., Jia, P., Wang, T., 2016. Furfural: A promising platform compound for sustainable production of C4 and C5 chemicals. ACS Catal. 6, 7621–7640.

Liang, J., Lalonde, J., Borup, B., Mitchell, V., Mundorff, E., Trinh, N., Kochrekar, D.A., Cherat, R.N., Pai, G.G., 2010. Development of a biocatalytic process as an alternative to the (-)-DIP-Cl-mediated asymmetric reduction of a key intermediate of montelukast. Org. Process Res. Dev. 14, 193–198.

Lim, S.A.H., Antony, J., 2019. Food industry and its contribution to the global economy, in : Statistical process control for the food industry: A guide for practitioners and managers 13–21.

Lim, T.K., 2012. *Lupinus albus*, in : Edible medicinal and non-medicinal plants:

Volume 2, Fruits 763–769.

Lin, K., Liu, W., Li, L., Gan, J., 2008. Single and joint acute toxicity of isocarbophos enantiomers to *Daphnia magna*. J. Agric. Food Chem. 56, 4273–4277.

Lister, D.L., Kanungo, G., Rathbone, D.A., Bruce, N.C., 1999. Transformations of codeine to important semisynthetic opiate derivatives by *Pseudomonas putida* m10. FEMS Microbiol. Lett. 181, 137–144.

Liu, Y., Wang, L., Huang, K., Wang, W., Nie, X., Jiang, Y., Li, P., Liu, S., Xu, P., Tang, H., 2014. Physiological and biochemical characterization of a novel nicotine-degrading bacterium *Pseudomonas geniculata* N1. PLoS One 9, e84399.

Lopez-Cabeza, R., Gamiz, B., Cornejo, J., Celis, R., 2017. Behavior of the enantiomers of the herbicide imazaquin in agricultural soils under different application regimes. Geoderma 293, 64–72.

Lopez-Gomez, J.P., Alexandri, M., Schneider, R., Latorre-Sanchez, M., Lozano, C.C., Venus, J., 2020. Organic fraction of municipal solid waste for the production of L-lactic acid with high optical purity. J. Clean. Prod. 247, e119165.

Lopez, P.C., Peng, C., Arneborg, N., Junicke, H., Gernaey, K.V., 2021. Analysis of the response of the cell membrane of *Saccharomyces cerevisiae* during the detoxification of common lignocellulosic inhibitors. Sci. Rep. 11, e6853.

Lopez, P.M.G., Mora, P.G., Wysocka, W., Maiztegui, B., Alzugaray, M.E., Zotto, H.D., Borelli, M.I., 2004. Quinolizidine alkaloids isolated from *Lupinus* species enhance insulin secretion. Eur. J. Pharmacol. 504, 139–142.

Lorenz, H., Seidel-Morgenstern, A., 2014. Processes to separate enantiomers. Angew. Chemie Int. Ed. 53, 1218–1250.

Lourenco, N.M.T., Afonso, C.A.M., 2007. One-pot enzymatic resolution and separation of sec-alcohols based on ionic acylating agents. Angew. Chemie 119, 8326–8329.

Lourenco, N.M.T., Monteiro, C.M., Afonso, C.A.M., 2010. Ionic acylating agents for the enzymatic resolution of sec-alcohols in ionic liquids. European J. Org. Chem. 6938–6943.

Luo, Y., Li, Z., Li, X., Liu, X., Fan, J., Clark, J.H., Hu, C., 2019. The production of furfural directly from hemicellulose in lignocellulosic biomass: A review. Catal.

Today 319, 14–24.

Luo, Z., Swaleh, S.M., Theil, F., Curran, D.P., 2002. Resolution of 1-(2-naphthyl)ethanol by a combination of an enzyme-catalyzed kinetic resolution with a fluorous triphasic separative reaction. Org. Lett. 4, 2585–2587.

Magalhaes, S.C.Q., Fernandes, F., Cabrita, A.R.J., Fonseca, A.J.M., Valentao, P., Andrade, P.B., 2017. Alkaloids in the valorization of European *Lupinus* spp. seeds crop. Ind. Crops Prod. 95, 286–295.

Mahajan, M., Kumar, V., Yadav, S.K., 2010. Alkaloids: Properties, applications and pharmacological effects, in : Cassiano, N.M. (Eds), Alkaloids: Properties, applications and pharmacological effects 1–36.

Maier, N.M., Franco, P., Lindner, W., 2001. Separation of enantiomers: Needs, challenges, perspectives. J. Chromatogr. A 906, 3–33.

Mane, S., 2016. Racemic drug resolution: A comprehensive guide. Anal. Methods 8, 7567–7586.

Mani, A., Dinabandhu, S., 2015. Green algae, in: Sahoo, D., Seckbach, J. (Eds). The algae world 91–120.

Manirakiza, P., Covaci, A., Schepens, P., 2001. Comparative study on total lipid determination using soxhlet, Roese-Gottlieb, Bligh & Dyer, and modified Bligh & Dyer extraction methods. J. Food Compos. Anal. 14, 93–100.

Mariscal, R., Maireles-Torres, P., Ojeda, M., Sádaba, I., Granados, M.L., 2018. Furfural: A renewable and versatile platform molecule for the synthesis of chemicals and fuels. Energy Environ. Sci. 9, 1144–1189.

Martinkova, L., Kren, V., 2018. Biocatalytic production of mandelic acid and analogues: A review and comparison with chemical processes. Appl. Microbiol. Biotechnol. 102, 3893–3900.

Martins, J., Teles, L.O., Vasconcelos, V., 2007. Assays with *Daphnia magna* and *Danio rerio* as alert systems in aquatic toxicology. Environ. Int. 33, 414–425.

Matusiak, A., Lewkowski, J., Rychter, P., Biczak, R., 2013. Phytotoxicity of new furan-derived aminophosphonic acids, *N*-Aryl furaldimines and 5-nitrofuraldimine. J. Agric. Food Chem. 61, 7673–7678.

Matzke, M., Stolte, S., Arning, J., Uebers, U., Filser, J., 2008. Imidazolium based ionic liquids in soils: Effects of the side chain length on wheat (*Triticum aestivum*) and cress (*Lepidium sativum*) as affected by different clays and organic matter. Green Chem. 10, 584–591.

Maugeri, Z., Leitner, W., Dominguez De Maria, P., 2012. Practical separation of alcohol-ester mixtures using Deep-Eutectic-Solvents. Tetrahedron Lett. 53, 6968–6971.

Maulide, N., Peng, B., Afonso, C.A.M., Frade, R.F.., 2016. Process for converting lupanine into sparteine. U.S. Patent No.: US2016/0096840A1.

Maulide, N., Peng, B., Afonso, C.A.M., Frade, R.F.M., 2014. Process for preparing enantiopure lupanine and sparteine. European Patent EP2808326A1.

Meneses, Y.E., Stratton, J., Flores, R.A., 2017. Water reconditioning and reuse in the food processing industry: Current situation and challenges. Trends Food Sci. Technol. 61, 72–79.

Mesnard, F., Girard, S., Fliniaux, O., Bhogal, R.K., Gillet, F., Lebreton, J., Fliniaux, M.A., Robins, R.J., 2001. Chiral specificity of the degradation of nicotine by *Nicotiana plumbaginifolia* cell suspension cultures. Plant Sci. 161, 1011–1018.

Metallinos, C., Szillat, H., Taylor, N.J., 2003. (-)-sparteine-mediated directed *ortho*-metalation of *N*-cumyl-*N*-ethylferrocenecarboxamide. Versatile routes to functionalized planar chiral ferrocenecarboxamides, amines, esters and phosphines. Adv. Synth. Catal. 345, 370–382.

Michalska, K., Bednarek, E., Gruba, E., Lewandowska, K., Mizera, M., Cielecka-Piontek, J., 2017. Comprehensive spectral identification of key intermediates to the final product of the chiral pool synthesis of radezolid. Chem. Cent. J. 11, e82.

Miller, G.L., 1959. Use of dinitrosalicylic acid reagent for determination of reducing sugar. Anal. Chem. 31, 426–428.

Mitkov, J., Danchev, N., Nikolova, I., Zlatkov, A., 2007. Synthesis and brain antihypoxic activity of some aminoalcoholic derivatives of caffeine-8-thioglycolic acid. Acta Pharm. 57, 361–370.

Mohan, S.V., Nikhil, G.N., Chiranjeevi, P., Reddy, C.N., Rohit, M.V., Kumar, A.N.,

Sarkar, O., 2016. Waste biorefinery models towards sustainable circular bioeconomy: Critical review and future perspectives. Bioresour. Technol. 215, 2–12.

Molero, P., Ramos-Quiroga, J.A., Martin-Santos, R., Calvo-Sánchez, E., Gutiérrez-Rojas, L., Meana, J.J., 2018. Antidepressant efficacy and tolerability of ketamine and esketamine: A critical review. CNS Drugs 32, 411–420.

Monteiro, C.M., Afonso, C.A.M., Lourenco, N.M.T., 2010. Enzymatic resolution and separation of secondary alcohols based on fatty esters as acylating agents. J. Chem. Educ. 87, 423–425.

Monteiro, C.M., Lourenço, N.M.T., Ferreira, F.C., Afonso, C.A.M., 2015. PEG 600-carboxylates as efficient reusable reaction media and acylating agents for the resolution of *sec*-alcohols. Chempluschem 80, 42–46.

Mozejko-Toczko, M., 1960. Decomposition of lupanine by *Pseudomonas lupanini*. Acta Microbiol. Pol. 9, 157–171.

Muralidhara, A., Bado-Nilles, A., Marlair, G., Engelen, V., Len, C., Pandard, P., 2019. Humins in the environment: Early stage insights on ecotoxicological aspects. Biofuels, Bioprod. Biorefining 13, 464–470.

Musa, M.M., 2020. Enzymatic racemization of alcohols and amines: An approach for bi-enzymatic dynamic kinetic resolution. Chirality 32, 147–157.

Musco, N., Cutrignelli, M.I., Calabro, S., Tudisco, R., Infascelli, F., Grazioli, R., Lo Presti, V., Gresta, F., Chiofalo, B., 2017. Comparison of nutritional and antinutritional traits among different species (*Lupinus albus* L., *Lupinus luteus* L., *Lupinus angustifolius* L.) and varieties of lupin seeds. J. Anim. Physiol. Anim. Nutr. (Berl). 101, 1227–1241.

Nagai, T., Taya, K., Annoh, H., Ishihara, S., 2013. Application of a fluorometric microplate algal toxicity assay for riverine periphytic algal species. Ecotoxicol. Environ. Saf. 94, 37–44.

Neri-Numa, I.A., Arruda, H.S., Geraldi, M.V., Marostica Junior, M.R., Pastore, G.M., 2020. Natural prebiotic carbohydrates, carotenoids and flavonoids as ingredients in food systems. Curr. Opin. Food Sci. 33, 98–107.

Neu, A.K., Pleissner, D., Mehlmann, K., Schneider, R., Puerta-Quintero, G.I., Venus, J., 2016. Fermentative utilization of coffee mucilage using *Bacillus coagulans* and investigation of down-stream processing of fermentation broth for optically pure L(+)-lactic acid production. Bioresour. Technol. 211, 398–405.

Nguyen, C.M., Kim, J.S., Nguyen, T.N., Kim, S.K., Choi, G.J., Choi, Y.H., Jang, K.S., Kim, J.C., 2013. Production of L- and D-lactic acid from waste *Curcuma longa* biomass through simultaneous saccharification and cofermentation. Bioresour. Technol. 146, 35–43.

Ni, K., Wang, H., Zhao, L., Zhang, M., Zhang, S., Ren, Y., Wei, D., 2013. Efficient production of (*R*)-(-)-mandelic acid in biphasic system by immobilized recombinant E. coli. J. Biotechnol. 167, 433–440.

Niedzielska, A., Rogozinski, J., 1973. Inducible lupanine hydroxylase from resting culture of *Pseudomonas lupanini*. Bull. Acad. Pol. Sci. Biol. 21, 1–5.

Nielsen, S.S., 2010. Phenol-sulfuric acid method for total carbohydrates, in : Food analysis laboratory manual 47–52.

OECD 201: 2006 - Organisation for Economic Co-operation and Development. Guidelines for the testing of chemicals–Freshwater alga and cyanobacteria, growth inhibition test.

OECD 208:2006 - Organisation for Economic Co-operation and Development. Guidelines for the testing of chemicals–Terrestrial plant test: Seedling emergence and seedling growth test.

Ohmiya, S., Saito, K., Murakoshi, I., 1995. Lupine Alkaloids, in: Cordell, G.A. (Eds). The alkaloids: chemistry and pharmacology 47, 1–114.

Ojima, I., 2010. Catalytic asymmetric synthesis 1–986.

Okudomi, M., Ageishi, K., Yamada, T., Chihara, N., Nakagawa, T., Mizuochi, K., Matsumoto, K., 2010. Enzyme-mediated enantioselective hydrolysis of soluble polymer-supported carboxylates. Tetrahedron 66, 8060–8067.

Oliveira, R.A., Komesu, A., Rossell, C.E.V., Filho, R.M., 2018. Challenges and opportunities in lactic acid bioprocess design - From economic to production aspects. Biochem. Eng. J. 133, 219–239.

Ooi, K.Y., Wu, J.C., 2015. Use of dry yeast cells as a cheap nitrogen source for lactic acid production by thermophilic *Bacillus coagulans* WCP10-4. Front. Chem. Sci. Eng. 9, 381–385.

Ozturk, B., Parkinson, C., Gonzalez-Miquel, M., 2018. Extraction of polyphenolic antioxidants from orange peel waste using deep eutectic solvents. Sep. Purif. Technol. 206, 1–13.

Pagliaro, M., 2017. C3-monomers, in : Glycerol: The renewable platform chemical 23–57.

Paiva, A., Vidinha, P., Angelova, M., Rebocho, S., Barreiros, S., Brunner, G., 2011. Biocatalytic separation of (*R, S*)-1-phenylethanol enantiomers and fractionation of reaction products with supercritical carbon dioxide. J. Supercrit. Fluids 55, 963–970.

Pamies, O., Backvall, J.E., 2003. Combination of enzymes and metal catalysts. A powerful approach in asymmetric catalysis. Chem. Rev. 103, 3247–3261.

Parker, B.M., Rogers, S.L., Lymperopoulos, A., 2018. Clinical pharmacogenomics of carvedilol: The stereo-selective metabolism angle. Pharmacogenomics 19, 1089–1093.

Parmaki, S., Tsipa, A., Vasquez, M.I., Gonçalves, J.M.J., Hadjiadamou, I., Ferreira, F.C., Afonso, C.A.M., Drouza, C., Koutinas, M., 2020. Resolution of alkaloid racemate: A novel microbial approach for the production of enantiopure lupanine via industrial wastewater valorization. Microb. Cell Fact. 19, e67.

Parmaki, S., Vyrides, I., Vasquez, M.I., Hartman, V., Zacharia, I., Hadjiadamou, I., Barbeitos, C.B.M., Ferreira, F.C., Afonso, C.A.M., Drouza, C., Koutinas, M., 2018. Bioconversion of alkaloids to high-value chemicals: Comparative analysis of newly isolated lupanine degrading strains. Chemosphere 193, 50–59.

Parvez, S., Venkataraman, C., Mukherji, S., 2006. A review on advantages of implementing luminescence inhibition test (*Vibrio fischeri*) for acute toxicity prediction of chemicals. Environ. Int. 32, 265–268.

Patil, M.D., Grogan, G., Bommarius, A., Yun, H., 2018. Oxidoreductase-Catalyzed synthesis of chiral amines. ACS Catal. 8, 10985–11015.

Patsalou, M., Chrysargyris, A., Tzortzakis, N., Koutinas, M., 2020. A biorefinery for conversion of citrus peel waste into essential oils, pectin, fertilizer and succinic acid via different fermentation strategies. Waste Manag. 113, 469–477.

Patsalou, M., Menikea, K.K., Makri, E., Vasquez, M.I., Drouza, C., Koutinas, M., 2017. Development of a citrus peel-based biorefinery strategy for the production of succinic acid. J. Clean. Prod. 166, 706–716.

Pejin, J., Radosavljevic, M., Pribic, M., Kocic-Tanackov, S., Mladenovic, D., Djukic-Vukovic, A., Mojovic, L., 2018. Possibility of L-(+)-lactic acid fermentation using malting, brewing, and oil production by-products. Waste Manag. 79, 153–163.

Peleteiro, S., Rivas, S., Alonso, J.L., Santos, V., Parajó, J.C., 2016. Furfural production using ionic liquids: A review. Bioresour. Technol. 202, 181–191.

Perazzolo, C., Saouter, E., 2013. REACH legislation in ecotoxicology, in: Ferard, J.F., Blaise, C. (Eds), Encyclopedia of aquatic ecotoxicology 967–972.

Petrickova, A., Sosedov, O., Baum, S., Stolz, A., Martinkova, L., 2012. Influence of point mutations near the active site on the catalytic properties of fungal arylacetonitrilases from Aspergillus niger and Neurospora crassa. J. Mol. Catal. B Enzym. 77, 74–80.

Petterson, D.S., Ellis, Z.L., Harris, D.J., Spadek, Z.E., 1987. Acute toxicity of the major alkaloids of cultivated *Lupinus angustifolius* seed to rats. J. Appl. Toxicol. 7, 51–53.

Pihlanto, A., Mattila, P., Mäkinen, S., Pajari, A.M., 2017. Bioactivities of alternative protein sources and their potential health benefits. Food Funct. 8, 3443–3458.

Pinxterhuis, E.B., Gualtierotti, J.B., Wezenberg, S.J., de Vries, J.G., Feringa, B.L., 2018. Highly efficient and robust enantioselective liquid–liquid extraction of 1,2-amino alcohols utilizing VAPOL- and VANOL-based phosphoric acid hosts. ChemSusChem 11, 178–184.

Pleissner, D., Neu, A.K., Mehlmann, K., Schneider, R., Puerta-Quintero, G.I., Venus, J., 2016. Fermentative lactic acid production from coffee pulp hydrolysate using *Bacillus coagulans* at laboratory and pilot scales. Bioresour. Technol. 218, 167–173.

Pothier, J., Cheav, S.L., Galand, N., Dormeau, C., Viel, C., 1998. A comparative study of the effects of sparteine, lupanine and lupin extract on the central nervous system of the mouse. J. Pharm. Pharmacol. 50, 949–954.

Prandini, A., Morlacchini, M., Moschini, M., Fusconi, G., Masoero, F., Piva, G., 2005. Raw and extruded pea (*Pisum sativum*) and lupin (*Lupinus albus* var. Multitalia) seeds as protein sources in weaned piglets' diets: Effect on growth rate and blood parameters. Ital. J. Anim. Sci. 4, 385–394.

Priyadarshini, S., Joseph, P.J.A., Srinivas, P., Maheswaran, H., Kantam, M.L., Bhargava, S., 2011. Bis(μ-iodo)bis((-)-sparteine)dicopper(I) catalyzed Sonogashira-type reaction under palladium and phosphine-free conditions. Tetrahedron Lett. 52, 1615–1618.

Przybyl, A.K., Kubicki, M., 2011. Simple and highly efficient preparation and characterization of (-)-lupanine and (+)-sparteine. Tetrahedron 67, 7787–7793.

Qian, Y., Zhu, L., Wang, Y., Lu, X., 2015. Recent progress in the development of biofuel 2,5-dimethylfuran. Renew. Sustain. Energy Rev. 41, 633–646.

Quiles, M.R.S., Oquendo-Jimenez, I., Herreno-Saenz, D., Antoun, M.D., 2010. Genotoxicity of alkaloid-rich extract from *Lupinus termis* seeds. Pharm. Crop. 18–23.

Rasouli, H., Yarani, R., Pociot, F., Popovic-Djordjevic, J., 2020. Anti-diabetic potential of plant alkaloids: Revisiting current findings and future perspectives. Pharmacol. Res. 155, e104723.

Rathbone, D.A., Bruce, N.C., 2002. Microbial transformation of alkaloids. Curr. Opin. Microbiol. 5, 274–281.

REACH, 2006. Regulation (EC) No 1907/2006 of the European parliament and of the council of 18 December 2006 concerning the Registration, Evaluation, Authorisation and Restriction of Chemicals (REACH), establishing a European Chemicals Agency, amending Directive 1999/4. Off. J. Eur. Union 396/1.

Reetz, M.T., Wiesenhofer, W., Francio, G., Leitner, W., 2003. Continuous flow enzymatic kinetic resolution and enantiomer separation using ionic liquid/supercritical carbon dioxide media. Adv. Synth. Catal. 345, 1221–1228.

Remus-Emsermann, M.N., Schmid, M., Gekenidis, M.T., Pelludat, C., Frey, J.E., Ahrens, C.H., Drissner, D., 2016. Complete genome sequence of *Pseudomonas citronellolis* P3B5, a candidate for microbial phyllo-remediation of hydrocarbon-contaminated sites. Stand. Genomic Sci. 11, e75.

Resta, D., Boschin, G., D'Agostina, A., Arnoldi, A., 2008. Evaluation of total quinolizidine alkaloids content in lupin flours, lupin-based ingredients, and foods. Mol. Nutr. Food Res. 52, 490–495.

Revelles, O., Espinosa-Urgel, M., Fuhrer, T., Sauer, U., Ramos, J.L., 2005. Multiple and interconnected pathways for L-lysine catabolism in *Pseudomonas putida* KT2440. J. Bacteriol. 187, 7500–7510.

Rischer, H., Szilvay, G.R., Oksman-Caldentey, K.M., 2020. Cellular agriculture — industrial biotechnology for food and materials. Curr. Opin. Biotechnol. 61, 128–134.

Risi, C., Bortolini, O., Carmine, G., Ragno, D., Massi, A., 2019. Kinetic resolution, dynamic kinetic resolution and asymmetric desymmetrization by *N*-heterocyclic carbene catalysis. Synthesis (Stuttg). 51, 1871–1891.

Ritter, S.K., 2017. Where has all the sparteine gone? Chem. Eng. News 95, 18–20.

Rocha, A., Teixeira, R., Lourenco, N.M.T., Afonso, C.A.M., 2017. Enzymatic kinetic resolution of secondary alcohols using an ionic anhydride generated in situ. ChemSusChem 10, 296–302.

Rojo, F., 2010. Carbon catabolite repression in *Pseudomonas*: Optimizing metabolic versatility and interactions with the environment. FEMS Microbiol. Rev. 34, 658–684.

Rosenbaum, R.K., Hauschild, H.Z., Boulay, A.M., Fantke, P., Laurent, A., Nunez, M., Vieira, M., 2018. Life cycle impact assessment, in : Hauschild, M.Z., Rosenbaum, R.K., Olsen, S.I. (Eds.), Life cycle assessment 167–270.

Rosenkranz, V., Wink, M., 2007. Induction of apoptosis by alkaloids, non-protein amino acids, and cardiac glycosides in human promyelotic HL-60 cells. Zeitschrift für Naturforsch. C 62, 458–466.

Roshan, A., Kumar, M., 2020. Water end-use estimation can support the urban water

crisis management: A critical review. J. Environ. Manage. 268, e110663.

Rouf, A., Taneja, S.C., 2014. Synthesis of single- enantiomer bioactive molecules: A brief overview. Chirality 26, 63–78.

Roy, A., Bharadvaja, N., 2018. Biotechnological approaches for the production of pharmaceutically important compound: Plumbagin. Curr. Pharm. Biotechnol. 19, 372–381.

Ruan, A., Min, H., Peng, X., Huang, Z., 2005. Isolation and characterization of *Pseudomonas* sp. strain HF-1, capable of degrading nicotine. Res. Microbiol. 156, 700–706.

Rybinski, W., Kroc, M., Swiecicki, W., Wilczura, P., Kamel, K., Barzyk, P., Mikulski, W., 2018. Preliminary estimation of variation of alkaloids content in white lupin (*Lupinus albus* L.) collection, in: Brazauskas, G., Statkeviciute, G., Jonaviciene, K. (Eds.), Breeding grasses and protein crops in the era of genomics 131–136.

Saavedra, L., Barbas, C., 2002. Optimization of the separation lactic acid enantiomers in body fluids by capillary electrophoresis. J. Chromatogr. B Anal. Technol. Biomed. Life Sci. 766, 235–242.

Sabelli, P.A., 2012. Seed development: A comparative overview on biology of morphology, physiology, and biochemistry between monocot and dicot plants, in : Agrawal, G.K., Rakwal, R. (Eds). Seed development: OMICS technologies toward improvement of seed quality and crop yield 3–25.

Sahin, E., 2019. Green synthesis of enantiopure (*S*)-1-(benzofuran-2-yl)ethanol by whole-cell biocatalyst. Chirality 31, 892–897.

Sahin, E., 2018. Production of (*R*)-1-(1,3-benzodioxol-5-yl)ethanol in high enantiomeric purity by *Lactobacillus paracasei* BD101. Chirality 30, 189–194.

Sahin, E., Dertli, E., 2017. Highly enantioselective production of chiral secondary alcohols with *Candida zeylanoides* as a new whole cell biocatalyst. Chem. Biodivers. 14, e1700121.

Salvatore, M., Carafa, A.M., Carratu, G., 2008. Assessment of heavy metals phytotoxicity using seed germination and root elongation tests: A comparison of two growth substrates. Chemosphere 73, 1461–1464.

Sanganyado, E., Lu, Z., Fu, Q., Schlenk, D., Gan, J., 2017. Chiral pharmaceuticals : A review on their environmental occurrence and fate processes. Water Res. 124, 527–542.

Santacesaria, E., Tesser, R., Serio, M.D., Casale, L., Verde, D., 2010. New process for producing epichlorohydrin via glycerol chlorination. Ind. Eng. Chem. Res. 49, 964–970.

Santana, F.C., Empis, J., 2001. Bacterial removal of quinolizidine alkaloids from *Lupinus albus* flours. Eur. Food Res. Technol. 212, 217–224.

Santana, F.M., Pinto, T., Fialho, A.M., Sá-Correia, I., Empis, J.M., 2002. Bacterial removal of quinolizidine alkaloids and other carbon sources from a *Lupinus albus* aqueous extract. J. Agric. Food Chem. 50, 2318–2323.

Santana, F.M.C., Fialho, A.M., Sá-Correia, I., Empis, J.M.A., 1996. Isolation of bacterial strains capable of using lupanine, the predominant quinolizidine alkaloid in white lupin, as sole carbon and energy source. J. Ind. Microbiol. 17, 110–115.

Sara, M., Brar, S.K., J.F., B., 2016. Production of drop-in and novel bio-based platform chemicals, in : Brar, S.K., Sarma, S.J., Pakshirajan, K. (Eds.), Platform chemical biorefinery: Future freen Industry 249–283.

Schrenk, D., Bodin, L., Chipman, J.K., Mazo, J., Grasl-Kraupp, B., Hogstrand, C., Hoogenboom, L., Leblanc, J.C., Nebbia, C.S., Nielsen, E., Ntzani, E., Petersen, A., Sand, S., Schwerdtle, T., Vleminckx, C., Wallace, H., Alexander, J., Cottrill, B., Dusemund, B., Mulder, P., Arcella, D., Baert, K., Cascio, C., Steinkellner, H., Bignami, M., 2019. Scientific opinion on the risks for animal and human health related to the presence of quinolizidine alkaloids in feed and food, in particular in lupins and lupin-derived products. EFSA J. 17, e5860.

Schuur, B., Verkuijl, B.J.V., Minnaard, A.J., Vries, J.G., Heeres, H.J., Feringa, B.L., 2011. Chiral separation by enantioselective liquid-liquid extraction. Org. Biomol. Chem. 9, 36–51.

Sekhon, B.S., 2013. Exploiting the power of stereochemistry in drugs: An overview of racemic and enantiopure drugs. J. Mod. Med. Chem. 1, 10–36.

Shang, Y.P., Chen, Q., Kong, X.D., Zhang, Y.J., Xu, J.H., Yu, H.L., 2017. Efficient

Synthesis of (*R*)-2-Chloro-1-(2,4-dichlorophenyl)ethanol with a Ketoreductase from *Scheffersomyces stipitis* CBS 6045. Adv. Synth. Catal. 359, 426–431.

Shen, J.D., Cai, X., Liu, Z.Q., Zheng, Y.G., 2021. Nitrilase: A promising biocatalyst in industrial applications for green chemistry. Crit. Rev. Biotechnol. 41, 72–93.

Shen, Z., Lv, C., Zeng, S., 2016. Significance and challenges of stereoselectivity assessing methods in drug metabolism. J. Pharm. Anal. 6, 1–10.

Sheng, B., Xu, J., Ge, Y., Zhang, S., Wang, D., Gao, C., Ma, C., Xu, P., 2016. Enzymatic resolution by a D-lactate oxidase catalyzed reaction for (*S*)-2-hydroxycarboxylic acids. ChemCatChem 8, 2630–2633.

Shimizu, K., 2011. Metabolic regulation analysis and metabolic engineering, in : Moo-Young, M. (Eds.), Comprehensive biotechnology 541–554.

Simola, F., Iosco, M., 2012. Continuous process for producing epichlorohydrin from glycerol. U.S. Patent No.: WO2014/049625A1.

Smerilli, M., Neureiter, M., Wurz, S., Haas, C., Frühauf, S., Fuchs, W., 2015. Direct fermentation of potato starch and potato residues to lactic acid by *Geobacillus stearothermophilus* under non-sterile conditions. J. Chem. Technol. Biotechnol. 90, 648–657.

Smith, B.T., Wendt, J.A., Aubé, J., 2002. First asymmetric total synthesis of (+)-sparteine. Org. Lett. 4, 2577–2579.

Smitha, M.S., Singh, S., Singh, R., 2017. Microbial biotransformation: A process for chemical alterations. J. Bacteriol. Mycol. Open Access 4, 47–51.

Soccol, C.R., Faraco, V., Karp, S.G., Vandenberghe, L.P.S., Thomaz-Soccol, V., Woiciechowski, A.L., Pandey, A., 2019. Lignocellulosic bioethanol: Current status and future perspectives, in : Pandey, A., Larroche, C., Dussap, C.G., Gnansounou, E., Khanal, S.K., Ricke, S. (Eds.), Biofuels: Alternative feedstocks and conversion processes for the production of liquid and gas 331–354.

Stead, D., O'Brien, P., Sanderson, A., 2008. A new sparteine surrogate for asymmetric deprotonation of *N*-Boc pyrrolidine. Org. Lett. 10, 1409–1412.

Stinson, S.C., 2001. Chiral chemistry: Driven by the needs of the drug industry and fueled by the ingenuity of chemists, sales of single-enantiomer chiral compounds

keep accelerating. Chem. Eng. News 79, 45–57.

Sujak, A., Kotlarz, A., Strobel, W., 2006. Compositional and nutritional evaluation of several lupin seeds. Food Chem. 98, 711–719.

Sujatha, P.S., 2008. Monitoring cytotoxic potentials of furfuryl alcohol and 2-furyl methyl ketone in mice. Food Chem. Toxicol. 46, 286–292.

Sun, J., Liu, D., Wang, Z., 2011. Representative chiral drugs, : Lin, G.Q., You, Q.D., Cheng, J.F. (Eds.), Chiral drugs: Chemistry and biological action 401–448.

Sun, Y., Wang, Z., Liu, Y., Meng, X., Qu, J., Liu, C., Qu, B., 2019. A review on the transformation of furfural residue for value-added products. Energies 13, e21.

Swart, E., Boer, T.E., Chen, G., Vooijs, R., Gestel, C.A.M., Straalen, N.M., Roelofs, D., 2019. Species-specific transcriptomic responses in *Daphnia magna* exposed to a bio-plastic production intermediate. Environ. Pollut. 252, 399–408.

Szekely, G., De Sousa, M.C.A., Gil, M., Ferreira, F.C., Heggie, W., 2015. Genotoxic impurities in pharmaceutical manufacturing: Sources, regulations, and mitigation. Chem. Rev. 115, 8182–8229.

Tadele, Y., 2015. White Lupin (*Lupinus albus*) grain, a potential source of protein for ruminants: A review. Res. J. Agric. Environ. Manag. 4, 180–188.

Tan, J., Abdel-Rahman, A.A., Sononmoto, K., 2018. Biorefinery-based lactic acid fermentation: Microbial production of pure monomer product, in : Lorenzo, M.L.D., Androsch, R. (Eds.), Synthesis, structure and properties of poly(lactic acid) 279, 27–66.

Tang, X.L., Lu, X.F., Wu, Z.M., Zheng, R.C., Zheng, Y.G., 2018. Biocatalytic production of (*S*)-2-aminobutanamide by a novel D-aminopeptidase from Brucella sp. with high activity and enantioselectivity. J. Biotechnol. 266, 20–26.

Taylor, L.N., Scroggins, R.P., 2013. Standardization of ecotoxicological tests: The process, in: Ferard, J.F., Blaise, C. (Eds), Encyclopedia of aquatic ecotoxicology 1072–1080.

Temple, J.L., Bernard, C., Lipshultz, S.E., Czachor, J.D., Westphal, J.A., Mestre, M.A., 2017. The safety of ingested caffeine: A comprehensive review. Front. Psychiatry 8, e80.

Thakur, A., Panesar, P.S., Saini, M.S., 2019. L(+)-lactic acid production by immobilized *Lactobacillus casei* using low cost agro-industrial waste as carbon and nitrogen sources. Waste and Biomass Valorization 10, 1119–1129.

Thamhesl, M., Apfelthaler, E., Schwartz-Zimmermann, H.E., Kunz-Vekiru, E., Krska, R., Kneifel, W., Schatzmayr, G., Moll, W.D., 2015. *Rhodococcus erythropolis* MTHt3 biotransforms ergopeptines to lysergic acid. BMC Microbiol. 15, e73.

Therapontos, C., Erskine, L., Gardner, E.R., Figg, W.D., Vargesson, N., 2009. Thalidomide induces limb defects by preventing angiogenic outgrowth during early limb formation. PNAS 106, 8573–8578.

Toczko, M., 1966. Induced lupanine hydroxylase from *Pseudomonas lupanini*. Biochim. Biophys. Acta (BBA)-Enzymology Biol. Oxid. 128, 570–573.

Todd, M., 2014. Introduction: A survey of how and why to separate enantiomers, in : Todd, M., (Eds.), Separation of enantiomers 1–11.

Torre, I., Acedos, M.G., Ladero, M., Santos, V.E., 2019a. On the use of resting *L. delbrueckii* spp. delbrueckii cells for D-lactic acid production from orange peel wastes hydrolysates. Biochem. Eng. J. 145, 162–169.

Torre, I., Ladero, M., Santos, V.E., 2020. D-lactic acid production from orange waste enzymatic hydrolysates with *L. delbrueckii* cells in growing and resting state. Ind. Crops Prod. 146, e112176.

Torre, I., Martin-Dominguez, V., Acedos, M.G., Esteban, J., Santos, V.E., Ladero, M., 2019b. Utilisation/upgrading of orange peel waste from a biological biorefinery perspective. Appl. Microbiol. Biotechnol. 103, 5975–5991.

Tseliou, V., Knaus, T., Masman, M.F., Corrado, M.L., Mutti, F.G., 2019. Generation of amine dehydrogenases with increased catalytic performance and substrate scope from ε-deaminating L-Lysine dehydrogenase. Nat. Commun. 10, e3717.

Tseliou, V., Knaus, T., Vilím, J., Masman, M.F., Mutti, F.G., 2020. Kinetic resolution of racemic primary amines using *Geobacillus stearothermophilus* amine dehydrogenase variant. ChemCatChem 12, 2184–2188.

Tsipa, A., Koutinas, M., Pistikopoulos, E.N., Mantalaris, A., 2016. Transcriptional kinetics of the cross-talk between the ortho-cleavage and TOL pathways of toluene

biodegradation in *Pseudomonas putida* mt-2. J. Biotechnol. 228, 112–123.

Tsipa, A., Koutinas, M., Usaku, C., Mantalaris, A., 2018. Optimal bioprocess design through a gene regulatory network-Growth kinetic hybrid model: Towards replacing Monod kinetics. Metab. Eng. 48, 129–137.

Tsouko, E., Maina, S., Ladakis, D., Kookos, I.K., Koutinas, A., 2020. Integrated biorefinery development for the extraction of value-added components and bacterial cellulose production from orange peel waste streams. Renew. Energy 160, 944–954.

U.S. Environmental Protection Agency (EPA). Method 1684: Total, fixed, and volatile solids in water, solids, and biosolids, 2001.

U.S. Environmental Protection Agency (EPA). Technical overview of ecological risk assessment - analysis phase: Ecological effects characterization.

U.S. Food and Drug Administration (FDA), 1992. FDA's Policy Statement for the Development of New Stereoisomeric Drugs. Fed. Regist.

Ubando, A.T., Felix, C.B., Chen, W.H., 2020. Biorefineries in circular bioeconomy: A comprehensive review. Bioresour. Technol. 299, e122585.

Valadez-Blanco, R., Ferreira, F.C., Jorge, R.F., Livingston, A.G., 2008. A membrane bioreactor for biotransformations of hydrophobic molecules using organic solvent nanofiltration (OSN) membranes. J. Memb. Sci. 317, 50–64.

Valta, K., Kosanovic, T., Malamis, D., Moustakas, K., Loizidou, M., 2015. Overview of water usage and wastewater management in the food and beverage industry. Desalin. Water Treat. 53, 3335–3347.

Vasas, G., Gáspár, A., Surányi, G., Batta, G., Gyémánt, G., M-Hamvas, M., Máthé, C., Grigorszky, I., Molnár, E., Borbély, G., 2002. Capillary electrophoretic assay and purification of cylindrospermopsin, a cyanobacterial toxin from *Aphanizomenon ovalisporum*, by plant test (Blue-Green Sinapis Test). Anal. Biochem. 302, 95–103.

Vasquez, Z.S., Carvalho Neto, D.P., Pereira, G.V.M., Vandenberghe, L.P.S., Oliveira, P.Z., Tiburcio, P.B., Rogez, H.L.G., Goes Neto, A., Soccol, C.R., 2019. Biotechnological approaches for cocoa waste management: A review. Waste Manag. 90, 72–83.

Ventura, S.P.M., Morais, P., Coelho, J.A.S., Sintra, T., Coutinho, J.A.P., Afonso, C.A.M., 2016. Evaluating the toxicity of biomass derived platform chemicals. Green Chem. 18, 4733–4742.

Villalpando-Vargas, F., Medina-Ceja, L., 2016. Sparteine as an anticonvulsant drug: Evidence and possible mechanism of action. Seizure 39, 49–55.

Villalpando-Vargas, F., Medina-Ceja, L., Santerre, A., Enciso-Madero, E.A., 2020. The anticonvulsant effect of sparteine on pentylenetetrazole-induced seizures in rats: A behavioral, electroencephalographic, morphological and molecular study. J. Mol. Histol. 51, 503–518.

Vonk, J.A., Kraak, M.H.S., 2020. Herbicide exposure and toxicity to aquatic primary producers, in : Voogt, P. (Eds.), Reviews of environmental contamination and toxicology 119–171.

Wang, Q., Li, Y., Li, J., Wang, Y., Wang, C., Wang, P., 2015. Experimental and kinetic study on the cometabolic biodegradation of phenol and 4-chlorophenol by psychrotrophic *Pseudomonas putida* LY1. Environ. Sci. Pollut. Res. 22, 565–573.

Wang, S.N., Xu, P., Tang, H.Z., Meng, J., Liu, X.L., Huang, J., Chen, H., Du, Y., Blankespoor, H.D., 2012. Biodegradation and detoxification of nicotine in tobacco solid waste by a *Pseudomonas* sp. Biotechnol. Lett. 26, 1493–1496.

Wang, T., Wang, M., Cai, D., Wang, B., Wang, Z., Qin, P., Tan, T., 2016. Efficient l-lactic acid production from sweet sorghum bagasse by open simultaneous saccharification and fermentation. RSC Adv. 6, 35771–35777.

Wang, Y., Tashiro, Y., Sonomoto, K., 2015. Fermentative production of lactic acid from renewable materials: Recent achievements, prospects, and limits. J. Biosci. Bioeng. 119, 10–18.

Ward, T.J., 2002. Chiral separations. Anal. Chem. 74, 2863–2872.

Wieczerzak, M., Namieśnik, J., Kudłak, B., 2016. Bioassays as one of the Green Chemistry tools for assessing environmental quality: A review. Environ. Int. 94, 341–361.

Wiedemann, M., Gurrola-Diaz, C.M., Vargas-Guerrero, B., Wink, M., Garcia-Lopez, P.M., Dufer, M., 2015. Lupanine improves glucose homeostasis by influencing

KATP channels and insulin gene expression. Molecules 20, 19085–19100.

Wink, M., 2019. Quinolizidine and pyrrolizidine alkaloid chemical ecology - a mini-review on their similarities and differences. J. Chem. Ecol. 45, 109–115.

Wink, M., Schmeller, T., Latz-Bruning, B., 1998. Modes of action of allelochemical alkaloids: Interaction with neuroreceptors, DNA, and other molecular targets. J. Chem. Ecol. 24, 1881–1937.

Wohlgemuth, R., 2010. Asymmetric biocatalysis with microbial enzymes and cells. Curr. Opin. Microbiol. 13, 283–292.

Wu, H.L., Zhang, J.D., Zhang, C.F., Fan, X.J., Chang, H.H., Wei, W.L., 2017. Characterization of four new distinct ω-transaminases from *Pseudomonas putida* NBRC 14164 for kinetic resolution of racemic amines and amino alcohols. Appl. Biochem. Biotechnol. 181, 972–985.

Wu, L., Moteki, T., Gokhale, A.A., Flaherty, D.W., Toste, F.D., 2016. Production of fuels and chemicals from biomass: Condensation reactions and beyond. Chem 1, 32–58.

Xue, F., Liu, Z.Q., Wan, N.W., Zhu, H.Q., Zheng, Y.G., 2015. Engineering the epoxide hydrolase from *Agromyces mediolanus* for enhanced enantioselectivity and activity in the kinetic resolution of racemic epichlorohydrin. RSC Adv. 5, 31525–31532.

Xue, F., Ya, X., Tong, Q., Xiu, Y., Huang, H., 2018. Heterologous overexpression of *Pseudomonas umsongensis* halohydrin dehalogenase in *Escherichia coli* and its application in epoxide asymmetric ring opening reactions. Process Biochem. 75, 139–145.

Yan, Y., Bu, C., Huang, X., Ouyang, J., 2019. Efficient whole-cell biotransformation of furfural to furfuryl alcohol by *Saccharomyces cerevisiae* NL22. J. Chem. Technol. Biotechnol. 94, 3825–3831.

Yang, G.Z., Zhang, J., Peng, J.W., Zhang, Z.J., Zhao, W.B., Wang, R.X., Ma, K.Y., Li, J.C., Liu, Y.Q., Zhao, Z.M., Shang, X.F., 2020. Discovery of luotonin A analogues as potent fungicides and insecticides: Design, synthesis and biological evaluation inspired by natural alkaloid. Eur. J. Med. Chem. 194, e112253.

Yaver, E., Bilgicli, N., 2021. Ultrasound-treated lupin (*Lupinus albus* L.) flour: Protein-

and fiber-rich ingredient to improve physical and textural quality of bread with a reduced glycemic index. LWT - Food Sci. Technol. 148, e111767.

Yorgancilar, M., Bilgicli, N., 2012. Chemical and nutritional changes in bitter and sweet lupin seeds (*Lupinus albus* L.) during bulgur production. J. Food Sci. Technol. 50, 1384–1389.

Yovo, K., Huguet, F., Pothier, J., Durand, M., Breteau, M., Narcisse, G., 1984. Comparative pharmacological study of sparteine and its ketonic derivative lupanine from seeds of *Lupinus albus*. Planta Med. 50, 420–424.

Yuan, X., Wang, L., Liu, G., Dai, G., Tang, K., 2019. Resolution of (*R*,*S*)-ibuprofen catalyzed by immobilized Novozym40086 in organic phase. Chirality 31, 445–456.

Yuan, Y.J., Lu, Z.X., Wu, N., Huang, L.J., Lü, F.X., Bie, X.M., 2005. Isolation and preliminary characterization of a novel nicotine-degrading bacterium, *Ochrobactrum intermedium* DN2. Int. Biodeterior. Biodegrad. 56, 45–50.

Yukawa, H., Ookino, S., Inui, M., 2010. L- aspartic acid, Production processes, in : Flickinger, M.C. (Eds.), Encyclopedia of industrial biotechnology: Bioprocess, bioseparation, and cell technology 1–3.

Zambrana, S., Lundqvist, L.C.E., Mamani, O., Catrina, S.B., Gonzales, E., Ostenson, C.G., 2018. *Lupinus mutabilis* extract exerts an anti-diabetic effect by improving insulin release in type 2 diabetic goto-kakizaki rats. Nutrients 10, e933.

Zamora-Natera, J.F., Ruiz-Lopez, M., Soto-Hernandez, M., Garcia-Lopez, P., Bernal-Alcocer, A., Przybyl, A.K., 2005. Mycelial growth inhibition of pathogenic fungi by lupanine and alkaloid extracts from *Lupinus exaltatus* and *Lupinus mexicanus*, in : Santen, E., Hill, G.D. (Eds.), Mexico, where old and new world lupins meet 139–141.

Zeitsch, K.J., 2000. Applications of furfural, in : The chemistry and technology of furfural and its many by-products 98–103.

Zhang, L., Li, X., Yong, Q., Yang, S.T., Ouyang, J., Yu, S., 2015. Simultaneous saccharification and fermentation of xylo-oligosaccharides manufacturing waste residue for L-lactic acid production by *Rhizopus oryzae*. Biochem. Eng. J. 94, 92–99.

Zheng, M., Xiang, X., Wang, S., Shi, J., Deng, Q., Huang, F., Cong, R., 2017. Lipase immobilized in ordered mesoporous silica: A powerful biocatalyst for ultrafast kinetic resolution of racemic secondary alcohols. Process Biochem. 53, 102–108.

Zheng, Y.C., Xu, J.H., Wang, H., Lin, G.Q., Hong, R., Yu, H.L., 2017. Hydroxynitrile lyase isozymes from *Prunus communis*: Identification, characterization and synthetic applications. Adv. Synth. Catal. 359, 1185–1193.

Zheng, Y.G., Yin, H.H., Yu, D.F., Chen, X., Tang, X.L., Zhang, X.J., Xue, Y.P., Wang, Y.J., Liu, Z.Q., 2017. Recent advances in biotechnological applications of alcohol dehydrogenases. Appl. Microbiol. Biotechnol. 101, 987–1001.

Zheng, Z., Xu, Q., Liu, P., Zhou, F., Ouyang, J., 2018. Enhanced inulin saccharification by self-produced inulinase from a newly isolated *Penicillium* sp. and its application in D-lactic acid production. Appl. Biochem. Biotechnol. 186, 122–131.

Zhong, W., Zhu, C., Shu, M., Sun, K., Zhao, L., Wang, C., Ye, Z., Chen, J., 2010. Degradation of nicotine in tobacco waste extract by newly isolated *Pseudomonas* sp. ZUTSKD. Bioresour. Technol. 101, 6935–6941.

Zhou, S., Lin, K., Li, L., Jin, M., Ye, J., Liu, W., 2009. Separation and toxicity of salithion enantiomers. Chirality 21, 922–928.

Zou, C., Li, Z., Yu, D., 2010. *Bacillus megaterium* strain XTBG34 promotes plant growth by producing 2-pentylfuran. J. Microbiol. 48, 460–466.

Zuriaga, E., Giner, B., Ribate, M.P., García, C.B., Lomba, L., 2018. Exploring the usefulness of key green physicochemical properties: Quantitative structure–activity relationship for solvents from biomass. Environ. Toxicol. Chem. 37, 1014–1023.

APPENDIX I

Details of furanic compounds

Table AP 1: Code name, chemical name, chemical formula, molecular weight and chemical structure of the furan compounds studied in this work.

Code name	Chemical name	Chemical formula	Chemical structure
Furfuryl alcohol	furan-2-yl-methanol	$C_5H_6O_2$	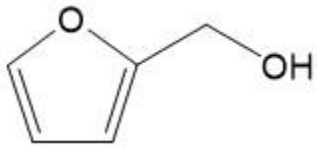
Furfural	furan-2-carbaldehyde	$C_5H_4O_2$	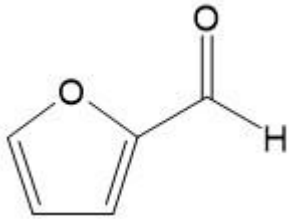
FA	furan-2-carboxylic acid or 2-furoic acid	$C_5H_4O_3$	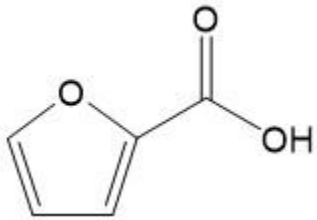

EFA	ethyl 2-furoate or ethyl furan-2-carboxylate	$C_7H_8O_3$	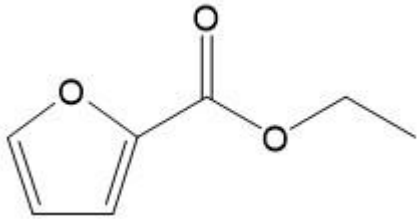
DMF	2,5-dimethylfuran	C_6H_2O	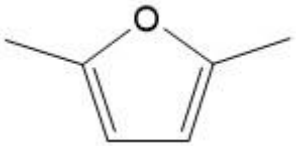
DHMF	furan-2,5-diyldimethanol or 2,5-bis(hydroxymethyl)furan	$C_6H_8O_3$	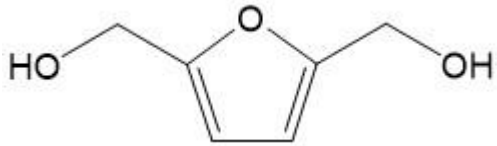
HMF	5-hydroxymethyl furfural or 5-(hydroxymethyl)furan-2-carbaldehyde	$C_6H_6O_3$	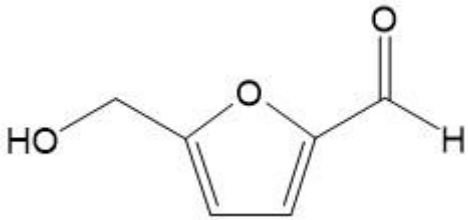

HMFA	5-(hydroxymethyl)furan-2-carboxylic acid	$C_6H_6O_4$	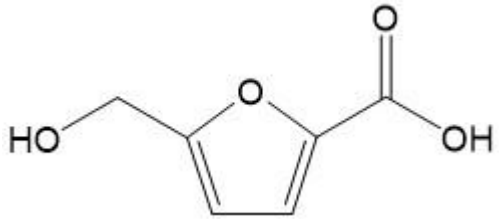
DFA	2,5-furandicarboxaldehyde or furan-2,5-dicarbaldehyde	$C_6H_4O_3$	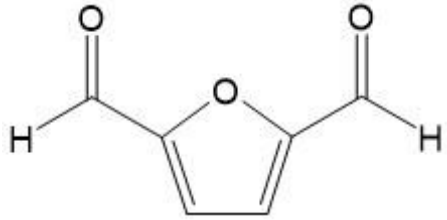
FDCA	2,5-furandicarboxylic acid or furan-2,5-dicarboxylic acid	$C_6H_4O_5$	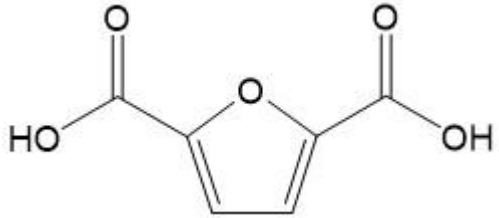
DFDC	dimethyl furan-2,5-dicarboxylate	$C_8H_8O_5$	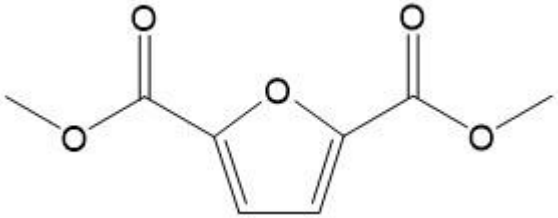

OBMFA	(5,5'-(oxybis(methylene))bis(furan-5,2-diyl))dimethanol	$C_{12}H_{14}O_3$	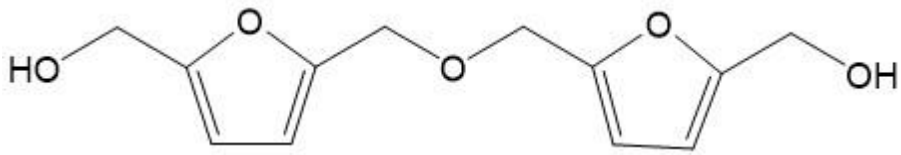
OBMF	5,5'-(oxybis(methylene))bis(furan-2-carbaldehyde)	$C_{12}H_{10}O_5$	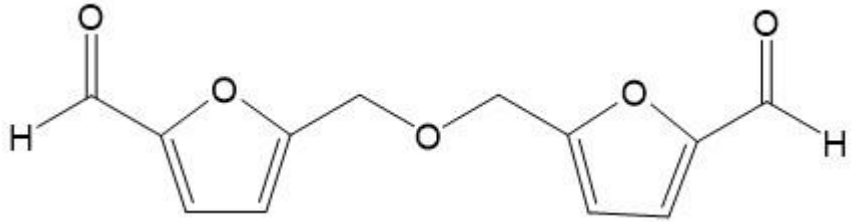
OBCA	5,5'-(oxybis(methylene))bis(furan-2-carboxylic acid)	$C_{12}H_{10}O_7$